Universidad de Valladolid

FACULTAD DE CIENCIAS

DEPARTAMENTO DE MATEMÁTICA APLICADA

TESIS DOCTORAL:

CUATRO ENSAYOS SOBRE VALORACIÓN DE DERIVADOS Y ESTRATEGIAS DE INVERSIÓN.

Presentada por Víctor Gatón Bustillo para optar al grado de doctor por la Universidad de Valladolid

Dirigida por:
Javier de Frutos Baraja

Agradecimientos

Quiero agradecer a Javier de Frutos la oportunidad de haber podido realizar esta tesis doctoral con él. Han sido unos años muy estimulantes, no sólo por el reto que este trabajo supone, sino también por las informales (y divertidas) charlas y reflexiones sobre economía y mercados. Le agradezco su dirección y guía durante mis primeros pasos en la investigación matemática.

A la profesora María Cruz Valsero le agradezco su ayuda cuando comencé a trabajar por primera vez con series históricas de datos. A la profesora Michèle Breton le agradezco todos los comentarios y sugerencias durante el desarrollo del Capítulo 1.

Al profesor Peter Christoffersen le agradezco que amablemente me proporcionara los datos reales de mercado que han sido empleados en los análisis de esta tesis.

Al Departamento de Matemática Aplicada, y en particular a la Sección de Ciencias, le agradezco su acogida y la oportunidad de haber podido colaborar en la docencia y en actividades como la organización del SciCADE. Muchas gracias a todos los profesores por los consejos y apoyo, tanto en el desarrollo de la tesis, como cuando me tocó estar al otro lado de la barrera al impartir mis primeras clases.

Por último, un cariñoso recuerdo a todos los profesores que me dieron clase a lo largo de la carrera y el Máster. Esta tesis ha sido posible gracias a ellos.

A mi Padre, aunque me saliera de letras
A Elena, matemática, compañera y amiga que siempre estuvo ahí
A Carmen y Pablo, los amigos de verdad lo son para siempre
A Sol-Leks, por la compañía en las noches de trabajo

"Doubt always of yourself until the data do not allow you to doubt anymore"

Louis Pasteur

Contents

List of Figures

Technical Remark

All the algorithms presented in this thesis have been implemented in Matlab vR2010a.

Numerical experiments have been realized in a personal computer with an Intel(R) Core(TM) i3 CPU , 540 @ 3.07GHz, memory RAM of 4,00 GB and a 64-bits operative system.

All the computational costs mentioned in the numerical examples are referred to the previous system.

Resumen

En esta tesis estudiaremos algunos modelos empleados en la valoración de derivados financieros. En particular, usaremos dos clases de técnicas de valoración, Réplica e Indifference Pricing (valoración por equivalencia entre resultados esperados). Abordaremos el problema de valoración en tiempo real, el de valoración de opciones con tipos de interés variables y los de inversión óptima y valoración de opciones cuando existen costes de transacción. El diseño de técnicas numéricas apropiadas es imprescindible para la obtención de resultados.

Un derivado financiero es un contrato entre dos partes cuyo precio depende, o es obtenido, de un activo subyacente. Los subyacentes más habituales incluyen acciones, bonos, materias primas, moneda, tipos de interés e índices de mercados. Aunque la negociación moderna de derivados en mercados oficiales comienza en los años setenta, en el Chicago Board of Options Exchange, los derivados no son un producto de reciente creación. Sus orígenes se remontan a varios siglos antes como, por ejemplo, los futuros de arroz en el Dojima Rice Exchange.

Un ejemplo de derivado es la Opción Europea, que da al comprador el derecho de comprar una acción (u otro subyacente), en una fecha futura fija y a un precio preestablecido. Existen muchos otros tipos de derivados (Opción Americana, Bermuda, Barrera...), clasificados según el tipo de acuerdo que se establezca entre el comprador y el vendedor. En [38] se puede encontrar un amplio recopilatorio de muchos de ellos.

La valoración de derivados no es una tarea sencilla. El precio futuro de la acción suele ser impredecible, por eso modelizar la acción como un proceso estocástico es un buen punto de partida. En [3], [28], [41] y [52] se puede encontrar un desarrollo detallado del cálculo estocástico y su aplicación a las matemáticas financieras.

Una vez que hemos modelizado la dinámica de la acción, el siguiente paso es obtener un precio "justo" del derivado. Una oportudinad de arbitraje se define en [38] como una estrategia de inversión que, sin requerir aportaciones de capital, tiene una probabilidad positiva de dar beneficios sin riesgo alguno de pérdidas. El precio de una opción se dice "justo" cuando no existen oportunidades de arbitraje. Esta propiedad lleva a la estrategia de valoración por réplica.

En sus artículos iniciales, Fischer Black y Myron Scholes [4] y Robert Merton [49] dieron los pasos para, siguiendo una estrategia dinámica, constuir una (única) cartera, formada por la acción y el bono, que replica en todo momento el valor de la Opción Europea negociada sobre la acción. Como no pueden existir oportunidades de arbritraje, el precio del derivado y el de la cartera de réplica deben coincidir.

Aparte de un modo de calcular el precio de la opción, Black-Scholes obtuvieron una fórmula explícita que apenas tiene coste computacional. Esto fue algo que contribuyó a que se convertiera en un método muy popular, y probablemente el más utilizado, para valorar Opciones Europeas o estimar los parámetros de mercado, como por ejemplo, la volatilidad implícita de la acción. Esta fórmula suele estar integrada en la mayoría de las calculadoras financieras.

Desafortunadamente, el análisis de datos de las series históricas de precios de la acción no verifica todas las hipótesis del modelo de Black-Scholes, por lo que hicieron falta modelos más complejos que replicaran las propiedades observadas empíricamente. Estos nuevos modelos ajustan mucho mejor cuando se emplean para calibrar los parámetros del mercado y además cometen menores errores cuando se utilizan para predecir los precios de las opciones tras, por ejemplo, un cambio en la cotización de la acción. Como contrapartida, y por regla general, no disponemos de una fórmula explícita.

De hecho, incluso asumiendo que se verificaran las hipótesis del modelo de Black-Scholes, tampoco suele existir fórmula explícita para derivados más complejos que la Opción Europea.

Cuando se carece de una fórmula explícita, el precio de un derivado debe obtenerse mediante métodos numéricos. Como cabría esperar, estos métodos tienden a ser bastante costosos computacionalmente (varios segundos para calcular el precio de una opción). Aunque existen técnicas para reducir el coste (técnicas de reducción de varianza para métodos de Monte-Carlo, paralelización en varios ordenadores...), generalmente se requiere el acceso a bastante capacidad computacional para ser competitivos si se quiere aplicar modelos complejos a la negociación en tiempo real. Es este coste computacional la principal desventaja de los modelos complejos y la razón por la que el modelo de Black-Scholes sigue siendo tan popular, al menos para conseguir precios aproximados, especialmente cuando el acceso a grandes capacidades computacionales no es posible.

Los precios de las acciones (y por tanto el precio de las opciones) cambia casi continuamente. Solamente en el mercado español, se negocian simultaneamente Opciones Europeas para 35 acciones distintas con distintos precios de ejercicio y vencimientos. Podemos darnos cuenta del problema de valoración en tiempo real cuando hay multitud de mercados abiertos simultáneamente a lo largo del mundo. La minimización de coste computacional es una propiedad deseada (y necesaria) para los inversores.

Uno de los objetivos de esta tesis es diseñar un método numérico, suficientemente general para ser aplicado a cualquier modelo complejo o tipo de derivado, que sea capaz de valorar opciones o calibrar los parámetros del modelo de una o varias acciones diferentes simultáneamente. De hecho, también buscamos que el método pueda ser implementado en una calculadora o un ordenador personal. Esto es abordado en el Capítulo 1.

El objetivo principal de este trabajo no es estudiar la idoneidad de diferentes modelos en su ajuste a la dinámica de la acción, pero creemos que merece la pena estudiar el otro componente de la cartera de réplica en la Opción Europea: el bono. Existen muchos modelos que incorporan tipos de interés estocástico a la dinámica del bono pero, en particular si los vencimientos son pequeños, se suele asumir que el tipo de interés del bono es constante.

Si tratamos el tipo de interés del bono como otro parámetro que debe ser estimado de

los precios de las opciones, se puede observar que los valores obtenidos están estrechamente relacionados con los valores negociados en el mercado. No obstante, especialmente en periodos de alta volatilidad, aparecen serias discrepancias.

Parte de este trabajo (Capítulo 2) incluye un estudio sobre cómo los tipos de interés variables, deterministas o estocásticos, se pueden incorporar a los modelos. Veremos cómo un modelo discreto se puede extender para admitir tipos variables deterministas y las técnicas necesarias para conseguir un precio justo de la opción. También estudiaremos un modelo continuo con tipos de interés estocásticos. Partiendo del modelo de volatilidad estocástica de Heston [34], y siguiendo la propuesta incluída en el mismo artículo, incorporaremos un bono que, dependiendo del valor de los parámetros, puede ser determinista o admitir una componente estocástica. Obtendremos una fórmula explícita para el bono y una fórmula semi-explícita para la opción. También realizaremos una estimación de parámetros con datos reales de mercado.

Para finalizar la tesis, Capítulos 3 y 4, nos centraremos en modelos de valoración que, en vez de buscar un precio justo, siguen un enfoque ligeramente distinto. Una de las hipótesis realizadas por los economistas sobre el comportamiento social es el principio: "Cuanto más, mejor". Para modelizar esto, primero tenemos que definir una función de Utilidad adecuada (dos veces derivable, estrictamente creciente (mejor más que menos) y estrictamente cóncava (los inversores son aversos al riesgo). Existen multitud de funciones que verifican estas propiedades, y cuál de ellas se adecúa mejor al comportamiento social es algo que preferimos dejar a los economistas o sociólogos. Eso sí, señalamos que cada una de las funciones de Utilidad tiene sus ventajas e inconvenientes y además suelen requerir distinto tratamiento numérico.

Cuando queremos resolver un problema de Inversión Óptima, se elige una función de Utilidad e intentamos encontrar una estrategia de inversión admisible que maximize la utilidad esperada de la riqueza al vencimiento. La técnica de Indifference Pricing (valoración por equivalencia entre resultados esperados) surge de aquí.

El desarrollo teórico completo y distintas aplicaciones de la técnica de Indifference Pricing se puede encontrar en [12]. Para valorar opciones, el objetivo es, en lineas generales, construir dos escenarios. En el primero no se negocia ningún derivado y simplemente resolvemos un problema de Inversión Óptima. En el segundo, negociamos un derivado, recibiendo/pagando una cierta cantidad de dinero, y resolvemos de nuevo el problema de Inversión Óptima bajo estas nuevas condiciones. El precio del derivado será aquel que nos deje indiferentes entre elegir cualquiera de los dos escenarios porque los resultados esperados sean iguales.

Esta técnica de valoración es especialmente útil cuando el subyacente del derivado no es directamente observable o cuando la estrategia de réplica no es aplicable, por ejemplo, si existen costes de transacción.

Los métodos espectrales (ver [10]) son una clase de discretizaciones espaciales para ecuaciones en derivadas parciales que suelen ofrecer una convergencia muy rápida permitiéndonos, con pocos nodos, representar funciones con bastante precisión. Otro de los objetivos de esta tesis es, bajo un escenario con costes proporcionales de transacción, aplicar métodos espectrales a dos de las funciones de Utilidad más habituales: Potencial y Exponencial. Como hemos

comentado antes, cada función de Utilidad tiene distintos pros y contras. La primera de ellas no permite trabajar con riquezas negativas y la segunda, aunque sí lo hace, presenta problemas en los modelos log-normales, como se comenta en [12].

Propondremos dos métodos espectrales especialmente adaptados a los problemas numéricos de cada función de Utilidad. Trabajaremos en el problema de Inversión Óptima bajo Utilidad Potencial y con el problema de valoración de opciones bajo Utilidad Exponencial. En ambos casos, asumiremos que existen costes proporcionales de transacción.

El esquema de la tesis es el siguiente:

En el Capítulo 1 propondremos un método de Base reducida de Funciones para el problema de valoración en tiempo real. Bajo la idea de pagar coste computacional sólo una vez, en un primer paso construiremos un polinomio interpolador en varias variables que admite *valoración tensorial* (calcula precios de opciones para distintos valores de los parámetros simultáneamente) y es computacionalmente muy eficiente. Los polinomios interpoladores en varias variables sufren de la conocida "Maldición de la dimensionalidad", que dispara el costo de almacenaje del polinomio. En una segunda etapa, desarrollaremos un método de reducción de la dimensión de las bases empleadas que se aplicará al polinomio interpolador calculado previamente. Este enfoque reduce el impacto de la maldición, dando lugar a un polinomio cuyo coste de almacenamiento es bastante menor y sigue permitiendo una *valoración tensorial* muy eficiente. Los algoritmos son lo suficientemente generales para aplicarse a modelos de n variables o distintos tipos de opciones. También estudiaremos los resultados de esta técnica cuando la apliquemos a un modelo concreto (GARCH) con datos reales de mercado.

El Capítulo 2 está dedicado a la extensión de modelos incorporando tipos de interés variables. Presentaremos un modelo discreto GARCH con tipos de interés variables deterministas. Así mismo, propondremos una extensión del modelo de volatilidad estocástica de Heston con un bono que es capaz de incorporar una componente estocástica. Para el modelo discreto se probará la existencia, bajo unas ciertas hipótesis, de una medida libre de riesgo. Para el modelo continuo, se obtendrá una fórmula semiexplícita y se realizarán análisis con datos reales de mercado.

En el Capítulo 3, en un escenario con costes proporcionales de transacción, se desarrolla un método de colocación de Chebyshev con malla adaptativa para resolver el problema de Inversión Óptima bajo Utilidad Potencial. En este problema se pueden calcular varias fórmulas explícitas para ciertos casos particulares que, por tanto, se emplearán en el análisis del error del método numérico.

El Capítulo 4 está dedicado a la valoración de opciones con costes de transacción bajo utilidad Exponencial. Después de lidiar con los problemas numéricos asociados a la función de Utilidad Exponencial, llegaremos a una nueva EDP no lineal. Se propondrá un método de Fourier pseudoespectral para resolver el problema numéricamente y se probará la estabilidad y convergencia teórica del método. También se llevarán a cabo experimentos para estudiar el efecto en el precio de la opción al incorporar costes de transacción.

Preface

In this thesis, we study some models used in pricing financial derivatives. In particular, we will use two kinds of valuation techniques, Replication and Indifference Pricing. We will deal with the real-time valuation problem, option pricing with variable interest rates and optimal investment and option pricing when transaction costs are present. The analysis and design of appropriate numerical techniques will be necessary in this study.

A financial derivative is a contract between two parts, whose price is dependent upon, or derived from, one or more underlying assets. The most common underlying assets include stocks, bonds, commodities, currencies, interest rates and market indexes. Though modern trading of derivatives at organized markets starts at the Chicago Board of Options Exchange, back in the early Seventies, they are not a product of recent creation. Their origins trace back several centuries as, for example, *rice futures* on the Dojima Rice Exchange.

An example of a derivative is the European Call Option, which gives the buyer the right to buy a stock (or other asset), at a fixed future date and at a fixed price. There exist several other types of options (American, Bermuda, Barrier, ...), depending on the kind of agreement between the buyer and the seller and in [38], a full review of many of them is presented.

To value derivatives is not an easy task. Since the future price of the underlying stock is not usually predictable, to model the stock price as a stochastic process is a good starting point. In [3], [28], [41], and [52] a full development of stochastic calculus and its application to financial mathematics can be found.

Once we have modelled the dynamic of the stock, the next step would be to obtain a "fair" price for the derivative. An arbitrage opportunity is defined in [38] as a trading strategy that, requiring no cash input, has some probability of making profits without any risk of a loss. An option price is said to be fair when arbitrage opportunities are not possible. This property leads to the Replication valuation strategy.

In their seminal papers, Fischer Black and Myron Scholes [4] and Robert Merton [49], gave the steps for, following a dynamic strategy, build a (unique) replicating portfolio, formed with a stock and a bond, which mimics the European Option of the stock. Since no arbitrage possibilities must exist, the fair price of the derivative has to be the one of the portfolio.

Besides a way of pricing options, an explicit and no computational-time consuming formula for the European Option was also obtained in the Black-Scholes model. This was something that contributed to make it the most popular and widespread used method to valuate Eu-

ropean Options or estimate market parameters, like the *implied volatility* of the stock. This formula is usually implemented in most financial calculators.

Unfortunately, data analysis of stock's historical prices, does not support all the hypothesis of the Black-Scholes' model, and more complex models were derived to replicate observed stock's properties. These new models fit much better when used to estimate market parameters and commit smaller errors when used to predict traded option prices after, for example, a change in the stock's price. As a counterpart, an explicit formula is not usually available.

In general, other kinds of derivatives, even if we suppose that the underling asset fulfills Black-Scholes conditions, also lack of an explicit formula.

When we do not have an explicit formula, the price of a derivative has to be obtained by numerical methods. As it could be expected, these methods tend to be quite time-consuming (several seconds to obtain just one option price). Although there exist techniques to reduce the time cost (variance reduction techniques for Monte-Carlo based methods, parallelization in several computers ...) they usually require quite a big computational power in order to be competitive when applied to on-line trading. This time consuming issue is the principal drawback of complex models and one of the reasons why Black-Scholes is still so popular, at least for obtaining an indicative price, specially when access to big computational resources is not possible.

Stock prices (therefore option prices) change almost continuously. Just in the Spanish market, European Options for 35 different stocks, with several different strikes and maturities, are simultaneously traded. We can become aware of the real-time valuation problem when there are many markets worldwide opened at the same time. Minimization of computational cost is a very much desired (and needed) property for traders.

One of the objectives of this work is to design a numerical method, general enough to be applied with any complex models for stock's dynamics or option type, which would be able to price simultaneously options from several stocks and/or model parameters. Beyond, we want that the method could be used in just one single computer or calculator.

Though it is not the main scope of this work to make a performance analysis of several models, we believe that it is worthy to study a bit the other component of the replication portfolio in the European Option: the bond. Replication models that incorporate stochastic interest rates for the bond have been widely developed and used, but many times, when short maturities are involved, it is assumed that the interest rate of the bond remains constant.

If we treat the interest rate as another parameter that must be estimated from option prices, we can observe that the values obtained are closely related with the ones traded at the market, but sometimes, specially in high-volatility periods, serious discrepancies can appear.

Part of this work includes a review of how variable interest rates, deterministic and stochastic, can be incorporated to models. We will see how a discrete model can be extended to admit variable deterministic interest rates and the techniques needed to obtain a fair price.

A more complex continuous model with stochastic interest rates will also be derived. Using the proposed extension of Heston's Stochastic Volatility model [34], we will incorporate

a bond which, depending on the parameter values, can be deterministic or admit a stochastic component. An explicit formula for the bond and a semi-explicit formula for the option price will be derived and parameter estimation will be carried out with market traded option prices.

Finally, we will deal with pricing models that, instead of searching a fair price, have a slightly different point of view. One of the basic hypothesis of social behaviour made by economists is the principle: "The more we have, the happier we are". In order to model this, first we have to define a suitable Utility function (twice differentiable, strictly increasing (more is better than less) and strictly concave (investors are risk averse)). There are many functions that verify these conditions, and which one would be the best is a topic that we prefer to leave for economists or sociologists. Though, it should be pointed out that each of them will usually require a different numerical treatment.

When we want to solve the Optimal Investment problem, we pick an Utility function and try to find the admissible trading strategy that maximizes the expected utility of the terminal wealth. The Indifference Pricing technique is developed from here.

A very complete theoretical development and several applications of the Indifference Pricing techniques can be found in [12]. The basics of this technique in option pricing, broadly speaking, are the following: Two scenarios are built. In the first one, no derivative contract is signed and we just solve the Optimal Investment problem. In the second one, we sign a derivative, obtaining/paying a certain amount of money and then we solve again the Optimal Investment problem under this new condition. The derivative price will be the one which leaves us indifferent between both scenarios.

This kind of valuation technique is specially useful when the underlying asset of the derivative is not directly observable or when the replication strategy is not feasible, like in the case when transactions costs are present.

Spectral methods, see [10], are a class of spatial discretizations for differential equations which usually offer a very rapid convergence, enabling us to represent functions very precisely with relatively few nodes.

Other of the objectives of this thesis is, under a scenario where proportional transaction costs are present, to apply spectral methods to two of the probably most used Utility functions: Potential and Exponential. As it has been mentioned before, each Utility function has different numerical problems or shortcomings. The first one does not allow negative wealth and the second, though usually offers more tractable equations, gives problems in log-normal models as pointed in [12].

We will propose two spectral methods specifically adapted to the numerical problems of each Utility function. We will deal with the Optimal Investment problem under Potential Utility and with the Option Pricing problem under Exponential Utility. In both cases, it is assumed that proportional transaction costs exist.

The outline of the thesis is as follows:

In Chapter 1 we will propose a Reduced Bases functions method for the real-time valuation problem. Under the idea of paying computational cost just once, in a first step we will construct an interpolant polynomial in several variables that admits *tensorial valuation* (computes option prices for several parameter values simultaneously) and it is computationally very efficient. Interpolant polynomials of models with several parameters suffer of the so called "Curse of dimensionality", which blows their storage cost. In a second step, a Reduced Bases function approach, designed and applied to the previous polynomial is presented. This approach will drastically reduce the impact of the mentioned curse, obtaining a low-storage and fast multiple-evaluation polynomial. The algorithms are described so that they can be applied to n-variable models and option types. Analysis of performance with a particular model (GARCH) and real market prices will also be presented.

Chapter 2 is devoted to model extension incorporating variable interest rates. We will present a discrete GARCH model with deterministic variable interest rates and an extension of Heston's SV model with a bond that is able to incorporate a stochastic component. The existence, under certain hypothesis, of a risk free measure for the discrete model is proved and the stock's dynamics is computed. For the continuous model, a semi-explicit formula is obtained and analysis with market data are carried out.

In Chapter 3, in a scenario with proportional transaction costs, a mesh-adaptative Chebyshev collocation method is developed to numerically solve the Optimal Investment problem under Potential Utility. Explicit analytical formulas can be obtained for certain interesting cases. Consequently, they are employed in the analysis of the numerical error of the method.

Chapter 4 is dedicated to Option Pricing with transaction costs under Exponential Utility. After dealing with the numerical problems associated to the Exponential Utility function, a new non-linear PDE is obtained and a Fourier pseudospectral method is proposed to numerically solve it. Theoretical stability and convergence of the method is proved. We also carry out numerical experiments to test the effects in the option price of incorporating transaction costs.

Chapter 1

Reduced Bases Function Approach to Option Valuation

1.1 Introduction to Option Valuation

An European Call Option is a financial instrument that gives the buyer the right, but not the obligation, to buy a stock or asset, at a fixed future date (maturity), and at a fixed price (strike or exercise price). The seller will have the obligation, if the buyer exercises his/her right, to sell the stock at the exercise price.

The buyer of the option will only exercise his/her right only if, at maturity (t_M), the market price of the asset ($\bar{S}(t_M)$) is higher than the strike (K) (this is referred as the option is "In the Money"). If the strike is higher than the market price ("Out of the Money"), the buyer will not exercise his/her right, since it would be cheaper to buy the asset directly in the market.

In the famous papers of Fischer Black and Myron Scholes [4] and Robert Merton [49], a fair price for the European Option was obtained. Assuming that the behaviour of the dynamics of the stock in the physical space P is given by:

$$d\bar{S}(t) = \mu\bar{S}(t)dt + \sigma\bar{S}(t)d\bar{z}(t), \tag{1.1}$$

where $\bar{z}(t)$ denotes the standard Brownian motion, and that a bond B exists,

$$dB(t) = rB(t)dt, \tag{1.2}$$

a replicating portfolio which mimics the option can be constructed buying and selling continuously both the stock and bond.

Since no arbitrage opportunities can exist, at any moment prior to maturity, the value of the option must coincide with the value of the portfolio, hence the valuation problem is solved.

Mathematically, this strategy is analogous to obtain the existence and uniqueness of an equivalent Risk-free measure Q, for which the dynamics of the stock is given by:

$$d\bar{S}(t) = r\bar{S}(t)dt + \sigma\bar{S}(t)d\bar{z}^Q(t), \tag{1.3}$$

where $\bar{z}^Q(t)$ is the standard Brownian motion with respect measure Q and where the option price is obtained as the discounted value of the expected future value of the contract at maturity. Formally,

$$C(S) = e^{-r(t_M - t)}\mathbb{E}^Q\left[\max\{\bar{S}(t_M) - K, 0\}\middle|\, \bar{S}(t) = S\right] \tag{1.4}$$

where $\mathbb{E}^Q$ denotes the conditional expectation at time t.

Besides a way of pricing options, an explicit and no computational-time consuming formula for the previous expression was obtained in the Black-Scholes model. The formula and its proof can be found, for example, in [4] or [38].

Data analysis of stock's historical prices show that not all the hypothesis of Black-Scholes' model hold. For example, volatility (σ) is assumed constant when, in fact, market data do not support this assertion. Even if we estimate today's volatility from traded options prices, different values for different maturities are obtained. A phenomena known as the "volatility smile".

More complex models, built to match the stock's observed dynamics and new fair prices for them ought to be obtained. These new models achieve better results both in pricing options and parameter estimation, but are much more time-consuming because they usually lack of an explicit formula. Furthermore, even if easy dynamics models are employed to price complex contracts, like the American Option (the right can be exercised any time prior to maturity), we also lack of an explicit formula.

Though it will be explained later, we point out that one way of doing estimation is through a least-square search of the error between theoretical and market traded option prices. Thus, obtaining option prices and the derivatives of the pricing function with respect to the variables that correspond to the model parameters are the principal problems we are facing in the real-time option valuation or model calibration.

The objective of this Chapter is, fixed a complex model for the stock's dynamics, to develop a fast numerical method able to price simultaneously options from several stocks and/or several model parameters. Furthermore, we want that the method can be used in just one single computer or calculator. Thus, there are three mutually related problems that must be handled: velocity, precision and storage cost.

Our first priority is to solve the velocity problem. In Section 1.3, a fast tensorial Chebyshev polynomial interpolation is developed. As expected with polynomial interpolation, the precision problem can be solved increasing the number of interpolation points. This leaves us with the third and last problem: storage-cost, commonly referred as "The Curse of Dimensionality".

This curse is drastically reduced in Section 1.4, where, focusing on retaining the solution of the velocity problem, a Reduced Bases Approximation method is constructed upon the polynomial obtained in Section 1.3. The result will be a low storage cost polynomial which is able to price options (or calibrate model parameters) very fast for several stocks at the same time.

The method is general enough to apply it with different models for stock dynamics or option types (most of other option types lack of an explicit formula either). In particular, we will test it for the NGARCH(1,1) model, which has 8 parameters, and use it to price S&P500 European Options. A brief introduction to GARCH models is done in Section 1.2 and numerical results with real market data are presented in Section 1.5.

1.2 GARCH Models.

As it has been mentioned before, market data do not satisfy, among others, the hypothesis of constant volatility in the Black-Scholes model. Furthermore, non-constant volatility is not the only empirical property observed. Others are:

(i) Thick tales: asset returns tend to be leptokurtic, i.e., the kurtosis value is large.

(ii) Volatility clustering: large changes tend to be followed by large changes and small changes tend to be followed by small changes.

(iii) Leverage effects: there is a tendency for changes in stock prices to be negatively correlated with changes in stock volatility.

(iv) Non-trading periods: information accumulates while markets are closed.

(v) Forecastable events: for example, volatility tends to be higher around earnings report dates.

ARCH models (AutoRegressive Conditional Heterodastic) introduced by Engle in [29] are a kind of stochastic processes in which recent past gives information about future variance. Several ARCH models have been proposed along the years, trying to capture some of the market properties.

In [7], a complete review of several ARCH models is presented. In that paper, the authors list a number of conditions that guarantee that the models are well defined. Also, the authors study the market properties that each model is able to capture and reference articles where these desirable properties are contrasted with empirical results.

Let $\{\bar{\epsilon}_t(\theta)\}_{t=0,1,\dots}$ denote a discrete time stochastic process with conditional mean and variance functions parametrized by the finite dimensional vector $\theta \in \Theta \subseteq \Re^m$. θ_0 will denote the parameters value, a priori unknown, that has to be estimated from the available market data.

Let $E_{t-1}(.)$ denote the mathematical expectation, conditional on the past, of the process, along with any other information available at time $t-1$. We say that the process $\{\bar{\epsilon}_t(\theta_0)\}$ follows an ARCH model if the conditional mean is zero

$$E_{t-1}(\bar{\epsilon}_t(\theta_0)) = 0, \quad t = 1, 2, ..., \tag{1.5}$$

and the conditional variance,

$$\sigma_t^2(\theta_0) \equiv Var_{t-1}(\bar{\epsilon}_t(\theta_0)) = E_{t-1}(\bar{\epsilon}_t^2(\theta_0)), \quad t = 1, 2, ..., \tag{1.6}$$

depends non-trivially on the σ-field generated by past observations $\{\bar{\epsilon}_{t-1}(\theta_0), \bar{\epsilon}_{t-2}(\theta_0), ...\}$.

Engle's first model was ARCH(q):

$$\sigma_t^2 = \omega + \sum_{i=1}^{q} \alpha_i \bar{\epsilon}_{t-i}^2, \tag{1.7}$$

where ω and $\{\alpha_i\}_{i=1}^q$ are the model parameters.

A more general type of models is the class GARCH(p, q) (Generalized ARCH), developed by Bollerslev in [6]. They are defined by:

$$\sigma_t^2 = \omega + \sum_{i=1}^{q} \alpha_i \bar{\epsilon}_{t-i}^2 + \sum_{j=1}^{p} \beta_j \sigma_{t-j}^2. \tag{1.8}$$

ARCH models must satisfy certain conditions in order to be well defined. For example, for model GARCH(p, q):

1. $\omega, \alpha_i, \beta_i \geq 0$ implies $\sigma_t^2 \geq 0$.
2. $\sum \alpha_i + \sum \beta_j < 1$ implies $E_{t-1}(\sigma_t^2) < \infty$.

GARCH models are suitable to capture thick tailed returns and volatility clustering, but are not directly suited to capture leverage effects, since the conditional variance depends just on the size of the lagged residuals but not on their sign.

Another model used in the literature is the Non-lineal ARCH, derived by Higgins and Vera in [36],

$$\sigma_t^\gamma = \omega + \sum_{i=1}^{q} \alpha_i \left|\bar{\epsilon}_{t-i}\right|^\gamma + \sum_{j=1}^{p} \beta_j \sigma_{t-j}^\gamma, \tag{1.9}$$

which can be slightly modified

$$\sigma_t^\gamma = \omega + \sum_{i=1}^{q} \alpha_i \left|\bar{\epsilon}_{t-i} - \kappa\right|^\gamma + \sum_{j=1}^{p} \beta_j \sigma_{t-j}^\gamma, \tag{1.10}$$

allowing now to capture leverage effect, since σ_t^γ depends both on the size and the sign of the lagged residuals.

It should be remarked now that all these models are broadly used in option valuation. [9], [26], [33], [54] and [59] are just a few examples where option prices are obtained through GARCH models.

Once we have chosen one particular GARCH specification, we have to calibrate or estimate the value of the parameters from market data. The two most common ways to calibrate the model are with respect to the stock prices or with respect to the option prices.

We must point out that the values obtained from both procedures usually do not match, existing a small gap between them. Any chosen GARCH specification probably will not incorporate all the information about the stock dynamics and options will be mispriced. If the main objective is option valuation, better results will be obtained calibrating directly from option prices.

In the first estimation procedure, a maximum likelihood estimator (see [60]) is employed in order to find the model parameters that have the best fit to the historical series of the stock price.

In the second one, we search the parameters that minimize the mean square error between the prices of a set of traded option contracts and the theoretical prices obtained by the model for the same contracts (see [13]).

We remark that even if we use the first technique and some models achieve a better theoretical fit, the may work worse than others when used to price traded options in the market. We refer to [13], [14] and references therein for a study of this phenomena.

Since our objective is option valuation, when estimating parameters, we will follow the minimization of the mean square error approach for the rest of Chapters 1 and 2. We will explain this technique in detail when we carry out a performance comparison between Black-Scholes and GARCH models.

In [13], a study of the performance of several GARCH models, following the two ways of model calibration mentioned above, is carried out. In this thesis, we have chosen one of the models that gave best results. This one will be referred as NGARCH(1,1), and it will be used for the rest of the Chapter.

This model is defined in the physical probability P by:

$$\begin{cases} \ln\left(\dfrac{\bar{S}_t}{\bar{S}_{t-1}}\right) \equiv \bar{R}_t = r + \lambda\sqrt{\sigma_t^2} - \dfrac{1}{2}\sigma_t^2 + \sqrt{\sigma_t^2}\bar{z}_t, \\ \sigma_t^2 = \beta_0 + \beta_1\sigma_{t-1}^2 + \beta_2\sigma_{t-1}^2(\bar{z}_{t-1} - \theta)^2, \end{cases} \tag{1.11}$$

where

(i) $\bar{S}_t$: denotes the stock price at date t.

(ii) σ_t^2: is the variance of the stock at date t.

(iii) r: is the risk-free rate.

(iv) $\beta_0,\ \beta_1,\ \beta_2,\ \lambda,\ \theta$: are the GARCH model parameters.

(v) $\bar{z}_t$ is a normally distributed random variable with mean 0 and variance 1.

For pricing options, we need to obtain the existence and uniqueness of a Risk-free measure Q that allows us, avoiding any arbitrage opportunity, to obtain today's option price as the discounted (at the risk-free rate) expectation of the future value. This has been done, with different arguments, both in [24] and in [40].

The dynamics of the stock in the new measure Q must be computed. Two different ways of analysis are presented in [24], [40]. We will go deeply in these results later in Chapter 2. Now, we directly move to the solution. The dynamics in the Risk-free measure Q is given by:

$$\begin{cases} \ln\left(\dfrac{\bar{S}_t}{\bar{S}_{t-1}}\right) \equiv \bar{R}_t = r - \dfrac{1}{2}\sigma_t^2 + \sqrt{\sigma_t^2}\bar{z}_t^Q, \\ \qquad\qquad \sigma_t^2 = \beta_0 + \beta_1\sigma_{t-1}^2 + \beta_2\sigma_{t-1}^2(\bar{z}_{t-1} - (\theta+\lambda))^2, \end{cases} \tag{1.12}$$

where $\bar{z}_t^Q$ is a normally distributed random variable with mean 0 and variance 1.

The dynamics in the Risk-free measure allow us to compute the option price as:

$$C(S) = e^{-r(t_M - t)}\mathbb{E}^Q\left[\max\{\bar{S}_{t_M} - K, 0\}|\bar{S}_t = S\right]. \tag{1.13}$$

For this model, there is no known closed form solution and several numerical methods can be employed, being Monte-Carlo based methods ([25], [59]), Lattice methods ([46], [54]), Finite Elements ([1]) or Spectral methods ([9]) some of them.

This Section finishes with a performance comparison between the Black-Scholes pricing model and the NGARCH(1,1) as a justification of the employment of this kind of models in option valuation.

1.2.1 In The Sample / Out The Sample analysis

We are going to carry out two kind of analysis with real market data (S&P500) following the lines developed in [13].

For the In The Sample daily analysis, we first fix a date t_0 and consider the set of all European Call contracts traded along that day. Let

(i) N_{t_0} denote the amount of contracts negotiated on day t_0.

(ii) $C_{t_0}^i$ denote the market price of contract i.

(iii) $C_i(S^i_{t_0}, t_{Mi}, K_i)$ denote the model's price (Black-Scholes or NGARCH(1,1)) of contract i.

(iv) r_{t_0} be the constant risk-free rate corresponding to the 3-months US bond negotiated on day t_0.

For simplicity reasons, we assume that for each t_0, the rate r_{t_0} is the constant interest rate r employed in the valuation formulas (1.12)-(1.13) or in the Black-Scholes explicit formula.

Our objective, for the In The Sample analysis (In), is to find, for each day t_0, the parameter values:

a) σ^2 for Black-Scholes.

b) $\{\sigma^2_{t_0}, \beta_0, \beta_1, \beta_2, (\lambda + \theta)\}$ for NGARCH(1,1).

that give the minimum mean square error (MSE) between the theoretical option prices and the traded ones. Therefore, our objective is to find, for each day t_0, the parameter values that minimize the function

$$\text{InMSE}(t_0) = \frac{1}{N_{t_0}} \sum_{i=1}^{N_{t_0}} \left(C^i_{t_0} - C_i(S^i_{t_0}, t_{Mi}, K_i)\right)^2. \tag{1.14}$$

The results plotted on Figure 1.1 are the square root of InMSE, which represent the daily error, in monetary terms, for all Wednesdays (or the closest day if the market was closed) between 12-26-1991 and 12-30-92 (54 days). We plot each negotiation day t_0 (horizontal axis) versus the root of InMSE (vertical axis) of Black-Scholes(blue) and NGARCH(1,1)(red).

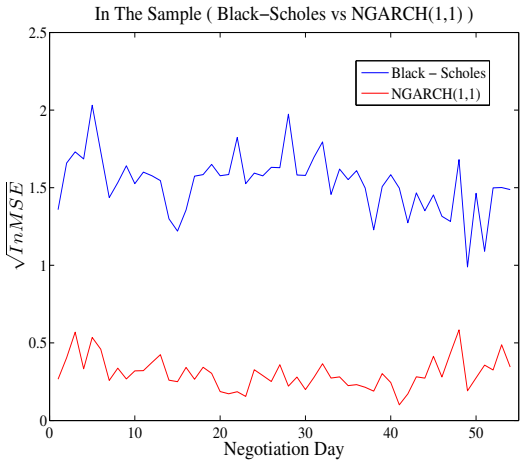

Figure 1.1: Error, in monetary terms, of the In The Sample analysis.

The mean values of the root of InMSE along the 54 days are 1.53 and 0.30 for Black-Scholes and NGARCH(1,1) respectively.

While this result represents a great improvement, it is not so surprising since in the Black-Scholes model we only have one degree of freedom (σ^2) while in NGARCH(1,1) we have five ($\sigma_{t_0}^2,\ \beta_0,\ \beta_1,\ \beta_2,\ (\lambda+\theta)$). More remarkable is the following result.

For the Out The Sample analysis (Out), we want to study how both models predict contract prices before the market opens. The procedure is the following:

1. Fix a date (t_0) and estimate the model parameter values for the contracts negotiated in the market a week ago (t_0-7).

2. Compute the theoretical prices of the contracts of day t_0 with the parameters obtained in t_0-7, all the information available between $[t_0-7,\ t_0]$ and the allowances of the model.

3. Compare the results with the real market prices of day t_0.

Since the Black-Scholes model assumes constant variance, in Step 2, we have to compute contract prices on day t_0 with the variance obtained on day t_0-7.

On the other hand, the NGARCH(1,1) model allows us to update the variance. If we know the S&P500 movements between $[t_0-7, t_0]$, using the model equations (1.12) we can obtain a volatility updating formula

$$\begin{cases} \hat{\sigma}_j^2 = \beta_0 + \beta_1\hat{\sigma}_{j-1}^2 + \beta_2\hat{\sigma}_{j-1}^2\left(\left[\dfrac{\left(\bar{R}_j - r + \frac{\hat{\sigma}_{j-1}^2}{2}\right)}{\sqrt{\hat{\sigma}_{j-1}^2}}\right] - (\lambda+\theta)\right)^2, \quad j = t_0-6, t_0-5, ..., t_0, \\ \hat{\sigma}_{t_0-7}^2 = \sigma_{t_0-7}^2, \end{cases} \tag{1.15}$$

where $\{\sigma_{t_0-7}^2, \beta_0, \beta_1, \beta_2, (\lambda+\theta)\}$ are the parameters estimated on date t_0-7 and $\bar{R}_j = \ln\left(\frac{\bar{S}_j}{\bar{S}_{j-1}}\right)$ are obtained from market data. We refer to [13] where this, and others, estimation procedures are described.

Concerning the risk-free rate r, and for simplicity reasons, we employ $r = r_{t_0-7}$ for the updating formula. We could have employed a variable interest rate in the updating formula, but this is postponed to Chapter 2. Within the time periods involved (1 week), the movements of the stock are much more relevant than the movements of the risk free rate.

Thus, an estimation of today's variance $\tilde{\sigma}_{t_0}$ is obtained: $\hat{\sigma}_{t_0}^2$ for the NGARCH(1,1) model and σ^2 of t_0-7 for the Black-Scholes model.

If N_{t_0} denotes the amount of contracts negotiated on day t_0, let $i \in \{1,\ 2,\ ...,\ N_{t_0}\}$. The option prices of day t_0 are computed with formula

$$C_i(S_{t_0}^i, t_{Mi}, K_i, \tilde{\sigma}_{t_0}^2),$$

where, for NGARCH(1,1), the values of the parameters $\{\beta_0, \beta_1, \beta_2, (\lambda + \theta)\}$ are those of date $t_0 - 7$.

If we want to know how well we have predicted option prices, we compare the results obtained with the traded prices computing the mean square error.

$$\text{OutMSE}(t_0) = \frac{1}{N_{t_0}} \sum_{i=1}^{N_{t_0}} \left(C^i_{t_0} - C_i(S^i_{t_0}, t_{Mi}, K_i, \bar{\sigma}^2_{t_0}) \right)^2 . \tag{1.16}$$

The results plotted on Figure 1.2 show the root of OutMSE, which represents the error, in monetary terms, when prices are predicted with both models for all Wednesdays between 2-01-1992 and 12-30-92 (53 days). We plot each negotiation day t_0 (horizontal axis) versus the root of OutMSE (vertical axis) of Black-Scholes(blue) and NGARCH(1,1)(red).

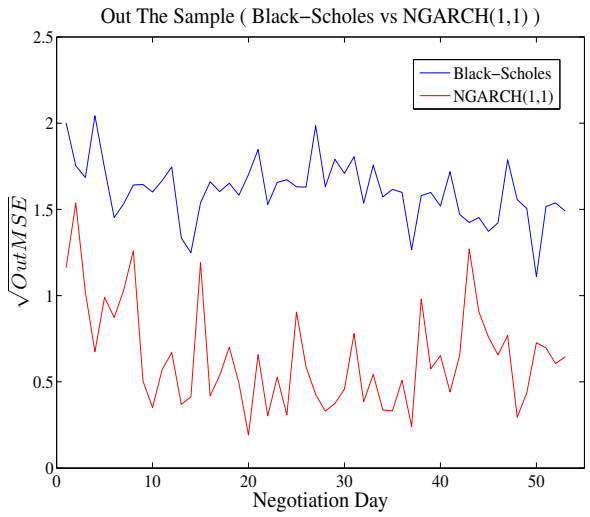

Figure 1.2: Error in monetary terms of the Out The Sample analysis.

The mean values of the square root of OutMSE are 1.60 and 0.64 for the Black-Scholes model and NGARCH(1,1) respectively.

In conclusion: GARCH models are better when used to fit to market data and, more relevant, they are also capable to incorporate changes in the stock market to option prices.

The principal drawback of GARCH models is their computational cost. It will depend on the numerical method employed, but all the ones mentioned (Monte-Carlo, Lattice, Spectral...) require several seconds to compute option prices and several minutes to estimate parameter values. This can result in an unpractical procedure, since option prices change almost continuously. The objective of the following Section is to design a numerical method that drastically reduces the computing time associated with the valuation of option prices with GARCH models.

1.3 Polynomial Interpolation

What we propose here is a Chebyshev polynomial interpolation procedure for option valuation with GARCH (or other) models.

Stock price changes almost constantly, so option prices must be continuously updated. The properties of Chebyshev polynomials (see [55]) enables us to use time-competitive and accurate enough techniques for computing polynomial coefficients, evaluation and differentiation.

Furthermore, many stocks from different companies are traded simultaneously. Several options, for different prices, maturities, possibly with different model parameter values, must be priced at the same time, what from now on will be referred as *tensorial valuation*. This will be achieved through a suitable defined multidimensional array operation and the employment of efficient algorithms.

The interpolation will be done using Chebyshev polynomials and nodes in the interval where the parameters are defined.

Definition 1.3.1. *Let us define*

$$T_n(x) = \cos\left(n \arccos(x)\right), \tag{1.17}$$

where $0 \leq \arccos(x) \leq \pi$.

It is well known (see [55]) that this function is a polynomial of degree n*, called the Chebyshev polynomial of degree* n.

Through the whole thesis, $T_n(x)$ will denote the Chebyshev polynomial of degree n.

Definition 1.3.2. *Let* $N \in \mathbb{N}$. *The* $N+1$ *Chebyshev nodes* $\{\tilde{\alpha}^k\}_{k=0}^N$ *in interval* $[a,\ b]$ *correspond to the extrema of* $T_n(x)$ *and they are given by:*

$$\tilde{\alpha}^k = \frac{1}{2}\left[\cos\left(\frac{\pi k}{N}\right)(b-a) + (b+a)\right], \quad k = 0, 1, ..., N. \tag{1.18}$$

We also define the $N+1$ *Chebyshev nodes* $\{\alpha^k\}_{k=0}^N$ *in interval* $[-1, 1]$*, where*

$$\alpha^k = \cos\left(\frac{\pi k}{N}\right), \quad k = 0, 1, ..., N. \tag{1.19}$$

Definition 1.3.3. *Let* $\tilde{F}(\tilde{x})$ *be a continuous function defined in* $\tilde{x} \in [\tilde{x}^{\min},\ \tilde{x}^{\max}]$.

We define the function $F(x),\ x \in [-1, 1]$ *as*

$$F(x) = \tilde{F}(\tilde{x}),$$

where

$$\tilde{x} = \frac{\tilde{x}^{\max} - \tilde{x}^{\min}}{2}x + \frac{\tilde{x}^{\max} + \tilde{x}^{\min}}{2}, \quad x \in [-1,\ 1]. \tag{1.20}$$

For $N \in \mathbb{N}$, let $I_N F(x)$ be the N degree interpolant of function $F(x)$ at the Chebyshev nodes $\{\alpha^k\}_{k=0}^N$, i.e. the polynomial which satisfies

$$I_N F(\alpha_k) = F(\alpha_k) = \tilde{F}(\tilde{\alpha}_k), \quad k = 0, 1, ..., N.$$

Polynomial $I_N F(x)$ will be given by

$$I_N F(x) = \sum_{l=0}^{N_1} \hat{p}_l T_l(x), \quad x \in [-1, 1], \tag{1.21}$$

where $\hat{p}_l \in \mathbb{R}$.

Here we present just the definitions that will be needed for the proposed method. The practical computation of the coefficients $\hat{p}_l$ is postponed to Subsection 1.3.1.

Definition 1.3.4. *Let $\tilde{\boldsymbol{x}} = (\tilde{x}_1, \tilde{x}_2, ..., \tilde{x}_n)$ and $\tilde{F}(\tilde{\boldsymbol{x}})$ be a continuous function defined in*

$$\tilde{x}_j \in [\tilde{x}_j^{\min},\ \tilde{x}_j^{\max}], \quad j = 1, 2, ..., n. \tag{1.22}$$

For $\boldsymbol{x} = (x_1, x_2, ..., x_n)$, we define the function $F(\boldsymbol{x})$, $\boldsymbol{x} \in [-1, 1]^n$ as

$$F(\boldsymbol{x}) = \tilde{F}(\tilde{\boldsymbol{x}}),$$

where

$$\tilde{x}_j = \frac{\tilde{x}_j^{\max} - \tilde{x}_j^{\min}}{2} x_j + \frac{\tilde{x}_j^{\max} + \tilde{x}_j^{\min}}{2}, \quad \begin{cases} x_j \in [-1,\ 1], \\ j = 1, 2, ..., n. \end{cases} \tag{1.23}$$

For $\boldsymbol{N} = \{N_1, N_2, ..., N_n\} \in \mathbb{N}^n$, we define

$$L^{\boldsymbol{N}} = \{\boldsymbol{l} = (l_1, l_2, ..., l_n) \ / \ 0 \leq l_j \leq N_j,\ j = 1, 2, ..., n\}. \tag{1.24}$$

For $j = 1, 2, ..., n$, let $\left\{\tilde{\alpha}_j^k\right\}_{k=0}^{N_j}$ be the $N_j + 1$ Chebyshev nodes in $[\tilde{x}_j^{\min},\ \tilde{x}_j^{\max}]$ and $\left\{\alpha_j^k\right\}_{k=0}^{N_j}$ be the $N_j + 1$ Chebyshev nodes in $[-1,\ 1]$.

We use the notation $\tilde{\boldsymbol{\alpha}}^{\boldsymbol{l}} = \left(\tilde{\alpha}_1^{l_1}, \tilde{\alpha}_2^{l_2}, ..., \tilde{\alpha}_n^{l_n}\right)$ and $\boldsymbol{\alpha}^{\boldsymbol{l}} = \left(\alpha_1^{l_1},\ \alpha_2^{l_2}, ..., \alpha_n^{l_n}\right)$.

Let $I_{\boldsymbol{N}} F(\boldsymbol{x})$ be the n-dimensional interpolant of function $F(\boldsymbol{x})$ at the Chebyshev nodes $\left\{\boldsymbol{\alpha}^{\boldsymbol{l}}\right\}_{\boldsymbol{l} \in L^{\boldsymbol{N}}}$, i.e. the polynomial which satisfies

$$I_{\boldsymbol{N}} F(\boldsymbol{\alpha}^{\boldsymbol{l}}) = F(\boldsymbol{\alpha}^{\boldsymbol{l}}) = \tilde{F}(\tilde{\boldsymbol{\alpha}}^{\boldsymbol{l}}), \quad \boldsymbol{l} \in L^{\boldsymbol{N}}.$$

Polynomial $I_{\boldsymbol{N}} F(\boldsymbol{x})$ will be given by

$$I_{\boldsymbol{N}} F(\boldsymbol{x}) = \sum_{\boldsymbol{l} \in L^{\boldsymbol{N}}} \hat{p}_{\boldsymbol{l}} T^{\boldsymbol{l}}(\boldsymbol{x}), \quad \boldsymbol{x} \in [-1, 1]^n, \tag{1.25}$$

where

$$\hat{p}_{\boldsymbol{l}} = \hat{p}_{(l_1, l_2, ..., l_n)} \in \mathbb{R},$$
$$T^{\boldsymbol{l}}(\boldsymbol{x}) = T_{l_1}(x_1) T_{l_2}(x_2) ... T_{l_n}(x_n).$$

The function we want to interpolate is the one which gives the option price of a stock whose dynamics are given by the NGARCH(1,1) model. Recall that in the Risk-free measure Q, this price was given by

$$C(S) = e^{-r(t_M - t)}\mathbb{E}^Q[\max\{\bar{S}_{t_M} - K, 0\}|S_t = S],$$

where the dynamics of the stock was modelled by

$$\begin{cases} \ln\left(\dfrac{\bar{S}_t}{\bar{S}_{t-1}}\right) \equiv \bar{R}_t = r - \dfrac{1}{2}\sigma_t^2 + \sqrt{\sigma_t^2}\bar{z}_t \\ \qquad\qquad \sigma_t^2 = \beta_0 + \beta_1\sigma_{t-1}^2 + \beta_2\sigma_{t-1}^2(\bar{z}_{t-1} - (\theta + \lambda))^2. \end{cases}$$

and

(i) t_M: is the maturity date of the contract.

(ii) σ_t^2: is the variance of the stock at date t.

(iii) $\bar{S}_t$: denotes the stock price at date t.

(iv) r: is the risk-free rate.

(v) $\beta_0,\ \beta_1,\ \beta_2,\ (\lambda + \theta)$: are the Garch model parameters.

Let today be $t = 0$ and S_0, σ_0^2 denote today's stock price and variance respectively. Since the pricing model is linear in the relation $\frac{S}{K}$, the strike of the option does not need to be included. We can fix it for $K = K_0$ and option prices for other strikes can be directly obtained by interpolation.

Therefore, the option price is a function of 8 real variables:

$$\tilde{F}\left(t_M, \sigma_0^2, S_0, r, \beta_0, \beta_1, \beta_2, (\lambda + \theta)\right) = \tilde{F}(\tilde{\mathbf{x}}), \tag{1.26}$$

where, in order to simplify the notation, we write

$$\tilde{\mathbf{x}} = [\tilde{x}_1, \tilde{x}_2, \tilde{x}_3, \tilde{x}_4, \tilde{x}_5, \tilde{x}_6, \tilde{x}_7, \tilde{x}_8] = [t_M, \sigma_0^2, S_0, r, \beta_0, \beta_1, \beta_2, (\lambda + \theta)].$$

We restrict to a bounded domain

$$\tilde{\Omega} = [\tilde{x}_1^{\min},\ \tilde{x}_1^{\max}] \times [\tilde{x}_2^{\min},\ \tilde{x}_2^{\max}] \times ... \times [\tilde{x}_8^{\min},\ \tilde{x}_8^{\max}], \tag{1.27}$$

where we can compute the 8-dimensional interpolant $I_{\boldsymbol{N}}F(\mathbf{x})$ as it has been given in Definition 1.3.4

We remark that the number of variables depends on the chosen GARCH specification. Although we are dealing with the NGARCH(1,1) model, all the following algorithms will be described for a function of n variables.

In the numerical examples, we will return to the original notation of the specific NGARCH(1,1) model and specify the values of the respective domains where the variables are defined.

Now we proceed to outline the main ideas of the proposed numerical method.

Polynomial Interpolation Strategy:
The procedure has two different steps that we next describe.

First step: Off line computation.

This step is called *Off line computation* because it corresponds to the construction of the interpolant of a function (an option pricing function in our case) and it has to be done just once.

When the polynomial has been built, we can employ it as many times as we want and whenever we want in order to price options in the market. We do not need to repeat this first step again.

Suppose that $\tilde{F}(\tilde{\mathbf{x}})$ is a n variable function as the one given in Definition 1.3.4. The degree of the interpolant is denoted by $\mathbf{N} = (N_1, ..., N_n) \in \mathbb{N}^n$.
$N_j + 1,\ j = 1, ..., N$ states the number of interpolation points (Chebyshev nodes in this case) for the interval $[\tilde{x}_j^{\min},\ \tilde{x}_j^{\max}],\ j = 1, ..., n$ of each of the variables. In the numerical examples we will state how to pick the intervals and study the behaviour of the interpolation error.

Once fixed $\mathbf{N}$, in order to construct the interpolant we will need to compute

$$\tilde{F}\left(\tilde{\alpha}_1^{k_1}, \tilde{\alpha}_2^{k_2}, ..., \tilde{\alpha}_n^{k_n}\right), \quad \begin{cases} \forall k_j \in \{0, ..., N_j\}, \\ j = 1, 2, ..., n, \end{cases}$$

where the $\tilde{\alpha}_j^{k_j}$ are the Chebyshev nodes from Definition 1.3.4. If $\tilde{F}(\tilde{\mathbf{x}})$ is an option pricing function, this can be done by means of one of the mentioned numerical methods (Monte Carlo, Lattice, Spectral ...).

In this thesis, the numerical method employed for computing the option prices in the Chebyshev nodes will be the spectral method developed in [9] and will be referred as B-F method. This numerical method gives enough precision with few grid points, and the employment of FFT techniques makes it a low-time consuming method. Besides, fixed a maturity t_M, it is implemented in a way that computes option prices for several stock prices, volatilities and all discrete maturities between $[0,\ t_M]$ at the same time.

Finally, with the function evaluated at the Chebyshev nodes, we build the interpolant

$$I_{\boldsymbol{N}} F(\mathbf{x}) = \sum_{\boldsymbol{l} \in L^{\boldsymbol{N}}} \hat{p}_{\boldsymbol{l}} T^{\boldsymbol{l}}(\mathbf{x}), \quad \mathbf{x} \in [-1, 1]^n,$$

with the Algorithm CnV described in Subsection 1.3.1. We remark that the interpolant has to be computed just once and it can be employed as many times as we want.

Second step: In line computation

This second step is called *In line computation* because we employ the polynomial built in the previous step to price contracts or calibrate model parameters from market data on real time.

As we mentioned before, several options for different asset prices, maturities and possibly with different model parameter values must be priced at the same time. Furthermore, the asset prices (upon the options are negotiated) change almost continuously while the markets are opened.

This means that, almost constantly, we will need to price options for a finite set of values $\mathbf{\Theta} \in \tilde{\Omega}$, such that for $q_j \in \mathbb{N},\ 1 \leq j \leq n$, we have that

$$\mathbf{\Theta} = \left\{ \tilde{\boldsymbol{x}} = (\tilde{x}_1, \tilde{x}_2, ..., \tilde{x}_n) \ / \ \tilde{x}_j \in \{\tilde{x}_j^1, ..., \tilde{x}_j^{q_j}\},\ \tilde{x}_j^k \in [\tilde{x}_j^{\min},\ \tilde{x}_j^{\max}],\ 1 \leq k \leq q_j \right\}.$$

We point that $|\mathbf{\Theta}| = \prod_{j=1}^{n} q_j$. It should be remarked that, in the real market, set $\mathbf{\Theta} \in \tilde{\Omega}$ probably varies with time.

These prices will be computed with polynomial $I_{\boldsymbol{N}} F(\mathbf{x})$, where the relation between $\tilde{\boldsymbol{x}}$ and $\boldsymbol{x}$ is given by formula (1.23).

The algorithms presented in Subsection 1.3.2 allow us to evaluate the interpolation polynomial in a set of points like $\mathbf{\Theta}$ very fast. Furthermore, numerical algorithms can be adapted in order to estimate the model parameters in the sense of the In The Sample analysis introduced in Subsection 1.2.1.

1.3.1 Computation of the interpolating polynomial.

One variable:

Let $\tilde{F}(\tilde{x})$ and $N \in \mathbb{N}$ be as given in Definition 1.3.3 and suppose that we want to compute the Chebyshev interpolant

$$I_{N_1} F(x) = \sum_{l=0}^{N_1} \hat{p}_l T_l(x), \quad x \in [-1, 1].$$

If we employ Definitions 1.3.1 and 1.3.2, it must hold that

$$\tilde{F}(\tilde{\alpha}^k) = F(\alpha^k) = \sum_{l=0}^{N} \hat{p}_l T_l(\alpha^k) = \sum_{l=0}^{N} \hat{p}_l \cos(l(\arccos(\alpha^k))) = \sum_{l=0}^{N} \hat{p}_l \cos\left(l \frac{\pi k}{N}\right),$$

where $\{\tilde{\alpha}^k\}_{k=0}^N,\ \{\alpha^k\}_{k=0}^N$ are the Chebyshev nodes in $[\tilde{x}^{\min}, \tilde{x}^{\max}]$ and $[-1,\ 1]$.

There are several efficient algorithms that allow us to obtain the coefficients $\{\hat{p}_l\}_{l=0}^N$. We are going to present one that can be found in [10].

We define $\hat{p}_l = \hat{p}_{2N-l}$ if $l > N$. Therefore, we can write:

$$F(\alpha^k) = \sum_{l=0}^{N} \frac{\hat{p}_l}{2} \cos\left(l\frac{2\pi k}{2N}\right) + \sum_{l=N}^{2N} \frac{\hat{p}_l}{2} \cos\left(l\frac{2\pi k}{2N}\right).$$

On the other hand

$$\begin{cases} \dfrac{\hat{p}_0}{2}\cos\left(0\dfrac{2\pi k}{2N}\right) = \dfrac{\hat{p}_{2N}}{2}\cos\left(2N\dfrac{2\pi k}{2N}\right), \\ \quad \sin\left(0\dfrac{2\pi k}{2N}\right) = \sin\left(N\dfrac{2\pi k}{2N}\right) = \sin\left(2N\dfrac{2\pi k}{2N}\right) = 0, \\ \dfrac{\hat{p}_l}{2}\sin\left(l\dfrac{2\pi k}{2N}\right) = -\dfrac{\hat{p}_{2N-l}}{2}\sin\left((2N-l)\dfrac{2\pi k}{2N}\right), \end{cases}$$

so we have that

$$\begin{aligned} F(\alpha^k) = \hat{p}_0\left(\cos\left(0\frac{2\pi k}{2N}\right) + i\sin\left(0\frac{2\pi k}{2N}\right)\right) + \sum_{l=1}^{N-1}\frac{\hat{p}_l}{2}\left(\cos\left(l\frac{2\pi k}{2N}\right) + i\sin\left(l\frac{2\pi k}{2N}\right)\right) \\ + \hat{p}_N\left(\cos\left(N\frac{2\pi k}{2N}\right) + i\sin\left(N\frac{2\pi k}{2N}\right)\right) + \sum_{l=N+1}^{2N-1}\frac{\hat{p}_l}{2}\left(\cos\left(l\frac{2\pi k}{2N}\right) + i\sin\left(l\frac{2\pi k}{2N}\right)\right) = \\ \frac{1}{2N}\sum_{l=0}^{2N-1} X_l \exp\left(il\frac{2\pi k}{2N}\right), \end{aligned}$$

because the $i\sin(.)$ part cancels in the expansion of the expression.

Now, we can apply time-optimal FFT-techniques for obtaining the $\{\hat{p}_l\}_{l=0}^N$.

Suppose we are given $\left\{F(\alpha^k)\right\}_{k=0}^N$. The algorithm that could be implemented is

Algorithm C1v:

1. Construct $z = \left[F(\alpha^0), F(\alpha^1), ..., F(\alpha^{N-1}), F(\alpha^N), F(\alpha^{N-1}), ..., F(\alpha^2), F(\alpha^1)\right]^T$.
2. Compute
$$y = \frac{\text{real}\left(\text{FFT}(z)\right)}{2N}.$$
3.
$$\begin{cases} \hat{p}_0 = y(1), \\ \hat{p}_l = y(l+1) + y(2N-(l-1)) \text{ if } 0 < l < N, \\ \hat{p}_N = y(N). \end{cases}$$

Several variables:

Definition 1.3.5. *Let A be an array of dimension $n_1 \times n_2 \times ... \times n_m$. We denote the vector*

$$A(j_1, ..., j_{n_{s-1}}, :, j_{n_{s+1}}, ..., j_m) = \{A(j_1, ..., j_{n_{s-1}}, j, j_{n_{s+1}}, ..., j_m)\}_{j=1}^{n_s},$$

where obviously $1 \leq j_i \leq n_i, \quad \forall i \in \{1, 2, ..., m\} - \{s\}$.

Let B be an array of dimension $a \times n_1 \times n_2 \times ... \times n_m$. We define the permutation operator $\mathcal{P}$ such that if:

$$D = \mathcal{P}(B),$$

we have that $\dim(D) = n_1 \times n_2 \times ... \times n_m \times a$ *and*

$$D(j_1, ..., j_m, :) = B(:, j_1, ..., j_m).$$

Let $\tilde{F}(\tilde{\mathbf{x}})$ and $\mathbf{N} \in \mathbb{N}^n$ be as given in Definition 1.3.4 and suppose that we want to construct the interpolant

$$I_{\boldsymbol{N}} F(\mathbf{x}) = \sum_{\boldsymbol{l} \in L^{\boldsymbol{N}}} \hat{p}_{\boldsymbol{l}} T^{\boldsymbol{l}}(\mathbf{x}), \quad \mathbf{x} \in [-1, 1]^n.$$

Suppose that we have already computed the function value at the Chebyshev nodes

$$\tilde{F}\left(\tilde{\alpha}_1^{k_1}, \tilde{\alpha}_2^{k_2}, ..., \tilde{\alpha}_n^{k_n}\right) = F\left(\alpha_1^{k_1}, \alpha_2^{k_2}, ..., \alpha_n^{k_n}\right), \quad \begin{cases} \forall k_j \in \{0, ..., N_j\}, \\ j = 1, 2, ..., n, \end{cases}$$

which are stored in an array $\Gamma_{(N_1+1)\times(N_2+1)\times...\times(N_n+1)}$ such that

$$\Gamma(k_1 + 1, k_2 + 1, ..., k_n + 1) = F\left(\alpha_1^{k_1}, \alpha_2^{k_2}, ..., \alpha_n^{k_n}\right).$$

The coefficients $\hat{p}_{\boldsymbol{l}}$ are obtained through the following algorithm.

Algorithm Cnv:

1. $B_1 = \Gamma$.

2. For i=1 to n

   2.1. $\{m_1, m_2, ..., m_n\} = \dim(B_i)$.

   2.2. For $j_2 = 1$ to m_2, for $j_3 = 1$ to m_3, ..., for $j_n = 1$ to m_n

   $$C_i(:, j_2, j_3, ..., j_n) = \text{Algorithm C1v}\left(B_i(:, j_2, j_3, ..., j_n)\right).$$

   2.3. $B_{i+1} = \mathcal{P}(C_i)$.

3. $\hat{p}_{\boldsymbol{l}} = B_{n+1}(l_1 + 1, l_2 + 1, ..., l_n + 1)$.

We remark that FFT routine in Matlab admits multidimensional valuation. Step 2.2 of the previous algorithm can be computed without using loops and barely takes a couple of seconds even with the biggest polynomials of the numerical examples.

1.3.2 Tensorial Evaluation and Differentiation of the interpolation polynomial.

Definition 1.3.6. *Let A and B be two arrays, $(A)_{a\times n_1\times n_2\times ...\times n_k}$ and $(B)_{a\times b}$ respectively, and such that $b>1$.*

We define the tensorial array operation $C=A\otimes B$, as the array C given by:

$$C(j_1,...,j_k,:)=\mathcal{P}\left(B'\cdot A(:,j_1,...,j_k)\right), \tag{1.28}$$

where $\cdot$ denotes the usual product of matrix times a vector and $\mathcal{P}$ is the permutation operator introduced in Definition 1.3.5.

It is easy to check that $\dim(C)=n_1\times n_2\times ...\times n_k\times b$.

Concerning the implementation in Matlab of the tensorial array operation,

$$C=\text{permute}\left(\text{multiprod}(B',A),[2:n\ 1]\right),$$

where *permute* is a standard procedure implemented in Matlab.

The algorithm *multiprod*, implemented by Paolo de Leva and available in Mathworks (see [50]), makes the required kind of tensorial operation simultaneously in all variables in a very efficient way.

Suppose now that we have a polynomial

$$I_{\boldsymbol{N}}F(\mathbf{x})=\sum_{\boldsymbol{l}\in L^{\boldsymbol{N}}}\hat{p}_{\boldsymbol{l}}T^{\boldsymbol{l}}(\mathbf{x})=\sum_{l_1=0}^{N_1}\sum_{l_2=0}^{N_2}...\sum_{l_n=0}^{N_n}\hat{p}_{\boldsymbol{l}}T_{l_1}(x_1)T_{l_2}(x_2)...T_{l_n}(x_n).$$

We want to evaluate the polynomial in a finite set of points $\boldsymbol{\Theta}$, such that for $q_j\in\mathbb{N},\ 1\leq j\leq n$, we have that

$$\boldsymbol{\Theta}=\left\{\tilde{\boldsymbol{x}}=(\tilde{x}_1,\tilde{x}_2,...,\tilde{x}_n)\ /\ \tilde{x}_j\in\{\tilde{x}_j^1,...,\tilde{x}_j^{q_j}\},\ \tilde{x}_j^k\in[\tilde{x}_j^{\min},\ \tilde{x}_j^{\max}],\ 1\leq k\leq q_j\right\}.$$

For computational reasons, that we detail below, we impose that $q_j>1,\ j=1,2,...,n$.

The evaluation algorithm has two steps.

1. Evaluate the Chebyshev polynomials:

We use the recurrence property of Chebyshev polynomials:

$$T_0(x)=1,\quad T_1(x)=x,\quad T_l(x)=2xT_{l-1}(x)-T_{l-2}(x),\quad l=2,3,4,...,$$

that with the number $\boldsymbol{N}$ of interpolation points involved in the option pricing problem works fairly well.

We employ the notation $\eta_j = \{x_j^k\}_{k=1}^{q_j}$, obtained from $\mathbf{\Theta}$ and (1.23). With the recurrence property, we compute

$$\begin{aligned}
\boldsymbol{T}(\eta_1) &= \boldsymbol{T}(\eta_1)_{(N_1+1)\times q_1} = \left(T_l(x_1^k)\right)_{0\le l\le N_1,\ 1\le k\le q_1}, \\
\boldsymbol{T}(\eta_2) &= \boldsymbol{T}(\eta_2)_{(N_2+1)\times q_2} = \left(T_l(x_2^k)\right)_{0\le l\le N_2,\ 1\le k\le q_2}, \\
&\ldots \\
\boldsymbol{T}(\eta_n) &= \boldsymbol{T}(\eta_n)_{(N_n+1)\times q_n} = \left(T_l(x_2^k)\right)_{0\le l\le N_n,\ 1\le k\le q_n},
\end{aligned}$$

where the results are stored in matrices.

2. Evaluate the rest of the polynomial.

The evaluation of the polynomial $I_{\boldsymbol{N}}F(\mathbf{x})$ for the whole set of points $\mathbf{\Theta}$ can be done at once using the tensorial array operation.

The polynomial coefficients are stored in a $(N_1+1)\times(N_2+1)\times\ldots\times(N_n+1)$-dimensional array A.

$$A(l_1+1, l_2+1, ..., l_n+1) = \hat{p}_{(l_1,l_2,...,l_n)},$$

and we compute

$$I_{\boldsymbol{N}}F(\mathbf{\Theta}) = (\ldots[(A\otimes\boldsymbol{T}(\eta_1))\otimes\boldsymbol{T}(\eta_2)]\ldots)\otimes\boldsymbol{T}(\eta_n), \tag{1.29}$$

where the result will be an $q_1\times q_2\times\ldots\times q_n$-dimensional array which contains the evaluation of the interpolant in all the points of set $\mathbf{\Theta}$.

We remark that the previous definition must not be seen as a product with the usual properties. The order of the parenthesis has to be strictly followed in order to be consistent with the dimensions.

The reason why we imposed $q_j > 1,\ j = 1, 2, ..., n$ is also related with the consistency of the dimensions. If $q_i = 1$, by default, *multiprod* algorithm does not recognize

$$q_1\times\ldots\times q_{i-1}\times 1\times q_{i+1}\times\ldots\times q_n - \text{dimension},$$

but collapses the array to

$$q_1\times\ldots\times q_{i-1}\times q_{i+1}\times\ldots\times q_n - \text{dimension}.$$

We recall that $\otimes$ consists of *multiprod* and a *permutation*. If $q_i = 1$, a wrong dimension will be permuted in the valuation algorithm.

Computationally it is easier to impose that set $\mathbf{\Theta}$ contains at least two different values for each of the variables and, as we will see in the numerical examples, this will not drastically affect the computational cost of the method.

Polynomial differentiation:

Concerning the option pricing problem we are dealing with, we include a brief commentary about the In the Sample analysis introduced in Subsection 1.2.1.

The estimation of the model parameters from real market prices is done with a standard Newton algorithm. Next, we describe the evaluation of the Jacobian that we need in the algorithm.

Note that if $\tilde{x} \in [a, b]$ and we have interpolated function $\tilde{F}(\tilde{x})$

$$\tilde{F}(\tilde{x}) \approx I_N F(x) = \sum_{l=0}^{N} \hat{p}_l T_l(x),$$

where

$$\tilde{x} = \frac{b-a}{2}x + \frac{b+a}{2}, \quad x \in [-1, 1],$$

we can approximate, if function F is regular enough (see [10]),

$$\tilde{F}'(\tilde{x}) \approx (I_N F(x))' = \frac{2}{b-a} \sum_{l=0}^{N-1} \hat{q}_l T_l(x),$$

where (see [10, (2.4.22)]) for $l = 0, 1, ..., N-1$:

$$\hat{q}_l = \frac{2}{c_l} + \sum_{\substack{j=l+1 \\ j+l \text{ odd}}}^{N} j\hat{p}_j, \quad \text{where } c_l = \begin{cases} 2, & l = 0, \\ 1, & l \geq 1. \end{cases}$$

This implies that the coefficients of the derivatives of the polynomials need to be computed each time or stored in memory. Both options do not fit with the objective of this work.

If the coefficients are computed each time they are needed, that would increase the total time cost of the In the Sample analysis. This worsens the objective of doing real time parameter calibration.

On the other hand, as we are about to see, there is a memory storage problem in the polynomial interpolation technique. To store the coefficients of the derivative means to almost double the memory requirements of the method.

For these reasons, we prefer to employ a fast computing way to approximate the derivative, which does not require any more memory storage. We approximate

$$\tilde{F}'(\tilde{x}) \approx \frac{2}{b-a} \frac{I_N F(x+h) - I_N F(x)}{h},$$

where $0 < h << 1$. This is the technique employed in the numerical examples.

As it has been seen, all the algorithms developed in Subsections 1.3.1 and 1.3.2 are general enough and can be exported to other kinds of models, contracts, etc.. The only thing that we need to know is how many variables the interpolated function has and everything is straightforward.

1.3.3 Interpolation Error

In the first place, we fix the intervals in which the interpolant of the option price will be constructed.

We recall that the model was linear in the relation $\frac{S}{K}$, so strike is fixed at $K = 1$. The rest of variables are defined as follows:

$$\begin{aligned} &t_M \in [0,\ 365], && \beta_0 \in [0,\ 2\cdot 10^{-6}],\\ &h_0 \in [0.25\cdot 10^{-4},\ 2.25\cdot 10^{-4}], && \beta_1 \in [0.60,\ 0.95],\\ &S_0 \in [0.75,\ 1.20], && \beta_2 \in [0.02,\ 0.25],\\ &r \in [0.02,\ 0.085], && (\lambda+\theta) \in [0.20,\ 2]. \end{aligned}$$

These intervals are chosen because they cover all the values empirically observed in market data along several years.

The stability condition $\beta_1+\beta_2 < 1$ (see [7]) guarantees that the volatility process does not blow to ∞. In the B-F numerical method, the volatility varies in a big, but finite interval. Therefore, no divergence problems appear since the volatility cannot grow over a certain level. This generates a numerical localization error (see [9]), but it can be made as small as desired. This error mainly affects to values $\beta_1 + \beta_2 > 1$ or extremely high volatilities.

The volatility interval in the B-F method was chosen big enough in order to cover all the volatility values observed in the market and minimize the localization error. Furthermore, parameter values such that $\beta_1 + \beta_2 > 1$ where not observed in any of the experiments with market data. For simplicity reasons, we do not impose this condition.

We are going to carry out a standard error analysis doubling the value of $\boldsymbol{N}$. Note that with Chebyshev nodes, each new set of points will contain all of the previous one. The following table details the degree N_* of the interpolation polynomial in each of the variables and the total storage cost of the polynomial coefficients. We remark that the number of interpolation points of variable x_* is $N_* + 1$.

	N_{t_M}	N_{β_1}	N_{β_2}	$N_{(\lambda+\theta)}$	N_r	N_{β_0}	N_{h_0}	N_S	Storage cost(bytes)
$I_{\mathbf{3}}F$	3	3	3	3	3	3	3	3	$5.24\cdot 10^5$
$I_{\mathbf{6}}F$	6	6	6	6	6	6	6	6	$4.61\cdot 10^7$
$I_{\mathbf{12}}F$	12	12	12	12	12	12	12	12	$6.52\cdot 10^9$

Table 1.1: Degree of the interpolation polynomial $I_{\boldsymbol{N}}F$ in each of the variables and storage cost of the polynomial coefficients. The number of interpolation points in each of the variables is $N_* + 1$.

The storage cost of the polynomials is explicitly computable. For the polynomials described in the table, this formula is $(N_* + 1)^8$. The growth of the storage cost, as we increase the value of N_*, is commonly referred as the "Curse of dimensionality".

Fixed an enough precision for the B-F method, we assume for the rest of the Chapter that the option price obtained with this method is the reference option price. The construction of the polynomial and the error analysis will be carried referencing to the values obtained with it.

Once fixed $\boldsymbol{N}$, we compute the Chebyshev nodes $\{\tilde{\boldsymbol{\alpha}}^{\boldsymbol{l}}\}_{l\in L^{\boldsymbol{N}}}$ with formula (1.18). We compute the function values $\{\tilde{F}\left(\tilde{\boldsymbol{\alpha}}^{\boldsymbol{l}}\right)\}_{l\in L^{\boldsymbol{N}}}$ with B-F method and construct $I_{\boldsymbol{N}}F$ with the algorithms developed in Subsection 1.3.1.

Independently, we have to build a control sample which allows us to measure how well the interpolation polynomial prices options in the domain $\tilde{\Omega}$. We have chosen a sample uniformly distributed on $\tilde{\Omega}$.

Definition 1.3.7. *For each variable $\tilde{x}_j \in [\tilde{x}_j^{\min},\ \tilde{x}_j^{\max}]$ and for a given $m \in \mathbb{N}$ we define*

$$\Delta_{\tilde{x}_j}^m = \frac{\tilde{x}_j^{\max} - \tilde{x}_j^{\min}}{m},$$

and the set of points

$$\Theta_{\tilde{x}_j}^m = \left\{\tilde{x}_{\min} + \Delta_{\tilde{x}_j}\cdot i\right\}_{i=1}^{m-1}, \quad j = 1, 2..., 8.$$

This set of equally spaced points will be used to build a control sample. Points that correspond to $i = \{0, m\}$ are not included because they always correspond to Chebyshev nodes.

Sample $\boldsymbol{\Theta}_m$ *will denote the set of option prices for all the possible combinations of values in sets $\Theta_{\tilde{x}_j}^m$, i.e.*

$$\text{Sample } \boldsymbol{\Theta}_m = \{\tilde{F}\left(\Theta_{\tilde{x}_1}^m, \Theta_{\tilde{x}_2}^m, ..., \Theta_{\tilde{x}_8}^m\right)\}, \quad |\text{Sample } \boldsymbol{\Theta}_m| = (m-1)^8,$$

computed with B-F method.

We compute Sample $\boldsymbol{\Theta}_m$ and numerate its elements. Let

- C_j^{B-F} be the j contract price of Sample $\boldsymbol{\Theta}_m$.
- $C_j^{I_{\boldsymbol{N}}F}$ be the j contract price evaluated with polynomial $I_{\boldsymbol{N}}F$.

We define

$$\text{MSE}_{\text{Sample } \boldsymbol{\Theta}_m}(I_{\boldsymbol{N}}F) = \frac{1}{(m-1)^8}\sum_{j=1}^{(m-1)^8}\left(C_j^{B-F} - C_j^{I_{\boldsymbol{N}}F}\right)^2.$$

For the numerical examples, we have built Sample $\boldsymbol{\Theta}_7$. The number of elements of this sample is $1679616 \approx 1.68\cdot 10^6$.

The following table shows, for $\boldsymbol{N} = \mathbf{3}, \mathbf{6}, \mathbf{12}$, the memory storage requirements of $I_{\boldsymbol{N}}F$, the computational cost (seconds) of computing Sample $\boldsymbol{\Theta}_7$ with $I_{\boldsymbol{N}}F$ and the $\mathrm{MSE}_{\mathrm{Sample}\ \boldsymbol{\Theta}_7}(I_{\boldsymbol{N}}F)$.

	Storage (bytes)	Computational Cost (seconds)	Mean Square Error (MSE)
$I_{\mathbf{3}}F$	$5.24 \cdot 10^5$	0.11	$0.69186 \cdot 10^{-4}$
$I_{\mathbf{6}}F$	$4.61 \cdot 10^7$	0.46	$0.12298 \cdot 10^{-4}$
$I_{\mathbf{12}}F$	$6.52 \cdot 10^9$	91	$0.01203 \cdot 10^{-4}$

Table 1.2: Storage cost of $I_{\boldsymbol{N}}F$, computational cost of evaluating Sample $\boldsymbol{\Theta}_7$ with $I_{\boldsymbol{N}}F$ and the Mean Square Error committed by the interpolation polynomial $I_{\boldsymbol{N}}F$ when evaluating the contract prices of Sample $\boldsymbol{\Theta}_7$.

In the previous table, we can check that the computational cost of $I_{\mathbf{3}}F$ and $I_{\mathbf{6}}F$ is fairly good, but it blows to 91 seconds in the case of $I_{\mathbf{12}}F$. Although this time might not seem too high for computing $\approx 1.68 \cdot 10^6$ contracts, it is unacceptable for practical applications in real time trade. In the markets, the stock price might have changed a few times before we have finished the computation, making the results worthless.

The reason why the computational cost has increased so much is due to the "Curse of dimensionality". We remark that $I_{\mathbf{12}}F$ is above the operational limit of the Matlab/computer employed in the analysis to be stored in just one single array. Although the storage problem can be handled, splitting the polynomial in several parts and loading/discarding the needed data, unfortunately, in velocity terms, this implies a great increase of computational work.

Concerning $I_{\mathbf{12}}F$, let $\{t_{Mi}\}_{i=0}^{12}$ denote the 13 Chebyshev nodes in interval $[0,\ 365]$. For each value of t_{Mi} we build the 7-variable interpolation polynomial for the rest of the variables. This way, we have polynomial $I_{\mathbf{12}}F$ stored as 13 smaller polynomials which can be handled.

In our example, the 91 seconds are mostly due to several uses of the function *load* when we call each of the 7-variable smaller polynomials.

We mention that if the polynomial was even bigger, the splitting procedure can be extended to other variables, so storage is not an unsolvable problem. Nevertheless, it worsens the computational costs because it implies that we need to load data from the memory very frequently.

We point that the objective of the next Section is to build a new smaller polynomial which preserves the information and that can be rapidly evaluated with the algorithms described in Subsection 1.3.2

Concerning the error of the interpolation polynomials, the following picture shows the log-log of the Memory Storage versus the Mean Square Error.

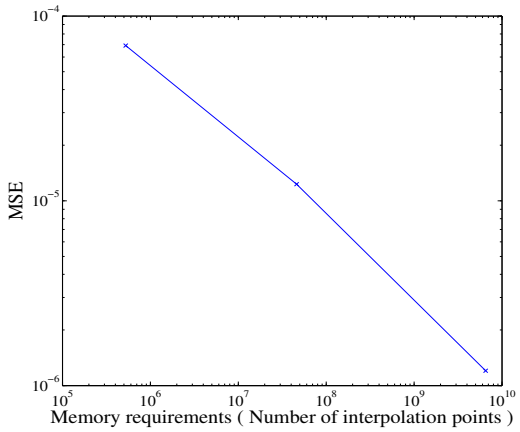

Figure 1.3: Interpolation Error Convergence. We plot the log-log of the Memory requirements (horizontal axis) vs the Mean Square Error (vertical axis) of each polynomial $I_{\mathbf{N}}F$.

The slope of the regression line of the previous figure is -0.43. We have a good error behaviour, achieving a precision of $0.01203 \cdot 10^{-4}$ with $\boldsymbol{N} = \{12, 12, ..., 12\}$. If more precision is required, we can build bigger interpolation polynomials, which can be handled thanks to the splitting technique that we described before.

For completing the analysis, we are going to study the error, in monetary terms, including an In the Sample / Out the Sample analysis with real market data.

We are going to repeat exactly the In/Out The Sample analysis done in Subsection 1.2.1. On Figure 1.4 we include the results obtained with polynomial $I_{\mathbf{12}}F$ (red) to see that, from a practical point of view, we are already really close to NGARCH(1,1) (green) and that we outperform Black-Scholes (blue).

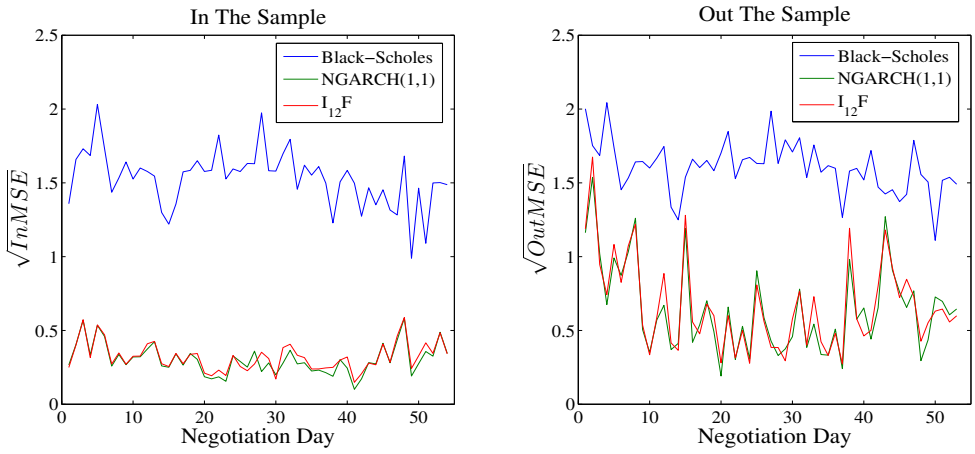

Figure 1.4: We plot each negotiation day t_0 (horizontal axis) vs the root of InMSE (left) and OutMSE (right) when prices are computed with Black-Scholes (blue),NGARCH(1,1) (green) and $I_{\mathbf{12}}F$ (red).

The mean values of the root of InMSE and OutMSE have been:

	Black-Scholes	NGARCH(1,1)	$I_{\mathbf{12}}F$
In The Sample	1.53	0.30	0.32
Out The Sample	1.60	0.64	0.66

Table 1.3: Mean error, in monetary terms, of the 54/53 different days when we adjust (In) or predict (Out) traded option prices with Black-Scholes model, NGARCH(1,1) and $I_{\mathbf{12}}F$.

The previous table shows that interpolant $I_{\mathbf{12}}F$ is capable to adjust / predict prices better than the Black-Scholes model and with a similar accuracy as the NGARCH(1,1) model, the function which interpolates.

These results also show that the interpolant is consistent in the sense that, although the parameters estimated In The Sample are not exactly the same (but are fairly close) to the ones obtained with NGARCH(1,1), when market conditions change and we try to predict (Out The Sample), the prices obtained are also close to the ones obtained with NGARCH(1,1).

Also note that we have two kinds of errors here. The first one is the error due to the adequacy of the NGARCH(1,1) model to market data, which cannot be reduced unless we change the model. It is given in the table by the column of NGARCH(1,1). The second one is the interpolation error, which is given by the differences between the columns of NGARCH(1,1) and $I_{\mathbf{12}}F$. This one can be reduced as much as we want increasing the number of interpolation points.

1.4 Reduced Bases Approach

The objective of this Section is to build a new polynomial which gives comparable accuracy, but which has less memory requirements.

Suppose we are given a high degree polynomial $P^{\mathbf{N}}$. The objective is to construct from it a smaller polynomial, as we will see in memory terms but not in degree, which globally values as well as the original one.

The method we are going to develop could be exported to other kinds of polynomials, but since our evaluation algorithms are designed for the Chebyshev ones, the construction is focused to take advantage of their properties. It is also general enough to be applied to any n-variables polynomial.

1.4.1 Hierarchical orthonormalization

Suppose we have a polynomial

$$P^{\boldsymbol{N}}(x_1,\ ...,\ x_n), \quad \boldsymbol{N} = [N_1, N_2, ..., N_n] \in \mathbb{N}^n, \tag{1.30}$$

where $\boldsymbol{N}$ denotes the degree in each of the variables.

Our objective is, given a set of points $\Phi = \{\phi_i\}_{i=1}^{m_\Phi}$ and $\epsilon > 0$, to construct a polynomial

$Q^{\boldsymbol{N}_\epsilon^\Phi}$ from $P^{\boldsymbol{N}}$, such that

$$\frac{1}{m_\Phi}\sum_{i=1}^{m_\Phi}||P^{\boldsymbol{N}}(\phi_i)-Q^{\boldsymbol{N}_\epsilon^\Phi}(\phi_i)||^2<\epsilon, \tag{1.31}$$

where polynomial $Q^{\boldsymbol{N}_\epsilon^\Phi}$ has the smallest size (in memory terms) compatible with (1.31).

Although another set of points could be chosen, since in our option pricing problem polynomial $P^{\boldsymbol{N}}=I_{\boldsymbol{N}}F$, the interpolation polynomial of a certain function $\tilde{F}(\tilde{\boldsymbol{x}})$, the natural set of points Φ will be the set of points used in the construction of the interpolation polynomial, i.e., the Chebyshev nodes $\Phi=\{\boldsymbol{\alpha_l}\}_{\boldsymbol{l}\in L^{\boldsymbol{N}}}$.

Our approach will be to use a set of Orthonormal Function Bases that will be hierarchically chosen. All polynomials that appear in the procedure we are going to construct must be written in function of Chebyshev polynomials. Hence, it is natural to employ the weighted norm associated with them and to exploit all the related properties which will simplify enormously all the calculus involved.

Definition 1.4.1. *Given two functions $f(x_1,...,x_n)$ and $g(x_1,...,x_n)$, where $(x_1,...,x_n)\in[-1,\ 1]^n$, we define the weighted scalar product $<f,g>_{\mathrm{L}_\omega}$ as:*

$$<f(x_1,...,x_n),g(x_1,...,x_n)>_{\mathrm{L}_\omega}=\int_{-1}^{1}...\int_{-1}^{1}\frac{f(x_1,...,x_n)g(x_1,...,x_n)}{\sqrt{1-x_1^2}...\sqrt{1-x_n^2}}dx_1...dx_n.$$

We denote by $||\cdot||_{\mathrm{L}_\omega}$ the norm induced by this scalar product.

Lemma 1.4.1. *The Chebyshev polynomials, $T_i(x)$, are orthogonal with respect to the scalar product $<f,g>_{\mathrm{L}_\omega}$. Furthermore, if $H(x)$ is a polynomial of degree less or equal to $2n+1$ then*

$$\int_{-1}^{1}\frac{H(x)}{\sqrt{1-x^2}}dx=\sum_{j=0}^{n}{}''\frac{\pi}{n}H(x_j)=\sum_{j=1}^{n-1}\frac{\pi}{n}H(x_j)+\frac{\pi}{2n}H(x_0)+\frac{\pi}{2n}H(x_n),$$

where $\{x_j\}_{j=0}^n$ are the Chebyshev nodes in [-1,1]. (Gauss-Lobato-Chebyshev cuadrature)

The proof can be found in [55].

Definition 1.4.2. *Let $f(x_j,x_{j+1},...,x_n)$ and $g(x_j,x_{j+1},...,x_n)$ be two functions such that $(x_j,x_{j+1}...,x_n)\in[-1,\ 1]^{n-j+1}$.*

Based on the previous scalar product, we define function

$$<f,g>_{\mathrm{L}_\omega^{\mathrm{j+1,n}}}(x_j)=\int_{-1}^{1}...\int_{-1}^{1}\frac{f(x_j,...,x_n)g(x_j,...,x_n)}{\sqrt{1-x_{j+1}^2}...\sqrt{1-x_n^2}}dx_{j+1}...dx_n.$$

For simplicity in the notation, we denote $<f,g>_{\mathrm{L}_\omega^{\mathrm{j+1,n}}}(x_j)=<f,g>_{\mathrm{L}_\omega^{\mathrm{j+1,n}}}$.

The algorithm of the hierarchical Gram-Schmidt procedure that we are about to propose has $n-1$ steps if the polynomial $P^{\boldsymbol{N}}(x_1,\ ...,\ x_n)$ has n variables.

Hierarchical orthonormalization procedure:

Let us consider $P^{\boldsymbol{N}}(x_1,\ ...,\ x_n)$ and for simplicity assume that $x_j \in [-1,\ 1]$. Let us consider also a set of points $\Phi = \{\phi_i\}_{i=1}^{m_\Phi},\ \phi_i \in [-1,1]^n$. (As mentioned before, in the numerical examples we take $\Phi = \{\boldsymbol{\alpha_l}\}_{\boldsymbol{l}\in L^{\boldsymbol{N}}}$ but other sets of points could be considered).

Step 1:
Let $\{\alpha_1^i\}_{i=0}^{N_1}$ denote the N_1+1 Chebyshev nodes in $[-1,\ 1]$ and define $P_i(x_2,...,x_n) = P^{\boldsymbol{N}}(\alpha_1^i, x_2, ..., x_n)$. It is easy to check that we can rewrite $P^{\boldsymbol{N}}$ as:

$$P^{\boldsymbol{N}}(x_1,\ ...,\ x_n) = \sum_{i=0}^{N_1} a_i(x_1)P_i(x_2,...,x_n) = R_1(x_1,...,x_n),$$

where $a_i(x_1)$ is a N_1-degree polynomial such that for $m = 0, 1, ..., N_1$ it holds that:

$$\begin{cases} a_i(\alpha_1^i) = 1, \\ a_i(\alpha_1^m) = 0, \quad i \neq m. \end{cases}$$

For $i_1 \in \{0,...,N_1\}$, we set $\tilde{q}_{i_1}^1 = P_{i_1}$ and $q_{i_1}^1 = \frac{\tilde{q}_{i_1}^1}{\left\|\tilde{q}_{i_1}^1\right\|_{L_\omega}}$ and look for:

$$j_1 = \underset{i_1}{\operatorname{argmin}} \left\| R_1 - < R_1, q_{i_1}^1 >_{L_\omega^{2,n}} q_{i_1}^1 \right\|_{L_\omega}.$$

We define $q_{j_1} = q_{j_1}^1$ and $R_2 = R_1 - < R_1, q_{j_1} >_{L_\omega^{2,n}} q_{j_1}$.

For $i_2 \in \{0,...,N_1\} - j_1$, we set $\tilde{q}_{i_2}^2 = P_{i_2} - < P_{i_2}, q_{j_1} >_{L_\omega^{2,n}} q_{j_1}$ and $q_{i_2}^2 = \frac{\tilde{q}_{i_1}^2}{\left\|\tilde{q}_{i_1}^2\right\|_{L_\omega}}$ and we look for

$$j_2 = \underset{i_2}{\operatorname{argmin}} \left\| R_2 - < R_2, q_{i_2}^2 >_{L_\omega^{2,n}} q_{i_2}^2 \right\|_{L_\omega}.$$

We define $q_{j_2} = q_{j_2}^2$ and $R_3 = R_2 - < R_2, q_{j_2} >_{L_\omega^{2,n}} q_{j_2}$.

If we proceed iteratively, at the end we will obtain a set of $\{q_{j_k}\}_{k=0}^{N_1}$ orthonormal polynomials such that

$$P^{\boldsymbol{N}}(x_1,\ ...,\ x_n) = \sum_{k=0}^{N_1} A_{j_k}^1(x_1) q_{j_k}(x_2,...,x_n),$$

where $A_{j_k}^1(x_1) =< P^{\boldsymbol{N}}, q_{j_k} >_{L_\omega^{2,n}},\ k = 0, 1, ..., N_1$.

We can now approximate $P^{\boldsymbol{N}}(x_1,\ ...,\ x_n)$ by

$$P^{\boldsymbol{N}}(x_1,\ ...,\ x_n) \approx Q_1 = \sum_{k=0}^{M_1} A_{j_k}^1(x_1) q_{j_k}(x_2,...,x_n),$$

where M_1 is the first index such that

$$\frac{1}{m_\Phi}\sum_{i=1}^{m_\Phi}\left\|P^{\boldsymbol{N}}(\phi_i)-Q_1(\phi_i)\right\|^2<\epsilon. \tag{1.32}$$

Let us observe that the polynomials q_{j_k} that were picked first were those that, in the sense of (1.32), had more "information" about $P^{\boldsymbol{N}}$. Indeed, usually with very few ones (depending on the variable), a good approximation to the original polynomial is achieved.

Furthermore, the amount of storage required is considerably reduced.

Step 2:

Each of the $q_{j_k}(x_2,...,x_n)$ is a $n-1$ variable polynomial, and we can proceed the same way as we did in **Step 1**.

For each of the j_k, let $\{\alpha_2^i\}_{i=0}^{N_2}$ be the N_2+1 Chebyshev nodes in $[-1,1]$ and

$$q_{j_k}(x_2,...,x_n)=\sum_{i=0}^{N_2}a_i^{j_k}(x_2)P_i^{j_k}(x_3,...,x_n)=R_1^{j_k}(x_2,...,x_n),$$

where $P_i^{j_k}(x_3,...,x_n)=q_{j_k}(\alpha_2^i,x_3,...,x_n)$.

For $i_1\in\{0,...,N_2\}$, we set $\tilde{q}_{i_1}^{j_k,1}=P_i^{j_k}$ and $q_{i_1}^{j_k,1}=\frac{\tilde{q}_{i_1}^{j_k,1}}{\left\|\tilde{q}_{i_1}^{j_k,1}\right\|_{L_\omega}}$ and look for:

$$l_1=\underset{i_1}{\operatorname{argmin}}\left\|R_1^{j_k}-<R_1^{j_k},q_{i_1}^{j_k,1}>_{L_\omega^{3,n}}q_{i_1}^{j_k,1}\right\|_{L_\omega}.$$

We define $q_{j_k,l_1}=q_{l_1}^{j_k,1}$ and $R_2^{j_k}=R_1^{j_k}-<R_1^{j_k},q_{j_k,l_1}>_{L_\omega^{3,n}}q_{j_k,l_1}$.

Now, for $i_2\in\{0,...,N_2\}-l_1$, we set $\tilde{q}_{i_2}^{j_k,2}=P_{i_2}^{j_k}-<P_{i_2}^{j_k},q_{j_k,l_1}>_{L_\omega^{3,n}}q_{j_k,l_1}$ and $q_{i_2}^{j_k,2}=\frac{\tilde{q}_{i_2}^{j_k,2}}{\left\|\tilde{q}_{i_2}^{j_k,2}\right\|_{L_\omega}}$. Again we look for

$$l_2=\underset{i_2}{\operatorname{argmin}}\left\|R_2^{j_k}-<R_2^{j_k},q_{i_2}^{j_k,2}>_{L_\omega^{3,n}}q_{i_2}^{j_k,2}\right\|_{L_\omega}.$$

We define $q_{j_k,l_2}=q_{l_2}^{j_k,2}$ and $R_3^{j_k}=R_2^{j_k}-<R_2^{j_k},q_{j_k,l_2}>_{L_\omega^{3,n}}q_{j_k,l_2}$.

If we proceed iteratively, at the end we will obtain

$$Q_1=\sum_{k=0}^{M_1}A_{j_k}^1(x_1)\left(\sum_{m=0}^{N_2}A_{j_k,l_m}^2(x_2)q_{j_k,l_m}(x_3,...,x_n)\right),$$

where $A_{j_k,l_m}^2(x_2)=<q_{j_k}(x_2,...,x_n),q_{j_k,l_m}(x_3,...,x_n)>_{L_\omega^{3,n}},\ m=0,1,...,N_2$.

We will approximate $P^{\boldsymbol{N}}(x_1,\ ...,\ x_n)$ by

$$P^{\boldsymbol{N}} \approx Q_2 = \sum_{k=0}^{M_1} A^1_{j_k}(x_1) \left(\sum_{m=0}^{M_2} A^2_{j_k,l_m}(x_2) q_{j_k,l_m}(x_3, ..., x_n) \right),$$

where M_2 is the first index such that

$$\frac{1}{m_\Phi} \sum_{i=0}^{m_\Phi} \left\| P^{\boldsymbol{N}}(\phi_i) - Q_2(\phi_i) \right\|^2 < \epsilon. \tag{1.33}$$

We proceed iteratively until completing **Step n-1** where we stop. We will have arrived to a new polynomial that can be written in the form

$$P^{\boldsymbol{N}} \approx Q^{\boldsymbol{N}^\Phi_\epsilon} = \sum_{i_1,i_2,...,i_{n-1}}^{M_1,M_2,...,M_{n-1}} A^1_{i_1}(x_1) A^2_{i_1,i_2}(x_2) ... A^{n-1}_{i_1,i_2,...,i_{n-1}}(x_{n-1}) q^{n-1}_{i_1,i_2,...,i_{n-1}}(x_n).$$

Note that $\boldsymbol{N}^\Phi_\epsilon = \{M_1, ..., M_{n-1}, N_n\}$ is the number of function bases used in each variable. Note also that, in general, the degree of $Q^{\boldsymbol{N}^\Phi_\epsilon}$ is still $N_1 \times N_2 \times ... \times N_n$.

We remark that the last value of $\boldsymbol{N}^\Phi_\epsilon$ is N_n because the last variable remains untouched. An improved result (in memory terms) can be obtained if the variables of polynomial $P^{\boldsymbol{N}}$ are reordered before the Reduced Bases procedure and N_n is the smallest among the N_i.

Visually, we can check the big memory saving. The following picture shows an example of the first three steps of the algorithm if $N_1 = 5,\ N_2 = 3,\ N_3 = 4, ...$

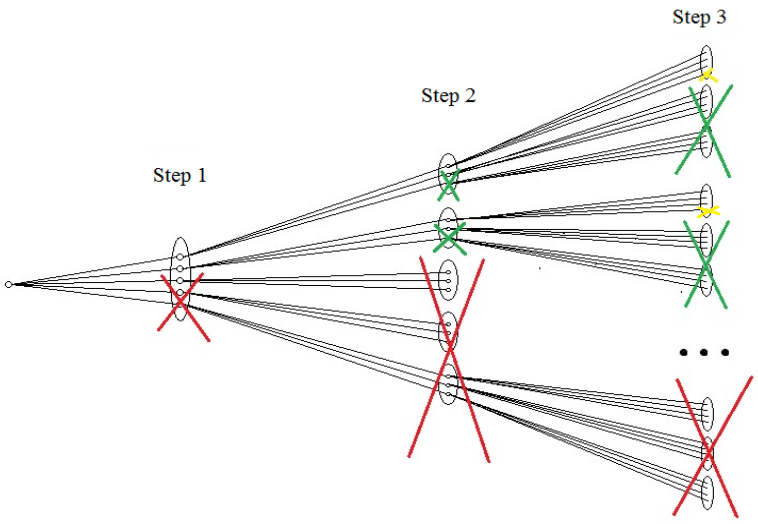

Figure 1.5: Truncated Orthonormal decomposition. The colored '×' mark the function bases discarded (equivalent to memory savings) in each step (Step 1-red, Step 2-green and Step 3-yellow) of the Hierarchical orthonormalization procedure.

The tree represents the orthonormal decomposition in each of the variables and the colored '×' the function bases that are discarded in each step: 3 function bases (Step 1-red), 2 function bases (Step 2-green) and 1 function bases (Step 3-yellow). The proportion of the tree that has been discarded represents approximately the memory savings with respect to the original polynomial P_N obtained by our method.

The last step is to adequate the algorithms for *tensorial valuation* to $Q^{\boldsymbol{N}_\epsilon^\Phi}$.

1.4.2 Tensorial valuation for Reduced Bases

Polynomial $Q^{\boldsymbol{N}_\epsilon^\Phi}$ is rewritten for tensorial evaluation as

$$\begin{aligned} Q^{\boldsymbol{N}_\epsilon^\Phi} &= \sum_{i_1,i_2,...,i_{n-1}}^{M_1,M_2,...,M_{n-1}} A^1_{i_1}(x_1)A^2_{i_1,i_2}(x_2)...A^{n-1}_{i_1,i_2,...,i_{n-1}}(x_{n-1})q^{n-1}_{i_1,i_2,...,i_{n-1}}(x_n) = \\ &= \sum_{i_1=0}^{M_1} A^1_{i_1}(x_1) \sum_{i_2=0}^{M_2} A^2_{i_1,2}(x_2)... \sum_{i_{n-2}=0}^{M_{n-2}} A^{n-2}_{i_{1,n-2}}(x_{n-2}) \sum_{i_{n-1}=0}^{M_{n-1}} A^{n-1}_{i_{1,n-1}}(x_{n-1})q^{n-1}_{i_{1,n-1}}(x_n). \end{aligned}$$

where we denote $i_{1,j} = (i_1, i_2, ..., i_j)$.

Each polynomial is written in function of the Chebyshev polynomials:

$$\begin{aligned} A^1_{i_1}(x_1) &= \sum_{j=0}^{N_1} a^1_{j,i_1} T(x_1), \\ A^2_{i_{1,2}}(x_2) &= \sum_{j=0}^{N_2} a^2_{j,i_{1,2}} T(x_2), \\ &... \\ A^{n-1}_{i_{1,n-1}}(x_{n-1}) &= \sum_{j=0}^{N_{n-1}} a^{n-1}_{j,i_{1,n-1}} T(x_{n-1}), \\ q^{n-1}_{i_{1,n-1}}(x_n) &= \sum_{j=0}^{N_n} a^n_{j,i_{1,n-1}} T(x_n), \end{aligned} \tag{1.34}$$

and $Q^{\boldsymbol{N}_\epsilon^\Phi}$ is kept in memory storing the coefficient of the previous polynomials in n different multidimensional arrays.

Suppose that we want to evaluate the polynomial in a finite set of points $\boldsymbol{\Theta}$, such that for $q_j \in \mathbb{N},\ 1 \leq j \leq n$, we have that

$$\boldsymbol{\Theta} = \left\{ \tilde{\boldsymbol{x}} = (\tilde{x}_1, \tilde{x}_2, ..., \tilde{x}_n) \ / \ \tilde{x}_j \in \{\tilde{x}_j^1, ..., \tilde{x}_j^{q_j}\},\ \tilde{x}_j^k \in [\tilde{x}_j^{\min},\ \tilde{x}_j^{\max}],\ 1 \leq k \leq q_j \right\}.$$

We employ the notation $\eta_j = \{x_j^k\}_{k=1}^{q_j}$, obtained from $\boldsymbol{\Theta}$ and (1.23).

The evaluation of polynomials $A^1_{i_1}(\eta_1)$, ..., $A^{n-1}_{i_{1,n-1}}(\eta_{n-1})$, $q^{n-1}_{i_{1,n-1}}(\eta_n)$ when they are given by (1.34) can be done efficiently using the first algorithm from Subsection 1.3.2.

Thus, suppose that we have evaluated them and stored the results in arrays:

$$\begin{aligned} A^1_{i_1}(\eta_1) &= (A^1)_{(M_1+1)\times q_1}, \\ A^2_{i_{1,2}}(\eta_2) &= (A^2)_{(M_1+1)\times(M_2+1)\times q_2}, \\ &\dots \\ A^{n-1}_{i_{1,n-1}}(\eta_{n-1}) &= (A^{n-1})_{(M_1+1)\times(M_2+1)\times\dots\times(M_{n-1}+1)\times q_{n-1}}, \\ q^{n-1}_{i_{1,n-1}}(\eta_n) &= (A^n)_{(M_1+1)\times(M_2+1)\times\dots\times(M_{n-1}+1)\times q_n}. \end{aligned}$$

Definition 1.4.3. *Let A and B be two arrays such that*

$$\begin{cases} (A)_{m_1\times m_2\times\dots\times m_k\times a}, \\ (B)_{m_1\times m_2\times\dots\times m_k\times b_1\times\dots\times b_s}. \end{cases}$$

We define the special tensorial array operation $C = A\tilde{\otimes}B$ as:

$$C(j_1,...,j_{k-1},:,j_{k+1},...,j_{k+s}) = A(j_1,...,j_{k-1},:,:)'\cdot B(j_1,...,j_{k-1},:,j_{k+1},...,j_{k+s}),$$

where $\cdot$ denotes the usual product of matrix times a vector.

It is straightforward that $\dim(C) = m_1\times m_2\times\dots\times m_{k-1}\times a\times b_1\times\dots\times b_s$.

multiprod command is employed again to implement the special tensorial array operation.

The *tensorial valuation* for the reduced bases polynomial can be written as:

$$Q^{\mathbf{N}^\Phi_\epsilon} = A^1_{i_1}(\eta_1)\tilde{\otimes}\left(\dots\tilde{\otimes}\left(A^{n-2}_{i_{1,n-2}}(\eta_{n-2})\tilde{\otimes}\left(A^{n-1}_{i_{1,n-1}}(\eta_{n-1})\tilde{\otimes}q^{n-1}_{i_{1,n-1}}(\eta_n)\right)\right)\dots\right),$$

where again the order fixed by the parenthesis must be strictly followed in order to be consistent with the dimensions of the arrays.

The result will be a $q_1\times q_2\times\dots\times q_n$-dimensional array which contains the evaluation of the polynomial with all the possible combinations of the given values to each of the variables.

1.4.3 Comments about the Reduced Bases method.

Although in the numerical experiments we will see that the results are quite good in the sense of reduction of memory requirements and computational time cost, we must point that the procedure presented could be improved.

We remark that $Q^{\boldsymbol{N}^{\Phi}_{\epsilon}}$ is not optimal in various senses. First of all, the hierarchical criteria to select the function bases is not necessarily the optimal. For example, there might exist a combination of several function bases that give a less overall error than the ones chosen by our criterium. The selection criterium that we employ is very fast because, when we have to order hierarchically the function bases in each step, we only need to reevaluate the function bases that have not already been ordered.

Another factor that could be improved is the criterium for truncation. We can orthonormally decompose the whole polynomial hierarchically

$$P^{\boldsymbol{N}} = \sum_{i_1,i_2,\ldots,i_{n-1}}^{N_1,N_2,\ldots,N_{n-1}} A^1_{i_1}(x_1)A^2_{i_1,i_2}(x_2)\ldots A^{n-1}_{i_1,i_2,\ldots,i_{n-1}}(x_{n-1})q^{n-1}_{i_1,i_2,\ldots,i_{n-1}}(x_n),$$

and notice that we can independently truncate one branch of the tree or another. For example:

$$P^{\boldsymbol{N}} \approx \sum_{i_1,i_2,\ldots,i_{n-1}}^{M_1,N_2,N_3\ldots,N_{n-1}} A^1_{i_1}(x_1)A^2_{i_1,i_2}(x_2)\ldots A^{n-1}_{i_1,i_2,\ldots,i_{n-1}}(x_{n-1})q^{n-1}_{i_1,i_2,\ldots,i_{n-1}}(x_n),$$

or

$$P^{\boldsymbol{N}} \approx \sum_{i_1,i_2,\ldots,i_{n-1}}^{N_1,M_2,N_3,\ldots,N_{n-1}} A^1_{i_1}(x_1)A^2_{i_1,i_2}(x_2)\ldots A^{n-1}_{i_1,i_2,\ldots,i_{n-1}}(x_{n-1})q^{n-1}_{i_1,i_2,\ldots,i_{n-1}}(x_n).$$

Our procedure does not maximize memory savings over the whole polynomial. A method which maximizes the memory savings versus the deterioration of the error when we truncate function bases of one or other variable could be designed.

1.5 Numerical Results

We are going to apply the Reduced Bases procedure developed in Section 1.4 to polynomial $I_{\mathbf{12}}F$ built in Subsection 1.3.3.

As mentioned before, although a different set of points could be used, the set of points employed in the Hierarchical procedure will be the set of interpolation points employed in the construction of the interpolation polynomial $I_{\mathbf{12}}F$, i.e. the Chebyshev nodes $\Phi = \{\boldsymbol{\alpha_l}\}_{\boldsymbol{l}\in L^{\boldsymbol{N}}}$.

We also want to know how the new polynomial valuates option prices over the whole domain $\tilde{\Omega}$. In order to check this, we are going to employ Sample $\boldsymbol{\Theta}_7$ ($\approx 1.68\cdot 10^6$ contracts) defined in Subsection 1.3.3, whose points do not correspond to those of Φ and are equally distributed over $\tilde{\Omega}$.

The first experiment that we are going to do is to check the numerical results when just **Step 1** of the algorithm of the Hierarchical orthonormalization is applied. Once we have

decomposed

$$I_{\mathbf{12}}F \approx \sum_{k=0}^{M_1} A^1_{j_k}(x_1) q_{j_k}(x_2, ..., x_n),$$

for $M_1 = 0, 1, ..., 12$, we check how does the approximation valuates options, both in Sample Φ and in Sample $\mathbf{\Theta}_7$.

The following table shows the number of function bases retained (M_1+1), the total storage cost in each case and the Mean Square Error when they are employed to compute the option prices of Sample Φ and of Sample $\mathbf{\Theta}_7$.

Function Bases	Storage cost (bytes)	$\text{MSE}_{\text{Sample } \Phi}$	$\text{MSE}_{\text{Sample } \mathbf{\Theta}_7}$
1	$5.01 \cdot 10^8$	$3.41 \cdot 10^{-4}$	$2.5459961130 \cdot 10^{-4}$
2	$1.00 \cdot 10^9$	$0.14 \cdot 10^{-4}$	$0.0886299162 \cdot 10^{-4}$
3	$1.51 \cdot 10^9$	$3.79 \cdot 10^{-6}$	$0.0241547107 \cdot 10^{-4}$
4	$2.00 \cdot 10^9$	$8.53 \cdot 10^{-7}$	$0.0180563533 \cdot 10^{-4}$
5	$2.50 \cdot 10^9$	$6.72 \cdot 10^{-8}$	$0.0123753987 \cdot 10^{-4}$
6	$3.01 \cdot 10^9$	$8.79 \cdot 10^{-9}$	$0.0121988751 \cdot 10^{-4}$
7	$3.51 \cdot 10^9$	$2.30 \cdot 10^{-9}$	$0.0120682703 \cdot 10^{-4}$
8	$4.01 \cdot 10^9$	$3.89 \cdot 10^{-10}$	$0.0120340513 \cdot 10^{-4}$
9	$4.51 \cdot 10^9$	$5.29 \cdot 10^{-11}$	$0.0120324036 \cdot 10^{-4}$
10	$5.01 \cdot 10^9$	$1.77 \cdot 10^{-12}$	$0.0120330154 \cdot 10^{-4}$
11	$5.52 \cdot 10^9$	$2.33 \cdot 10^{-14}$	$0.0120330374 \cdot 10^{-4}$
12	$6.02 \cdot 10^9$	$3.22 \cdot 10^{-16}$	$0.0120330568 \cdot 10^{-4}$
13	$6.52 \cdot 10^9$	$1.18 \cdot 10^{-28}$	$0.0120330555 \cdot 10^{-4}$
$I_{\mathbf{12}}F$	$6.52 \cdot 10^9$	0	$0.0120330555 \cdot 10^{-4}$

Table 1.4: Number of function bases retained after **Step 1** of the Hierarchical orthonormalization. We include the storage costs in each case and the MSE committed when evaluating Sample Φ and Sample $\mathbf{\Theta}_7$.

In the previous table we can check that, as expected, the error over Sample Φ worsens each time that we discard one of the function bases. But our objective is to obtain a polynomial which valuates options over the whole domain $\tilde{\Omega}$, not just over Sample Φ.

The global error is represented by $\text{MSE}_{\text{Sample } \mathbf{\Theta}_7}$. Note that with just 5 or 6 function bases for the first variable, we obtain a polynomial which valuates with comparable accuracy as $I_{\mathbf{12}}F$ but which requires half the storage cost.

We run now the Hierarchical orthonormalization algorithm completely (**Steps 1-7**). We fix three different values of the parameter ϵ. Remember that ϵ limits the maximum Mean Square Error allowed when we evaluate Sample Φ with the polynomials obtained from the procedure.

In the following table, we include the memory requirements of each polynomial and the error committed when they are employed to compute the contracts of Sample $\mathbf{\Theta}_7$.

	ϵ	MSE (Sample $\mathbf{\Theta}_7$)	Storage cost (bytes)	Memory Savings
$I_{\mathbf{12}}F$		$0.01203 \cdot 10^{-4}$	$6.52 \cdot 10^{9}$	
Q_1	$4 \cdot 10^{-7}$	$0.01194 \cdot 10^{-4}$	$6.263 \cdot 10^{7}$	99.038 %
Q_2	$5.5 \cdot 10^{-7}$	$0.01229 \cdot 10^{-4}$	$4.431 \cdot 10^{7}$	99.319 %
Q_3	$6 \cdot 10^{-7}$	$0.01249 \cdot 10^{-4}$	$3.325 \cdot 10^{7}$	99.489 %

Table 1.5: Mean Square Error committed when evaluating Sample $\mathbf{\Theta}_7$ with three different polynomials constructed from $I_{\mathbf{12}}F$ after applying the Hierarchical orthonormalization procedure. We include the storage cost and the memory savings with respect to the storage cost of $I_{\mathbf{12}}F$.

The previous table shows that with the Reduced Bases approach we obtain much smaller polynomials (in memory terms) which give an overall error of the same order as the original $I_{\mathbf{12}}F$. We remark that, as expected, if $\epsilon \to 0$, the error committed when evaluating Sample $\mathbf{\Theta}_7$ converges to $0.01203 \cdot 10^{-4}$, the interpolation error of $I_{\mathbf{12}}F$.

Concerning the computational cost, we recall that B-F method admits tensorial valuation in three variables: volatility, stock price and maturity. We define the following sets of points:

1. One value for each of the variables: 1 contract.
2. 7 different stock prices, 6 different volatilities, 5 different maturities and one value for the rest of the variables: 210 contracts.
3. Sample $\mathbf{\Theta}_7$, i.e. 6 different values for each of the variables: 1679616 contracts

We remark that evaluate Sample $\mathbf{\Theta}_7$ would be equivalent to price options in the real market for several stocks with different parameter values for the NGARCH(1,1) model. The following table summarizes the results.

	1 contract	210 contracts	Sample $\mathbf{\Theta}_7$ ($\approx 1.68 \cdot 10^6$ contracts)
B-F method	41 s	41 s	$3 \cdot 10^5$ s
$I_{\mathbf{12}}F$	91 s	91 s	91 s
Q_1	0.301 s	0.303 s	0.768 s
Q_2	0.216 s	0.218 s	0.583 s
Q_3	0.162 s	0.164 s	0.499 s

Table 1.6: Computational cost of evaluating different sets of contracts with B-F method, the interpolation polynomial $I_{\mathbf{12}}F$ and different polynomials constructed from $I_{\mathbf{12}}F$ with the Reduced Bases approach.

B-F method needs the same time for computing 1 or 210 contracts (because it admits tensorial valuation for S, σ_0^2 and T). For computing Sample $\mathbf{\Theta}_7$, B-F method needs to be evaluated for each different value of $\{\beta_0, \beta_1, \beta_2, r, (\lambda + \theta)\}$, which requires 7776 different evaluations of 41 seconds each.

$I_{\mathbf{12}}F$ requires the same computational time in the three examples because, as it was mentioned in Subsection 1.3.3, the polynomial is too big and it has to be stored in different parts. The computational cost is due to several employments of function *load*.

With the polynomials obtained from the Reduced Bases approach, we have retrieved the *tensorial valuation* velocity achieved when we were working with the smaller polynomials $I_{\mathbf{3}}F$, $I_{\mathbf{6}}F$ but with more precision. This can be checked in the following table.

	MSE (Sample $\mathbf{\Theta}_7$)	Memory Storage (bytes)	Computational cost
$I_{\mathbf{3}}F$	$0.69186 \cdot 10^{-4}$	$5.24 \cdot 10^{5}$	0.11 s
$I_{\mathbf{6}}F$	$0.12298 \cdot 10^{-4}$	$4.61 \cdot 10^{7}$	0.46 s
Q_3	$0.01249 \cdot 10^{-4}$	$3.325 \cdot 10^{7}$	0.49 s

Table 1.7: Mean Square Error committed by interpolation polynomials $I_{\mathbf{3}}F$ and $I_{\mathbf{6}}F$ and by polynomial Q_3 when evaluating Sample $\mathbf{\Theta}_7$, their storage cost and their computational cost when used to evaluate Sample $\mathbf{\Theta}_7$.

As we can see in the previous table, polynomial Q_3 requires the same memory storage as $I_{\mathbf{6}}F$ but it gives one digit more of precision. Now we have polynomials that can be stored in memory without problems and are capable of valuate multiple option prices for several model parameter values at once.

Finally, we check the performance of polynomials Q_i when they are applied to the problem of estimating parameters with real market data. Concerning the In the Sample analysis, the results are plotted in Figure 1.6.

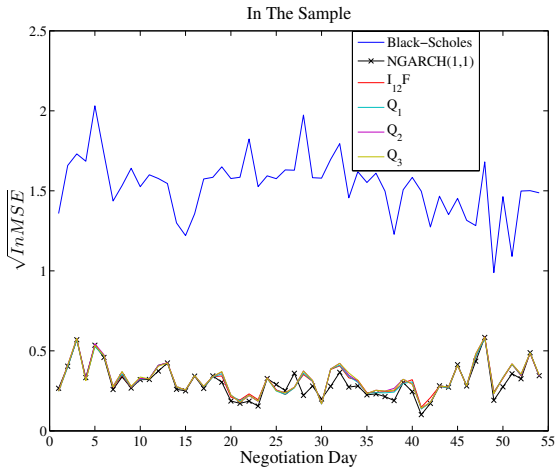

Figure 1.6: Error, in monetary terms, of the In the Sample analysis. We plot each negotiation day t_0 (horizontal axis) vs the root of the InMSE (vertical axis) of Black-Scholes (blue), B-F(NGARCH(1,1)) (black), $I_{\mathbf{12}}F$ (red), Q_1 (cyan), Q_2 (violet), Q_3 (yellow).

On the previous picture we can observe the difference between B-F method and $I_{\mathbf{12}}F$ due to the interpolation error. We can also observe that polynomials Q_i are fairly close to $I_{\mathbf{12}}F$. Polynomials $Q_i, i = 1, 2, 3$ outperform Black-Scholes every day.

The average In the Sample error committed in 1992 has been:

	Black-Scholes	B-F	$I_{\mathbf{12}}F$	Q_1	Q_2	Q_3
Mean$\left(\sqrt{\text{InMSE}}\right)$	1.53	0.303	0.321	0.319	0.324	0.323

Table 1.8: Mean error, in monetary terms, committed when adjusting model parameters to traded option prices with the Black-Scholes model, Garch, interpolation polynomial $I_{\mathbf{12}}F$ and the three different polynomials obtained after applying the Reduction Bases approach.

We can compute the mean of the absolute value of the daily difference (MDD) between each of the polynomials Q_i and $I_{\mathbf{12}}F$ to see how much have they moved away from $I_{\mathbf{12}}F$:

$$\text{InMDD}_{Q_i} = \frac{1}{54}\sum_{j=1}^{54}\left|\sqrt{\text{InMSE}}_j^{Q_i} - \sqrt{\text{InMSE}}_j^{I_{\mathbf{12}}F}\right|,$$

which gives

	Q_1	Q_2	Q_3
InMDD_{Q_i}	0.00482	0.00806	0.00811

Table 1.9: Mean of the absolute value of the daily monetary error difference between interpolation polynomial $I_{\mathbf{12}}F$ and polynomials Q_i, when adjusting model parameters.

This table, jointly with the previous one, show that while ϵ grows (moderately), we move away from $I_{\mathbf{12}}F$ more and more. Some days achieve a better adjust while others get a worse one. Obviously, until certain limit value of ϵ, where the error will grow much more.

Concerning the Out the Sample analysis, the following Figure shows the results obtained:

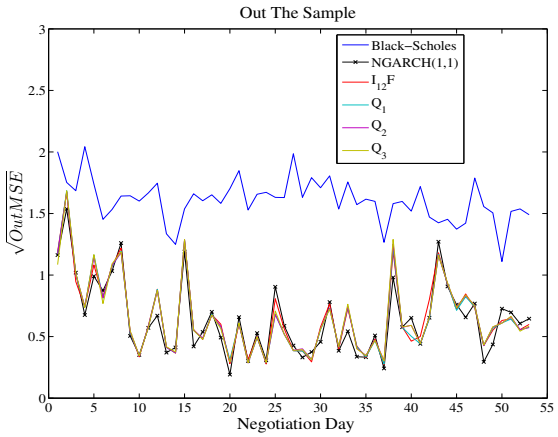

Figure 1.7: Error, in monetary terms, of the Out the Sample analysis. We plot each negotiation day t_0 (horizontal axis) vs the root of the OutMSE (vertical axis) of Black-Scholes (blue), B-F (NGARCH(1,1)) (black), $I_{\mathbf{12}}F$ (red), Q_1 (cyan), Q_2 (violet), Q_3 (yellow).

The previous Figure implies that the Reduced Basis approach is consistent. The polynomials obtained with it can be employed to predict option prices from the market.

The average Out the Sample error committed in 1992 has been:

	Black-Scholes	B-F	$I_{\mathbf{12}}F$	Q_1	Q_2	Q_3
$\text{Mean}\left(\sqrt{\text{OutMSE}}\right)$	1.60	0.642	0.664	0.658	0.662	0.662

Table 1.10: Error, in monetary terms, when predicting traded option prices with the Black-Scholes model, Garch, interpolation polynomial $I_{\mathbf{12}}F$ and three polynomials obtained after applying the Reduction Bases approach.

We also compute the mean of the absolute value of the daily difference between each of the polynomials Q_i and $I_{\mathbf{12}}F$.

$$\text{OutMDD}_{Q_i} = \frac{1}{53}\sum_{j=1}^{53}\left|\sqrt{\text{OutMSE}}_j^{Q_i} - \sqrt{\text{OutMSE}}_j^{I_{\mathbf{12}}F}\right|,$$

which gives

	Q_1	Q_2	Q_3
OutMDD_{Q_i}	0.0203	0.0241	0.0286

Table 1.11: Mean of the absolute value of the daily monetary error difference between interpolation polynomial $I_{\mathbf{12}}F$ and and polynomials Q_i, when predicting traded option prices.

This table and the previous one give the same conclusions as the ones of the In the Sample analysis. This analysis can be also seen as a consistency one. Although slightly different parameters were obtained for each of the Q_i in the In the Sample analysis, the new prices obtained when trying to predict with each polynomial Q_i are fairly close.

Concerning the computational cost of the In the Sample analysis (a least square search), we point out that while with the usual methods (Monte-Carlo, Lattice, Spectral) it takes several minutes to estimate the parameters of one negotiation day t_0, this can be done in a few seconds with polynomials Q_i.

Chapter 2

Option Pricing with Variable Interest Rates.

2.1 Introduction

In the previous Chapter, GARCH models were introduced in order to obtain an approximation to the stock's dynamics more realistic than the Black-Scholes dynamics. The objective of this Chapter is to study the other component of the Option replicating portfolio, the bond.

We recall that in the Black-Scholes model, the bond's dynamics is deterministic. However, the market trades several bonds with different risk-free rates. Furthermore, traded risk-free rates do not remain constant in time.

It is usually assumed that, specially for short maturities, constant interest rates can be used for the purpose of pricing options. Moreover, a deeper study is certainly of interest.

When a constant interest rate is assumed $r(t) \equiv r_0$, the bond price is given by the formula

$$B(t_0, T) = e^{-r_0(T-t_0)}, \tag{2.1}$$

where t_0 denotes the current date and T denotes maturity.

For the rest of the Chapter, we denote by $B^{3-US}\left(t_0, t_0 + \frac{1}{4}\right)$ the price of the 3 months US Treasury Bond negotiated at date t_0 in the Bond market (with t measured in years). We denote by $r_{t_0}^{3-US}$ the annualized constant risk-free rate of the 3-month US Treasury Bond, i.e. the value which satisfies, at date t_0, that

$$B^{3-US}\left(t_0, t_0 + \frac{1}{4}\right) = e^{-\frac{1}{4} r_{t_0}^{3-US}}. \tag{2.2}$$

As a first approach, we will employ the NGARCH(1,1) model defined in equation (1.11). We will perform a daily In the Sample analysis with the S&P500 European Option contracts negotiated on Wednesdays between 1990 and 1992, as described in Subsection 1.2.1. The interest rate r of the NGARCH(1,1) model is treated just as another parameter that must be estimated from traded option prices on day t_0.

The results obtained are plotted in Figure 2.1. In the left side we have plotted, for each Wednesday t_0 between 1990 and 1992, the value of $r_{t_0}^{3-US}$ (blue) and the estimated value r_{t_0} (red). In the right side, we have plotted the estimated variance (green) of the market for each negotiation day (σ_0^2 of NGARCH(1,1) model at date t_0).

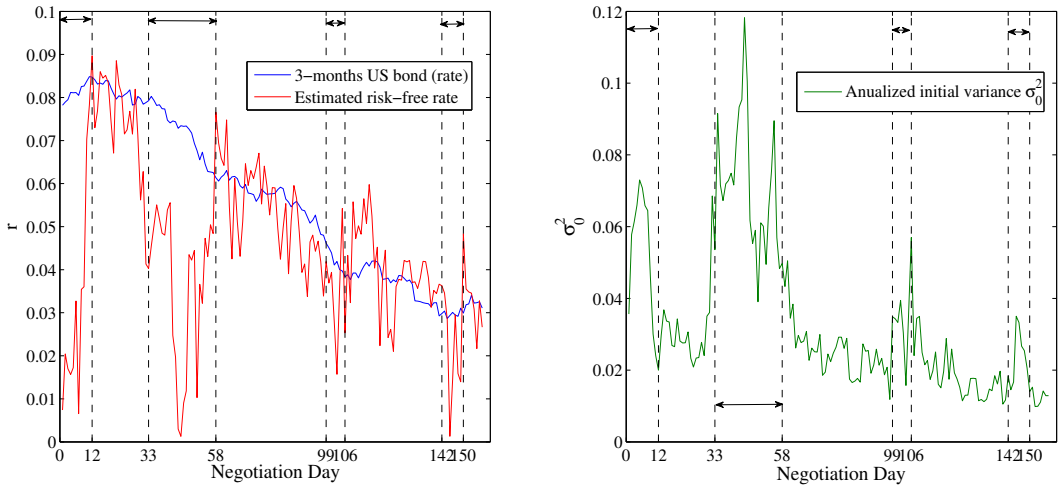

Figure 2.1: On both Figures we plot each negotiation day t_0 (horizontal axis) vs the estimated (from option prices) risk-free rate (left-red), the negotiated rate in the bond market, r^{3-US} (left-blue) and the estimated (from option prices) initial variance (σ_0^2 of NGARCH(1,1) (right-green).

As we can observe on the left side of Figure 2.1, the values of $r_{t_0}^{3-US}$ and r_{t_0} are pretty close many days. Nevertheless, there are some discrepancies at zones marked between discontinuous vertical lines, and which correspond to high volatility periods in the stock market (implied variance σ_0^2 of option prices), as it can be checked on the right side of Figure 2.1. The previous results show that the interest rate of the pricing model is closely related with the one negotiated in the bond market, except at periods of high volatility, where the model is unable to reproduce the market behaviour.

The first natural extension is to consider deterministic variable interest rates in the context of the NGARCH(1,1) model. In Section 2.2, following the line presented in [24], we include a proof of the valuation formula for this case. An alternative proof, following the line of [40], can also be derived.

Though this model may be a good first approach, it has several shortcomings. The usual models for variable interest rates tend to have several parameters and they have also to be estimated. If we do so just employing the traded options, we found ourselves with very few data (around 60 contracts per day and just four different maturities) that make it unlikely that the parameter estimation will produce a reasonable fit.

A way of constructing a model without increasing unacceptably the number of parameters

is to consider variable stochastic interest rates, assuming that the stock and the bond share the same underlying volatility process. In Section 2.3 a continuous model with Stochastic Volatility (SV) and Stochastic Interest Rates (SIR) is derived. Starting from Heston's SV model, introduced in [34], an extension that allows SIR will be derived, following the lines proposed in the same article.

An explicit formula for the bond and a semi-explicit formula for the option price will be given and analysis with real market data will be carried out. The results will be presented in Section 2.4.

2.2 GARCH with variable deterministic interest rates

Let $(\Omega, \mathscr{F}, P)$ be a filtered probability space, where P denotes the physical probability measure.

The initial hypothesis that we need are:

1. Future interest rates (r_t) are considered deterministic.

2. Interest rates only change at discrete times and are right continuous.

3. Under the physical probability measure, the stock $(\bar{S}_t)$ dynamics is given by:

$$\begin{cases} \ln\left(\dfrac{\bar{S}_t}{\bar{S}_{t-1}}\right) \equiv \bar{R}_t = r_{t-1} + \lambda\sqrt{\sigma_t^2} - \dfrac{1}{2}\sigma_t^2 + \sqrt{\sigma_t^2}\bar{z}_t, \\ \sigma_t^2 = g(\sigma_{t'}^2, \bar{z}_{t'}), \quad t' \leq t-1, \end{cases} \tag{2.3}$$

where λ is a constant, $r_t = r(t)$ is a (known a priori) function of time, positive, right continuous and which only changes at discrete times, g is a given function (which corresponds to a GARCH specification) and $\bar{z}_t | \mathscr{F}_{t-1}$ is a normally distributed random variable with 0 mean and variance 1.

Following the line presented in [24], we define:

Definition 2.2.1. *A probability measure Q is said to satisfy the locally Risk-Neutral valuation relationship with variable Deterministic Rate (RNDR) if:*

1. *Q is absolutely continuous with respect to the physical measure P.*
2. $\left.\dfrac{\bar{S}_t}{\bar{S}_{t-1}}\right| \mathscr{F}_{t-1}$ *has a log-normal distribution under Q.*
3. $E^Q\left(\left.\dfrac{\bar{S}_t}{\bar{S}_{t-1}}\right| \mathscr{F}_{t-1}\right) = e^{r_{t-1}}$.
4. $Var^Q\left(\left.\dfrac{\bar{S}_t}{\bar{S}_{t-1}}\right| \mathscr{F}_{t-1}\right) = Var^P\left(\left.\dfrac{\bar{S}_t}{\bar{S}_{t-1}}\right| \mathscr{F}_{t-1}\right) = \sigma_t^2$.

almost surely with respect to measure P.

The results that we are going to present are very similar to the ones in [24]. Prior to the main theorems, we present a definition and two auxiliary lemmas that will be needed.

Given $\bar{Z}_t$, a random variable such that $\bar{Z}_t \big| \mathscr{F}_{t-1}$ is normally distributed with 0 mean and variance K under probability P, we define a new measure Q by:

$$dQ = e^{\sum_{t=1}^{t=T} (r_{t-1} - \rho + \bar{Y}_t)} dP. \tag{2.4}$$

where

$$\begin{cases} \bar{Y}_t = \nu_{t-1} + \bar{Z}_t, \\ \nu_{t-1} = -r_{t-1} + \rho - \dfrac{K^2}{2}, \end{cases} \tag{2.5}$$

and ρ is a constant.

Lemma 2.2.1. *Q is a probability measure absolutely continuous with respect to measure P. Furthermore, for each random variable $\bar{W}_t$ that is $\mathscr{F}_t$-measurable, we have that*

$$E^Q(\bar{W}_t | \mathscr{F}_{t-1}) = E^P(\bar{W}_t e^{(r_{t-1} - \rho) + \bar{Y}_t} | \mathscr{F}_{t-1}).$$

Proof. By the definition of $\bar{Y}_t$, it is clear that

$$\sum_{t=1}^{T} (r_{t-1} - \rho + \bar{Y}_t) = \sum_{t=1}^{T} (r_{t-1} - \rho + \nu_{t-1} + \bar{Z}_t) = \sum_{t=1}^{T} \left(\bar{Z}_t - \frac{K^2}{2} \right),$$

where we recall that $\bar{Z}_t$ is a random variable such that $\bar{Z}_t \big| \mathscr{F}_{t-1}$ is normally distributed with 0 mean and variance K under probability P. Therefore,

$$E^P(e^{-\rho + \bar{Y}_t} | \mathscr{F}_{t-1}) = e^{-r_{t-1}}.$$

Let us check that Q is a probability measure $\left(\int_\Omega 1 dQ = 1 \right)$.

$$\int_\Omega 1 dQ = E^P \left[e^{\sum_{i=1}^{T} (r_{i-1} - \rho + \bar{Y}_i)} \middle| \mathscr{F}_0 \right] = E^P \left[e^{\sum_{i=1}^{T-1} (r_{i-1} - \rho + \bar{Y}_i)} e^{r_{T-1} - \rho + \bar{Y}_T} \middle| \mathscr{F}_0 \right] =$$

$$= E^P \left[e^{\sum_{i=1}^{T-1} (r_{i-1} - \rho + \bar{Y}_i)} e^{r_{T-1}} E^P(e^{-\rho + \bar{Y}_T} | \mathscr{F}_{T-1}) \middle| \mathscr{F}_0 \right] = E^P \left[e^{\sum_{i=1}^{T-1} (r_{i-1} - \rho + \bar{Y}_i)} \middle| \mathscr{F}_0 \right],$$

so, we obtain the desired result reasoning recursively.

The second part of the Lemma is given by Radon-Nikodym's theorem. □

Although we detail it below (see Theorem 2.2.1), we mention now that, under the hypothesis over the representative agent and the utility function, it exists a probability measure Q, given as in (2.4), such that

$$\bar{S}_{t-1} = E^P(e^{-\rho+\bar{Y}_t}\bar{S}_t|\mathscr{F}_{t-1}) \tag{2.6}$$

Lemma 2.2.2. *Suppose that $\bar{S}_t$ follows (2.3) under probability P and that (2.6) holds. This implies:*

1. $\left.\frac{\bar{S}_t}{\bar{S}_{t-1}}\right| \mathscr{F}_{t-1}$ *has a log-normal distribution under Q.*
2. $E^Q\left(\left.\frac{\bar{S}_t}{\bar{S}_{t-1}}\right| \mathscr{F}_{t-1}\right) = e^{r_{t-1}}$.
3. $Var^Q\left(\left.\frac{\bar{S}_t}{\bar{S}_{t-1}}\right| \mathscr{F}_{t-1}\right) = Var^P\left(\left.\frac{\bar{S}_t}{\bar{S}_{t-1}}\right| \mathscr{F}_{t-1}\right) = \sigma_t^2$ *a.s. with respect to measure Q.*

Proof. In order to prove statement (2), we use Lemma 2.2.1:

$$E^Q\left(\left.\frac{\bar{S}_t}{\bar{S}_{t-1}}\right| \mathscr{F}_{t-1}\right) = E^P\left(\left.\frac{\bar{S}_t}{\bar{S}_{t-1}}e^{(r_{t-1}-\rho)+\bar{Y}_t}\right| \mathscr{F}_{t-1}\right) = \frac{e^{r_{t-1}}}{S_{t-1}}E^P(\bar{S}_t e^{-\rho+\bar{Y}_t}|\mathscr{F}_{t-1}) = e^{r_{t-1}}.$$

by the hypothesis of the lemma.

To prove statements (1) and (3), consider the conditional moment generating function

$$\bar{W}_t = \log\left(\frac{\bar{S}_t}{\bar{S}_{t-1}}\right)$$

under measure Q. Thus,

$$E^Q\left(\left.e^{c\bar{W}_t}\right| \mathscr{F}_{t-1}\right) = E^P\left(\left.e^{c\bar{W}_t+(r_{t-1}-\rho)+\bar{Y}_t}\right| \mathscr{F}_{t-1}\right),$$

where c is a constant.

Under measure P, since $\bar{S}_t$ follows process (2.3), it holds that $\bar{W}_t\big| \mathscr{F}_{t-1}$ is normally distributed, with variance σ_t^2 and mean $\mu_t = E^P\left(\left.\log\left(\frac{\bar{S}_t}{\bar{S}_{t-1}}\right)\right| \mathscr{F}_{t-1}\right) = r_{t-1} + \lambda\sqrt{\sigma_t^2}$.

On the other hand, $\bar{Y}_t$ is $\mathscr{F}_{t-1}$-conditionally normal, thus

$$\bar{Y}_t = \alpha + \beta\bar{W}_t + \bar{U}_t,$$

where $\bar{W}_t$ and $\bar{U}_t$ are independent normal processes and $\alpha,\ \beta$ are constants. It holds that

$$\begin{aligned}
E^Q\left(\left.e^{c\bar{W}_t}\right| \mathscr{F}_{t-1}\right) &= e^{\alpha+(r_{t-1}-\rho)}E^P\left(\left.e^{(\beta+c)\bar{W}_t+\bar{U}_t}\right| \mathscr{F}_{t-1}\right) \\
&= e^{\alpha+(r_{t-1}-\rho)+\frac{E\left(\left.\bar{U}_t^2\right|\mathscr{F}_{t-1}\right)}{2}}E^P\left(\left.e^{(\beta+c)\bar{W}_t}\right| \mathscr{F}_{t-1}\right) \\
&= e^{\alpha+(r_{t-1}-\rho)+\frac{E\left(\left.\bar{U}_t^2\right|\mathscr{F}_{t-1}\right)}{2}+\beta\mu_t+\beta^2\frac{\sigma_t^2}{2}+c(\mu_t+\beta\sigma_t^2)+c^2\frac{\sigma_t^2}{2}}.
\end{aligned}$$

Now, if $c = 0$,

$$e^{\alpha+(r_{t-1}-\rho)+\frac{E\left(\bar{U}_t^2\middle|\mathscr{F}_{t-1}\right)}{2}+\beta\mu_t+\beta^2\frac{\sigma_t^2}{2}} = 1,$$

since $E^Q\left(1\middle|\mathscr{F}_{t-1}\right) = 1$. This leads us to

$$E^Q\left(e^{cW_t}\middle|\mathscr{F}_{t-1}\right) = e^{c(\mu_t+\beta\sigma_t^2)+c^2\frac{\sigma_t^2}{2}},$$

which implies that

$$\log\left(\left(\frac{\bar{S}_t}{\bar{S}_{t-1}}\right)\middle|\mathscr{F}_{t-1}\right)$$

is normally distributed with mean $\mu_t + \beta\sigma_t^2$ and variance σ_t^2 under measure Q.

□

Definition 2.2.2. *A utility function $U(x)$ is a strictly increasing and strictly concave function with continuous second order derivative.*

The increasing property models that investors prefer more to less (wealth or consumption) and the concave property models that investors are risk-averse.

Definition 2.2.3. *The coefficient of absolute risk aversion for a given utility function $U(x)$, is*

$$R_a(x) = -\frac{U''(x)}{U'(x)}, \tag{2.7}$$

and the coefficient of relative risk aversion is defined by

$$R_r(x) = xR_a(x). \tag{2.8}$$

Theorem 2.2.1. *If the representative agent is an expected utility maximizer and the utility function is time separable and additive, then RNDR holds under any of the following two conditions:*

1. *The utility function is of constant relative risk aversion and changes in the logarithmic aggregate consumption are distributed normally, under measure P, with deterministic mean (known a priori) and constant variance.*

2. *The utility function is of constant absolute risk aversion and changes in the aggregate consumption are distributed normally, under measure P, with deterministic mean (known a priori) and constant variance.*

Proof. Let $U(C_t)$ and C_t be the utility function and aggregate consumption at instant t. If ρ is the impatience factor, the maximization of the utility function gives the following equation (see [24]):

$$\bar{S}_{t-1} = E^P\left[e^{-\rho}\frac{U'(C_t)}{U'(C_{t-1})}\bar{S}_t\middle|\mathscr{F}_{t-1}\right].$$

If $U(C_t)$ is a utility function of constant absolute risk aversion $R_a(C_t) = \kappa$, then it holds that

$$\frac{U''(C)}{U'(C)} = -\kappa,$$

which implies

$$\int_{t-1}^{t} \frac{U''(C)}{U'(C)} dt = \int_{t-1}^{t} -\kappa dt,$$

leading to

$$\log\left(\frac{U'(C_t)}{U'(C_{t-1})}\right) = -\kappa(C_t - C_{t-1}).$$

On the other hand if $U(C_t)$ is a utility function of relative risk aversion $R_r(C_t) = \kappa$, then it holds that

$$\frac{U''(C)}{U'(C)} = -\frac{\kappa}{C},$$

which employing the same arguments leads to

$$\log\left(\frac{U'(C_t)}{U'(C_{t-1})}\right) = -\kappa \log\left(\frac{C_t}{C_{t-1}}\right).$$

In any case, under the hypothesis of the Theorem, $\ln\left(\frac{U'(C_t)}{U'(C_{t-1})}\right)$ distributes normally. This, jointly with Lemmas 2.2.1 and 2.2.1 completes the proof.

□

Theorem 2.2.2. *The stock's dynamics in measure Q is given by:*

$$\begin{cases} \ln\left(\frac{\bar{S}_t}{\bar{S}_{t-1}}\right) \equiv \bar{R}_t = r_{t-1} - \frac{1}{2}\sigma_t^2 + \sqrt{\sigma_t^2}\bar{\epsilon}_t, \\ \qquad\qquad \sigma_t^2 = g(\sigma_{t'}^2, \bar{\epsilon}_{t'} - \lambda), \quad t' \leq t-1. \end{cases}$$

where $\bar{\epsilon}_t$ is a normally distributed random variable with mean 0 and variance 1.

Proof. Identical to the one of Theorem 2.2 in [24] with the corresponding r_{t-1}.

□

Corollary 2.2.1.

$$\bar{S}_T = \bar{S}_t \exp\left[\sum_{i=t+1}^{T} r_{i-1} - \frac{1}{2}\sum_{i=t+1}^{T} \sigma_i^2 + \sum_{i=t+1}^{T} \bar{\epsilon}_i\right].$$

Corollary 2.2.2. *The discounted price process $e^{-\sum_{i=1}^{T} r_{i-1}} \bar{S}_t$ is a Q-martingale.*

Corollary 2.2.3. *The price of the European Option price is given by the conditional expectation:*

$$C(S) = e^{-\sum_{i=t+1}^{T} r_{i-1}} E^Q\left[\max(\bar{S}_T - K, 0) | \bar{S}_t = S\right].$$

There are two different possibilities to estimate the model parameter values from market data.

The first one is to do a cross estimation. We fix an interest rate model. With the set of historical data of the Bond market, we estimate its parameter values. Afterwards, we estimate the future interest rates. Assuming that the results obtained for future interest rates are deterministic, we enforce their values into the pricing model of the option.

Another option is to assume that the option price incorporates all the information. On a fixed date t_0, we can try to estimate the parameter values of the pricing model and those of the interest rate model with just the traded options and the bond price on date t_0. This is the criteria that we prefer to follow (and the criteria employed in the analysis of Subsection 1.2.1).

Unfortunately, we usually have very few contracts and very few maturities (around 60 contracts per day with just 4 different maturities). This makes difficult to carry out a parameter estimation with a reasonable fit. If we employ complex rate models, the number of total parameters grows too much and we do not have enough differentiated contracts.

Trying to solve the lack of enough traded contracts, we relaxed the assumption of deterministic rates. The idea is to incorporate a stochastic interest rate model directly to the pricing model of the option. We will modify a continuous pricing model in order to do so. Another objective is to not increase much the total number of parameters, so a good estimation can be carried out with the available contracts.

2.3 Stochastic Volatility and Stochastic Interest Rates

In [34], Heston proposes a Stochastic Volatility model with constant interest rate and derives a semi-explicit valuation formula. Heston also describes, in general terms, how the model could be extended to incorporate Stochastic Interest Rates. This Section is devoted to the construction of an extension of Heston's Stochastic Volatility model with a particular stochastic bond model.

The Subsection will be organized as follows.

First, we will review Heston's original model with constant interest rates.

In a second step, we will make the theoretical development of the extended model as presented in [34].

In a third step, we will search for a stochastic bond formula that can be nested within this framework, i.e., that fits with the specifications of the pricing model. The construction of the bond model must be considered independent of the rest of the text. Our first objective will be

to find an explicit and suitable bond formula that can be incorporated to the pricing model of the option. The second objective will be to do not increase too much the total number of parameters.

Finally, we will assume that the market is composed by the stock and the discounted bond computed in the previous step. We will see that, under certain parameter restrictions, the resulting model is of the type proposed by Heston in [34]. We will derive a semi-explicit formula and obtain a pricing model which has just one more parameter than the original Heston's SV. Thus, we will have incorporated stochastic interest rates without increasing much the number of parameters. Therefore, a satisfactory estimation can be carried out with the available traded contracts.

2.3.1 Heston SV model

We recall that in Heston's model [34], the dynamics is:

$$\begin{cases} d\bar{S}(t) = \mu\bar{S}(t)dt + \sqrt{\bar{v}(t)}\bar{S}(t)d\bar{z}_1(t), \\ d\bar{v}(t) = \kappa[\theta - \bar{v}(t)]dt + \sigma\sqrt{\bar{v}(t)}d\bar{z}_2(t), \end{cases} \tag{2.9}$$

where $\bar{z}_1$ and $\bar{z}_2$ are Wiener processes. Employing the notation of [3] or [34], we define the (instantaneous) correlation coefficient ρ by

$$\rho dt = \mathrm{Cov}(d\bar{z}_1, d\bar{z}_2) \tag{2.10}$$

where $\mathrm{Cov}(.\,,.\,)$ stands for covariance.

We assume that a constant rate risk-free bond exists: $B(t,T) = e^{-r_0(T-t)}$.

In [34], it is claimed that these assumptions are insufficient to price contingent claims, because we have not made an assumption that gives the price of "volatility risk". By no arbitrage arguments (see [3] or [34]), the value of any claim must satisfy:

$$\frac{1}{2}vS^2\frac{\partial^2 U}{\partial S^2} + \rho\sigma vS\frac{\partial^2 U}{\partial S\partial v} + \frac{1}{2}\sigma^2 v\frac{\partial^2 U}{\partial v^2} + r_0 S\frac{\partial U}{\partial S} + (\kappa(\theta - v) - \lambda(S,v,t))\frac{\partial U}{\partial v} - r_0 U + \frac{\partial U}{\partial t} = 0 \tag{2.11}$$

where $\bar{S}(t) = S$, $\bar{v}(t) = v$ and $\lambda(S,v,t)$ represents the price of volatility risk.

For the rest of the Chapter, we will assume that any risk premia is of the form $\lambda(S,v,t) = \lambda v$. It should be remarked that, once fixed the components of the market, the risk premia is independent of the claim, i. e. the same risk premia is used to price all the claims (see [3]).

Remark 2.3.1. As Heston claims in ([34]), this choice of risk premia is not arbitrary. In the consumption model derived in [8],

$$\lambda(S,v,t)dt = \gamma\mathrm{Cov}\left[d\bar{v}, \frac{d\bar{C}}{\bar{C}}\right],$$

where γ is the relative risk aversion of an investor, $\bar{C}(t)$ is the consumption and $\mathrm{Cov}(.,.)$ denotes the covariance. The consumption process in [17] is

$$d\bar{C}(t) = \mu_c \bar{v}(t)\bar{C}(t)dt + \sigma_c\sqrt{\bar{v}(t)}\bar{C}(t)dz,$$

where consumption growth has constant correlation with the spot-asset return, which leads to the indicated risk premia.

Thus, the price of the European Call Option $U(S,v,t)$ satisfies the partial differential equation:

$$\frac{1}{2}vS^2\frac{\partial^2 U}{\partial S^2} + \rho\sigma vS\frac{\partial^2 U}{\partial S\partial v} + \frac{1}{2}\sigma^2 v\frac{\partial^2 U}{\partial v^2} + r_0 S\frac{\partial U}{\partial S} + (\kappa(\theta - v) - \lambda v)\frac{\partial U}{\partial v} - r_0 U + \frac{\partial U}{\partial t} = 0, \quad (2.12)$$

subject to the following conditions:

$$\begin{aligned} U(S,v,T) &= \max(0, S-K), \\ U(0,v,t) &= 0, \\ \frac{\partial U}{\partial S}(\infty,v,t) &= 1, \\ r_0 S\frac{\partial U}{\partial S} + \kappa\theta\frac{\partial U}{\partial v} - r_0 U + U_t\Big|_{(S,0,t)} &= 0, \\ U(S,\infty,t) &= S. \end{aligned} \quad (2.13)$$

Heston conjectures a solution similar to the Black-Scholes model:

$$U(S,v,t,T,K) = S\cdot R_1 - K\cdot B(t,T)\cdot R_2, \quad (2.14)$$

The following semi-explicit formula for the price of the European Option is obtained

$$U\left(x,v,\tau,\ln(K)\right) = x\cdot R_1\left(x,v,\tau;\ln(K)\right) - \ln(K)\cdot B(t,T)\cdot R_2\left(x,v,\tau;\ln(K)\right), \quad (2.15)$$

where $x = \ln(S)$, $\tau = T - t$ and function $R_j,\ j\in\{1,2\}$ is given by

$$R_j(x,v,\tau;\ln(K)) = \frac{1}{2} + \frac{1}{\pi}\int_0^\infty Re\left[\frac{e^{-i\phi\ln(K)}f_j(x,v,\tau,\phi)}{i\phi}\right]d\phi, \quad (2.16)$$

where

$$\begin{aligned} f_j(x,v,\tau;\phi) &= e^{C(\tau;\phi)+D(\tau;\phi)+i\phi x}, \\ C(\tau;\phi) &= r_0\phi i\tau + \frac{a}{\sigma^2}\left\{(b_j - \rho\sigma\phi i + d)\tau - 2\ln\left[\frac{1-ge^{d\tau}}{1-g}\right]\right\}, \\ D(\tau;\phi) &= \frac{b_j - \rho\sigma\phi i + d}{\sigma^2}\left[\frac{1-e^{d\tau}}{1-ge^{d\tau}}\right], \\ g &= \frac{b_j - \rho\sigma\phi i + d}{b_j - \rho\sigma\phi i - d}, \\ d &= \sqrt{(\rho\sigma\phi i - b_j)^2 - \sigma^2(2\zeta_j\phi i - \phi^2)}, \\ \zeta_1 &= \frac{1}{2}, \quad \zeta_2 = -\frac{1}{2}, \quad a = \kappa\theta, \quad b_1 = \kappa + \lambda - \rho\sigma, \quad b_2 = \kappa + \lambda. \end{aligned} \quad (2.17)$$

The following result is also given in [34]:

Theorem 2.3.1. *Given the processes:*

$$\begin{cases} d\bar{x}(t) = [r_0 + \zeta_j \bar{v}(t)]dt + \sqrt{\bar{v}(t)}d\bar{z}_1, \\ d\bar{v}(t) = (a - b_j)\bar{v}(t)dt + \sigma\sqrt{\bar{v}(t)}d\bar{z}_2, \end{cases}$$

then R_j, given by (2.16)-(2.17), is the probability that the contract finishes "In the money".

$$R_j(x, v, t; \ln(K)) = Pr[\bar{x}(T) \geq \ln(K) | \, \bar{x}(t) = x, \bar{v}(t) = v] \, . \tag{2.18}$$

Proof. See [34]

□

2.3.2 The extended model

We propose (see [34]) the following market dynamics in the physical measure:

$$\begin{cases} d\bar{S}(t) = \mu_S \bar{S}(t)dt + \sigma_s(t)\sqrt{\bar{v}(t)}\bar{S}(t)d\bar{z}_1(t), \\ d\bar{v}(t) = \kappa[\theta - \bar{v}(t)]dt + \sigma\sqrt{\bar{v}(t)}d\bar{z}_2(t), \\ d\bar{B}(t,T) = \mu_b \bar{B}(t,T)dt + \sigma_b(t)\sqrt{\bar{v}(t)}\bar{B}(t,T)d\bar{z}_3(t), \end{cases} \tag{2.19}$$

We also denote

$$\begin{aligned} \rho_{sv}dt &= \text{Cov}(d\bar{z}_1, d\bar{z}_2), \\ \rho_{sb}dt &= \text{Cov}(d\bar{z}_1, d\bar{z}_3), \\ \rho_{vb}dt &= \text{Cov}(d\bar{z}_2, d\bar{z}_3). \end{aligned} \tag{2.20}$$

Let $\bar{\mathbf{X}}(t) = (\bar{S}(t), \bar{v}(t), \bar{B}(t,T))$. Let us assume that the short rate of interest is a deterministic function of the state factors, i.e. $\bar{r} = \bar{r}(\bar{\mathbf{X}}(t))$, (short rates are stochastic but, at any fixed time t, they can be computed from the state of the market). Assuming as in [34] that the risk premia is of the form λv, any claim satisfies the partial differential equation (see [3], pg 218):

$$\begin{aligned} &\frac{\partial U}{\partial t} + \frac{1}{2}\sigma_s^2 v S^2 \frac{\partial^2 U}{\partial S^2} + \frac{1}{2}\sigma^2 v \frac{\partial^2 U}{\partial v^2} + \frac{1}{2}\sigma_b^2 v B^2 \frac{\partial^2 U}{\partial B^2} + \rho_{sv}\sigma_s \sigma S v \frac{\partial^2 U}{\partial s \partial v} + \rho_{sb}\sigma_s \sigma_b v S B \frac{\partial^2 U}{\partial S \partial B} \\ &\quad + \rho_{vb}\sigma_b \sigma B v \frac{\partial^2 U}{\partial v \partial B} + rS\frac{\partial U}{\partial S} + [k(\theta - v) - \lambda v]\frac{\partial U}{\partial v} - rU + rB\frac{\partial U}{\partial B} = 0, \end{aligned} \tag{2.21}$$

where $\bar{\mathbf{X}}(t) = \mathbf{X} = (S, v, B)$, $r = r(\mathbf{X})$ and subject to the terminal condition of the claim (European Call) and proper boundary data (see (2.13)) and $B(T,T) = 1$.

There also exists a risk-neutral measure π. The value of any T-claim $U(t, \mathbf{X})$ is given by the conditional expectation:

$$U(t, \mathbf{X}) = E^{\pi}\left[e^{-\int_t^T \bar{r}(\bar{\mathbf{X}}(s))ds} U(\bar{\mathbf{X}}(T)) \Big| \, \bar{\mathbf{X}}(t) = \mathbf{X} \right], \tag{2.22}$$

and the market dynamics in the risk neutral measure is given by

$$\begin{cases} d\bar{S}(t) = r\bar{S}(t)dt + \sigma_s(t)\sqrt{\bar{v}(t)}\bar{S}(t)d\bar{z}_1(t), \\ d\bar{v}(t) = [k\theta - k\bar{v}(t) - \lambda\bar{v}(t)]dt + \sigma\sqrt{\bar{v}(t)}d\bar{z}_2(t), \\ d\bar{B}(t,T) = r\bar{B}(t,T)dt + \sigma_b(t)\sqrt{\bar{v}(t)}\bar{B}(t,T)d\bar{z}_3(t). \end{cases} \tag{2.23}$$

The change of variable $x = \ln\left(\frac{S}{B(t,T)}\right)$ implies that the PDE in the new variable can be written as:

$$\begin{aligned} &\frac{\partial U}{\partial t} + \left(\frac{1}{2}\sigma_s^2 v + \frac{1}{2}\sigma_b^2 v - \rho_{sb}\sigma_s\sigma_b v\right)\frac{\partial^2 U}{\partial x^2} + \frac{1}{2}\sigma^2 v\frac{\partial^2 U}{\partial v^2} + \frac{1}{2}\sigma_b^2 v B^2\frac{\partial^2 U}{\partial B^2} \\ &+ \left(-\sigma_b^2 vP + \rho_{sb}\sigma_s\sigma_b vB\right)\frac{\partial^2 U}{\partial x\partial B} + \left(\rho_{sv}\sigma_s\sigma v - \rho_{vb}\sigma_b\sigma v\right)\frac{\partial^2 U}{\partial x\partial v} + \left(\rho_{vb}\sigma_b\sigma vB\right)\frac{\partial^2 U}{\partial v\partial B} \\ &+ \left(-\frac{1}{2}\sigma_s^2 v + \frac{1}{2}\sigma_b^2 v\right)\frac{\partial U}{\partial x} + [k(\theta - v) - \lambda v]\frac{\partial U}{\partial v} + rB\frac{\partial U}{\partial B} - rU = 0. \end{aligned} \tag{2.24}$$

Similar to the simple SV model, Heston conjectures a solution of the form:

$$U(t,x,P,v) = e^x B(t,T)R_1(t,x,v) - KB(t,T)R_2(t,x,v), \tag{2.25}$$

Substituting (2.25) into equation (2.24), we obtain that $R_j(t,x,v)$ must satisfy, for $j = 1, 2$:

$$\frac{1}{2}\sigma_x^2 v\frac{\partial^2 R_j}{\partial x^2} + \rho_{xv}\sigma_x\sigma v\frac{\partial^2 R_j}{\partial x\partial v} + \frac{1}{2}\sigma^2 v\frac{\partial^2 R_j}{\partial v^2} + \zeta_j v\frac{\partial R_j}{\partial x} + (a - b_j v)\frac{\partial R_j}{\partial v} + \frac{\partial R_j}{\partial t} = 0, \tag{2.26}$$

where

$$\begin{aligned} \frac{1}{2}\sigma_x^2 &= \frac{1}{2}\sigma_s^2 - \rho_{sb}\sigma_s\sigma_b + \frac{1}{2}\sigma_b^2, \\ \rho_{xv} &= \frac{\rho_{sv}\sigma_s\sigma - \rho_{bv}\sigma_b\sigma}{\sigma_x\sigma}, \\ \zeta_1 &= \frac{1}{2}\sigma_x^2, \quad \zeta_2 = -\frac{1}{2}\sigma_x^2, \quad a = k\theta, \\ b_1 &= k + \lambda - \rho_{sv}\sigma_s\sigma, \\ b_2 &= k + \lambda - \rho_{bv}\sigma_b\sigma, \end{aligned} \tag{2.27}$$

subject to the condition at maturity corresponding to the European Option Call:

$$R_j(T,x,v;\ln(K)) = I_{\{x\geq\ln(K)\}},$$

where I denotes the indicator function.

Remark 2.3.2. In Subsection 2.3.4 we will see that, with the bond model that we are going to propose, short rates are of the form $r = \mu + \beta v$ (μ, β constant) and, using no arbitrage arguments, that the risk premia must be $\lambda(S,P,v,t) = \lambda v$, so we can apply Heston's results.

The following proposition is proven in [34].

Proposition 2.3.1. *Functions R_j, $j \in \{1,2\}$ in (2.25) can be interpreted as the probabilities that process x finishes in the money. There exists a semi-explicit pricing formula (that we derive in Subsection 2.3.4) which is obtained through the characteristic function.*

2.3.3 The stochastic bond.

We are looking for a bond formula which can be nested in (2.19). Longstaff and Schwartz develop in [45] a model for interest rates that we are partly going to use.

The interest rate model derived in [45] depends on 6 different parameters. Since we do not want to increase too much the total number of parameters in the pricing model of the option, we are going to develop a simpler model based in it.

We mentioned before that the construction of the bond model should be considered independent of the rest of the text.

Without loss of generality, we can assume that the bond is offered to the market by an entity (the US government for example), whose unique function in the market is to trade the bond. This bond is constructed, by no arbitrage arguments, upon a certain asset $\bar{Q}$. We assume that asset $\bar{Q}$, although dependant of the state of the market, is only accessible to the the entity which offers the bond. Therefore, any other investor who invests in the market described by (2.19) can only negotiate upon the traded stock $\bar{S}$ and the bond.

We suppose the existence of an asset with dynamics:

$$\begin{cases} d\bar{Q} = (\mu + \delta\bar{v})\bar{Q}dt + \sigma_{\bar{Q}}\sqrt{\bar{v}}\bar{Q}d\bar{Z}, \\ d\bar{v} = [k(\theta - \bar{v})]dt + \sigma\sqrt{\bar{v}}d\bar{z}_2. \end{cases} \tag{2.28}$$

where $\bar{v}(t)$ is the same volatility process of (2.19).

Following the development in [45], we assume that individuals have time-additive preferences of the form

$$E_t\left[\int_t^\infty \exp(-\rho s)\log(\bar{C}_s)ds\right], \tag{2.29}$$

where $E[\cdot\,]$ is the conditional expectation operator, ρ is the utility discount factor and $\bar{C}_s$ represents consumption at time s.

The representative investor's decision problem is equivalent to maximizing (2.29) subject to the budget constraint

$$d\bar{W} = \bar{W}\frac{d\bar{Q}}{\bar{Q}} - \bar{C}dt, \tag{2.30}$$

where $\bar{W}$ denotes wealth.

Standard maximization arguments employed in [45] lead to the following equation for the wealth dynamics

$$d\bar{W} = (\mu + \delta\bar{v}(t) - \rho)\bar{W}dt + \sigma_{\bar{Q}}\bar{W}\sqrt{\bar{v}(t)}d\bar{Z}. \tag{2.31}$$

Applying Theorem 3 in [16], the value of a contingent claim $B(\tau, v)$ must satisfy the partial differential equation

$$-B_t = \frac{\sigma^2 v}{2}B_{vv} + (k\theta - kv - \lambda v)B_v - rB, \tag{2.32}$$

where $\bar{v}(t) = v$, the market price of risk is λv and $\bar{r}(t) = r$ is the instantaneous riskless rate.

To obtain the equilibrium interest rate $\bar{r}$, Theorem 1 of [16] is applied. This theorem relates the riskless rate to the expected rate of change in marginal utility. The result obtained is that

$$\bar{r}(t) = \mu + (\delta - \sigma_Q^2)\bar{v}(t) = \mu + \beta\bar{v}(t), \tag{2.33}$$

The price of a riskless unit discount bond $B(\tau, v)$, where $\tau = T - t$ is obtained solving equation (2.32) subject to the maturity condition $B(0, v) = 1$.

Remark 2.3.3. In Subsection 2.3.4 we will prove that $\bar{r}$ is the instantaneous interest rate employed in the market dynamics given in equation (2.23) of Subsection 2.3.2.

For the rest of the text, we assume that $\beta > 0$. We will see that when parameter $\beta \to 0^+$, the function $B(\tau, v)$ approaches to the bond price when the risk-free rate is considered constant ($B(\tau, v) = e^{-\mu\tau}$).

Now, we proceed to give the main result of this Subsection.

Theorem 2.3.2. *The riskless unit discount bond $B(\tau, v)$, where $\tau = T - t$ denotes the time until maturity, $\bar{v}(\tau) = v$ and $\bar{r}(t) = r = \mu + \beta v$, is given by the formula:*

$$B(\tau, v) = F(\tau)e^{G(\tau)v}, \tag{2.34}$$

where

$$\begin{aligned} F(\tau) &= \exp\left(-\left(\mu + \frac{k\theta}{b}\right)\tau + k\theta\left(\frac{b+c}{bc}\right)\ln\left(b + ce^{d\tau}\right) - k\theta\left(\frac{b+c}{bc}\right)\ln(b+c)\right), \\ G(\tau) &= \frac{e^{d\tau} - 1}{b + ce^{d\tau}}, \end{aligned} \tag{2.35}$$

and

$$\begin{aligned} d &= -\sqrt{(k+\lambda)^2 + 2\beta\sigma^2}, \\ b &= \frac{(k+\lambda) - d}{2\beta}, \\ c &= \frac{-(k+\lambda) - d}{2\beta}. \end{aligned} \tag{2.36}$$

Proof. For simplicity, along the proof, we will employ the notation:

$$\eta = k\theta, \quad \alpha = k + \lambda.$$

The claim satisfies the partial differential equation (2.32) subject to the maturity condition $B(0, v) = 1$. With the notation that we have just introduced, we have to solve:

$$\begin{cases} B_\tau = \dfrac{\sigma^2}{2}vB_{vv} + (\eta - \alpha v)B_v - (\mu + \beta v)B, \\ B(0, v) = 1. \end{cases}$$

We conjecture a solution of the form:

$$B(\tau, v) = F(\tau)e^{G(\tau)v}.$$

Thus, we have that

$$\begin{aligned} B_v &= F(\tau)G(\tau)\exp(G(\tau)v), \\ B_{vv} &= F(\tau)G^2(\tau)\exp(G(\tau)v), \\ B_\tau &= [F'(\tau) + F(\tau)G'(\tau)v]\exp(G(\tau)v), \end{aligned}$$

and condition $B(0, v) = 1$ imposes that $F(0) = 1$ and $G(0) = 0$.

Substituting into the PDE

$$\frac{\sigma^2}{2}vF(\tau)G^2(\tau) + (\eta - \alpha v)F(\tau)G(\tau) - (\mu + \beta v)F(\tau) = F'(\tau) + F(\tau)G'(\tau)v. \tag{2.37}$$

As the previous equation is an identity in v, we obtain two equations:

$$\begin{cases} \dfrac{\sigma^2}{2}F(\tau)G^2(\tau) - \alpha F(\tau)G(\tau) - \beta F(\tau) = F(\tau)G'(\tau), \\ \eta F(\tau)G(\tau) - \mu F(\tau) = F'(\tau). \end{cases}$$

For the first one, as candidate for solution we take:

$$G(\tau) = \frac{a + e^{d\tau}}{b + ce^{d\tau}} = \frac{e^{d\tau} - 1}{b + ce^{d\tau}},$$

as $G(0) = 0$ implies $a = -1$ and $b \neq -c$.

Thus, obtaining $G^2(\tau)$, $G'(\tau)$ and substituting, we obtain a second degree equation given in function of $\exp(2d\tau), \exp(d\tau), 1$, which implies that:

$$\begin{aligned} \sigma^2 - 2\alpha c - 2\beta c^2 &= 0, \\ -2\sigma^2 - 2\alpha(b - c) - 4\beta bc &= 2(bd + cd), \\ \sigma^2 + 2\alpha b - 2\beta b^2 &= 0. \end{aligned}$$

Solved for b and c, we obtain:

$$\begin{aligned} c &= \frac{-\alpha \pm \sqrt{\alpha^2 + 2\beta\sigma^2}}{2\beta}, \\ b &= \frac{\alpha \pm \sqrt{\alpha^2 + 2\beta\sigma^2}}{2\beta}. \end{aligned}$$

As $b \neq -c$, two solutions are eliminated. Another one is rejected when solving the other ODE as it appears $\ln(b + c)$, which must be positive. The solution is then:

$$
\begin{aligned}
c &= \frac{-\alpha + \sqrt{\alpha^2 + 2\beta\sigma^2}}{2\beta}, \\
b &= \frac{\alpha + \sqrt{\alpha^2 + 2\beta\sigma^2}}{2\beta}, \\
d &= -\sqrt{\alpha^2 + 2\beta\sigma^2}.
\end{aligned}
$$

For the second equation, we obtain:

$$
\begin{cases}
\eta F(\tau)G(\tau) - \mu F(\tau) = F'(\tau), \\
F(0) = 1.
\end{cases}
$$

After substituting, we arrive to:

$$
F(\tau) = \exp\left(-\left(\mu + \frac{\eta}{b}\right)\tau + \eta\frac{b+c}{bc}\ln(b + ce^{d\tau}) - \eta\frac{b+c}{bc}\ln(b+c)\right),
$$

which completes the proof.

□

For the rest of the Chapter, we denote $\bar{B}(\tau, \bar{v}) = B(\tau, \bar{v})$.

Proposition 2.3.2. *The bond dynamics in the physical measure is given by*

$$
\begin{aligned}
d\bar{B}(\tau,\bar{v}) &= \left[\mu + \beta\bar{v} + \lambda\bar{v}\right]\bar{B}(\tau,\bar{v})dt + G(\tau)\sigma\sqrt{\bar{v}}\bar{B}(\tau,\bar{v})d\bar{z}_2 \\
&= (\bar{r}(t) + \lambda\bar{v})\bar{B}(\tau,\bar{v})dt + G(\tau)\sigma\sqrt{\bar{v}}\bar{B}(\tau,\bar{v})d\bar{z}_2,
\end{aligned}
\tag{2.38}
$$

where $\bar{r}(t)$ denotes the instantaneous riskless rate and $\bar{z}_2$ is the same Wiener process as in equation (2.19).

Proof. We have that

$$
\begin{aligned}
d\bar{v} &= [k(\theta - \bar{v})]dt + \sigma\sqrt{\bar{v}}d\bar{z}_2, \\
B(\tau, v) &= F(\tau)e^{G(\tau)v},
\end{aligned}
$$

so applying Itô's formula we get to

$$
\begin{aligned}
d\bar{B}(\tau,\bar{v}) = &-\left[F'(\tau) + F(\tau)G'(\tau)\bar{v}\right]e^{G(\tau)\bar{v}}dt + G(\tau)\bar{B}(\tau,\bar{v})\left(\left[k(\theta-\bar{v})\right]dt + \sigma\sqrt{\bar{v}}d\bar{z}_2\right) + \\
&+ \frac{1}{2}G^2(\tau)\bar{B}(\tau,\bar{v})\sigma^2\bar{v}dt,
\end{aligned}
$$

where we have used that $B_t = -B_\tau$.

Now, taking in account equation (2.37)

$$
F'(\tau) + F(\tau)G'(\tau)v = F(\tau)\left[\frac{\sigma^2}{2}vG^2(\tau) + [k\theta - (k+\lambda)v]G(\tau) - (\mu + \beta v)\right],
$$

we come to

$$d\bar{B}(\tau,\bar{v}) = -\left[\frac{\sigma^2}{2}\bar{v}G^2(\tau) + [k\theta - (k+\lambda)\bar{v}]G(\tau) - (\mu+\beta\bar{v})\right]\bar{B}(\tau,\bar{v})dt + \\ + G(\tau)\bar{B}(\tau,\bar{v})\left([k(\theta-\bar{v})]\,dt + \sigma\sqrt{\bar{v}}d\bar{z}_2\right) + \frac{1}{2}G^2(\tau)\bar{B}(\tau,\bar{v})\sigma^2\bar{v}dt,$$

and rearranging terms the proof is complete.

□

The following result will be interesting in the following Subsection, where we incorporate the bond to the pricing model of the option. It states that when parameter β approaches to 0^+, then function $B(\tau, v)$ converges to the price of the bond when constant risk-free rates are employed, i.e., the bond employed in the simple SV model.

Proposition 2.3.3. *Consider the functions given by*

$$F(\tau) = \exp\left(-\left(\mu + \frac{k\theta}{b}\right)\tau + k\theta\left(\frac{b+c}{bc}\right)\ln\left(b+ce^{d\tau}\right) - k\theta\left(\frac{b+c}{bc}\right)\ln(b+c)\right),$$
$$G(\tau) = \frac{e^{d\tau}-1}{b+ce^{d\tau}},$$

and

$$d = -\sqrt{(k+\lambda)^2 + 2\beta\sigma^2},$$
$$b = \frac{(k+\lambda)-d}{2\beta},$$
$$c = \frac{-(k+\lambda)-d}{2\beta}.$$

If $\beta \to 0^+$, then we have that:

$$F(\tau) \to \exp(-\mu\tau),$$
$$G(\tau) \to 0.$$

Proof. Expanding the previous definitions for $F(\tau)$ and $G(\tau)$ and condensing the terms in function of β, we will get to an expression equivalent to

$$\frac{k\theta}{b} = 2\beta\alpha_1(\beta),$$
$$k\theta\left(\frac{b+c}{bc}\right)\ln\left(b+ce^{d\tau}\right) = \alpha_2(\beta)\beta\ln\left(\frac{\alpha_3(\beta)}{\beta}\right),$$
$$k\theta\left(\frac{b+c}{bc}\right)\ln(b+c) = \alpha_4(\beta)\beta\ln\left(\frac{\alpha_5(\beta)}{\beta}\right),$$
$$\frac{e^{d\tau}-1}{b+ce^{d\tau}} = \beta\alpha_6(\beta),$$

where it is easy to check that $\lim_{\beta\to 0^+}\alpha_i(\beta) \in \mathbb{R}, \forall i = 1,...,6$ and $\lim_{\beta\to 0^+}\alpha_i(\beta) > 0,\ i = 3,5$, being then straightforward the result.

□

Lemma 2.3.1. *Let $G(\tau)$ be given by (2.35). Then it holds:*

$$\begin{cases} G(\tau) = \dfrac{e^{d\tau}-1}{b+ce^{d\tau}} \underset{\tau\to 0}{\longrightarrow} 0, \\ G(\tau) \neq 0, \quad \tau > 0, \\ G(0) = 0. \end{cases}$$

Proof. We recall that $G(\tau)$ is given by

$$G(\tau) = \frac{e^{d\tau}-1}{b+ce^{d\tau}}$$

where

$$\begin{aligned} d &= -\sqrt{(k+\lambda)^2+2\beta\sigma^2}, \\ b &= \frac{(k+\lambda)-d}{2\beta}, \\ c &= \frac{-(k+\lambda)-d}{2\beta}. \end{aligned}$$

and since, by hypothesis $\beta, \sigma^2 > 0$, the result follows.

□

Remark 2.3.4. As $\bar{B}(\tau, \bar{v})$ is the stochastic process of a bond price, the stochastic component $G(\tau)\sigma\sqrt{\bar{v}}$ of equation (2.38) must vanish at maturity so the bond reaches par at maturity with probability one.

This is also satisfied due to the previous Lemma.

2.3.4 Valuation Formula

Suppose that the market is formed by a stock given by (physical measure)

$$\begin{cases} d\bar{S}(t) = \mu_S \bar{S}(t)dt + \sigma_s(t)\sqrt{\bar{v}(t)}\bar{S}(t)d\bar{z}_1(t), \\ d\bar{v}(t) = \kappa[\theta - \bar{v}(t)]dt + \sigma\sqrt{\bar{v}(t)}d\bar{z}_2(t), \end{cases}$$

and by a bond

$$\bar{B}(t,T;\bar{v}) = \bar{B}(\tau;\bar{v}) = F(\tau)e^{G(\tau)\bar{v}},$$

where $\tau = T-t$ and $F(\tau),\ G(\tau)$ are explicitly given by formulas (2.35)-(2.36).

If we compute the bond dynamics, Proposition 2.3.2 enforces that, in order to be consistent with model (2.19),

$$\begin{cases} \sigma_b(\tau) = \sigma G(\tau), \\ \rho_{bv} = 1, \\ \rho_{bs} = \rho_{vs}, \end{cases} \tag{2.39}$$

and for simplicity reasons we have taken $\sigma_S(t) \equiv 1$.

The sign and magnitude of the correlation between the bond and the stock seems to be difficult to estimate from market data (see [39]). Condition $\rho_{bs} = \rho_{vs}$, although restrictive, does not violate market empirical observations in the sense of the sign (positive/negative).

Proposition 2.3.4. *The short interest rate is given by $r = \mu + \beta v$ and the risk premia $\lambda(S, v, B, t) = \lambda v$ where λ is the constant employed in the bond formula (2.34).*

Proof. Let us assume that it exists a deterministic function $\bar{r} = \bar{r}\left(\bar{\mathbf{X}}(t)\right)$ where $\bar{\mathbf{X}}(t) = (\bar{S}(t), \bar{v}(t), \bar{B}(t,T))$ for the short interest rate. Using the results in [3], pg 218, any contingent claim must satisfy

$$\frac{\partial U}{\partial t} + \frac{1}{2}\sigma_s^2 v S^2 \frac{\partial^2 U}{\partial S^2} + \frac{1}{2}\sigma^2 v \frac{\partial^2 U}{\partial v^2} + \frac{1}{2}\sigma_b^2 v B^2 \frac{\partial^2 U}{\partial B^2} + \rho_{sv}\sigma_s \sigma S v \frac{\partial^2 U}{\partial s \partial v} + \rho_{sb}\sigma_s \sigma_b v S B \frac{\partial^2 U}{\partial S \partial B} +$$
$$+ \rho_{vb}\sigma_b \sigma B v \frac{\partial^2 U}{\partial v \partial B} + rS\frac{\partial U}{\partial S} + [k(\theta - v) - \lambda(S, v, B, t)]\frac{\partial U}{\partial v} - rU + rB\frac{\partial U}{\partial B} = 0.$$

where $\bar{\mathbf{X}}(t) = \mathbf{X} = (S, v, B)$.

Suppose that, fixed a maturity T ($\tau = T - t$), we want to price the contingent claim which values 1 at maturity. In order to avoid any arbitrage opportunity, this claim has to be the bond,

$$U(S, v, B, \tau) = F(\tau)e^{G(\tau)v},$$

thus, it must hold that

$$-\left(F'(\tau)e^{G(\tau)v} + F(\tau)G'(\tau)ve^{G(\tau)v}\right) + \frac{1}{2}\sigma^2 v F(\tau)G^2(\tau)e^{G(\tau)v} +$$
$$+ [k(\theta - v) - \lambda(S, v, B, t)]F(\tau)G(\tau)e^{G(\tau)v} - rF(\tau)e^{G(\tau)v} = 0.$$

On the other hand, by construction of the bond, we know that

$$-\left(F'(\tau)e^{G(\tau)v} + F(\tau)G'(\tau)ve^{G(\tau)v}\right) + \frac{1}{2}\sigma^2 v F(\tau)G^2(\tau)e^{G(\tau)v} +$$
$$+ [k(\theta - v) - \lambda v]F(\tau)G(\tau)e^{G(\tau)v} - (\mu + \beta v)F(\tau)e^{G(\tau)v} = 0.$$

We subtract both expressions and divide by $F(\tau)e^{G(\tau)v}$ to get to

$$\left(-\lambda(S, v, B, t) + \lambda v\right) G(\tau) + \left(-r + (\mu + \beta v)\right) = 0.$$

The previous expression must hold for all v, τ. From Proposition 2.3.1 we know that $G(\tau) \neq 0$, $\tau \neq 0$ and that $G(0) = 0$. Standard arguments yield the desired result.

□

In the riskless measure, the dynamics is:

$$\begin{cases} d\bar{S}(t) = r\bar{S}(t)dt + \sqrt{\bar{v}(t)}\bar{S}(t)d\bar{z}_1(t), \\ d\bar{v}(t) = [k\theta - k\bar{v}(t) - \lambda\bar{v}(t)]dt + \sigma\sqrt{\bar{v}(t)}d\bar{z}_2(t), \\ d\bar{B}(t,T) = r\bar{B}(t,T)dt + \sigma G(\tau)\sqrt{\bar{v}(t)}\bar{B}(t,T)d\bar{z}_2(t), \end{cases} \tag{2.40}$$

where the riskless rate is $\bar{r}(t) = \mu + \beta\bar{v}(t)$.

If we compare it with the original SV model of Heston, note that just one new parameter has appeared, β, which models the stochastic component of the bond.

Proposition 2.3.3 states that, as β approaches to 0^+, the function which gives the bond price $B(\tau, v)$ converges, for any fixed v, to $e^{-\mu\tau}$, which is the price of a bond when constant risk free rates are employed. Therefore, the original SV model can be considered a particular case of this one. This will be used to check, in the numerical experiments, the general assumption of constant interest rates when pricing options.

For the rest of the Chapter, we impose $\beta \geq 0$ where $\beta = 0$ denotes the the original SV model.

Now we are going to develop a semi-explicit formula. We recall that Heston conjectured in [34] a solution

$$U(t, x, P, v) = e^x B(t, T) R_1(t, x, v) - KB(t, T) R_2(t, x, v),$$

where $R_j,\ j \in \{1, 2\}$ satisfies (2.26)-(2.27).

Substituting the parameter restrictions (2.39) into (2.26)-(2.27), we obtain

$$\frac{1}{2}\sigma_x^2 v\frac{\partial^2 R_j}{\partial x^2} + \rho_{xv}\sigma_x\sigma v\frac{\partial^2 R_j}{\partial x\partial v} + \frac{1}{2}\sigma^2 v\frac{\partial^2 R_j}{\partial v^2} + \zeta_j v\frac{\partial R_j}{\partial x} + (a - b_j v)\frac{\partial R_j}{\partial v} + \frac{\partial R_j}{\partial t} = 0, \tag{2.41}$$

where

$$\begin{aligned}
\frac{1}{2}\sigma_x^2 &= \frac{1}{2} - \rho_{sv}\sigma G(\tau) + \frac{1}{2}\sigma^2 G^2(\tau),\\
\rho_{xv} &= \frac{\rho_{sv} - \sigma G(\tau)}{\sigma_x},\\
\zeta_1 &= \frac{1}{2}\sigma_x^2, \quad \zeta_2 = -\frac{1}{2}\sigma_x^2, \quad a = k\theta,\\
b_1 &= k + \lambda - \rho_{sv}\sigma,\\
b_2 &= k + \lambda - \sigma^2 G(\tau).
\end{aligned} \tag{2.42}$$

Lemma 2.3.2. *Let $\tau = T - t$. The solution of equation*

$$\frac{1}{2}\sigma_x^2 v\frac{\partial^2 f_j}{\partial x^2} + \rho_{xv}\sigma_x\sigma v\frac{\partial^2 f_j}{\partial x\partial v} + \frac{1}{2}\sigma^2 v\frac{\partial^2 f_j}{\partial v^2} + \zeta_j v\frac{\partial f_j}{\partial x} + (a - b_j v)\frac{\partial f_j}{\partial v} - \frac{\partial f_j}{\partial \tau} = 0, \tag{2.43}$$

subject to $f(x, v, 0; \phi) = e^{i\phi x}$ is the characteristic function of R_j.

Proof. See Appendix in [34].

□

In order to obtain the solution (2.43), the characteristic function is conjectured to be

$$f_j(x, \upsilon, \tau, \phi) = e^{C(\tau,\phi) + D(\tau,\phi)\upsilon + i\phi x}.$$

Thus it holds that:

$$\begin{aligned}
&\frac{\partial f}{\partial t} = f\left(\frac{\partial C}{\partial t} + \frac{\partial D}{\partial t}\upsilon\right) = f\left(-\frac{\partial C}{\partial \tau} - \frac{\partial D}{\partial \tau}\upsilon\right),\\
&\frac{\partial f}{\partial x} = fi\phi, \quad \frac{\partial f}{\partial v} = fD,\\
&\frac{\partial^2 f}{\partial x^2} = -f\phi^2, \quad \frac{\partial^2 f}{\partial v^2} = fD^2, \quad \frac{\partial^2 f}{\partial v \partial x} = i\phi Df.
\end{aligned}$$

Substituting in the PDE, we come to:

$$-\frac{1}{2}\sigma_x^2 \upsilon f\phi^2 + \rho_{xv}\sigma_x\sigma\upsilon i\phi Df + \frac{1}{2}\sigma^2\upsilon fD^2 + u_j\upsilon fi\phi + (a - b_j\upsilon)fD + f\left(-\frac{\partial C}{\partial \tau} - \frac{\partial D}{\partial \tau}\upsilon\right) = 0.$$

As the previous expression in an identity in υ we obtain the next two equations:

$$\begin{cases} -\frac{1}{2}\sigma_x^2\phi^2 + \rho_{xv}\sigma_x\sigma i\phi D + \frac{1}{2}\sigma^2 D^2 + u_j i\phi - b_j D - \frac{\partial D}{\partial \tau} = 0, \\ aD - \frac{\partial C}{\partial \tau} = 0, \end{cases}$$

plus the condition $C(0) = D(0) = 0$.

The first equation is a Ricatti equation, but as $\sigma_x(t)$ depends on time and not being constant, a direct solution has not been found and it has to be solved numerically, for example, by means of the routine of matlab ode 45.

Corollary 2.3.1. *The price of the option is then given by:*

$$R_j(x, v, \tau, \ln(K)) = \frac{1}{2} + \frac{1}{\pi}\int_0^\infty Re\left[\frac{e^{-i\phi\ln(K)} f_j(x, \upsilon, \tau, \phi)}{i\phi}\right] d\phi,$$

where

$$f_j(x, \upsilon, \tau, \phi) = e^{C(\tau,\phi) + D(\tau,\phi)\upsilon + i\phi x}.$$

Remark 2.3.5. For both SV and SVSIR models, a change of variables has been realized

$$\begin{cases} k^* = k + \lambda, \\ \theta^* = \dfrac{k\theta}{k + \lambda}, \end{cases}$$

so the variance equation reads in the risk-neutral measure as

$$d\bar{v} = k^*\left[\theta^* - \bar{v}(t)\right]dt + \sigma\sqrt{\bar{v}(t)}d\bar{z}_2(t). \tag{2.44}$$

2.4 Numerical Results

2.4.1 Analysis with the SV model

In this Subsection we will perform an In/Out the Sample analysis, similar to the one we performed in Chapter 1, with real market data and Heston's SV model. We will employ the S&P500 options negotiated all Wednesdays (or the closest if the market was closed) between 01-03-1990 and 12-30-92 (157 days).

For the In The Sample daily analysis, we fix a date t_0 and consider all European Call contracts traded along that day. Our objective is to find the parameter values for day t_0 that minimize:

$$\text{InMSE}(t_0) = \frac{1}{N_{t_0}} \sum_{i=1}^{N_{t_0}} \left(C_{t_0}^i - C_i(S_{t_0}^i, t_M^i, K_i) \right)^2, \tag{2.45}$$

where

(i) N_{t_0} denotes the amount of contracts negotiated on day t_0.

(ii) $C_{t_0}^i$ denotes the market price of contract i.

(iii) t_M^i and K_i denote respectively the maturity and strike of contract i.

(iv) $C_i(S_{t_0}^i, t_M^i, K_i)$ denotes the model's price of contract i.

In order to compare results, we compute $C_i(S_{t_0}^i, t_M^i, K_i)$ for Heston's SV model, for the Black-Scholes model and for the NGARCH(1,1) model employed in Chapter 1. In all the models, the risk-free rate employed was $r_{t_0}^{3-US}$, i.e. the annualized constant risk-free rate of the 3-month US Treasury Bond.

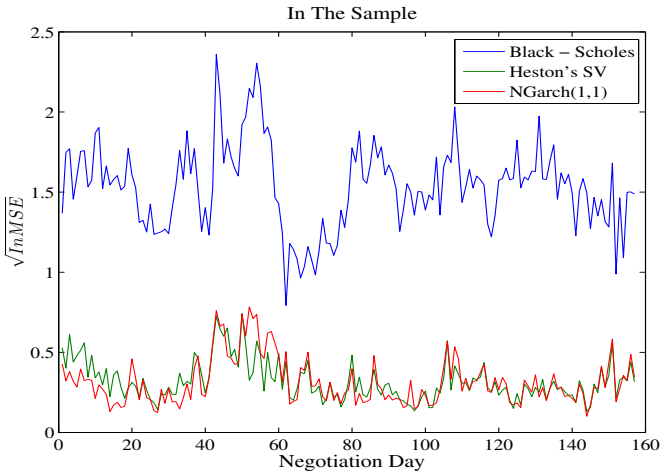

Figure 2.2: Error in monetary terms for the In The Sample analysis. We plot each negotiation day (horizontal axis) vs the root of InMSE (vertical axis) with Black-Scholes (blue), Heston's SV (green) and NGARCH(1,1) (red).

The results plotted in Figure 2.2 are the square root of InMSE for each negotiation day t_0. This error represents the daily error, in monetary terms, for all Wednesdays (or the closest if the market was closed) between 01-03-1990 and 12-30-92 (157 days) for the three models.

As we can see, Heston's model performs much better than the Black-Scholes model and very similar as the NGARCH(1,1) model. The mean value of the root of InMSE along the 157 days has been 1.534 for the Black-Scholes model, 0.321 for the Heston's SV model and 0.315 for the NGARCH(1,1) model.

The fact that the results of the NGARCH(1,1) and the SV models are so similar is not surprising. The close relation between ARCH and SV models can be found, for example, in [15] or [51], where it is proven that ARCH models could be seen as a discrete counterpart of SV models.

Furthermore, due to their close relation, we can combine the information obtained from both in the Out the Sample analysis as we are about to see.

The Out The Sample analysis is identical to the one explained in Section 1.2.1. Suppose that we are at day t_0. With the estimated parameters on date $t_0 - 7$, the stock movements along the week $[t_0 - 7, t_0]$ and the allowances of the model, we try to predict the option prices before the market opens.

We recall that for the NGARCH(1,1) model, we gave in Chapter 1 an updating volatility formula

$$\sigma_t^2 = \beta_0 + \beta_1 \sigma_{t-1}^2 + \beta_2 \sigma_{t-1}^2 \left(\left[\frac{\left(R_{t-1} - r + \frac{\sigma_{t-1}^2}{2} \right)}{\sqrt{\sigma_{t-1}^2}} \right] - (\lambda + \theta) \right)^2 , \tag{2.46}$$

as an estimator (from the movements of the stock) of today's market's volatility.

For the SV model, we are going to employ the empirically observed close relation between SV and NGARCH(1,1). The following technique is similar to the one found in [45]. We employ (2.46) as a volatility estimator in the SV model.

Although (2.46) is possibly not the best volatility estimator, it is interesting to check if the results obtained so far are consistent when we employ the information from one model into the other when we try to predict future option prices.

Let t_0 denote today. The procedure for the Out the Sample analysis is as follows:

a) Estimate the NGARCH(1,1) and SV parameters on day $t_0 - 7$. Estimate Black-Scholes implied volatility on day $t_0 - 7$.

b) Enforce the NGARCH(1,1) parameters into the updating formula (2.46).

c) With the stock movements along $[t_0 - 7, t_0]$ and the last Wednesday markets's volatility estimated for NGARCH(1,1) and Heston's SV, compute an estimation of todays market's volatility for both models. For the Black-Scholes model, the volatility is not updated (since it is assumed constant).

d) Option prices are computed for each model with their respective parameters and their respective volatility estimation.

If N_{t_0} denotes the amount of contracts negotiated on day t_0, let $i \in \{1,\ 2,\ ...,\ N_{t_0}\}$. The option prices of day t_0 are computed with formula

$$C_i(S^i_{t_0}, t_{Mi}, K_i, \tilde{\sigma}^2_{t_0}),$$

where, for NGARCH(1,1) and SV models, the values of the parameters are those of date $t_0 - 7$ and $\tilde{\sigma}^2_{t_0}$ corresponds to the estimation of market's volatility of each model.

If we want to know how well we have predicted option prices, we compare the results obtained with the traded prices computing the mean square error.

$$\text{OutMSE}(t_0) = \frac{1}{N_{t_0}} \sum_{i=1}^{N_{t_0}} \left(C^i_{t_0} - C_i(S^i_{t_0}, t_{Mi}, K_i, \tilde{\sigma}^2_{t_0})\right)^2. \tag{2.47}$$

The results of Figure 2.3 show the square root of the OutMSE when prices are predicted with all the models for all Wednesdays between 2-01-1992 and 12-30-92 (53 days).

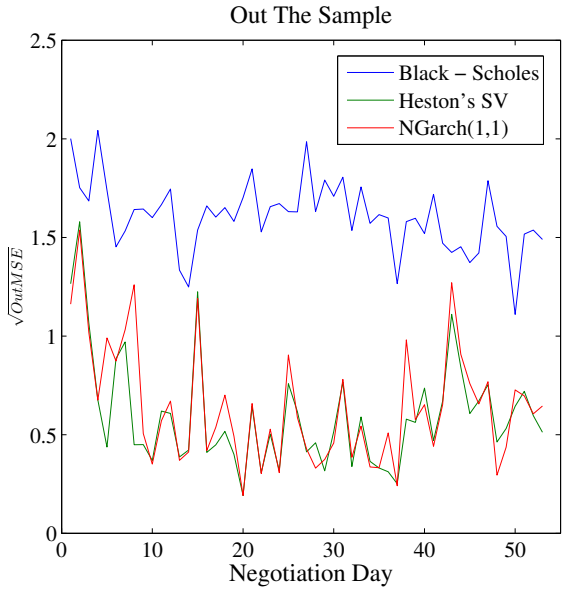

Figure 2.3: Error in monetary terms for the Out The Sample analysis. We plot each negotiation day (horizontal axis) vs the root of OutMSE (vertical axis) with Black-Scholes (blue), Heston's SV (green) and NGARCH(1,1) (red).

The mean values of the root of OutMSE along the 53 days have been 1.606 for Black-Scholes, 0.597 for Heston's SV and 0.642 for NGARCH(1,1) models.

Again, SV and NGARCH(1,1) perform similar and much better than Black-Scholes. The estimator employed for updating the volatility seems to have been consistent. Although it is not the objective of this work, we have empirically checked the close relation between Garch and SV when they are applied to option pricing.

2.4.2 Analysis with the SVSIR model

We establish how we deal with the parameters of the stochastic bond.

At a fixed day t_0, in order to make an equivalent comparison with the simple SV model, we enforce that the stochastic bond value matches with the value negotiated in the market for the 3-months ($\tau = 0.25$) US Bond, which is denoted by $B^{3-US}(t_0)$. This gives us the first constraint:

$$B(0.25, v) = B^{3-US}(t_0) \tag{2.48}$$

We recall that the stochastic interest rate depends on two parameters $r = \mu + \beta v$, where β modules the stochastic component. We have already imposed that $\beta \geq 0$ ($\beta = 0$ corresponds to the SV model). We also impose $\mu \geq 0$ to ensure the positiveness of the interest rate.

Our criteria, in the In the Sample analysis, has been to let, if possible, β free and enforce the value of μ so (2.48) and $\mu \geq 0$ are fulfilled.

If we substitute constraint (2.48) into the bond formula (2.34) we obtain

$$\mu = -\frac{1}{0.25} \log \left(B^{3-US}(t_0)\, e^{-G(0.25)v} \exp \left(k\theta \left[\frac{0.25}{b} - \frac{b+c}{bc} \ln \left(\frac{b + ce^{0.25d}}{b+c} \right) \right] \right) \right) \tag{2.49}$$

The In the Sample analysis is identical to the one described in the previous Subsection but, for the bond parameters μ and β, we impose:

a) β free (estimated from option prices) if $\mu > 0$ where μ is computed with formula (2.49).

b) $\mu = 0$ and $\beta = \underset{\beta}{\arg} \left\{ B(v, 0.25) = B^{3-US}(t_0) : \mu = 0 \right\}$ otherwise.

subject to $\beta \geq 0$ in both cases ($\beta = 0$ corresponds to the SV model).

Constant rate assumption:
It is generally assumed that constant interest rates ($\beta \equiv 0$) can be employed to value options, specially for those with short maturities. Our first objective is to check if traded option prices seem to incorporate a stochastic component to the bond.

Figure 2.4 shows, for each negotiation day t_0, the estimated initial volatility $v(t_0)$ and a colored mark depending on the estimated value of β_{t_0}.

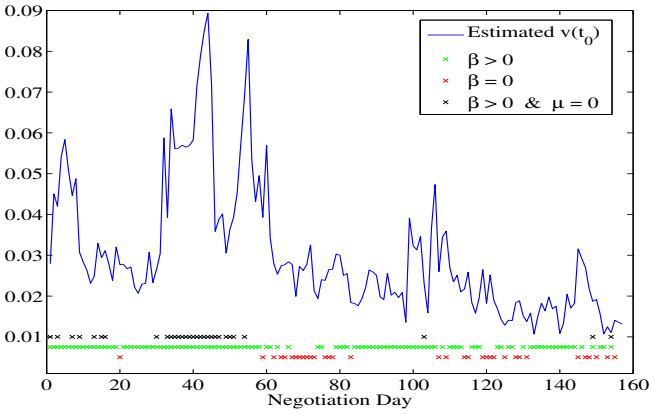

Figure 2.4: Analysis of Constant / Non Constant interest rates assumption from market data. For each negotiation day t_0 (horizontal axis), we plot the estimated initial volatility $v(t_0)$ (blue) and mark with a colored '$\times$' the cases: $\beta_{t_0} = 0$ (red), $\beta_{t_0},\ \mu_{t_0} > 0$ (green) and $\beta_{t_0} > 0,\ \mu_{t_0} = 0$ (black).

We recall that the instantaneous interest rate is given by $r = \mu + \beta v$, where β modules the stochastic component. $\beta = 0$ implies that the market has employed a constant interest rates to price the options. The numerical values estimated for β vary between $\beta \in [0,\ 0.4269]$. Of the 157 days of the estimation, 34 of them (21 %) correspond to $\beta = 0$ (constant rate bond) and 26 of them (16 %) to $\mu = 0$ ("purely" stochastic).

We are going to study the performance results. The In The Sample analysis is identical to the one of the previous subsection.

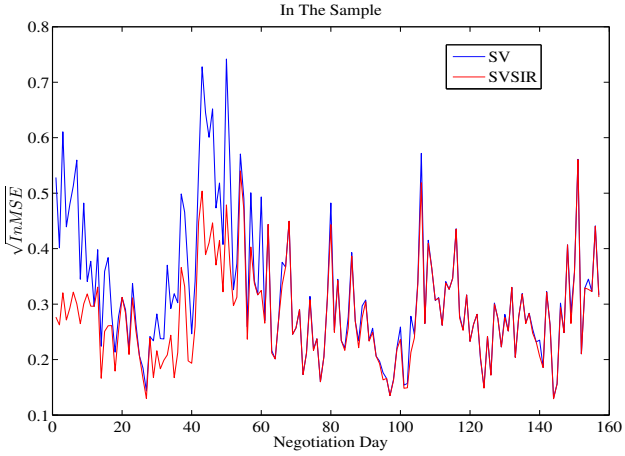

Figure 2.5: Error in monetary terms of the In The Sample analysis. We plot each negotiation day t_0 (horizontal axis) vs the root of the InMSE (vertical axis) with Heston's SV (blue) and SVSIR (red).

Obviously, as SV model can be considered a particular case of the SVSIR model, the results of the second one will always be equal or better than those of the first one. We plot, for each negotiation day t_0, the InMSE of SV and SVSIR models.

The mean values of the square root of InMSE have been 0.321 and 0.281 for the SV and SVSIR respectively. There is only a significant gain (in the sense of InMSE) for the SVSIR model in the 60 first days (which correspond to high-volatility periods (see Figure 2.4)), being the results very similar for both models for the rest of the days.

Concerning the Out The Sample analysis, we employ the same updating volatility formula as in the previous Subsection with the same estimated parameters of the NGARCH(1,1) model. Although this estimator would not be suitable for this model (in NGARCH(1,1) no stochastic rates were allowed), the results are again fairly close for both models. We will go back to this point at the end of the analysis.

The root of the OutMSE obtained for the prediction are plotted, for each negotiation day t_0, in the following picture:

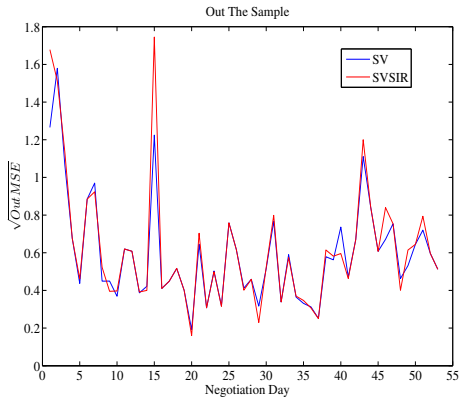

Figure 2.6: Error in monetary terms of the Out The Sample analysis. We have plotted the root of the OutMSE (vertical axis) for each negotiation day t_0 (horizontal axis). We present the results obtained for Heston's SV (blue) and SVSIR (red) models.

The mean values of the root of OutMSE have been 0.597 and 0.619 for the SV and SVSIR respectively. The prediction is very similar with both models.

It should be remarked that, although the results obtained are quite close, only 18 of the 53 days correspond to $\beta = 0$ (the same parameter values for both SV and SVSIR). The parameter values obtained for the other 35 days vary from one model to another.

The similar results obtained with both models have an empirical explanation. The estimated values of k^* and θ^* (see equation (2.44)) are different in both models.

Nevertheless, the estimated value of $k^*\theta^*$ (the stationary value which the volatility process approaches) seems to follow a certain distribution. The following picture shows the histogram of the values obtained for $k^*\theta^*$:

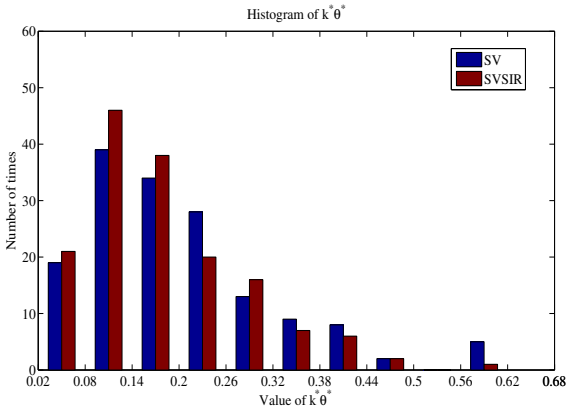

Figure 2.7: Histogram of parameter $k^*\theta^*$. With the estimated parameters of the In the Sample analysis, we have divided the horizontal axis (value of $k^*\theta^*$) in 11 equal subintervals. We have plotted, in the vertical axis, the number of times that the value $k^*\theta^*$ lies in each of the subintervals for the SV(blue) and SVSIR(red) models.

The empirically observed distribution of the market value of $k^*\theta^*$ is very similar with both models. Although different values for k^* and θ^* are obtained with each model, the value of $k^*\theta^*$ does not differ that much. Indeed, the greatest differences seem to occur in high-volatility periods, when the SVSIR model performs significantly better than the SV model in the In the Sample analysis (see Figures 2.4 and 2.5).

Summarizing the results, the SVSIR achieves a better error in the In The Sample analysis. If our objective is just to obtain indicative market prices (Out the Sample), the constant rate assumption seems to be not too far from reality. Stochastic rates have a limited effect in the performance of the model (in the sense of OutMSE). This may be a consequence of the model choice of volatility estimator.

Concerning the updating volatility formula, it must be remarked that, in practice, it is a rough predictor not only for the SVSIR model, but also for the SV one. Numerical experiments show that it may be not very reliable when big shocks occur in the market along the week: The values obtained for the new volatility tend to be higher than those that the market will actually employ.

As a future research, it could be worthy to explore other volatility predictors (see [61] for example) for the Out The Sample analysis.

Chapter 3

Optimal Investment with Transaction Costs under Potential Utility.

3.1 Introduction

Let us consider an investor whose wealth can be inverted in a risky stock and in a riskless bank account. Assume that the investor's decisions are driven by the objective of maximizing the utility that his future wealth will provide him, one hypothesis of social behaviour frequently assumed in Economy.

In order to model this, we define a suitable Utility function (twice differentiable, strictly increasing (more is better than less) and strictly concave (investors are risk averse), which reflects the preferences of the investor. The Optimal Investment problem in a finite horizon consists in finding the trading strategy which maximizes the expected future value of the utility of the terminal wealth.

This problem is usually formulated in terms of a Hamilton-Jacobi-Bellman equation. If the investor is of Constant Relative Risk Aversion (CRRA) (see Definition 2.2.2 in Chapter 2), the problem can be explicitly solved (see [48]) and the solution consists in keeping a fixed proportion between the money invested in the risky asset and in the bank account.

Since the stock price changes continuously, the solution proposed by Merton in [48] implies that, without any cost, we can transfer the money from the bank account to the stock and viceversa. Otherwise, if each time that we buy or sell the stock we have to pay an extra amount of money, we would incur in huge transaction costs due to the continuous rebalancing of the portfolio. This would make Merton's strategy unfeasible.

On the other hand, given that the hypothesis of the absence of transaction costs is unrealistic, proportional transaction costs were introduced in [47]. In this case, we usually lack an explicit solution of the problem, which has to be solved by numerical methods.

Spectral methods (see [10]), are a class of spatial discretizations for partial differential

equations which usually offer a very fast convergence, enabling us to represent functions very precisely with relatively few nodes.

The main objective of this Chapter is to construct a spectral method specifically adapted to the Optimal Investment problem with Potential Utility when proportional transaction costs are present.

The outline of the Chapter is as follows. In Section 3.2, a description of the Optimal Investment problem as it can be found in [21] or [56] is presented. In Section 3.3, the problem is reformulated as a parabolic double obstacle problem as it was done in [23], where some explicit formulas and properties of the problem were derived. In Section 3.4 we propose an equivalent formulation of the problem employing polar coordinates. Sections 3.5 and 3.6 are respectively devoted to the development of a Central Finite Differences method and a Mesh-adapted Chebyshev-collocation method which solve the problem developed in Section 3.4. Section 3.7 is devoted to the numerical analysis of both methods and a performance comparison (error committed vs computational cost) between them.

3.2 The Optimal Investment Problem

Let us consider an investor who holds $\bar{X}(t)$ and $\bar{Y}(t)$ in bank and stock accounts respectively. Let $(\Omega, \mathscr{F}, P)$ be a filtered probability space. In absence of transactions costs, we assume (see [48]) that the dynamics of both processes are given by:

$$\begin{cases} d\bar{X}(t) = r\bar{X}(t)dt, \\ d\bar{Y}(t) = \alpha\bar{Y}(t)dt + \sigma\bar{Y}(t)d\bar{z}_t, \end{cases} \tag{3.1}$$

where r denotes the constant risk-free rate, α is the constant expected rate of return of the stock, $\sigma > 0$ is the constant volatility of the stock and $\bar{z}_t$ is a standard Brownian motion such that $\mathscr{F}_t^{\bar{z}} \subseteq \mathscr{F}$ where $\mathscr{F}_t^{\bar{z}}$ is the natural filtration induced by $\bar{z}_t$.

Remark 3.2.1. The bank account plays the same role as the bond in the two previous Chapters. Notation has been slightly altered to emphasize that in this model we work with the amount of money invested in the stock and in the bank account instead of the stock price and the bond price.

The investor can change, at any time t, the amount of money invested in the stock to the bank account or viceversa. Thus, in absence of transaction costs (TC), the evolution of $\bar{X}(t)$, $\bar{Y}(t)$ can be modelled by the following equations:

$$\begin{cases} d\bar{X}(t) = r\bar{X}(t)dt - dL(t) + dM(t), \\ d\bar{Y}(t) = \alpha\bar{Y}(t)dt + \sigma\bar{Y}(t)d\bar{z}_t + dL(t) - dM(t), \end{cases} \tag{3.2}$$

where $L(t)$, $M(t)$ are adapted right-continuous, nonnegative and nondecreasing processes which represent the cumulative monetary values of the stock purchased or sold respectively.

The net wealth, or the money the investor would have if he closes his positions, in absence of transaction costs, is given by

$$\bar{W}(t) = \bar{X}(t) + \bar{Y}(t). \tag{3.3}$$

Let U be a Utility function, i.e. a function with continuous second order derivatives, strictly increasing and strictly concave (see Definition 2.2.2 in Chapter 2). The Optimal Investment problem at time $t = t_0$ consists in finding an admissible strategy that maximizes the Expected Utility of the terminal wealth:

$$\sup_{(L,M)\in A_{t_0}(x,y)} \mathbb{E}\left[U\left(\bar{W}(T)\right)\middle|\, (\bar{X}(t_0), \bar{Y}(t_0)) = (x,y)\right], \tag{3.4}$$

where $\mathbb{E}$ is the conditional expectation at time t_0 subject to $(\bar{X}(t_0), \bar{Y}(t_0)) = (x,y) \in \mathbb{S}$ and $\mathbb{S}$ denotes the Solvency Region. The Solvency Region is defined after the particular choice of the Utility Function, so we ensure that the problem is well defined. The set $A_{t_0}(x,y)$ denotes the set of all admissible strategies starting at (x,y) for $t \in [t_0, T]$.

Suppose that the investor is of Constant Relative Risk Aversion (CRRA). This means (see Definition 2.2.3 in Chapter 2) that the Utility function satisfies

$$-W\frac{U''(W)}{U'(W)} = 1 - \gamma,$$

where γ is a constant.

In [48], this problem is solved in terms of a Hamilton-Jacobi-Bellman equation which is explicitly solved. The optimal investment strategy can be analytically obtained, and consists in keeping a fixed proportion between the wealth in the bank and in the stock:

$$\frac{\bar{X}(t)}{\bar{Y}(t)} = -\frac{\alpha - r - (1-\gamma)\sigma^2}{\alpha - r} = x_M, \tag{3.5}$$

which is commonly referred as the Merton Line.

Since the stock value changes continuously, the portfolio needs to be constantly updated. In practice, the implementation of the optimal strategy would require negligible transaction costs.

In presence of transaction costs equal to a fixed percentage of the transacted amount (proportional transaction costs), the evolution of $\bar{X}(t)$, $\bar{Y}(t)$ is given by the following equations:

$$\begin{cases} d\bar{X}(t) = r\bar{X}(t)dt - (1+\lambda)dL(t) + (1-\mu)dM(t), & \bar{X}(t_0) = x, \\ d\bar{Y}(t) = \alpha\bar{Y}(t)dt + \sigma\bar{Y}(t)d\bar{z}_t + dL(t) - dM(t), & \bar{Y}(t_0) = y, \end{cases} \tag{3.6}$$

where $\lambda,\ \mu \in [0,1)$ represent the constant proportional transaction costs incurred on the purchase or sale of the stock.

In this case, the net wealth is given by:

$$\bar{W}(t) = \begin{cases} \bar{X}(t) + (1-\mu)\bar{Y}(t), & \text{if } \bar{Y}(t) \geq 0, \\ \bar{X}(t) + (1+\lambda)\bar{Y}(t), & \text{if } \bar{Y}(t) < 0, \end{cases} \tag{3.7}$$

for the cases where the investor is long or short in the stock respectively.

This Chapter is devoted to the numerical solution of the problem

$$\sup_{(L,M)\in A_{t_0}(x,y)} \mathbb{E}\left[U\left(\bar{W}(T)\right) \middle| \left(\bar{X}(t_0), \bar{Y}(t_0)\right) = (x,y)\right], \tag{3.8}$$

subject to equations (3.6)-(3.7) when U is the Potential Utility function

$$U(W) = \frac{W^\gamma}{\gamma}, \quad \gamma < 1, \quad \gamma \neq 0. \tag{3.9}$$

Since the Potential Utility function is defined only for positive values (no negative wealth is allowed), we define the Solvency Region as:

$$\mathbb{S} = \left\{(x,y) \in \mathbb{R}^2 \quad | \quad x + (1+\lambda)y > 0, \quad x + (1-\mu)y > 0\right\}. \tag{3.10}$$

The Solvency Region is represented in Figure 3.1, where the x and y axis respectively correspond to the amount of money invested in the bank account and in the stock account. The investor's position in the bank and stock accounts must lie above the frontier of the Solvency Region (blue lines) in order to have a positive wealth.

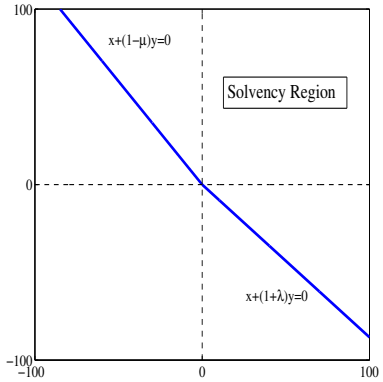

Figure 3.1: Solvency Region in Cartesian coordinates. Horizontal axis: capital invested in the bank account. Vertical axis: capital invested in the stock account.

We say that $(L,M) = (L(t), M(t)),\ t \in [t_0, T]$ is an admissible investment strategy if, given an initial condition $(\bar{X}(t_0),\ \bar{Y}(t_0)) = (x,\ y) \in \mathbb{S}$, then $(\bar{X}(t),\ \bar{Y}(t)) \in \mathbb{S},\ \forall t \in [t_0, T]$.

The Solvency Region implies that, at any time, the investor's positions in the stock and the bank account can be one of the following:

1. A positive amount of money invested in the stock and in the bank accounts.
2. A negative amount of money in the bank account but positive in the stock (leverage).
3. A negative amount of money in the stock account but positive in the bank account (short-selling).

and in the three cases the necessary condition is that, for any $t \in [t_0, T]$, the investor's total wealth is positive.

Let $t_0 = 0$. We denote by $\varphi(x, y, t)$ the optimal value function, i.e. the function that is given by:

$$\varphi(x, y, t) = \sup_{(L,M)\in A_t(x,y)} E\left[U\left(\bar{W}(T)\right) \middle| (\bar{X}(t), \bar{Y}(t)) = (x, y)\right], \quad (x, y, t) \in \mathbb{S} \times [0, T]. \quad (3.11)$$

As remarked in [21], the choice of the Potential Utility function is interesting since it leads to the homothetic property in the optimal value function,

$$\varphi(\rho x, \rho y, t) = \rho^{\gamma}\varphi(x, y, t), \quad \rho > 0,$$

which allows us to reduce the problem to another with one spatial-like variable.

For the rest of the chapter, we will suppose that $\lambda+\mu > 0$ (note that this means that transaction costs exist). In terms of the corresponding Hamilton-Jacobi-Bellman (HJB) equation (see [56]), the optimal value function is the viscosity solution of:

$$\min\left\{-\varphi_t - \hat{\mathcal{L}}\varphi,\ -(1-\mu)\varphi_x + \varphi_y,\ (1+\lambda)\varphi_x - \varphi_y\right\} = 0, \quad (x, y) \in \mathbb{S}, \quad t \in [0, T), \quad (3.12)$$

subject to:

$$\varphi(x, y, T) = \begin{cases} U(x + (1-\mu)y), & \text{if } y > 0, \\ U(x + (1+\lambda)y), & \text{if } y \leq 0, \end{cases} \quad (3.13)$$

where

$$\hat{\mathcal{L}}\varphi = \frac{1}{2}\sigma^2 y^2 \varphi_{yy} + \alpha y \varphi_y + rx\varphi_x. \quad (3.14)$$

The existence and uniqueness of a viscosity solution of the problem is proved in [21]. We refer the reader to it or to Chapter 4 where the arguments used to find the optimal trading strategies in this kind of problems are presented. Here, we are interested in the formulation of the problem presented in [23], where some regularity properties and explicit formulas for certain cases are obtained.

For simplicity reasons, we will suppose that $\alpha > r$. With this hypothesis, whether we are in a scenario with or without transaction costs, short-selling will always be a suboptimal strategy (see [48] and [20] or [56] respectively for each case). This means that the optimal trading strategy is always to have a nonnegative amount of money invested in the stock.

At any time t, the spatial domain is divided in three regions, namely in financial terms, the Buying Region ($(1+\lambda)\varphi_x - \varphi_y = 0$), the Selling Region ($-(1-\mu)\varphi_x + \varphi_y = 0$) and the No Transactions Region ($-\varphi_t - \hat{\mathcal{L}}\varphi = 0$). The Selling and Buying Regions do not intersect (the No Transactions Region will lie between them) and the optimal trading strategy is:

(a) If we are in the Buying Region, to buy the stock with the bank account money until reaching the frontier between the Buying and No Transactions regions.

(b) If we are in the Selling Region, to sell the stock and invest the money in the bank account until reaching the frontier between the Selling and No Transactions regions.

(c) If we are in the No Transactions Region, to do nothing.

For finishing the Subsection, we give the following result.

Proposition 3.2.1. *The value function*

$$\varphi(x,y,t) = \sup_{(L,M)\in A_t(x,y)} E\left[U\left(\bar{W}(T)\right)\middle|\,(\bar{X}(t),\bar{Y}(t)) = (x,y)\right], \quad (x,y,t)\in\mathbb{S}\times[0,T].$$

is a strictly increasing function of x and y.

Proof. For any fixed (x,y,t), consider the associated optimal trading strategy π^o.

Let $W^{\pi^o}(T)$ be the expected terminal wealth when strategy π^o is followed. The value function $\varphi(x,y,t)$ is given by

$$\varphi(x,y,t) = U\left(W_j^{\pi^o}(T)\right).$$

For any initial position $(x+\Delta x, y, t)$, where $\Delta x > 0$, consider the (suboptimal) trading strategy π^{s_1} which consists in retain $\epsilon_1 = \Delta x$ in the bank account until maturity while we independently follow strategy π^o with the rest of the holdings.

For any initial position $(x, y+\Delta y, t)$, where $\Delta y > 0$, consider the (suboptimal) trading strategy π^{s_2} which consists in selling Δy of the stock and then retain $\epsilon_2 = \Delta y(1-\mu)$ in the bank account until maturity while we independently follow strategy π^o with the rest of the holdings.

For any of the two options ($i=1$ or $i=2$), the expected terminal wealth is:

$$W^{\pi^{s_i}}(T) = \epsilon_i e^{r(T-t)} + W^{\pi^o}(T).$$

Therefore, by the suboptimality of the strategy, it holds that

$$\varphi(x+\Delta x,y,t) \geq U\left(W_j^{\pi^{s_1}}(T)\right) = U\left(\epsilon_1\cdot e^{r(T-t)} + W^{\pi^o}(T)\right) > U\left(W^{\pi^o}(T)\right) = \varphi(x,y,t),$$
$$\varphi(x,y+\Delta y,t) \geq U\left(W_j^{\pi^{s_2}}(T)\right) = U\left(\epsilon_2\cdot e^{r(T-t)} + W^{\pi^o}(T)\right) > U\left(W^{\pi^o}(T)\right) = \varphi(x,y,t),$$

because the Utility function is a strictly increasing function. □

3.3 Parabolic double obstacle problem.

In [23], the equivalence of the previous problem to a parabolic double obstacle problem with two free boundaries is proved. Also, several properties and some explicit formulas are obtained.

A brief development of the problem is as follows. Using the homothetic property, we can introduce a new function $V(x,t) = \varphi(x,1,t)$ so that:

$$\varphi(x,y,t) = y^\gamma V\left(\frac{x}{y},t\right) = y^\gamma V(z,t) \tag{3.15}$$

where $z = \frac{x}{y}$ for the rest of the Chapter.

It is straightforward (see [23]) to check that function $V(z,t)$ is the solution of the problem:

$$\min\left\{-V_t - \hat{\mathcal{L}}_1 V,\ -(1+z-\mu)V_z + \gamma V,\ (1+z+\lambda)V_z - \gamma V\right\} = 0, \tag{3.16}$$

where

$$\hat{\mathcal{L}}_1 V = \frac{1}{2}\sigma^2 z^2 V_{zz} + \beta_2 z V_z + \beta_1 V, \tag{3.17}$$

and V satisfies the terminal condition $V(z,T) = \frac{1}{\gamma}(z+1-\mu)^\gamma$.

Function V is defined in $\hat{\Omega}\times(0,T)$, where $\hat{\Omega} = (-(1-\mu),\ \infty)$. We rewrite equation (3.16) as:

$$\begin{cases} -V_t - \hat{\mathcal{L}}_1 V = 0, & \text{if } \dfrac{1}{z+1+\lambda} < \dfrac{V_z}{\gamma V} < \dfrac{1}{z+1-\mu}, \\ -V_t - \hat{\mathcal{L}}_1 V \geq 0, & \text{if } \dfrac{V_z}{\gamma V} = \dfrac{1}{z+1-\mu} \text{ or } \dfrac{V_z}{\gamma V} = \dfrac{1}{z+1+\lambda,} \\ V(z,T) = \dfrac{1}{\gamma}(z+1-\mu)^\gamma. \end{cases} \tag{3.18}$$

Let be $w = \frac{1}{\gamma}\log(\gamma V)$ and $v(z,t) = w_z(z,t)$. In [23] it is proved that function $v(z,t)$ satisfies the following, and equivalent to problem (3.18), parabolic double obstacle problem:

$$\begin{cases} -v_t - \mathcal{L}v = 0, & \text{if } \dfrac{1}{z+1+\lambda} < v < \dfrac{1}{z+1-\mu}, \\ -v_t - \mathcal{L}v \geq 0, & \text{if } v = \dfrac{1}{z+1+\lambda}, \\ -v_t - \mathcal{L}v \leq 0, & \text{if } v = \dfrac{1}{z+1-\mu}, \\ v(z,T) = \dfrac{1}{z+1-\mu}, \end{cases} \tag{3.19}$$

where

$$\mathcal{L}v = \frac{1}{2}\sigma^2 z^2 v_{zz} + (\alpha - r - (2-\gamma)\sigma^2)z v_z - (\alpha - r - (1-\gamma)\sigma^2)v + \frac{1}{2}\gamma\sigma^2\left(z^2 v^2\right)_z. \tag{3.20}$$

The double obstacle problem involves two free boundaries which divide the space in three regions. Taking into account the relation between (3.18) and (3.19), these regions are

a) The Selling Region:

$$\mathbf{SR} = \left\{ (z,t) \in \hat{\Omega} \times [0,T] \;\middle|\; v(z,t) = \frac{1}{z+1-\mu} \right\}.$$

b) The Buying Region:

$$\mathbf{BR} = \left\{ (z,t) \in \hat{\Omega} \times [0,T] \;\middle|\; v(z,t) = \frac{1}{z+1+\lambda} \right\}.$$

c) The No Transaction Region:

$$\mathbf{NT} = \left\{ (z,t) \in \hat{\Omega} \times [0,T] \;\middle|\; \frac{1}{z+1+\lambda} < v(z,t) < \frac{1}{z+1-\mu} \right\}.$$

The proof of existence and regularity of the solution to the double obstacle problem presents some technical difficulties. For example, the degeneracy of operator $\mathcal{L}$ at $z = 0$ and the fact that the upper obstacle is infinite on the boundary $z = -(1-\mu)$.

We now present one of the main results in [23]. We define

$$\tilde{\Omega} = \{z > z^*, 0 < t < T\}, \quad z^* > -(1-\mu),$$

and

$$v(z^*,t) = \frac{1}{z^*+1-\mu}, \quad t \in [0,T].$$

Let $W_p^{a,b}(\tilde{\Omega})$ denote the class of functions $u(z,t) \in L^p(\tilde{\Omega})$ such that the weak derivatives up to order a with respect to z and up to order b with respect to t belong to $L^p(\tilde{\Omega})$ (see [31]).

Theorem 3.3.1. *The double obstacle problem (3.19) has a unique solution*

$$v(z,t) \in W_p^{2,1}\left(\tilde{\Omega}_N \backslash \{\|z\| < \delta\}\right), \quad \delta > 0,\ 1 < p < +\infty,$$

where $\tilde{\Omega}_N$ is any bounded set in $\tilde{\Omega}$.

Proof. See [23].

□

For finishing this Subsection, we present some interesting properties and explicit formulas that are obtained in [23].

3.3.1 Explicit formulas and properties

Problem (3.19) has been numerically solved in [2]. A complete review of all the properties and explicit formulas can be found in the same article, where they are numerically checked. Here we compile the results that are employed in the error analysis (explicit formulas) or that justify some assumptions made when we design the numerical methods.

a) There exist two continuous monotonically increasing functions

$$\mathrm{BR}_F^c(t), \mathrm{SR}_F^c(t) : [0,T] \to (-(1-\mu), +\infty], \tag{3.21}$$

such that $\mathrm{BR}_F^c(t) > \mathrm{SR}_F^c(t)$ and the Buying and Selling Regions are characterized by

$$\mathbf{SR} = \left\{ (z,t) \in \hat{\Omega} \times [0,T] \ \mid z \leq \mathrm{SR}_F^c(t), t \in [0,\ T] \right\},$$
$$\mathbf{BR} = \left\{ (z,t) \in \hat{\Omega} \times [0,T] \ \mid z \geq \mathrm{BR}_F^c(t), t \in [0,\ T] \right\}.$$

Furthermore, function $\mathrm{SR}_F^c(t)$ is $\mathcal{C}^\infty[0,T)$. (Superscript c stands for cartesian coordinates).

b) The function

$$\mathrm{BR}_F^c(t) = +\infty, \quad t \in [\hat{t}_0,\ T], \tag{3.22}$$

where

$$\hat{t}_0 = T - \frac{1}{\alpha - r} \log\left(\frac{1+\lambda}{1-\mu}\right). \tag{3.23}$$

This period of time has a direct and meaningful physical interpretation: "If we are near maturity and we do not have any amount invested in the stock, it is optimal not to invest since the return will not compensate the transaction costs associated to the investment".

c) If $\alpha - r - (1-\gamma)\sigma^2 > 0$, then

$$\begin{aligned} \mathrm{BR}_F^c(t) &< 0, \quad t \in (0,\ \hat{t}_1), \\ \mathrm{BR}_F^c(\hat{t}_1) &= 0, \\ \mathrm{BR}_F^c(t) &> 0, \quad t \in (\hat{t}_1,\ T), \end{aligned} \tag{3.24}$$

where

$$\hat{t}_1 = T - \frac{1}{\alpha - r - (1-\gamma)\sigma^2} \log\left(\frac{1+\lambda}{1-\mu}\right). \tag{3.25}$$

d) Function $v(0,t)$ has an analytical expression:

d.1) If $\alpha - r - (1-\gamma)\sigma^2 \leq 0$

$$v(0,t) = \frac{1}{1-\mu}. \tag{3.26}$$

d.2) If $\alpha - r - (1-\gamma)\sigma^2 > 0$

$$v(0,t) = \begin{cases} \dfrac{1}{1+\lambda} & \text{if } \ 0 \leq t \leq \hat{t}_1, \\ \dfrac{1}{1-\mu} e^{-(\alpha - r - (1-\gamma)\sigma^2)(T-t)} & \text{if } \ \hat{t}_1 < t \leq T. \end{cases} \tag{3.27}$$

e) Frontiers approach to a stationary state.

As $T \to \infty$, there exist two values $\mathrm{BR}_s^c, \mathrm{SR}_s^c \in \mathbb{R}$, such that

$$\begin{aligned} \lim_{t \to 0^+} \mathrm{BR}_F^c(t) &= \mathrm{BR}_s^c, \\ \lim_{t \to 0^+} \mathrm{SR}_F^c(t) &= \mathrm{SR}_s^c, \end{aligned} \tag{3.28}$$

where

$$\begin{aligned} &\mathrm{BR}_s^c = -\frac{d}{d + \frac{k}{k-1}}(1+\lambda), && \mathrm{SR}_s^c = -\frac{d}{d+k}(1-\mu), \\ &d = \frac{\alpha - r - (1-\gamma)\sigma^2}{\frac{1}{2}(1-\gamma)\sigma^2}, && \beta = (1-\gamma)d - 2\gamma C, \\ &C = -\frac{2(k-1)d^2}{k^2\left(d + \frac{1}{1-\gamma} + \sqrt{(d+\frac{1}{1-\gamma})^2 + 4\frac{\gamma}{1-\gamma}\frac{k-1}{k^2}d^2}\right)}, \end{aligned} \tag{3.29}$$

and k is the root of

$$\begin{aligned} &\frac{d + \frac{k}{k-1}}{d+k}\left(\frac{\frac{\gamma}{\beta+1} + \frac{1}{\frac{d}{k}+C}}{\frac{\gamma}{\beta+1} + \frac{1}{\frac{k-1}{k}d+C}}\right)^{\frac{1}{\beta+1}} = \frac{1+\lambda}{1-\mu}, && \text{if } \beta \neq -1, \\ &\frac{d + \frac{k}{k-1}}{d+k} \exp\left(\frac{1}{\gamma}\left(\frac{1}{\frac{d}{k}+C} - \frac{1}{\frac{k-1}{k}d+C}\right)\right) = \frac{1+\lambda}{1-\mu}, && \text{if } \beta = -1. \end{aligned} \tag{3.30}$$

f) $\lim_{t \to T^-} \mathrm{SR}_F^c(t) = (1-\mu)x_M$ where remember that x_M denotes the Merton line.

Proposition 3.3.1. *It holds that*

$$-(1-\mu) < SR^c(t). \tag{3.31}$$

Proof. We argue by contradiction. Properties a) (monotonicity), e), f) state that

$$-\frac{d}{d+k}(1-\mu) = \mathrm{SR}_s^c \leq \mathrm{SR}^c(t) \leq (1-\mu)x_M,$$

$-\frac{d}{d+k}(1-\mu) < -(1-\mu)$ is absurd because that would mean that it exists a finite time such that the Selling Frontier is defined outside the Solvency Region.

$-\frac{d}{d+k}(1-\mu) = -(1-\mu)$ implies $k = 0$, which violates a bound over $k \in [1,2]$ given in [23]. □

In the following Section, a change of variables to polar coordinates will be proposed. We include a numerical example of how the location of the Buying and Selling frontiers evolve in the cartesian coordinates.

On Figure 3.2 we have plotted functions $BR_F^c(t)$ (left) and $SR_F^c(t)$ (right) and include several of the properties compiled in this Subsection. We have enforced $\alpha - r - (1-\gamma)\sigma^2 > 0$ so Property c) can be applied.

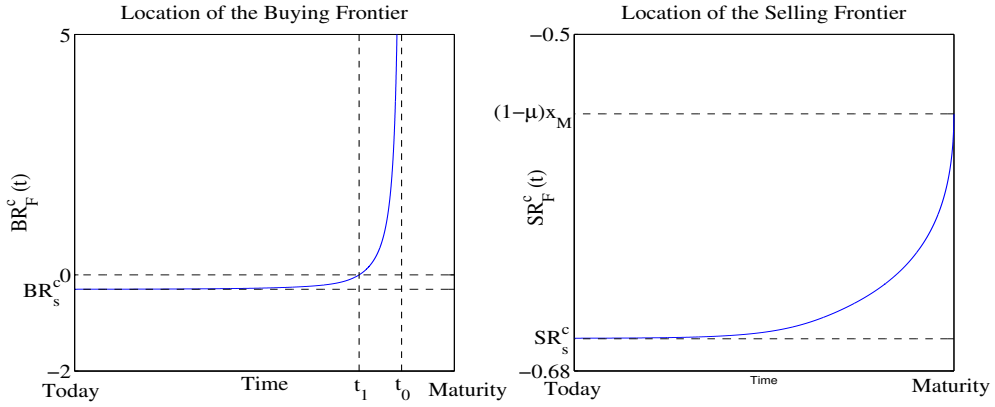

Figure 3.2: Graph of functions $BR_F^c(t)$ (left) and $SR_F^c(t)$ (right).

On Figure 3.2, we can observe that $BR_F^c(t)$ (left) is an increasing function of time. We can also check that the value of $BR_F^c(t)$ tends to $+\infty$ when t approaches to $\hat{t}_0$ by the left and that it holds $BR_F^c(\hat{t}_1) = 0$. Function $BR_F^c(t)$ tends to the stationary state BR_s^c when we move away from Maturity.

On the right side of Figure 3.2, we can observe that $SR_F^c(t)$ is an increasing function of time. It holds that $\lim_{t \to \text{Maturity}^-} \text{SR}^c(t) = (1-\mu)x_M$ and that $\text{SR}^c(t)$ tends to SR_s^c when we move away from Maturity.

We remark that, when we want to numerically solve the problem, one of the technical difficulties is Property b), i.e., the fact that

$$\text{BR}_F^c(t) = +\infty, \quad t \in [\hat{t}_0,\ T],$$

3.4 Alternative approach: Polar coordinates

What we propose here is to attack the problem numerically via polar coordinates:

$$x = a\cos\theta,$$
$$y = a\sin\theta.$$

When we apply this change of variable to equations (3.12)-(3.14) we get

$$\begin{aligned} \min \Bigg\{ & -\varphi_t - \hat{\mathcal{L}}\varphi,\ -(1-\mu)\left[\cos(\theta)\varphi_a - \frac{\sin(\theta)}{a}\varphi_\theta\right] + \left[\sin(\theta)\varphi_a + \frac{\cos(\theta)}{a}\varphi_\theta\right], \\ & (1+\lambda)\left[\cos(\theta)\varphi_a - \frac{\sin(\theta)}{a}\varphi_\theta\right] - \left[\sin(\theta)\varphi_a + \frac{\cos(\theta)}{a}\varphi_\theta\right] \Bigg\} = 0, \end{aligned} \tag{3.32}$$

subject to $\varphi(\theta, a, T)$:

$$\begin{aligned} &U(a\cdot\cos(\theta) + (1-\mu)a\sin(\theta)), \quad \text{if } \theta > 0, \\ &U(a\cdot\cos(\theta) + (1+\lambda)a\sin(\theta)), \quad \text{if } \theta \leq 0, \end{aligned} \tag{3.33}$$

where

$$\begin{aligned} \hat{\mathcal{L}}\varphi =& \frac{1}{2}\sigma^2 (a\sin(\theta))^2 \left[\sin^2(\theta)\varphi_{aa} + \frac{2\sin(\theta)\cos(\theta)}{a}\varphi_{a\theta} + \frac{\cos^2(\theta)}{a^2}\varphi_{\theta\theta} + \frac{\cos^2(\theta)}{a}\varphi_a - \frac{2\sin(\theta)\cos(\theta)}{a^2}\varphi_\theta\right] \\ &+ \alpha a\sin(\theta)\left[\sin(\theta)\varphi_a + \frac{\cos(\theta)}{a}\varphi_\theta\right] + ra\cos(\theta)\left[\cos(\theta)\varphi_a - \frac{\sin(\theta)}{a}\varphi_\theta\right]. \end{aligned} \tag{3.34}$$

The Solvency Region in the new coordinates is given by:

$$\begin{aligned} &a \in [0,\ \infty), \\ &\theta \in (\beta_1,\ \beta_2), \end{aligned} \tag{3.35}$$

where

$$\begin{aligned} \beta_1 &= \arctan\left(\frac{-1}{1+\lambda}\right), \\ \beta_2 &= \arctan\left(\frac{-1}{1-\mu}\right) + \pi. \end{aligned} \tag{3.36}$$

On the left side of Figure 3.3, we have represented the Solvency Region in variables (x, y), where x and y respectively represent the amount of money invested in the bank and stock accounts. We also plot the Solvency Region in polar (a, θ) coordinates (right), where $x = a\cos(\theta),\ y = a\sin(\theta)$. The blue lines represent the points where our total wealth is 0 in variables (x, y) and the red lines represent the same region in polar coordinates.

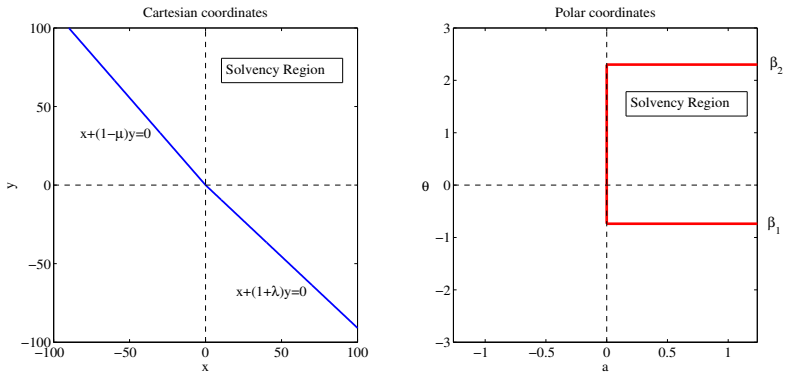

Figure 3.3: Solvency Region in cartesian (left) and polar (right) coordinates. The cartesian coordinates (x, y) represent (Money in the bank account, Money in the stock account).

We conjecture a solution to (3.32) of the form:

$$\varphi(a, \theta, t) = a^\gamma \cdot V(\theta, t). \tag{3.37}$$

Taking into account that

$$\begin{aligned} \varphi_a &= \gamma a^{\gamma-1} V, & \varphi_{aa} &= \gamma(\gamma-1) a^{\gamma-2} V, \\ \varphi_\theta &= a^\gamma V_\theta, & \varphi_{a\theta} &= \gamma a^{\gamma-1} V_\theta, \\ \varphi_t &= a^\gamma V_t, & \varphi_{\theta\theta} &= a^\gamma V_{\theta\theta}, \end{aligned} \tag{3.38}$$

we obtain:

1. In the Buying Region, $\theta \in (\beta_1,\ \mathrm{BR}_F(t)]$, equation $(1+\lambda)\varphi_x - \varphi_y = 0$ is equivalent to:

$$V_\theta = V\gamma \frac{(1+\lambda)\cos(\theta) - \sin(\theta)}{(1+\lambda)\sin(\theta) + \cos(\theta)}, \tag{3.39}$$

where $\mathrm{BR}_F(t) : [0,T] \to (\beta_1, \beta_2)$ is a function such that

$$\mathrm{BR}_F^c(t) = \cot\left(\mathrm{BR}_F(t)\right), \tag{3.40}$$

and $\mathrm{BR}_F^c(t)$ is the function which gives the location of the Buying frontier (Subsection 3.3.1).

2. In the Selling Region, $\theta \in [\mathrm{SR}_F(t), \beta_2)$, equation $-(1-\mu)\varphi_x + \varphi_y = 0$ is equivalent to:

$$V_\theta = V\gamma \frac{(1-\mu)\cos(\theta) - \sin(\theta)}{(1-\mu)\sin(\theta) + \cos(\theta)}, \tag{3.41}$$

where $\mathrm{SR}_F(t) : [0,T] \to (\beta_1, \beta_2)$ is a function such that

$$\mathrm{SR}_F^c(t) = \cot\left(\mathrm{SR}_F(t)\right), \tag{3.42}$$

and $\mathrm{SR}_F^c(t)$ is the function which gives the location of the Selling frontier (Subsection 3.3.1).

3. In the No Transaction Region, $\theta \in (\mathrm{BR}_F(t),\ \mathrm{SR}_F(t))$, equation $-\varphi_t - \hat{\mathcal{L}}\varphi = 0$ is equivalent to:

$$V_t + g_2(\theta) V_{\theta\theta} + g_1(\theta) V_\theta + g_0(\theta) V = 0, \tag{3.43}$$

where

$$\begin{aligned} g_2(\theta) &= \frac{1}{2}\sigma^2 \sin^2(\theta)\cos^2(\theta), \\ g_1(\theta) &= (\gamma-1)\sigma^2 \cos(\theta)\sin^3(\theta) + (\alpha - r)\sin(\theta)\cos(\theta), \\ g_0(\theta) &= \gamma\left[\left((\gamma-1)\sin^2(\theta) + \cos^2(\theta)\right)\frac{1}{2}\sigma^2\sin^2(\theta) + \alpha\sin^2(\theta) + r\cos^2(\theta)\right]. \end{aligned} \tag{3.44}$$

The objective of the change of variables to polar coordinates is to circumvent two of the technical difficulties that appear when we work with function $v(z,t)$ given by (3.19).

The first one is that the spatial-like variable z was defined in an unbounded domain $(-(1-\mu), +\infty)$. Now, we can work in a bounded domain $\theta \in (\beta_1,\ \beta_2)$. We remark Property b)

in Subsection 3.3.1, which stated the importance of $+\infty$ in this problem. In polar coordinates, this point corresponds to $\theta = 0$.

The second advantage of this formulation is that there are not non linear terms like $(z^2 v^2)_z$ that can be found in equation (3.19).

Summarizing the development, the problem that we want to numerically solve is:

$$\begin{aligned} \min \Bigg\{ & -V_t - g_2(\theta) V_{\theta\theta} - g_1(\theta) V_\theta - g_0(\theta) V, \; -V_\theta + V \cdot \gamma \frac{(1+\lambda)\cos(\theta) - \sin(\theta)}{(1+\lambda)\sin(\theta) + \cos(\theta)}, \\ & V_\theta - V \cdot \gamma \frac{(1-\mu)\cos(\theta) - \sin(\theta)}{(1-\mu)\sin(\theta) + \cos(\theta)} \Bigg\} = 0, \quad \theta \in (\beta_1, \beta_2), \quad t \in [0, T), \end{aligned} \tag{3.45}$$

subject to:

$$V(\theta, T) = \begin{cases} \dfrac{(\cos(\theta) + (1-\mu)\sin(\theta))^\gamma}{\gamma}, & \text{if } \theta > 0, \\ \dfrac{(\cos(\theta) + (1+\lambda)\sin(\theta))^\gamma}{\gamma}, & \text{if } \theta \leq 0. \end{cases} \tag{3.46}$$

where functions g_i are given by (3.44).

With the results shown in the previous Subsections, it is expected that the Spatial domain could be divided in three regions: Buying, No Transactions and Selling, where $\mathrm{BR}_F(t)$, $\mathrm{SR}_F(t)$ are the respective frontiers at time t.

If this holds, let $t \in [0, T]$. Suppose that we know the exact location of the Buying ($\mathrm{BR}_F(t)$) and Selling ($\mathrm{SR}_F(t)$) frontiers. Suppose also that we know the values $V(\mathrm{BR}_F(t), t)$ and $V(\mathrm{SR}_F(t), t)$. We can compute the function value $V(\theta, t)$ in the Buying and Selling Regions integrating equations (3.39) and (3.41):

$$\begin{aligned} V(\theta, t) &= V(\mathrm{BR}_F(t), t) \left[\frac{(1+\lambda)\sin(\theta) + \cos(\theta)}{(1+\lambda)\sin(\mathrm{BR}_F(t)) + \cos(\mathrm{BR}_F(t))} \right]^\gamma, \quad \theta < \mathrm{BR}_F(t), \\ V(\theta, t) &= V(\mathrm{SR}_F(t), t) \left[\frac{(1-\mu)\sin(\theta) + \cos(\theta)}{(1-\mu)\sin(\mathrm{SR}_F(t)) + \cos(\mathrm{SR}_F(t))} \right]^\gamma, \quad \theta > \mathrm{SR}_F(t). \end{aligned} \tag{3.47}$$

3.4.1 Explicit formulas and properties

The relation between function $V(\theta, t)$ and function $v(z, t)$ given by (3.19), can be explicitly computed:

$$\begin{aligned} v(z, t) &= -\left(\frac{V_\theta(\theta, t)\sin^2(\theta) - \gamma \sin(\theta)\cos(\theta) V(\theta, t)}{\gamma V(\theta, t)} \right), \\ z &= \cot(\theta). \end{aligned} \tag{3.48}$$

We can also derive some properties of functions $\mathrm{SR}_F(t)$, $\mathrm{BR}_F(t)$ from the properties of functions $\mathrm{SR}_F^c(t)$, $\mathrm{BR}_F^c(t)$ compiled in Subsection 3.3.1.

Proposition 3.4.1. *Functions $SR_F(t)$, $BR_F(t)$ given by (3.40) and (3.42) are monotonically decreasing functions.*

It holds that $BR_F(t) < SR_F(t)$ *and that*

$$BR_F(t) = 0, \quad t \in [\hat{t}_0,\ T].$$

where $\hat{t}_0$ *was defined in (3.23).*

If $\alpha - r - (1-\gamma)\sigma^2 > 0$, *then*

$$BR_F(\hat{t}_1) = \frac{\pi}{2}$$

where $\hat{t}_1$ *was defined in (3.25).*

If $T = \infty$, *there exist two values* $BR_s, SR_s \in (\beta_1, \beta_2)$, *such that*

$$\lim_{t\to 0^+} BR_F(t) = BR_s,$$
$$\lim_{t\to 0^+} SR_F(t) = SR_s.$$

It hods that $\lim_{t\to T^-} \cot\left(SR_F(t)\right) = (1-\mu)x_M$.

Proof. This result is a direct consequence of Properties a), b), c), e) and f) of Subsection 3.3.1 and the relation which corresponds to the change of variable to polar coordinates

$$\mathrm{BR}_F^c(t) = \cot\left(\mathrm{BR}_F(t)\right), \quad \mathrm{SR}_F^c(t) = \cot\left(\mathrm{SR}_F(t)\right).$$

□

We give a numerical example on Figure 3.4. We plot functions $BR_F(t)$ and $SR_F(t)$ and include the results of the previous Proposition. We have enforced the parameter values so $\alpha - r - (1-\gamma)\sigma^2 > 0$ holds.

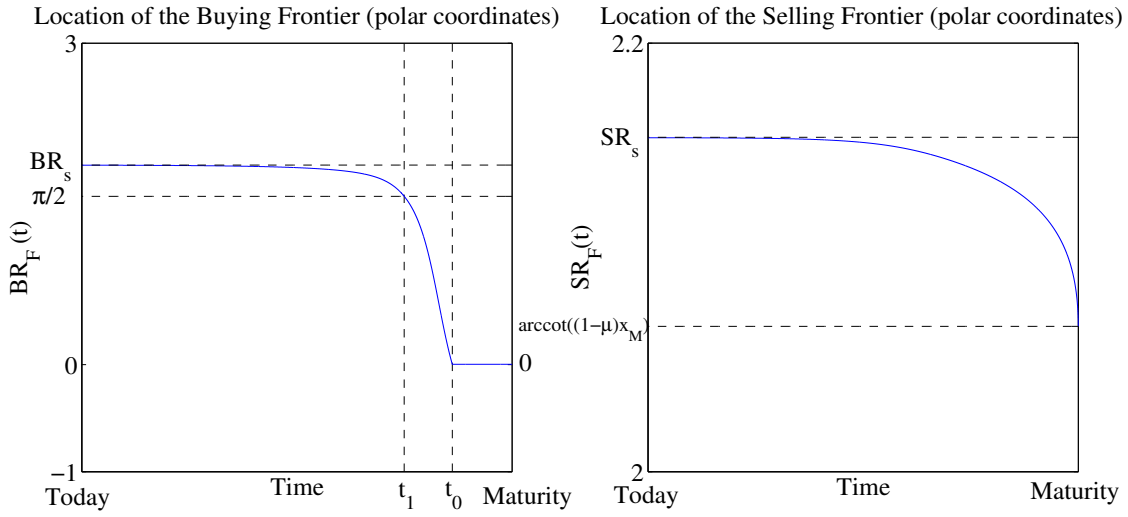

Figure 3.4: Graph of functions $BR_F(t)$ (left) and $SR_F(t)$ (right).

On Figure 3.4, we can see that $BR_F(t)$ (left) is a decreasing function of time. It holds that $BR_F(\hat{t}_1) = \pi/2$ and that $BR_F(t) = 0,\ t \in [\hat{t}_0, \text{Maturity}]$. Function $BR_F(t)$ tends to the stationary value BR_s as we move away from Maturity.

On the right side of Figure 3.4, we see that function $SR_F(t)$ is a decreasing function of time. Furthermore, it tends to the stationary value SR_s as we move away from Maturity and it holds that $\lim_{t\to T^-} \text{SR}(t) = \text{arccot}\left((1-\mu)x_M\right) \in (\beta_1, \beta_2)$.

The relation between Figure 3.4 and Figure 3.2 is given by $\text{BR}_F^c(t) = \cot\left(\text{BR}_F(t)\right)$, $\text{SR}_F^c(t) = \cot\left(\text{SR}_F(t)\right)$.

Proposition 3.4.2. *Let SR_s^c be the stationary value given by formula (3.28) and $SR_s \in (\beta_1, \beta_2)$ be such that $SR_s^c = \cot(SR_s)$.*

It holds that functions $SR_F(t)$, $BR_F(t)$ given by (3.40) and (3.42) satisfy

$$\beta_1 < 0 \leq BR(t) \leq SR(t) \leq SR_s < \beta_2, \quad t \in [0, T],$$

Proof. This result is a direct consequence of the monotonicity, the limit values when t approaches T, Proposition 3.3.1 and the relation

$$\text{SR}_F^c(t) = \cot\left(\text{SR}_F(t)\right), \quad \text{SR}_F^c(t) = \cot\left(\text{SR}_F(t)\right).$$

□

This Proposition justifies the two numerical methods that are proposed in the following Sections.

3.5 Central Finite Differences Method

The numerical methods that we are going to develop are constructed upon the following strategy.

Let $\pi \in A_0(x, y)$ denote an admissible trading strategy where x and y are the amount of money in the bank and stock accounts at $t = 0$. Let π^o denote the optimal trading strategy which solves (3.8).

Let $\alpha_1 \in (\beta_1, 0)$ and $\alpha_2 \in (SR_s, \beta_2)$ and define

$$A_0^{\alpha_1,\alpha_2}(x, y) = \{\pi \in A_0(x, y) : \theta^\pi \in (\alpha_1, \alpha_2)\} \tag{3.49}$$

where $\theta^\pi = \text{arccot}\left(\dfrac{x^\pi}{y^\pi}\right) \in (\alpha_1, \alpha_2)$ and $x^\pi,\ y^\pi$ are the amounts in the bank and stock accounts if strategy π is followed.

Corollary 3.5.1. *Proposition 3.4.2 implies that $\pi^o \in A_0^{\alpha_1,\alpha_2}(x, y)$.*

Therefore, the solution of the problem can be found solving (3.45)-(3.46) in $(\alpha_1, \alpha_2)\times[0,T]$ subject to the boundary conditions:

$$\begin{aligned} V_\theta(\alpha_1, t) &= V(\alpha_1, t)\,\gamma\frac{(1+\lambda)\cos(\alpha_1) - \sin(\alpha_1)}{(1+\lambda)\sin(\alpha_1) + \cos(\alpha_1)}, \\ V_\theta(\alpha_2, t) &= V(\alpha_2, t)\,\gamma\frac{(1-\mu)\cos(\alpha_2) - \sin(\alpha_2)}{(1-\mu)\sin(\alpha_2) + \cos(\alpha_2)}. \end{aligned} \tag{3.50}$$

where we note that these conditions are equivalent to a mandatory buying or selling the stock if θ reaches α_1 or α_2 respectively (see formulas (3.39)-(3.41)).

The solution is extended to $(\beta_1, \beta_2)\times[0,T]$ stating that for $t\in[0,T]$:

$$\begin{aligned} \theta \le \alpha_1 \quad &\text{is in the Buying Region,} \\ \theta \ge \alpha_2 \quad &\text{is in the Selling Region,} \end{aligned}$$

and computing $V(\theta, t)$ with (3.47).

Let $t\in[0,T]$. Fixed a number $N_t\in\mathbb{N}$, we define the time mesh $\{t_l\}_{l=0}^{N_t}$ by

$$t_l = l\Delta t, \quad l = 0,1,...,N_t, \quad \Delta t = \frac{T}{N_t} \tag{3.51}$$

The numerical method is based on the computation of V^{N_t}, which is an approximation in time to function V in $(\alpha_1,\alpha_2)\times[0,T]$. Function V^{N_t} is the function value which corresponds to the optimization problem (3.8) when the allowed transactions are:

1. The minimal which ensure that $\theta\in(\alpha_1,\alpha_2)$ for $t\in[0,T]$.
2. Any, if $t = t_{l_0}\in\{t_l\}_{l=0}^{N_t}$ and we remain in (α_1,α_2).

Function V^{N_t} converges to V as Δt tends to 0 because the allowed strategies given by 1. and 2. approach to $A_0^{\alpha_1,\alpha_2}(x,y)$. This implies that the optimal trading strategy $\pi_o^{N_t}$ of the discrete (in time) problem approaches to π_o.

The objective of this Section is to numerically solve problem (3.45)-(3.46) with a Central Finite Differences (FD) method.

Although the numerical algorithm will be fully described in Subsection 3.5.4, we mention now that, at any time step $t_{l_0}\in\{t_l\}_{l=0}^{N_t}$, we will have to:

a) Solve the the partial differential equation which corresponds to the No Transactions Region subject to the proper terminal condition.

b) Locate the Buying and Selling frontiers at t_{l_0} and recompute the function value in the Buying and Selling Regions.

The Section is organized as follows: First, we will explain how to choose the spatial mesh that will be employed for any time step $t_{l_0} \in \{t_l\}_{l=0}^{N_t}$. Afterwards, we will detail the FD method. Finally, we will explain how to numerically compute the location of the Buying and Selling frontiers.

The Section finishes with a detailed description of the numerical algorithm that must be followed to solve the problem and a brief example of the results obtained.

3.5.1 Fixed spatial mesh

We point out that the derivative of the function value $V(\theta, t)$ in the Buying and Selling regions grows to ∞ as we approximate the limits of the Solvency Region β_1 or β_2. This is the reason why, in order to avoid numerical difficulties, the limits of the Spatial domain have been chosen inside the Solvency Region.

We define the spatial mesh $\{\theta_j\}_{j=0}^{N_\theta}$ by

$$\theta_j = (j - N_1)\,\Delta\theta, \quad j = 0, 1, 2, ..., N_1 + N_2 = N_\theta, \tag{3.52}$$

where $\Delta\theta > 0$, $N_1, N_2 \in \mathbb{N}$ are parameters satisfying

$$\begin{aligned} &\Delta\theta < \min\left\{|\beta_1|, \beta_2 - \mathrm{SR}_s\right\}, \\ &\left\{\frac{|\beta_1|}{\Delta\theta}, \quad \frac{\beta_2}{\Delta\theta}, \quad \frac{\mathrm{SR}_s}{\Delta\theta}\right\} \notin \mathbb{N}, \\ &1 \leq N_1 \leq \left\lfloor \frac{|\beta_1|}{\Delta\theta} \right\rfloor, \quad \frac{SR_s}{\Delta\theta} < N_2 \leq \left\lfloor \frac{\beta_2}{\Delta\theta} \right\rfloor. \end{aligned} \tag{3.53}$$

and $N_\theta = N_1 + N_2$.

It is easy to check that, by construction and thanks to Proposition 3.4.2, it holds

$$\beta_1 < \theta_0 = -\Delta\theta N_1 < 0, \;\; \mathrm{SR}_s < \theta_{N_\theta} = \Delta\theta N_2 < \beta_2,$$

which implies that θ_0 is always inside the Buying Region and that θ_{N_θ} is always inside the Selling Region for all $t_l \in [0, T]$.

We point out that, with this definition, $\theta_{N_1} = 0$ and that the user is free to chose the size of $\Delta\theta$ and how close are θ_0 and θ_{N_θ} to the limits of the Solvency Region.

From now on, for any function f, the superscript $f^{\mathbf{N}}$ denotes its numerical approximation, where $\mathbf{N} = (N_t, N_\theta)$ describes the size of the time and spatial meshes.

3.5.2 The Central Finite Differences method

At a fixed time step t_l of the time discretization given by (3.51), suppose that we know the function value $V(\theta, t_l),\ \theta \in (\beta_1, \beta_2)$.

Let the spatial mesh $\{\theta_j\}_{j=0}^{N_\theta}$ be given by (3.52) and consider $(\theta_0, \theta_{N_\theta}) \subset (\beta_1, \beta_2)$.

Let $\hat{V}(\theta, t),\ (\theta, t) \in (\theta_0, \theta_{N_\theta}) \times [t_{l-1}, t_l]$ be the the function value which gives the expected terminal value when the trading strategy is not perform transactions if $\theta \in (\theta_0, \theta_{N_\theta})$, buy the stock if $\theta = \theta_0$ and sell the stock if $\theta = \theta_{N_\theta}$, subject to $\hat{V}(\theta, t_l) = V(\theta, t_l)$.

Therefore, $\hat{V}(\theta, t)$ is the solution of equation:

$$-\hat{V}_t + g_2(\theta)\hat{V}_{\theta\theta} + g_1(\theta)\hat{V}_\theta + g_0(\theta)\hat{V} = 0, \tag{3.54}$$

subject to

$$\begin{aligned} V_\theta(\theta_0, t) &= V(\theta_0, t)\,\gamma\frac{(1+\lambda)\cos(\theta_0) - \sin(\theta_0)}{(1+\lambda)\sin(\theta_0) + \cos(\theta_0)}, \\ V_\theta(\theta_{N_\theta}, t) &= V(\theta_{N_\theta}, t)\,\gamma\frac{(1-\mu)\cos(\theta_{N_\theta}) - \sin(\theta_{N_\theta})}{(1-\mu)\sin(\theta_{N_\theta}) + \cos(\theta_{N_\theta})}, \\ \hat{V}(\theta, t_l) &= V(\theta, t_l), \end{aligned} \tag{3.55}$$

where we note that the boundary conditions are equivalent to a mandatory buying or selling the stock if θ reaches θ_0 or θ_{N_θ} respectively (see formulas (3.39)-(3.41)).

The FD method will be invoked for $l = N_t,\ N_t - 1, ..., 1$ in the numerical algorithm developed in Subsection 3.5.4. If $t_l = t_{N_t} = T$, the function value $V(\theta, T)$ is a known data of the problem. If $t_l < T$, the value of $V(\theta, t_l)$ is substituted by its numerical approximation $V^{\mathbf{N}}(\theta, t_l)$, which has been computed in the previous step of the numerical algorithm.

The numerical approximation $\left\{\hat{V}^{\mathbf{N}}(\theta_j, t_{l-1})\right\}_{j=0}^{N_\theta}$ to function $\hat{V}$ in interval (θ_0, θ_N) is given by the solution of:

$$\left.\frac{\partial \hat{V}^{\mathbf{N}}}{\partial t}\right|_{\theta=\theta_j} = g_2(\theta)\frac{\partial^2 \hat{V}^{\mathbf{N}}}{\partial \theta^2} + g_1(\theta)\frac{\partial \hat{V}^{\mathbf{N}}}{\partial \theta} + g_0(\theta)\hat{V}^{\mathbf{N}}\Big|_{\theta=\theta_j} = L\left(\hat{V}^{\mathbf{N}}\right)\Big|_{\theta=\theta_j}, \quad j = 1, ..., N_\theta - 1, \tag{3.56}$$

subject to

$$\hat{V}^{\mathbf{N}}(\theta_j, t_l) = V(\theta_j, t_l), \quad j = 1, 2, ..., N_\theta - 1,$$

where we impose Neumann boundary conditions (discussed at the end of the Subsection), so that, for $t \in [t_{l-1}, t_l]$:

$$\begin{aligned} \hat{V}_\theta^{\mathbf{N}}(\theta_0, t) &= V_\theta(\theta_0, t_l) = V(\theta_0, t_l)\gamma\frac{(1+\lambda)\cos(\theta_0) - \sin(\theta_0)}{(1+\lambda)\sin(\theta_0) + \cos(\theta_0)}, \\ \hat{V}_\theta^{\mathbf{N}}(\theta_{N_\theta}, t) &= V_\theta(\theta_{N_\theta}, t_l) = V(\theta_{N_\theta}, t_l)\gamma\frac{(1-\mu)\cos(\theta_{N_\theta}) - \sin(\theta_{N_\theta})}{(1-\mu)\sin(\theta_{N_\theta}) + \cos(\theta_{N_\theta})}. \end{aligned} \tag{3.57}$$

It is understood that in (3.56), the derivatives with respect θ of order 1 and 2 are representations of the second order central finite differences, that is, for $f = V$ or $\hat{V}$ and $t = t_{l-1}$ or t_l,

the derivatives are approximated for $j = 1, ..., N_\theta - 1$ by

$$\begin{aligned} f_\theta(\theta_j, t) &\approx \frac{f(\theta_{j+1}, t) - f(\theta_{j-1}, t)}{2\Delta\theta}, \\ f_{\theta\theta}(\theta_j, t) &\approx \frac{f(\theta_{j+1}, t) - 2f(\theta_j, t) + f(\theta_{j-1}, t)}{(\Delta\theta)^2}. \end{aligned} \tag{3.58}$$

The temporal derivative is substituted by the implicit midpoint rule

$$\frac{\hat{V}(\theta, t_{l-1}) - V(\theta, t_l)}{\Delta t} = L\left(\frac{\hat{V}(\theta, t_{l-1}) + V(\theta, t_l)}{2}\right). \tag{3.59}$$

Since operator L is linear in V, the numerical scheme can be written as

$$\begin{cases} \hat{V}^{\mathbf{N}} - \dfrac{\Delta t}{2} L\left(\hat{V}^{\mathbf{N}}\right)\Big|_{\theta=\theta_j,\ t=t_{l-1}} = V + \dfrac{\Delta t}{2} L\left(V\right)\Big|_{\theta=\theta_j,\ t=t_l}, \quad j = 1, ..., N_\theta - 1, \\ \hat{V}_\theta^{\mathbf{N}}(\theta_0, t_{l-1}) = V(\theta_0, t_l)\gamma \dfrac{(1+\lambda)\cos(\theta_0) - \sin(\theta_0)}{(1+\lambda)\sin(\theta_0) + \cos(\theta_0)}, \\ \hat{V}_\theta^{\mathbf{N}}(\theta_{N_\theta}, t_{l-1}) = V(\theta_{N_\theta}, t_l)\gamma \dfrac{(1-\mu)\cos(\theta_{N_\theta}) - \sin(\theta_{N_\theta})}{(1-\mu)\sin(\theta_{N_\theta}) + \cos(\theta_{N_\theta})}. \end{cases} \tag{3.60}$$

To finish the Subsection, we make some remarks.

We point out that the values of $V_\theta(\theta_0, t_l)$ and $V_\theta(\theta_{N_\theta}, t_l)$ given in (3.57) are exact since, by construction, θ_0 and θ_N, are always respectively in the Buying and Selling Regions at $t = t_l$ (see the previous Subsection and formulas (3.39) and (3.41)).

Concerning the choice of Neumann boundary conditions, a priori, neither $\hat{V}(\theta)$ nor $\hat{V}_\theta(\theta)$ remain constant in time at $\theta = \{\theta_0,\ \theta_{N_\theta}\}$. Indeed, the true boundary conditions are of Robin type and would be given by (3.55).

In order to guarantee the stability of the numerical methods that we are going to develop and to perform an equivalent comparison between them, we have imposed the Neumann conditions in both (instead of Dirichlet ones, which gave higher errors). Therefore, we are generating a numerical error, that will be referred as the boundary error.

The computation of $\hat{V}^{\mathbf{N}}(t_{l-1})$ is just an intermediate step in order to compute the value of $V^{\mathbf{N}}(t_{l-1})$, the numerical approximation of the objective function. At each time step $l = N_t,\ N_t - 1, ..., 1$ of the Numerical Algorithm, (see Subsection 3.5.4), we will compute a numerical approximation of the Buying and Selling frontiers, and recompute the values in the Buying and Selling regions with explicit formulas. Therefore, the boundary error in the value of $V^{\mathbf{N}}$ will be controlled by the size of $\Delta\theta$ and Δt.

3.5.3 Location of the Buying/Selling frontiers

At a fixed time step t_l of the time discretization given by (3.51), suppose that we know the function value $V(\theta, t_l),\ \theta \in (\beta_1,\ \beta_2)$.

Let the spatial mesh $\{\theta_j\}_{j=0}^{N_\theta}$ be given by (3.52) and consider $(\theta_0, \theta_{N_\theta}) \subset (\beta_1, \beta_2)$.

Let $\hat{V}(\theta, t),\ (\theta, t) \in (\theta_0, \theta_{N_\theta}) \times [t_{l-1}, t_l]$ be the solution of (3.54)-(3.55). Function $\hat{V}(\theta, t)$ is the function value which gives the expected terminal value when the trading strategy is to not perform transactions if $\theta \in (\theta_0, \theta_{N_\theta})$, to buy the stock if $\theta = \theta_0$ and to sell the stock if $\theta = \theta_{N_\theta}$, subject to $\hat{V}(\theta, t_l) = V(\theta, t_l)$.

Suppose that we are allowed to perform a transaction (buy or sell the stock) at $t = t_{l-1}$. Since it can never be optimal to buy and sell the stock at the same time, we compare if it would be better to perform no transactions versus buy or sell the stock. We define:

$$\begin{aligned} P_1^{l-1}(\theta) &= \hat{V}_\theta(\theta, t_{l-1}) - \hat{V}(\theta, t_{l-1})\gamma \frac{(1+\lambda)\cos(\theta) - \sin(\theta)}{(1+\lambda)\sin(\theta) + \cos(\theta)}, \\ P_2^{l-1}(\theta) &= \hat{V}_\theta(\theta, t_{l-1}) - \hat{V}(\theta, t_{l-1})\gamma \frac{(1-\mu)\cos(\theta) - \sin(\theta)}{(1-\mu)\sin(\theta) + \cos(\theta)}, \end{aligned} \tag{3.61}$$

whose sign has a meaningful physical interpretation for each $\theta \in (\theta_0, \theta_N)$:

a) The sign of $P_1^{l-1}(\theta)$ implies that the result of buying the stock would be strictly better ($<$), equivalent ($=$) or strictly worse ($>$) to not performing transactions.

b) The sign of $P_2^{l-1}(\theta)$ implies that the result of selling the stock would be strictly better ($<$), equivalent ($=$) or strictly worse ($>$) to not performing transactions.

It is clear that the sign of $P_i^{l-1}(\theta),\ i = 1, 2$ must approach to the optimal trading strategy of the problem given by variational inequality (3.45) at $t = t_l$ when Δt tends to 0.

For defining an approximation in time of the Buying (BR_F^{l-1}) and Selling (SR_F^{l-1}) frontiers, we need to prove that for $i = 1, 2$, the sign of $P_i^{l-1}(\theta),\ \theta \in (\theta_0,\ \theta_{N_\theta})$ unambiguously divides the spatial domain in just three regions, which respectively correspond to a Buying, a No Transactions and a Selling Region.

Functions $P_i^{l-1}(\theta),\ i = 1, 2$ are not (empirical) strictly increasing or decreasing functions in $(\theta_0, \theta_{N_\theta})$. Nevertheless, we can argue, employing optimality arguments, that for $i = 1$ or 2, the following result holds.

Theorem 3.5.1. *It exists $\beta_i \in (\theta_0, \theta_{N_\theta}),\ i = 1, 2$ such that*

$$\begin{aligned} P_1^{l-1}(\theta) < 0 \text{ if and only if } \theta < \beta_1, \\ P_2^{l-1}(\theta) < 0 \text{ if and only if } \theta > \beta_2. \end{aligned}$$

To see that the previous theorem is true (the proof is detailed below), we need to pull back to the optimization statement of the problem to see what have we computed and which properties does it satisfy. Let x and y be the amount of money in the bank and stock accounts.

We define

$$\mathbb{S}^{N_\theta} = ((x,y) \in \mathbb{R} \times \mathbb{R} : x + \cot(\alpha_0)y > 0, \quad x + \cot(\alpha_{N_\theta})y > 0)), \tag{3.62}$$

and the trading strategy

$$\pi_{NT}(x,y) = \left\{(L(t), M(t)) : \left(\bar{X}(t_{l-1}), \bar{Y}(t_{l-1})\right) = (x,y)\right\}, \tag{3.63}$$

which ensures that $\left(\bar{X}(t), \bar{Y}(t)\right) \in \mathbb{S}^{N_\theta},\ t \in [t_{l-1}, t_l]$, but no transactions are realized if this occurs. We note that, from the linearity of equations (3.6), the trading strategy for an initial position $(\rho x, \rho y),\ \rho > 0$ is $\pi_{NT}(\rho x, \rho y) = \rho \pi_{NT} = \{(\rho L(t), \rho M(t)) :\ (L(t), M(t)) \in \pi_{NT}(x,y)\}$.

We define the function value:

$$\hat{\varphi}(x, y, t_{l-1}) = \mathbb{E}_{\pi_{NT}(x,y)} \left\{\varphi\left(\bar{X}(t_l), \bar{Y}(t_l), t_l\right) \mid \left(\bar{X}(t_{l-1}), \bar{Y}(t_{l-1})\right) = (x,y)\right\}, \tag{3.64}$$

where function φ was given in (3.11), processes $\bar{X}(t),\ \bar{Y}(t)$ are modelled by (3.6) and $\mathbb{E}_{\pi_{NT}(x,y)}$ is the conditional expectation at $t = t_{l-1}$ subject to $\left(\bar{X}(t_{l-1}), \bar{Y}(t_{l-1})\right) = (x,y)$ and to follow strategy $\pi_{NT}(x,y)$.

We recall that $\varphi(x,y,t)$ is strictly increasing in x and y (see Proposition 3.2.1). Furthermore, it has the homothetic property ($\varphi(\rho x, \rho y, t) = \rho^\gamma \varphi(x,y,t),\ \rho > 0$) and is concave (see [21]).

We note that function $\hat{\varphi}(x, y, t_{l-1})$ corresponds to $\hat{V}(\theta, t_{l-1})$ up to the change to polar coordinates.

Suppose now that we are allowed to perform a transaction at time t_{l-1}. Our objective is to maximize the expected terminal value. Therefore, we define:

$$\hat{\varphi}^{t_{l-1}}(x,y) = \sup_{L,M} \left\{\hat{\varphi}\left(x - (1+\lambda)L + (1-\mu)M, y - L + M, t_{l-1}\right)\right\}. \tag{3.65}$$

Employing the same arguments as in [21, Theorem 3.1], from the linearity of equations (3.6) and strategy π_{NT}, function $\hat{\varphi}^{t_{l-1}}(x,y)$ inherits the concavity and homothetic properties.

Proposition 3.5.1. *Function $\hat{\varphi}^{t_{l-1}}(x,y)$ is strictly increasing in x and y.*

Proof. Let (x,y) be the position at t_{l-1} and suppose that $\hat{\varphi}^{t_{l-1}}(x,y)$ is known.

For an initial position $(x + \Delta x, y),\ \Delta x > 0$, we are allowed to buy or sell the stock at t_{l-1}. Consider the, a priori suboptimal, trading strategy which consists in buying a certain amount $\epsilon > 0$ of the stock such that

$$(x + \Delta x - (1+\lambda)\epsilon, y + \epsilon) = (\rho x, \rho y)$$

with $\rho > 1$.

It holds, by the suboptimality of the strategy, that

$$\hat{\varphi}^{t_{l-1}}(x+\Delta x, y) \geq \hat{\varphi}^{t_{l-1}}(x+\Delta x-(1+\lambda)\epsilon, y+\epsilon) = \rho^{\gamma}\hat{\varphi}^{t_{l-1}}(x,y) > \hat{\varphi}^{t_{l-1}}(x,y)$$

employing the homothetic property.

The same argument can be applied to an initial position $(x, y+\Delta y),\ \Delta y > 0$.

□

Function $\hat{\varphi}^{t_{l-1}}(x,y)$ is the function value at $t = t_{l-1}$ of the maximization of the expected terminal utility when we allow a transaction at t_{l-1}, the minimal transactions to remain in $\mathbb{S}^{N_\theta}$ for $t \in [t_{l-1}, T]$ and any transactions for $t \in [t_l, T]$.

Employing optimization arguments (see [21]), the Hamilton-Jacobi-Bellman equation (3.12) holds at $t = t_{l-1}$ because we are allowed to perform a transaction (not for $t \in (t_{l-1}, t_l)$ where we do not have any control but to remain in $\mathbb{S}^{N_\theta}$). We note that the sign of $P_i^{l-1}(\theta)$ marks when the different inequalities occur.

As it is remarked in [21], the homothetic property only holds when we are allowed to buy or sell at the maximum rate, inducing the so called "bang-bang" strategies. If we are in the Buying Region, the optimal trading strategy is to immediately buy the stock until reaching the point where it is not optimal to do so (and the equivalent strategy in the Selling Region). This justifies the employment of the explicit formulas for the Buying and Selling Region.

Thanks to the homothetic property of function $\hat{\varphi}^{t_{l-1}}$, if it is optimal to buy or sell at $t = t_{l-1}$ for (x,y), so it is for $(\rho x, \rho y)$. This implies that the frontiers between regions are rays from the origin. For finishing the argument, note that the investors try to maximize their benefits and are risk-averse (concavity).

Let y be fixed. Suppose that for an initial position (x,y) it is optimal to buy. For any initial position $(x+\Delta x, y),\ \Delta x > 0$, we have increased our expected results ($\hat{\varphi}^{t_{l-1}}$ is strictly increasing) without increasing the risk, so we will be willing to buy. On the contrary, suppose that it is not optimal to buy. For any initial position $(x-\Delta x, y),\ \Delta x > 0$ we have reduced our expected results without reducing the risk, so we will not be willing to buy more.

Similar arguments for the Selling Region can be obtained. This suggests that the No Transactions Region is a wedge, lying the Buying Region above and the Selling Region below. From now on, we assume that this conjecture is correct.

We move back to polar coordinates. We note that (see (3.35) and Figure 3.3):

$$\begin{aligned}
&\theta < 0 \Rightarrow y < 0,\ x > -(1-\mu)y,\\
&\theta = 0 \Rightarrow y = 0,\ x \geq 0,\\
&\theta > 0 \Rightarrow y > 0,\ x > -(1+\lambda)y,
\end{aligned}$$

which implies,

$$\begin{aligned}
&\text{if } y > 0,\ \text{then } x \uparrow +\infty \Rightarrow \theta \downarrow 0^+,\\
&\text{if } y < 0,\ \text{then } x \uparrow +\infty \Rightarrow \theta \uparrow 0^-.
\end{aligned} \tag{3.66}$$

Proposition 3.5.2. $P_1^{l-1}(\theta_0) = P_2^{l-1}(\theta_{N_\theta}) = 0$.

Proof. This result is a direct consequence of the boundary conditions imposed in the definition of $\hat{V}$ (see (3.55)) □

We remark that there is no contradiction in the physical meaning of the sign of P_i^{l-1} since the boundary conditions are a mandatory buying or selling the stock if we respectively reach θ_0 or θ_{N_θ}.

Proposition 3.5.3. $P_1^{l-1}(\theta_{N_\theta}), P_2^{l-1}(\theta_0) > 0$.

Proof. We only prove $P_1^{l-1}(\theta_{N_\theta}) > 0$. The other result is obtained with identical arguments.

Suppose that $P_1^{l-1}(\theta_{N_\theta}) = 0$. This implies that $P_1^{l-1}(\theta_{N_\theta}) = P_2^{l-1}(\theta_{N_\theta})$ due to the previous Proposition. This equality leads to $\lambda = -\mu$, which is a contradiction with the hypothesis that transaction costs exist $\lambda + \mu > 0$.

The boundary condition at θ_{N_θ} (see (3.55)) is equivalent to the mandatory selling the stock. Therefore, $P_1^{l-1}(\theta_{N_\theta}) > 0$ since $P_1^{l-1}(\theta_{N_\theta}) < 0$ would imply that we have to buy and sell the stock at the same time, something which is always strictly suboptimal. □

Proof of Theorem 3.5.1. Since $\alpha > r$, we know that it is always suboptimal to have a negative amount of the stock. From the change to polar coordinates, this implies that

$$P_1^{l-1}(\theta) < 0, \quad \theta \in (\theta_0, 0)$$
$$P_2^{l-1}(\theta) > 0, \quad \theta \in (\theta_0, 0)$$

and it is enough to study $\theta \in (0, \theta_{N_\theta})$. Therefore, $y > 0$ for the rest of the proof.

Let $\beta \in (0, \theta_{N_\theta})$ and suppose that $P_1^{l-1}(\beta) < 0$ (it is optimal to buy). From the homothetic property, it is enough to study an initial position (x_0, y_0) such that $\operatorname{arccot}(x_0/y_0) = \beta$. With the optimization arguments shown before (the No Transactions Region is a wedge which separates the space in three regions), the investor will be in the Buying Region for any $(x_0 + \Delta x, y_0), \Delta x > 0$.

Let $\beta_{\Delta x} = \operatorname{arccot}((x_0 + \Delta x)/y_0) \in (\theta_0, \theta_{N_\theta})$. From (3.66), it holds $0 < \beta_{\Delta x} < \beta$ which implies $P_1^{l-1}(\theta) < 0,\ \theta \in (0, \beta]$.

Suppose now that $P_1^{l-1}(\beta) > 0$. This means that (x_0, y_0) it is not in the Buying Region. With the optimization arguments shown before (the No Transactions Region is a wedge which separates the space in three regions), the investor will not be in the Buying Region for any $(x_0 - \Delta x, y_0), \Delta x > 0$.

From (3.66), it holds $\beta < \beta_{\Delta x} < \theta_{N_\theta}$ which implies $P_1^{l-1}(\theta) \geq 0,\ \theta \in [\beta, \theta_{N_\theta})$.

A similar argument can be derived for function $P_2^{l-1}(\theta)$.

This arguments, jointly with Propositions 3.5.2 and 3.5.2 completes the proof of the Theorem and guarantees that we will be able to define a Buying and a Selling Region. □

We define

$$\begin{aligned} BR_F^{l-1} &= \min\left\{\beta : P_1^{l-1}(\theta) \geq 0,\ \theta \in [\beta, \theta_{N_\theta})\right\}, \\ SR_F^{l-1} &= \max\left\{\beta : P_2^{l-1}(\theta) \geq 0,\ \theta \in (\theta_0, \beta]\right\}. \end{aligned} \tag{3.67}$$

In order to check that the frontiers are well defined, we need a last result.

Proposition 3.5.4. *It holds* $BR_F^{l-1} < SR_F^{l-1}$.

Proof. We argue by contradiction.

If $BR_F^{l-1} > SR_F^{l-1}$, then it holds that it exists $\theta \in (\theta_0, \theta_{N_\theta})$ such that $P_i^{l-1}(\theta) < 0,\ i = 1, 2$, which is absurd, because it can never be optimal to buy and sell the stock at the same time.

Suppose that $BR_F^{l-1} = SR_F^{l-1}$. Then it holds $P_1^{l-1}(BR_F^{l-1}) = P_2^{l-1}(BR_F^{l-1})$, leading to $\lambda = -\mu$ which is a contradiction with $\lambda + \mu > 0$. □

Therefore BR_F^{l-1} and SR_F^{l-1} divide the spatial domain in three Regions:

a) $\theta < BR_F^{l-1}$ where it would be strictly better to buy the stock.

b) $BR_F^{l-1} \leq \theta \leq SR_F^{l-1}$ where it would be better or equivalent to do nothing.

c) $SR_F^{l-1} < \theta$ where it would be strictly better to sell the stock.

which define an approximation (in time) to the Buying, No Transactions and Selling Regions.

We recompute the function value $\hat{V}$ in the Buying and Selling Regions employing formulas (3.47), which are consistent, since with the arguments shown we know that the optimal trading strategies are "bang-bang" and the optimal trading strategy is to buy or sell at the maximum rate until reaching the No Transactions Region. Once done, we have obtained the value function which corresponds, up to the change to polar coordinates, to function $\hat{\varphi}^{t_{l-1}}(x, y)$.

In Subsection 3.5.2, we have computed $\left\{\hat{V}^{\mathbf{N}}(\theta_j, t_{l-1})\right\}_{j=0}^{N_\theta}$.

We define the numerical approximation $P_i^{\mathbf{N},l-1}$ to functions P_i^{l-1} by:

$$\begin{aligned} P_1^{(\mathbf{N},l-1)}(\theta_j) &= \hat{V}_\theta^{\mathbf{N}}(\theta_j, t_{l-1}) - \hat{V}^{\mathbf{N}}(\theta_j, t_{l-1})\gamma\frac{(1+\lambda)\cos(\theta_j) - \sin(\theta_j)}{(1+\lambda)\sin(\theta_j) + \cos(\theta_j)}, \\ P_2^{(\mathbf{N},l-1)}(\theta_j) &= \hat{V}_\theta^{\mathbf{N}}(\theta_j, t_{l-1}) - \hat{V}^{\mathbf{N}}(\theta_j, t_{l-1})\gamma\frac{(1-\mu)\cos(\theta_j) - \sin(\theta_j)}{(1-\mu)\sin(\theta_j) + \cos(\theta_j)}, \end{aligned} \tag{3.68}$$

where $\hat{V}_\theta^{\mathbf{N}}(\theta_j, t),\ j = 1, ..., N_\theta - 1$ are computed with finite differences (see (3.58)).

The numerical approximation to the location of the Buying / Selling Frontiers at $t = t_{l-1}$ is given by:

$$\begin{aligned} \mathrm{BR}_F^{\mathbf{N}}(t_{l-1}) &= \theta_{j_1}, \quad j_1 = \min\left\{j_i : P_1^{(\mathbf{N},l-1)}(\theta_j) \geq 0,\ j \geq j_i\right\}, \\ \mathrm{SR}_F^{\mathbf{N}}(t_{l-1}) &= \theta_{j_2}, \quad j_2 = \max\left\{j_i : P_2^{(\mathbf{N},l-1)}(\theta_j) \geq 0,\ j \leq j_i\right\}. \end{aligned} \tag{3.69}$$

We point out that with this definition, the numerical location of the frontiers will be points of the spatial mesh $\{\theta_j\}_{j=0}^{N_\theta}$ and its time evolution will be piecewise constant. In the following numerical method (see Section 3.6), $P_i^{(\mathbf{N},l-1)}$ will be functions and we will evaluate them in order to find the location of the frontiers.

Therefore, we define the numerical approximation $V^{\mathbf{N}}(\theta, t_{l-1})$ to function $V(\theta, t_{l-1})$ in the Buying and Selling Regions by

$$\begin{aligned} V^{\mathbf{N}}(\theta,t) &= \hat{V}^{\mathbf{N}}(\mathrm{BR}_F^{\mathbf{N}}(t),t)\left[\frac{(1+\lambda)\sin(\theta)+\cos(\theta)}{(1+\lambda)\sin(\mathrm{BR}_F^{\mathbf{N}}(t))+\cos(\mathrm{BR}_F^{\mathbf{N}}(t))}\right]^{\gamma}, \quad \theta < \mathrm{BR}_F^{\mathbf{N}}(t), \\ V^{\mathbf{N}}(\theta,t) &= \hat{V}^{\mathbf{N}}(\mathrm{SR}_F^{\mathbf{N}}(t),t)\left[\frac{(1-\mu)\sin(\theta)+\cos(\theta)}{(1-\mu)\sin(\mathrm{SR}_F^{\mathbf{N}}(t))+\cos(\mathrm{SR}_F^{\mathbf{N}}(t))}\right]^{\gamma}, \quad \theta > \mathrm{SR}_F^{\mathbf{N}}(t). \end{aligned} \tag{3.70}$$

3.5.4 Numerical Algorithm

We define now the Numerical Algorithm that must be followed in order to solve the problem. We suppose $t \in [0,T]$.

Step 0. Fix $\Delta\theta > 0$, $N_1, N_2 \in \mathbb{N}$, satisfying (3.53). Build the spatial mesh

$$\theta_j = (j - N_1)\,\Delta\theta, \quad j = 0,1,2,...,N_1+N_2$$

and define $N_\theta = N_1 + N_2$.

Fix $N_t \in \mathbb{N}$, compute $\Delta t = \frac{T}{N_t}$ and define the temporal mesh $\{t_l\}_{l=0}^{N_t}$

$$t_l = l\Delta t, \quad l = 0,1,...,N_t$$

Define $\mathbf{N} = (N_t, N_\theta)$ and compute $V^{\mathbf{N}}(\theta,T) = \{V(\theta_j,T)\}_{j=0}^{N_\theta}$ using formula (3.46). Set $l = N_t$.

Step 1. Compute $\hat{V}^{\mathbf{N}}(\theta, t_{l-1})$ solving

$$\begin{cases} \hat{V}^{\mathbf{N}} - \dfrac{\Delta t}{2} L\left(\hat{V}^{\mathbf{N}}\right)\Big|_{\theta=\theta_j,\ t=t_{l-1}} = V + \dfrac{\Delta t}{2} L\left(V\right)\Big|_{\theta=\theta_j,\ t=t_l}, \quad j = 1,...,N_\theta - 1, \\ \hat{V}_\theta^{\mathbf{N}}(\theta_0,t_{l-1}) = V(\theta_0,t_l)\gamma\dfrac{(1+\lambda)\cos(\theta_0)-\sin(\theta_0)}{(1+\lambda)\sin(\theta_0)+\cos(\theta_0)}, \\ \hat{V}_\theta^{\mathbf{N}}(\theta_{N_\theta},t_{l-1}) = V(\theta_{N_\theta},t_l)\gamma\dfrac{(1-\mu)\cos(\theta_{N_\theta})-\sin(\theta_{N_\theta})}{(1-\mu)\sin(\theta_{N_\theta})+\cos(\theta_{N_\theta})}. \end{cases}$$

where operator L is defined in (3.81).

Step 2. Locate the Buying and Selling Frontiers with formulas (3.68) and (3.69). Compute:

$$\begin{aligned} P_1^{\mathbf{N},l-1}(\theta_j) &= \hat{V}_\theta(\theta_j,t_{l-1}) - \hat{V}(\theta_j,t_{l-1})\gamma\frac{(1+\lambda)\cos(\theta_j)-\sin(\theta_j)}{(1+\lambda)\sin(\theta_j)+\cos(\theta_j)}, \\ P_2^{\mathbf{N},l-1}(\theta_j) &= \hat{V}_\theta(\theta_j,t_{l-1}) - \hat{V}(\theta_j,t_{l-1})\gamma\frac{(1-\mu)\cos(\theta_j)-\sin(\theta_j)}{(1-\mu)\sin(\theta_j)+\cos(\theta_j)}, \end{aligned}$$

and define

$$\mathrm{BR}_F^{\mathbf{N}}(t_{l-1}) = \theta_{j_1}, \quad j_1 = \min\left\{j_i : P_1^{\mathbf{N},l-1}(\theta_j) \geq 0,\ j \geq j_i\right\},$$
$$\mathrm{SR}_F^{\mathbf{N}}(t_{l-1}) = \theta_{j_2}, \quad j_2 = \max\left\{j_i : P_2^{\mathbf{N},l-1}(\theta_j) \geq 0,\ j \leq j_i\right\}.$$

Step 3. The numerical solution $V^{\mathbf{N}}$ of the function $V(\theta,t)$ at time t_{l-1} is defined by:

$$V^{\mathbf{N}}(\theta_j,t_{l-1}) = \begin{cases} \hat{V}^{\mathbf{N}}(\mathrm{BR}_F^{\mathbf{N}}(t_{l-1}),t_{l-1})\left[\dfrac{(1+\lambda)\sin(\theta_j)+\cos(\theta_j)}{(1+\lambda)\sin(\mathrm{BR}_F^{\mathbf{N}}(t_l))+\cos(\mathrm{BR}_F^{\mathbf{N}}(t_l))}\right]^{\gamma}, & \theta_j < \mathrm{BR}_F^{\mathbf{N}}(t_{l-1}), \\ \hat{V}^{\mathbf{N}}(\theta_j,t_{l-1}), \quad \mathrm{BR}_F^{\mathbf{N}}(t_{l-1}) \leq \theta_j \leq \mathrm{SR}_F^{\mathbf{N}}(t_{l-1}), & \\ \hat{V}^{\mathbf{N}}(\mathrm{SR}_F^{\mathbf{N}}(t_{l-1}),t_{l-1})\left[\dfrac{(1-\mu)\sin(\theta_j)+\cos(\theta_j)}{(1-\mu)\sin(\mathrm{SR}_F^{\mathbf{N}}(t_l))+\cos(\mathrm{SR}_F^{\mathbf{N}}(t_l))}\right]^{\gamma}, & \theta_j > \mathrm{SR}_F^{\mathbf{N}}(t_l), \end{cases}$$

where we have employed formula (3.70).

Step 4. Set $l = l-1$. If $l = 0$ we have finished. Otherwise, proceed to **Step 1**.

We now justify why the numerical solution is convergent.

Without considering the boundary error due to the imposition of Neumann conditions, as $\Delta x \to 0$, we approach to V^{N_t}. Function V^{N_t} corresponds, up to the change to polar coordinates, to

$$\varphi^{N_t}(x,y,t) = \sup_{(L,M)\in A_t^{N_t,\mathbb{S}^{N_\theta}}(x,y)} \mathbb{E}\left[U\left(\bar{W}(T)\right)\middle|\,(\bar{X}(t),\bar{Y}(t)) = (x,y)\right]$$

where the set of allowed trading strategies $A_0^{N_t,\mathbb{S}^{N_\theta}}(x,y)$ includes no transactions for $t \notin \{t_l\}_{l=0}^{N_t}$ but those needed to remain in $\mathbb{S}^{N_\theta}$, given in (3.62), and admits any transactions (subject to remain in $\mathbb{S}^{N_\theta}$) at discrete times $\{t_l\}_{l=0}^{N_t}$.

We point out that the previous statement is correct because strictly increasing, concavity and homothetic properties are inherited from one time step to the following one, so the arguments of the previous Subsection can be applied in an iterative way.

As N_t tends to ∞ (note that it is then when the boundary error completely vanishes), set $A_t^{N_t,\mathbb{S}^{N_\theta}}(x,y)$ tends to $A_t^{\mathbb{S}^{N_\theta}}(x,y)$, the set which includes any trading strategy subject to remain in $\mathbb{S}^{N_\theta}$. As pointed before, the optimal trading strategy π_o which solves (3.11) belongs to $A_t^{\mathbb{S}^{N_\theta}}(x,y)$.

Therefore, function $V^{\mathbf{N}}$ converges to V as N_t and N_θ tend to ∞.

3.5.5 Numerical Example

Although the error analysis of the method is postponed to Section 3.7, it is interesting to show now the numerical results obtained with this method.

We choose the same parameter values as in the first numerical experiment of reference [2]:

$$\sigma = 0.25, \quad r = 0.03, \quad \alpha = 0.10, \quad \gamma = 0.5, \quad \lambda = 0.08, \quad \mu = 0.02,$$

We fix a maturity $T = 30$ years in order to check the stationary values of the Buying and Selling frontiers when maturity is big enough (see Proposition 3.4.1).

The numerical approximation $V^{\mathbf{N}}(\theta, t)$ is plotted on Figure 3.5, where we have colored the function value depending on whether (θ, t) is in the Buying (blue), No Transactions (green) or Selling (red) Regions.

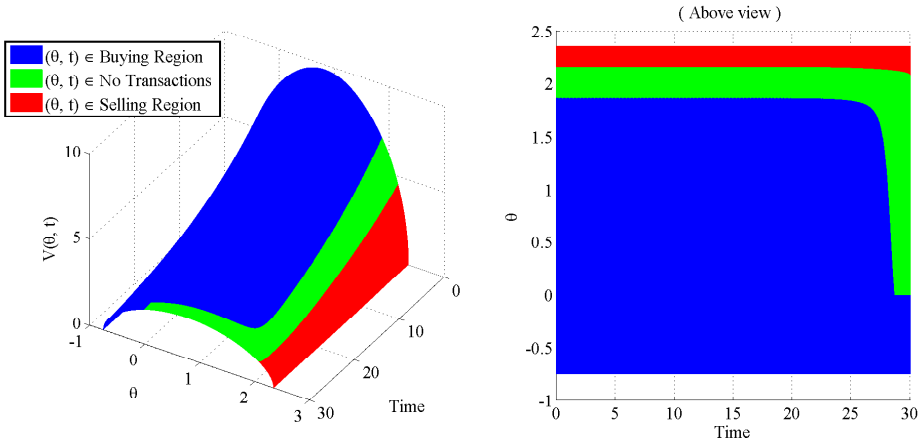

Figure 3.5: Value function $V^{\mathbf{N}}(\theta, t)$, $(\theta, t) \in [\beta_1, \beta_2] \times [0, 30]$. View in perspective (left) and from above (right).

At a fixed time t, the optimal trading strategy for a position

$$\theta = \operatorname{arccot}\left(\frac{\text{Money in Bank account}}{\text{Money in the Stock Account}}\right) \in [\beta_1,\ \beta_2],$$

is:

1. If (θ, t) is in the Buying Region (blue in Figure 3.5), to immediately buy stock until reaching the No Transactions Region (green in Figure 3.5).

2. If (θ, t) is in the No Transactions Region (green in Figure 3.5), to do nothing.

3. If (θ, t) is in the Selling Region (red in Figure 3.5), to immediately sell stock until reaching the No Transactions (green in Figure 3.5).

On the right side of the previous figure (projection over the (t, θ) plane), we can check some of the properties mentioned in Proposition 3.4.1. Consider the curve which divides the Buying and No Transaction Regions (frontier between blue and green colors), which is the numerical estimation of the Buying frontier ($\mathrm{BR}_F^{\mathbf{N}}(t)$). Consider also the curve which divides the Selling and No Transaction Regions (frontier between red and green colors), which is the numerical estimation of the Selling frontier ($\mathrm{SR}_F^{\mathbf{N}}(t)$).

(i) $\mathrm{BR}_F^{\mathbf{N}}(t)$ and $\mathrm{SR}_F^{\mathbf{N}}(t)$ are decreasing functions in time.

(ii) There is a time interval $[\hat{t}_0, T]$ such that $\mathrm{BR}_F^{\mathbf{N}}(t)$ remains constant at $\theta = 0$ ($z = +\infty$ in (3.19)).

(iii) $\mathrm{BR}_F^{\mathbf{N}}(t)$ and $\mathrm{SR}_F^{\mathbf{N}}(t)$ tend to a steady state as t approaches to 0^+.

3.6 Mesh-adapted Chebyshev-collocation method

Our objective is to design a second numerical method, for the solution of problem (3.45)-(3.46), more efficient than the previous one in terms of computational cost versus error tolerance.

The better performance is obtained looking for more spatial precision with less computational requirements. We will implement a spectral method, specifically adapted for this problem.

Let $t \in [0, T]$. Fix $N_t \in \mathbb{N}$ and define Δt and the time mesh $\{t_l\}_{l=0}^{N_t}$ as in (3.51).

We note that, thanks to formulas (3.39) and (3.41), it is enough to know the location of the Buying and Selling frontiers and the values of $V(\theta, t)$ in the No Transactions region in order to completely define the function $V(\theta, t)$. The problem will be solved with a spatial time dependent adapted mesh defined in a proper interval $I(t_l) = [C_1^{t_l},\ C_2^{t_l}]$.

Fix $N_\theta \in \mathbb{N}$. From now on, for any function f, the superscript $f^{\mathbf{N}}$ denotes its numerical approximation, where $\mathbf{N} = (N_t, N_\theta)$, N_t describes the size of the time mesh and $N_\theta + 1$ is the number of Chebyshev nodes.

The numerical solution at $t_{l_0} \in \{t_l\}_{l=0}^{N_t}$ is $V^{\mathbf{N}}(\theta, t_l)$, which will be a polynomial of degree N_θ defined in interval $I(t_{l_0})$ by its values at the $N_\theta + 1$ Chebyshev nodes of interval $I(t_{l_0})$.

The Section is organized as follows: First, we will explain how to choose the spatial mesh that depends on the time step. Afterwards, we will detail the Chebyshev Collocation method. Finally, we will study the computation of the Buying/Selling frontiers.

The Section finishes with the Numerical Algorithm that must be followed in order to solve the problem.

3.6.1 The adaptive mesh

Let N_t be a nonnegative integer and compute $\{t_l\}_{l=0}^{N_t}$ with (3.51).

Our objective is to give a general criteria to construct an adaptive interval $I(t_l)$ that will be employed in the numerical solution of our problem.

We are going to give the formulas to compute $I(t_l)$ and, afterwards, we will detail the properties that they satisfy. In the construction of interval $I(t_l)$, we will take advantage of the behaviour of the frontiers of the different regions that were detailed in Subsection 3.4.1.

Let $\delta \in (0, 0.5)$ be a control parameter and assumed fixed along the numerical algorithm. We define

$$\begin{aligned} k_1 &= \frac{\beta_2 - \mathrm{SR}_s}{\beta_2 - \mathrm{BR}_F(T)}, \\ k &= \min\{\delta, k_1,\ \mathrm{BR}_F(T) - \beta_1\}, \end{aligned} \tag{3.71}$$

where we recall that $\mathrm{BR}_F(T) = 0$ and that $\mathrm{SR}_s = \operatorname{arccot}(\mathrm{SR}_s^c) \in [\beta_1, \beta_2]$ is the stationary state of the Selling frontier. The value SR_s^c is explicitly computable from the initial data of the problem (see (3.28)).

Let $N \in \mathbb{N}$. We recall from Chapter 1 that the $N+1$ Chebyshev nodes in $[-1,\ 1]$ are

$$\tilde{\theta}_j = \cos\left(\frac{\pi j}{N_\theta}\right), \quad j = 0, 1, ..., N. \tag{3.72}$$

For $N \in \mathbb{N}$ fixed, let $j_k \in \{0, 1, 2, ..., N\}$ be the only value such that

$$\left|\tilde{\theta}_{N-j_k} - \tilde{\theta}_N\right| \leq 2k < \left|\tilde{\theta}_{N-(j_k+1)} - \tilde{\theta}_N\right|. \tag{3.73}$$

j_k is well defined because $0 < k \leq \delta < 0.5$. From the definition of the Chebyshev nodes, it is easy to check that it exists N_0 such that for all $N \geq N_0$, it holds that $j_k \geq 1$.

Suppose that we are at $t = t_l$ and that we know $BR_F(t_l)$ and $SR_F(t_l)$.

Let $N_\theta \in \mathbb{N}$, $N_\theta > N_0$ fixed along the numerical algorithm. Interval $I(t_l)$ is given by:

Case a) If $\mathrm{BR}_F(t_l) = 0$.

$$I_1(t_l) = \left[0,\ \frac{2}{\tilde{\theta}_{j_k} - \tilde{\theta}_{N_\theta}} \mathrm{SR}_F(t_l)\right]. \tag{3.74}$$

Case b) If $\mathrm{BR}_F(t_l) > 0$.

$$I_2(t_l) = \left[\mathrm{BR}_F(t_l) - M\frac{\tilde{\theta}_{N_\theta - j_k} - \tilde{\theta}_{N_\theta}}{\tilde{\theta}_{j_k} - \tilde{\theta}_{N_\theta - j_k}},\ SR_F(t_l) + M\frac{\tilde{\theta}_0 - \tilde{\theta}_{j_k}}{\tilde{\theta}_{j_k} - \tilde{\theta}_{N_\theta - j_k}}\right], \tag{3.75}$$

where $M = \mathrm{SR}_F(t_l) - \mathrm{BR}_F(t_l)$.

We note that the numerical algorithm is solved for $l = N_t, N_t - 1, ..., 2, 1$. Note that for $t_{N_t} = T$, the values

$$\mathrm{BR}_F(T) = 0, \quad \mathrm{SR}_F(T) = \operatorname{arccot}((1-\mu)x_M) \in (\beta_1, \beta_2)$$

where x_M is the Merton line, are known data. For $t_l < T$, the values $BR_F(t_l)$ and $SR_F(t_l)$ are substituted by $BR_F^{\mathbf{N}}(t_l)$ and $SR_F^{\mathbf{N}}(t_l)$, their numerical approximation, which has been computed prior to the construction of $I(t_l)$ (see Subsection 3.6.5).

The reason why two different intervals are defined is given in Subsection 3.6.4.

From the properties of the Buying Frontier (see Subsection 3.4.1), we know that it exists an explicitly computable value $\hat{t}_0$ such that $\mathrm{BR}_F(t) = 0,\ t \in [\hat{t}_0, T]$ and $\mathrm{BR}_F(t) > 0,\ t < \hat{t}_0$. We have taken advantage of this property in the definition of $I(t_l)$, but we remark that $\hat{t}_0$ is not employed in the implementation of the algorithm.

Since the numerical algorithm is solved for $l = N_t, N_t-1, ..., 2, 1$, we always start employing the interval defined in **Case a)** and we may or may not employ the interval defined in **Case b)**. The criteria to change the kind of interval from **Case a)** to **Case b)** is when we find $\mathrm{BR}_F^{\mathbf{N}}(t_{l_0}) > 0$ for the first time, and not the exact value of $\hat{t}_0$, which we do not compute.

The criterium to choose $I(t_l)$ is that it covers the three regions. In the definition that we have given, a $100\delta\%$ (maximum) of interval $I(t_l)$ will be in the Selling Region, another $100\delta\%$ (maximum) will be in the Buying Region and $100(1-2\delta)\%$ (minimum) will be in the No Transactions Region. Furthermore, value k ensures that $I(t_l) \subset [\beta_1, \beta_2]$, the Solvency Region.

Note that we have forced that both $\mathrm{BR}_F(t_l)$ and $\mathrm{SR}_F(t_l)$ are always one of the $N_\theta + 1$ Chebyshev nodes of interval $I(t_l)$. Note also that the restriction $N_\theta > N_0$ ($j_k \geq 1$) implies that $\mathrm{SR}_F(t_l)$ is always in the interior of $I(t_l)$.

We have indirectly imposed, assumed N_t is big enough, that $\mathrm{BR}_F(t_{l-1}), \mathrm{SR}_F(t_{l-1}) \in I(t_l)$. Since the numerical algorithm is solved for $l = N_t, N_t - 1, ..., 2, 1$, this implies that we can compute a numerical approximation to the Buying and Selling frontiers in the next step. This assertion is guaranteed for the exact solution of the problem by the following result.

Proposition 3.6.1. *Let $NT(t) = [BR_F(t),\ SR_F(t)]$ where $BR_F(t)$ and $SR_F(t)$ are the exact location of the Buying and Selling frontiers.*

For any $N_\theta > N_0$, where N_0 is the restriction which guarantees that $SR_F^N(t)$ will be in the interior of $I(t)$, compute $I(t)$ with (3.74) or (3.75).

It exists $N_1 > 0$ such that for any time mesh $\{t_l\}_{l=0}^{N_t},\ N_t > N_1$ given by (3.51), it holds

$$NT(t_{l_0-1}),\ NT(t_{l_0}) \subset I(t_{l_0}). \tag{3.76}$$

for any $t_{l_0} \in \{t_l\}_{l=0}^{N_t}$.

Proof. From Property a) of Subsection 3.3.1, we know that $\mathrm{SR}_F^c(t) \in \mathscr{C}^\infty[0, T)$. Therefore, $\mathrm{SR}_F(t) = \operatorname{arccot}(\mathrm{SR}_F^c(t)) \in (\beta_1,\ \beta_2)$ is $\mathscr{C}^\infty[0, T)$.

Let k from (3.71) be fixed. Since $\mathrm{SR}_F(t)$ is in the interior of $I(t)$, it will exist Δt_k such that $\forall \Delta t < \Delta t_k$ it holds:

$$SR_F(t - \Delta t) \in I(t), \quad t \in [0,\ T) \tag{3.77}$$

This guarantees that for any time mesh $\{t_l\}_{l=0}^{N_t}$, where $N_t > \frac{1}{\Delta t_k}$, it holds that $SR_F(t_{l-1}) \in I(t_l)$.

To finish the proof, note that $\mathrm{BR}_F(t)$ is a decreasing function and $\mathrm{BR}_F(t_{l-1}) \leq \mathrm{SR}_F(t_{l-1})$ (see Proposition 3.4.1), so the result follows directly from the definition of $I(t_l)$. □

3.6.2 Chebyshev collocation.

At a fixed time step t_l of the time discretization given by (3.51), suppose that we know the function value $V(\theta, t_l),\ \theta \in (\beta_1, \beta_2)$ and the values of $\mathrm{BR}_F(t_l)$ and $\mathrm{SR}_F(t_l)$.

For N_θ fixed, compute

$$I(t_l) = [C_1^{t_l},\ C_2^{t_l}]$$

with (3.74) if $\mathrm{BR}_F(t_l) = 0$ or with (3.75) otherwise.

As in Subsection 3.5.2, for $t \in [t_{l-1}, t_l]$, consider $\hat{V}$, the function value which gives the expected terminal value when the trading strategy is to not perform transactions if $\theta \in (C_1^{t_l},\ C_2^{t_l})$, to buy the stock if $\theta = C_1^{t_l}$ and to sell the stock if $\theta = C_2^{t_l}$, subject to $\hat{V}(\theta, t_l) = V(\theta, t_l)$.

Therefore, $\hat{V}$ is the solution of equation

$$-\hat{V}_t + g_2(\theta)\hat{V}_{\theta\theta} + g_1(\theta)\hat{V}_\theta + g_0(\theta)\hat{V} = 0, \tag{3.78}$$

subject to

$$\begin{aligned}
\hat{V}_\theta\left(C_1^{t_l}, t\right) &= \hat{V}\left(C_1^{t_l}, t\right)\gamma\frac{(1+\lambda)\cos(C_1^{t_l}) - \sin(C_1^{t_l})}{(1+\lambda)\sin(C_1^{t_l}) + \cos(C_1^{t_l})},\\
\hat{V}_\theta\left(C_2^{t_l}, t\right) &= \hat{V}\left(C_2^{t_l}, t\right)\gamma\frac{(1-\mu)\cos(C_2^{t_l}) - \sin(C_2^{t_l})}{(1-\mu)\sin(C_2^{t_l}) + \cos(C_2^{t_l})},\\
\hat{V}(\theta, t_l) &= V(\theta, t_l).
\end{aligned} \tag{3.79}$$

Note that the boundary conditions are a mandatory buying or selling the stock if θ reaches respectively $C_1^{t_l}$ or $C_2^{t_l}$ (see equations (3.39), so θ always remains inside $(C_1^{t_l},\ C_2^{t_l})$.

The numerical algorithm is solved for $l = N_t, N_t - 1, ..., 1$. Function $V(\theta, T)$ is a known data and if $l < N_t$, function $V(\theta, t_l)$ is substituted by its numerical approximation which will have been computed in the previous step.

Consider $\{\tilde{\theta}_j\}_{j=0}^{N_\theta}$, the $N_\theta + 1$ Chebyshev nodes in $[-1,\ 1]$, which are given by (3.72). The employment of the Chebyshev nodes in $[-1,\ 1]$ is due to implementation purposes. Note that the value of $\tilde{\theta}_j,\ j = 0, 1, ..., N_\theta$ does not depend of the time step t_l.

We compute $\{\theta_j\}_{j=0}^{N_\theta}$, the $N_\theta + 1$ Chebyshev nodes in $[C_1^{t_l},\ C_2^{t_l}]$ through the change of variable:

$$\theta_j = \frac{C_2^{t_l} - C_1^{t_l}}{2}\tilde{\theta}_j + \frac{C_2^{t_l} + C_1^{t_l}}{2},\ j = 0, 1, ..., N_\theta. \tag{3.80}$$

We note that $\theta_j = \theta_j(t_l)$, i.e. they depend on which time step we are. We also note that $\theta_0 = C_2^{t_l}$ and $\theta_{N_\theta} = C_1^{t_l}$ (Chebyshev nodes are ordered up-down).

The numerical approximation $\hat{V}^{\mathbf{N}}(\theta, t_{l-1}),\ \theta \in (\theta_{N_\theta}, \theta_0)$ is the collocation polynomial of degree N_θ defined by:

$$\left.\frac{\partial \hat{V}^{\mathbf{N}}}{\partial t}\right|_{\theta=\theta_j} = g_2(\theta)\frac{\partial^2 \hat{V}^{\mathbf{N}}}{\partial \theta^2} + g_1(\theta)\frac{\partial \hat{V}^{\mathbf{N}}}{\partial \theta} + g_0(\theta)\hat{V}^{\mathbf{N}}\Big|_{\theta=\theta_j} = L\left(\hat{V}^{\mathbf{N}}\right)\Big|_{\theta=\theta_j},\ j = 1, ..., N_\theta - 1 \tag{3.81}$$

subject to

$$\hat{V}^{\mathbf{N}}(\theta_j, t_l) = V(\theta_j, t_l),\ j = 1, 2, ..., N_\theta - 1, \tag{3.82}$$

and where we impose Neumann boundary conditions. For $t \in [t_{l-1}, t_l]$,

$$\begin{aligned} \hat{V}_\theta^{\mathbf{N}}(\theta_{N_\theta}, t) = V_\theta(\theta_{N_\theta}, t_l) = V(\theta_{N_\theta}, t_l)\gamma\frac{(1+\lambda)\cos(\theta_{N_\theta}) - \sin(\theta_{N_\theta})}{(1+\lambda)\sin(\theta_{N_\theta}) + \cos(\theta_{N_\theta})}, \\ \hat{V}_\theta^{\mathbf{N}}(\theta_0, t) = V_\theta(\theta_0, t_l) = V(\theta_0, t_l)\gamma\frac{(1-\mu)\cos(\theta_0) - \sin(\theta_0)}{(1-\mu)\sin(\theta_0) + \cos(\theta_0)}. \end{aligned} \tag{3.83}$$

We remark that the formulas for $V_\theta(\theta_0, t_l)$ and $V_\theta(\theta_{N_\theta}, t_l)$ are again consistent because, by definition of the adaptive interval, θ_0 is always inside the Selling Region and θ_{N_θ} is inside the Buying Region or it is the Buying Frontier. We detail this in Subsection 3.6.3.

For $j = 0, 1, 2, ..., N_\theta$, consider the Chebyshev polynomials $T_j\left(\tilde{\theta}\right),\ \tilde{\theta} \in [-1,\ 1]$, which were introduced in Definition 1.3.1 in Chapter 1.

Polynomial $\hat{V}^{\mathbf{N}}(\theta, t)$ and the collocation method are defined in function of variable θ but, taking into account the relation between θ and $\tilde{\theta}$ given by (3.80), the implementation will be done in function of variable $\tilde{\theta}$ and with polynomial $\hat{V}^{\mathbf{N}}(\theta, t)$ written in function of the Chebyshev polynomials:

$$\hat{V}^{\mathbf{N}}(\theta, t) = \sum_{j=0}^{N_\theta} \hat{a}_j(t) T_j(\tilde{\theta}), \quad (\tilde{\theta}, t) \in [-1, 1] \times [t_{l-1}, t_l]. \tag{3.84}$$

We note that the values $\{\hat{a}_j(t_l)\}_{j=0}^{N_\theta}$ are known by assumption ($V(\theta, t_l)$ known in (3.82)), and that we want to find the values $\{\hat{a}_j(t_{l-1})\}_{j=0}^{N_\theta}$ which satisfy (3.81)-(3.83).

The spatial derivatives of $\hat{V}^{\mathbf{N}}(\theta, t)$ are given by

$$\frac{\partial^k \hat{V}^{\mathbf{N}}(\theta, t)}{\partial \theta^k} = \left(\frac{2}{C_2^t - C_1^t}\right)^k \sum_{j=0}^{N_\theta} \hat{a}_j(t)\frac{\partial^k T_j(\tilde{\theta})}{\partial \tilde{\theta}^k}, \tag{3.85}$$

The temporal derivative is substituted by the implicit midpoint rule:

$$\frac{\hat{V}^{\mathbf{N}}(\theta, t_{l-1}) - \hat{V}^{\mathbf{N}}(\theta, t_l)}{\Delta t} = L\left(\frac{\hat{V}^{\mathbf{N}}(\theta, t_{l-1}) + \hat{V}^{\mathbf{N}}(\theta, t_l)}{2}\right).$$

Operator L, given in (3.81), is linear in V. Jointly with the boundary conditions, the collocation method is

$$\begin{cases} \hat{V}^{\mathbf{N}} - \dfrac{\Delta t}{2} L\left(\hat{V}^{\mathbf{N}}\right)\Big|_{\theta=\theta_j,\ t=t_{l-1}} = \hat{V}^{\mathbf{N}} + \dfrac{\Delta t}{2} L\left(\hat{V}^{\mathbf{N}}\right)\Big|_{\theta=\theta_j,\ t=t_l}, \quad j = 1, ..., N_\theta - 1, \\ \hat{V}_\theta^{\mathbf{N}}(\theta_{N_\theta}, t_{l-1}) = V(\theta_{N_\theta}, t_l)\gamma \dfrac{(1+\lambda)\cos(\theta_{N_\theta}) - \sin(\theta_{N_\theta})}{(1+\lambda)\sin(\theta_{N_\theta}) + \cos(\theta_{N_\theta})}, \\ \hat{V}_\theta^{\mathbf{N}}(\theta_0, t_{l-1}) = V(\theta_0, t_l)\gamma \dfrac{(1-\mu)\cos(\theta_0) - \sin(\theta_0)}{(1-\mu)\sin(\theta_0) + \cos(\theta_0)}. \end{cases} \tag{3.86}$$

Let us see now how to write the Collocation method in function of the Chebyshev polynomials and explicitly obtain the values of $\hat{a}(t_{l-1})$.

We define the matrices:

$$A_0 = \begin{pmatrix} T_0(\tilde{\theta}_0) & T_1(\tilde{\theta}_0) & ... & T_{N_\theta}(\tilde{\theta}_0) \\ T_0(\tilde{\theta}_1) & T_1(\tilde{\theta}_1) & ... & T_{N_\theta}(\tilde{\theta}_1) \\ ... & ... & ... & ... \\ T_0(\tilde{\theta}_{N_\theta}) & T_1(\tilde{\theta}_{N_\theta}) & ... & T_{N_\theta}(\tilde{\theta}_{N_\theta}) \end{pmatrix}, \quad A_1 = \begin{pmatrix} T_0'(\tilde{\theta}_0) & T_1'(\tilde{\theta}_0) & ... & T_{N_\theta}'(\tilde{\theta}_0) \\ T_0'(\tilde{\theta}_1) & T_1'(\tilde{\theta}_1) & ... & T_{N_\theta}'(\tilde{\theta}_1) \\ ... & ... & ... & ... \\ T_0'(\tilde{\theta}_{N_\theta}) & T_1'(\tilde{\theta}_{N_\theta}) & ... & T_{N_\theta}'(\tilde{\theta}_{N_\theta}) \end{pmatrix},$$

$$A_2 = \begin{pmatrix} T_0''(\tilde{\theta}_0) & T_1''(\tilde{\theta}_0) & ... & T_{N_\theta}''(\tilde{\theta}_0) \\ T_0''(\tilde{\theta}_1) & T_1''(\tilde{\theta}_1) & ... & T_{N_\theta}''(\tilde{\theta}_1) \\ ... & ... & ... & ... \\ T_0''(\tilde{\theta}_{N_\theta}) & T_1''(\tilde{\theta}_{N_\theta}) & ... & T_{N_\theta}''(\tilde{\theta}_{N_\theta}) \end{pmatrix}, \tag{3.87}$$

where we remark that matrices $A_i,\ i = 1, 2, 3$ can be computed once at the beginning of the numerical algorithm (they do not depend of the value of t_l).

For $k = 0, 1, 2$, we define the vectors

$$\mathbf{g}_k = \begin{pmatrix} g_k(\theta_0) \\ g_k(\theta_1) \\ ... \\ g_k(\theta_{N_\theta}) \end{pmatrix}_{(N_\theta+1)\times 1}, \quad \hat{\mathbf{V}}_l^{\mathbf{N}} = \begin{pmatrix} \hat{V}^{\mathbf{N}}(\theta_0, t_l) \\ \hat{V}^{\mathbf{N}}(\theta_1, t_l) \\ ... \\ \hat{V}^{\mathbf{N}}(\theta_{N_\theta}, t_l) \end{pmatrix}_{(N_\theta+1)\times 1},$$

and the matrix

$$G_k = \begin{pmatrix} g_k(\theta_0) & g_k(\theta_0) & ... & g_k(\theta_0) \\ g_k(\theta_1) & g_k(\theta_1) & ... & g_k(\theta_1) \\ ... & ... & ... & ... \\ g_k(\theta_{N_\theta}) & g_k(\theta_{N_\theta}) & ... & g_k(\theta_{N_\theta}) \end{pmatrix}_{(N_\theta+1)\times(N_\theta+1)},$$

We write the first equation of (3.86) employing matrix notation. For simplicity, we include the nodes which correspond to $j = 0$ and $j = N_\theta$, which will be altered below in order to

impose the boundary conditions. Let the matrix B_{l-1} and vector $\mathbf{W}_l$ be given:

$$\begin{aligned} B_{l-1} &= A_0 - \frac{\Delta t}{2}\left[G_0 \circ A_0 + \frac{2}{C_2^{t_l} - C_1^{t_l}} G_1 \circ A_1 + \left(\frac{2}{C_2^{t_l} - C_1^{t_l}}\right)^2 G_2 \circ A_2\right], \\ \mathbf{W}_l &= \hat{\mathbf{V}}_l^{\mathbf{N}} + \frac{\Delta t}{2}\left(\mathbf{g}_0 \circ \hat{\mathbf{V}}_l^{\mathbf{N}} + \mathbf{g}_1 \circ \left(\hat{\mathbf{V}}_l^{\mathbf{N}}\right)' + \mathbf{g}_2 \circ \left(\hat{\mathbf{V}}_l^{\mathbf{N}}\right)''\right). \end{aligned} \tag{3.88}$$

where $\circ$ is the Hadamard (pointwise) product and

$$\left(\hat{\mathbf{V}}_l^{\mathbf{N}}\right)' = \begin{pmatrix} \hat{V}_\theta^{\mathbf{N}}(\theta_0, t_l) \\ \hat{V}_\theta^{\mathbf{N}}(\theta_1, t_l) \\ \dots \\ \hat{V}_\theta^{\mathbf{N}}(\theta_{N_\theta}, t_l) \end{pmatrix}_{(N_\theta+1)\times 1}, \quad \left(\hat{\mathbf{V}}_l^{\mathbf{N}}\right)'' = \begin{pmatrix} \hat{V}_{\theta\theta}^{\mathbf{N}}(\theta_0, t_l) \\ \hat{V}_{\theta\theta}^{\mathbf{N}}(\theta_1, t_l) \\ \dots \\ \hat{V}_{\theta\theta}^{\mathbf{N}}(\theta_{N_\theta}, t_l) \end{pmatrix}_{(N_\theta+1)\times 1}.$$

This way, when the spatial mesh is changed in the numerical algorithm (see Subsection 3.6.5), we only have to recompute for $k = 0, 1, 2$ the vectors $\mathbf{g}_k$, the matrices G_k and the two derivatives of $\mathbf{V}_l^{\mathbf{N}}$, multiply and sum to obtain matrix B_{l-1} and vector $\mathbf{W}_l$.

Boundary conditions are imposed changing two of the rows of B_{l-1}. For $j = 1, ..., N_\theta + 1$

$$\begin{aligned} B_{l-1}(1, j) &= \frac{2}{C_2^{t_l} - C_1^{t_l}} T'_{j-1}(\hat{\theta}_0), \\ B_{l-1}(N_\theta + 1, j) &= \frac{2}{C_2^{t_l} - C_1^{t_l}} T'_{j-1}(\hat{\theta}_{N_\theta}), \end{aligned} \tag{3.89}$$

and two elements of $\mathbf{W}_l$:

$$\begin{aligned} \mathbf{W}_l(1, 1) &= V(\theta_0, t_l)\gamma \frac{(1-\mu)\cos(\theta_0) - \sin(\theta_0)}{(1-\mu)\sin(\theta_0) + \cos(\theta_0)}, \\ \mathbf{W}_l(N_\theta + 1, 1) &= V(\theta_N, t_l)\gamma \frac{(1+\lambda)\cos(\theta_N) - \sin(\theta_N)}{(1+\lambda)\sin(\theta_N) + \cos(\theta_N)}. \end{aligned} \tag{3.90}$$

The Collocation method (3.86) is given by:

$$B_{l-1} \begin{pmatrix} \hat{a}_0^{l-1} \\ \hat{a}_1^{l-1} \\ \dots \\ \hat{a}_{N_\theta-1}^{l-1} \\ \hat{a}_{N_\theta}^{l-1} \end{pmatrix} = \mathbf{W}_l,$$

where $\hat{a}_j^{l-1} = \hat{a}_j(t_{l-1})$, $j = 0, 1...N_\theta$, are the coefficients of the polynomial $\hat{V}^{\mathbf{N}}(\theta, t_{l-1})$, $\theta \in [\theta_{N_\theta}, \theta_0]$ given in function of the Chebyshev polynomials.

A priori, the system is dense and $O(N^3)$ operations will be necessary to solve it. The fact that, with relative few nodes for the spatial mesh we achieve a great precision, makes this method competitive with respect to the Central differences method depending on the precision that it is required.

3.6.3 Comments about the boundary condition in the Chebyshev collocation method

We must point that for $t \in [\hat{t}_0,\ T]$, the lower limit of the interval $I(t)$ is $C_1(t) = 0$, which is the Buying Frontier, so that, it is not inside the Buying Region.

We note that $V(\theta, T)$

$$\begin{aligned} &\frac{(\cos(\theta) + (1-\mu)\sin(\theta))^\gamma}{\gamma}, \quad \text{if } \theta > 0, \\ &\frac{(\cos(\theta) + (1+\lambda)\sin(\theta))^\gamma}{\gamma}, \quad \text{if } \theta \leq 0. \end{aligned}$$

is continuous but not differentiable at $\theta = 0$.

If we choose $C_1(T) < 0$, oscillatory phenomena, known as the Gibbs effect, will appear. These oscillations complicate the numerical location of the Buying frontier, described in the following Subsection. Nevertheless, note that when we compute function $\hat{V}$, the boundary condition at $C_1(t) = 0,\ t \in [\hat{t}_0, T]$ must be the mandatory of buying the stock. Therefore, the definition

$$V_\theta(0,t) = \lim_{\theta \to 0^-} V_\theta(\theta, t) = V(0,t)\gamma \frac{(1+\lambda)\cos(0) - \sin(0)}{(1+\lambda)\sin(0) + \cos(0)}$$

employed in (3.55) is the correct one.

Fixed $t = t_l$, the numerical error related with the boundary is due to the imposition of Neumann conditions for $t \in [t_{l-1}, t_l]$, which are not the correct ones. As it was pointed in the FD method, a priori, neither $\hat{V}_\theta(\theta, t)$ nor $\hat{V}(\theta, t)$ remain constant in time. We do not employ the Robin condition in order to guarantee the stability of the method.

The computation of $\hat{V}^{\mathbf{N}}(\theta, t_{l-1})$ is just and intermediate step in the computation of $V^{\mathbf{N}}(\theta, t_{l-1})$. The error due to the imposition of Neumann conditions is controlled by the size of Δt and N_θ.

3.6.4 Location of the Buying/Selling frontiers

At a fixed time step t_l of the time discretization (3.51), suppose that we know the function value $V(\theta, t_l)$ and the values $\mathrm{BR}_F(t_l)$ and $\mathrm{SR}_F(t_l)$.

Compute $I(t_l) = [C_1^{t_l},\ C_2^{t_l}]$ with (3.74) if $\mathrm{BR}_F(t_l) = 0$ or with (3.75) otherwise.

For $t \in [t_{l-1}, t_l]$, let $\hat{V}$ be the solution of (3.78)-(3.79), i.e. $\hat{V}$, is the function value where the only trading strategy is $\theta \in (C_1^{t_l},\ C_2^{t_l})$ but no transactions are realized if $\theta \in (C_1^{t_l},\ C_2^{t_l})$ subject to $\hat{V}(\theta, t_l) = V(\theta, t_l)$.

We compute $P_i^{l-1}(\theta),\ i=1,2$ with (3.61). We know that the sign of $P_i^{l-1}(\theta),\ i=1,2$ unambiguously divide the spatial domain in three Regions which correspond to the approximation in time to the Buying, No Transactions and Selling Regions (see Subsection 3.5.3).

For the Chebyshev method, we define the numerical approximation $P_i^{(\mathbf{N},l-1)}(\theta),\ i=1,2$ by :

$$\begin{aligned} P_1^{(\mathbf{N},l-1)}(\theta) &= \hat{V}_\theta^{\mathbf{N}}(\theta,t_{l-1}) - \hat{V}^{\mathbf{N}}(\theta,t_{l-1})\cdot\gamma\frac{(1+\lambda)\cos(\theta)-\sin(\theta)}{(1+\lambda)\sin(\theta)+\cos(\theta)},\\ P_2^{(\mathbf{N},l-1)}(\theta) &= \hat{V}_\theta^{\mathbf{N}}(\theta,t_{l-1}) - \hat{V}^{\mathbf{N}}(\theta,t_{l})\cdot\gamma\frac{(1-\mu)\cos(\theta)-\sin(\theta)}{(1-\mu)\sin(\theta)+\cos(\theta)}, \end{aligned} \tag{3.91}$$

which in this case are explicit functions because $\hat{V}^{\mathbf{N}}$ is a known polynomial in θ.

The numerical approximation to the Buying and Selling frontiers is given by:

$$\begin{aligned} \mathrm{BR}_F^{\mathbf{N}}(t_{l-1}) &= \min\left\{\beta : P_1^{(\mathbf{N},l-1)}(\theta)\geq 0, \theta\in[\beta, C_2^{t_l})\right\},\\ \mathrm{SR}_F^{\mathbf{N}}(t_{l-1}) &= \max\left\{\beta : P_2^{(\mathbf{N},l-1)}(\theta)\geq 0, \theta\in(C_1^{t_l}, \beta]\right\}, \end{aligned}$$

Once we know the location of the frontiers and the function value in that points, we can compute the function value in the Buying and Selling regions through the explicit formulas given in (3.47).

3.6.5 Numerical Algorithm

The following numerical algorithm solves completely the problem. Let $t\in[0,T]$

Step 0. Fix a number N_t and a number $N_\theta > N_0$ where N_0 is the bound given in (3.73).
Compute $\Delta t = \frac{T}{N_t}$ and $\{t_l\}_{l=0}^{N_t}$ as in (3.51).
Set $l=N_t$. We recall properties b) and f) of Subsection 3.3.1:

$$\begin{aligned} \mathrm{BR}_F(T) &= 0,\\ \mathrm{SR}_F(T) &= \operatorname{arccot}\left((1-\mu)x_M\right)\in[\beta_1,\ \beta_2]. \end{aligned}$$

Compute $I(t_{N_t})$ with formula (3.74) and let $\{\theta_j^T\}_{j=0}^{N_\theta}$ denote the Chebyshev nodes in $I(T)$.
Compute $V^{\mathbf{N}}(\theta,T)$ with (3.46).
Compute matrices $A_1,\ A_2$ and A_3 defined in (3.87).

Step 1. Compute the polynomial $\hat{V}^{\mathbf{N}}(\theta,t_{l-1}) = \sum_{j=0}^{N_\theta}\hat{a}_j(t_{l-1})T_j(\tilde{\theta})$ solving

$$B_{l-1}\begin{pmatrix}\hat{a}_0^{l-1}\\ \hat{a}_1^{l-1}\\ \dots\\ \hat{a}_{N_\theta-1}^{l-1}\\ \hat{a}_{N_\theta}^{l-1}\end{pmatrix} = \mathbf{W}_l,$$

where B_{l-1} and $\mathbf{W}_l$ are defined in (3.88)-(3.90).

$\hat{V}^{\mathbf{N}}(\theta, t_{l-1})$ is a polynomial defined in $I(t_l)$.

Step 2. Locate the Buying / Selling Frontiers

$$\mathrm{BR}_F^{\mathbf{N}}(t_{l-1}) = \min\left\{\alpha : P_1^{(\mathbf{N},l-1)}(\theta) \geq 0, \theta \in [\alpha, C_2^{t_l})\right\},$$
$$\mathrm{SR}_F^{\mathbf{N}}(t_{l-1}) = \max\left\{\alpha : P_2^{(\mathbf{N},l-1)}(\theta) \geq 0, \theta \in (C_2^{t_l}, \alpha]\right\},$$

where $P_1^{(\mathbf{N},l-1)}(\theta)$, $P_1^{(\mathbf{N},l-1)}(\theta)$ are defined in (3.91).

Step 3. Compute the interval $I(t_{l-1})$ with (3.74) if $\mathrm{BR}_F(t_{l-1}) = 0$ or with (3.75) otherwise.

Compute the Chebyshev nodes $\{\theta_j^{t_{l-1}}\}_{j=0}^{N_\theta}$ in $I(t_{l-1})$.

The numerical approximation $V^{\mathbf{N}}$ at time t_{l-1} is the Chebyshev interpolation polynomial in $I(t_{l-1})$ such that for $j = 0,\ 1,\ ..., N_\theta$:

$$V^{\mathbf{N}}(\theta_j^{t_{l-1}}, t_{l-1}) =$$
$$\hat{V}^{\mathbf{N}}(\mathrm{BR}_F^{\mathbf{N}}(t_{l-1}), t_{l-1})\left[\frac{(1+\lambda)\sin(\theta_j^{t_{l-1}}) + \cos(\theta_j^{t_{l-1}})}{(1+\lambda)\sin(\mathrm{BR}_F^{\mathbf{N}}(t_{l-1})) + \cos(\mathrm{BR}_F^{N_\theta}(t_{l-1}))}\right]^\gamma, \quad \theta_j^{t_{l-1}} < \mathrm{BR}_F^{\mathbf{N}}(t_{l-1}),$$
$$\hat{V}^{\mathbf{N}}(\theta_j^{t_{l-1}}, t_{l-1}), \quad \mathrm{BR}_F^{\mathbf{N}}(t_{l-1}) \leq \theta_j^{t_{l-1}} \leq \mathrm{SR}_F^{\mathbf{N}}(t_{l-1}),$$
$$\hat{V}^{\mathbf{N}}(\mathrm{SR}_F^{\mathbf{N}}(t_{l-1}), t_{l-1})\left[\frac{(1-\mu)\sin(\theta_j^{t_{l-1}}) + \cos(\theta_j^{t_{l-1}})}{(1-\mu)\sin(\mathrm{SR}_F^{\mathbf{N}}(t_{l-1})) + \cos(\mathrm{SR}_F^{\mathbf{N}}(t_{l-1}))}\right]^\gamma, \quad \theta_j^{t_{l-1}} > \mathrm{SR}_F^{\mathbf{N}}(t_{l-1}),$$

where we have employed (3.47).

Step 4. Set $l = l - 1$. If $l = 0$ we have finished. Otherwise, proceed to **Step 1**.

To finish this Subsection and with clarifying purposes, we are going to check visually how does the adaptive interval $I(t_l)$ evolves through time. In the numerical algorithm, suppose that we are in time step t_l.

We are going to project the function value over the spatial axis, coloring in blue the Buying, in green the No transactions and in red the Selling Regions. The plot represent how the different steps of the algorithm make the adaptive interval evolve through time. The operations that will be represented are:

1. We are in interval $I(t_l)$. Let $\{\theta_j^{t_0}\}_{j=0}^{N_\theta}$ denote the Chebyshev nodes in $I(t_l)$. We remark that the Buying / Selling frontiers $\mathrm{BR}_F^{\mathbf{N}}(t_l)$, $\mathrm{BR}_F^{\mathbf{N}}(t_l)$ are one of the Chebyshev nodes.

2. We solve the PDE through the Chebyshev collocation method (**Step 1** of the numerical algorithm).

3. We locate the new Buying / Selling frontiers $\mathrm{BR}_F^{\mathbf{N}}(t_{l-1})$, $\mathrm{BR}_F^{\mathbf{N}}(t_{l-1})$ (**Step 2** of the numerical algorithm).

4. We recompute the function values in the Buying / Selling regions. Recompute the new interval $I(t_{l-1})$ and its Chebyshev nodes and again $\mathrm{BR}_F^{\mathbf{N}}(t_{l-1})$, $\mathrm{BR}_F^{\mathbf{N}}(t_{l-1})$ are one of them (**Step 3** of the numerical algorithm). If $t_{l-1} > 0$ we repeat for the previous time step.

In the following Figure, each interval is split in The Buying (blue), No transactions (green) and Selling (red) regions. The '×' correspond to the $N_\theta + 1$ Chebyshev nodes of each interval. The left Figure corresponds to the first kind of interval ($\mathrm{BR}_F^{\mathbf{N}}(t_l) = 0$) and the right Figure to the second one ($\mathrm{BR}_F^{\mathbf{N}}(t_l) > 0$).

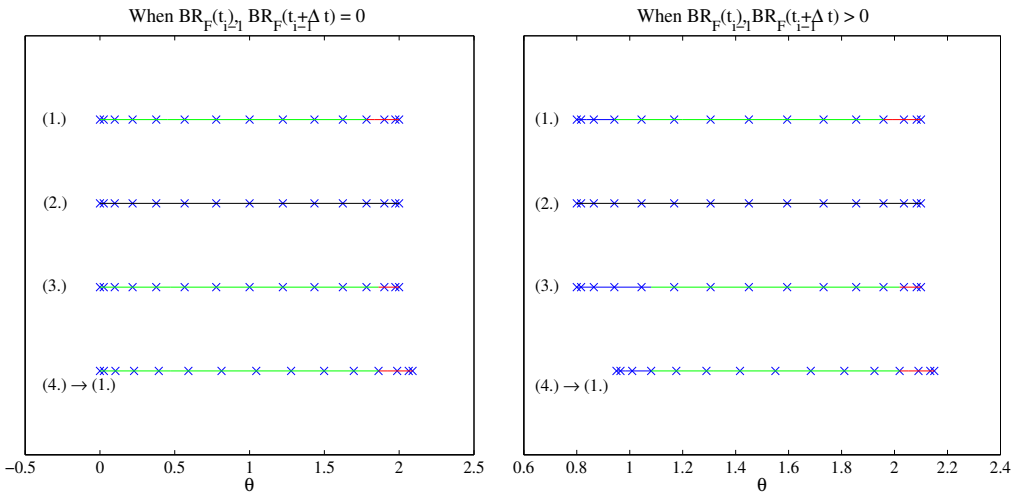

Figure 3.6: Evolution of the adaptive Mesh (Spatial domain) $I_{t_l} \to I_{t_{l-1}}$.

If Figure 3.6, (1) represents interval $I(t_l)$ of a certain time step t_l. In (2) we solve the PDE which corresponds to the No Transaction region. In (3) we locate the Buying/Selling frontiers of the time step t_{l-1}. In (4) we recompute the new interval $I(t_{l-1})$.

3.7 Numerical Results

We establish the criteria employed in the experiments to build the spatial meshes.

For the FD method, we have fixed $\Delta\theta_0 > 0$ and N_1^0, N_2^0 subject to (3.53) and computed $\{\theta_j\}_{j=0}^{N_1^0+N_2^0}$ with (3.52). Afterwards, we have defined

$$\theta_{\min} = \theta_0, \quad \theta_{\max} = \theta_{N_1^0+N_2^0}$$

When carrying the spatial error analysis, we halve the spatial mesh size and choose values N_1 and N_2 so that, when we define the new spatial mesh, it holds

$$\theta_0 = \theta_{\min}, \quad , \theta_{N_\theta} = \theta_{\max}$$

i.e., the limits of the spatial mesh of the FD method are the same in all the experiments. We note that the rate of convergence of the error in the FD method does not depend of the particular choice of values $\Delta\theta_0$, N_1^0 or N_2^0.

In the Chebyshev method, we have fixed the control parameter $\delta = 0.1$, so that, at least 80% of the interval corresponds to the No Transactions Region. The particular choice of δ does not affect the rate of convergence of the error in the Chebyshev method.

In the implementation of the Chebyshev method, we point that the Gibbs effect has been eliminated due to the definition of the adaptive interval $I(t_l)$. Nevertheless, we have observed that it may still appear if the following (empirical) bounds are violated

$$\Delta t > 0.1, \quad \Delta t < \frac{C}{N_\theta^{C_1}}, \tag{3.92}$$

where $C_1 \geq 1$ and numerical experiments suggest that C_1 might be a growing function of N_θ.

If the previous bounds are violated, functions $P_i^{(\mathbf{N},l-1)}(\theta)$, $i = 1, 2$ given in (3.91) may oscillate, complicating the location of $BR_F^{\mathbf{N}}$ and $SR_F^{\mathbf{N}}$.

We consider the parameter values as in the first experiment in [2]. For $t \in [0, 4]$, ($t = 0$ today), let:

$$\sigma = 0.25, \quad r = 0.03, \quad \alpha = 0.10, \quad \gamma = 0.5, \quad \lambda = 0.08, \quad \mu = 0.02,$$

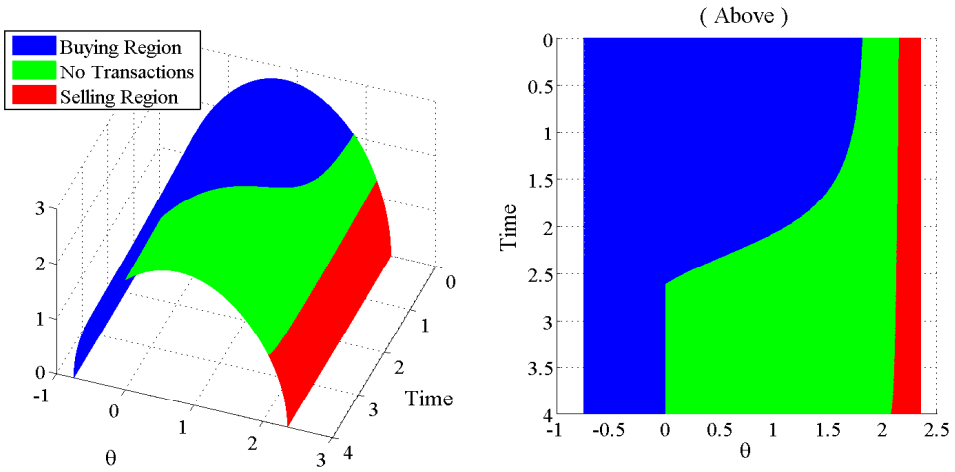

Figure 3.7: Value of $V^{\mathbf{N}}(\theta, t)$ indicating in blue if (θ, t) is in the Buying, in green if it is in the No Transactions and in red if it is in the Selling Region.

The previous figure shows the numerical values obtained for function $V^{\mathbf{N}}(\theta, t)$. We have colored the function depending in whether (θ, t) is in the Buying, Selling or No Transactions region. We can visually check the expected monotonicity of the Buying and Selling frontiers

studying from above (right) the two curves which divide the different colors. The Buying frontier remains constant for a certain period $[\hat{t}_0^{\mathbf{N}}, T]$.

Many properties of the problem have been obtained in [23], like the monotonicity of the location of the frontiers, their limit values and some explicit formulas for certain cases. We have included the most important of them in Subsection 3.3.1, and the rest can be found summarized between (P1)-(P7) in [2].

The formal study of the error will be conducted for the cases where explicit formulas are available, comparing the results of the Central differences and Chebyshev methods. The rest of the properties, although not included, were also checked.

3.7.1 Value of the function in $v(0,t)$

For $z = 0$, we employ Property d) in Subsection 3.3.1. Since $\alpha - r - (1-\gamma)\sigma^2 > 0$, it holds that:

$$v(0,t) = \begin{cases} \dfrac{1}{1+\lambda}, & 0 \leq t \leq \hat{t}_1, \\ \dfrac{1}{1-\mu} e^{-(\alpha - r - (1-\gamma)\sigma^2)(T-t)}, & \hat{t}_1 < t \leq T, \end{cases} \tag{3.93}$$

where

$$\hat{t}_1 = T - \frac{1}{\alpha - r - (1-\gamma)\sigma^2} \log\left(\frac{1+\lambda}{1-\mu}\right). \tag{3.94}$$

In Figure 3.8 we plot the value of $v(0,t)$ for $t \in [0,4]$. We note that (3.93) is continuous but not derivable at $\hat{t}_1$.

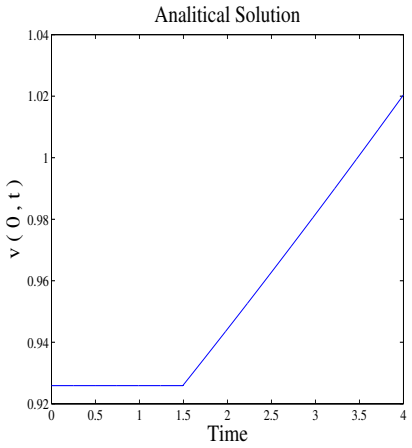

Figure 3.8: Analytical solution of $v(0,t)$, $t \in [0,4]$.

The value $z = 0$ corresponds in polar coordinates to $\theta = \frac{\pi}{2}$. A numerical solution $v^{\mathbf{N}}(0,t_i)$ can be computed explicitly using $V^{\mathbf{N}}\left(\frac{\pi}{2}, t_i\right)$ and the formula (3.48) which relates the function in polar coordinates and in the original variables.

$$v^{\mathbf{N}}(z,t) = -\left(\frac{V_\theta^{\mathbf{N}}(\theta,t)\sin^2(\theta) - \gamma\sin(\theta)\cos(\theta)V^{\mathbf{N}}(\theta,t)}{\gamma V^{\mathbf{N}}(\theta,t)}\right),$$
$$z = \cot(\theta).$$

Fixed a time partition $\Delta t = 3.9\cdot 10^{-4}$, we compute the difference between the analytical and the numerical solution for both methods: Central differences and Chebyshev. We do so for different number of spatial nodes N_θ. The results are plotted on the following figure.

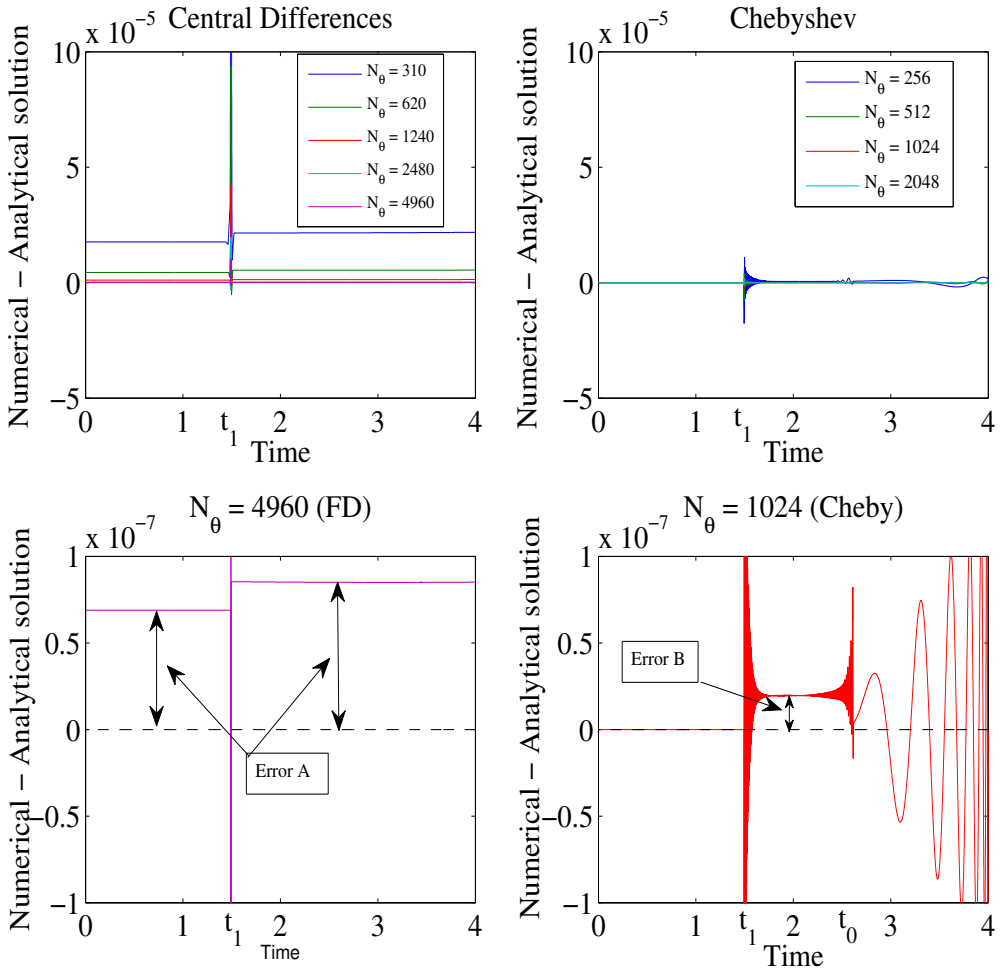

Figure 3.9: Difference between the exact value of $v(0,t)$, $t \in [0,4]$ and the numerical solution obtained with FD (left) and Chebyshev (right) methods for different N_θ. Upper scale is $\pm 5\cdot 10^{-5}$ and lower scale $\pm 10^{-7}$.

The upper and the lower pictures of Figure 3.9 are respectively in the same scale. The left side pictures correspond to the Central Finite Differences method and the right side pictures

correspond to the Chebyshev method for several values of N_θ. The lower pictures (plotted with the same scale) represent the result for $N_\theta = 4960$ (FD) and $N_\theta = 1024$ (Chebyshev).

On Figure 3.9 we can observe, in both methods, an error discontinuity at time $\hat{t}_1$, the instant when point $\theta = \frac{\pi}{2}$ moves from the No transactions to the Selling region. From equation (3.93), we know that the function $v(0,t)$ is not derivable (respect time) at instant $\hat{t}_1$. The same phenomena can be observed in the numerical experiments in [2].

In the Central Differences method (left side of Figure 3.9), the error marked as "Error A" is related with the error of approximating the derivatives $V_\theta^{\mathbf{N}}$ by central differences or with the interpolation error when computing the value at $\theta = \frac{\pi}{2}$ which, a priori, is not included in the spatial mesh.

In the Chebyshev method (right side of Figure 3.9), we can see that the frequency of the oscillations changes at time

$$\hat{t}_0 = T - \frac{1}{\alpha - r} \log\left(\frac{1+\lambda}{1-\mu}\right),$$

the instant when the Buying frontier starts to move. We recall that this point is where we change the kind of adaptive mesh $I(t_i)$ (Subsection 3.6.1).

The hump marked as "Error B" on Figure 3.9 probably corresponds to the error generated by the imposed Neumann boundary conditions for $t \in [\hat{t}_0,\ T]$, which we know that are not the exact boundary conditions of the problem, since they are of Robin type (see Subsection 3.5.2).

The following pictures compares the difference between the analytical solution $v(0,t),\ t \in [0,4]$ and the numerical solution obtained with the Central Differences method for $N_\theta = 310$ and $N_\theta = 4960$.

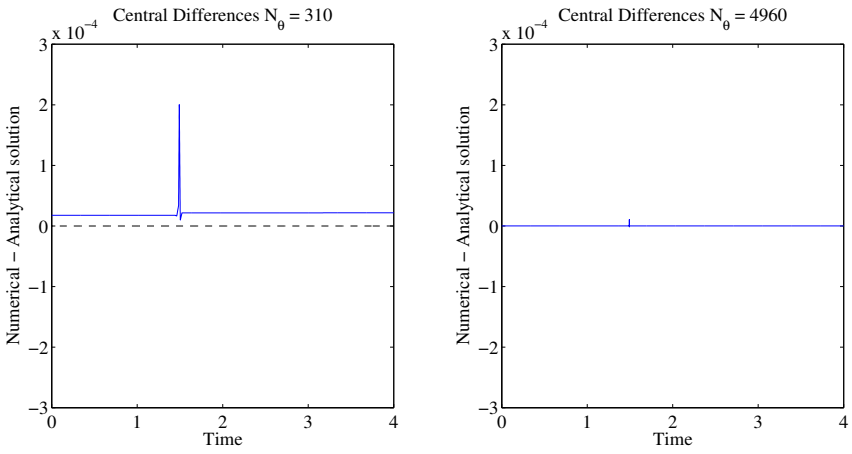

Figure 3.10: Difference between the exact value of $v(0,t),\ t \in [0,4]$ and the numerical solution of FD method with $N_\theta = 310$ (left) and $N_\theta = 4960$ (right).

Both pictures on Figure 3.10 are in the same scale. We can check that both the error discontinuity at time $\hat{t}_1$ and "Error A" reduce as we increase the number of spatial nodes.

The following pictures compares the difference between the analytical solution $v(0,t),\ t \in [0,4]$ and the numerical solution obtained with the Chebyshev method for $N_\theta = 256$ and $N_\theta = 2048$.

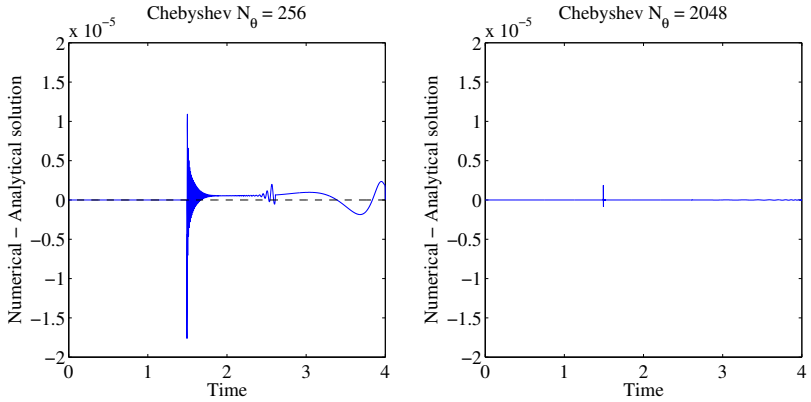

Figure 3.11: Difference between the exact value of $v(0,t),\ t \in [0,4]$ and the numerical solution of Chebyshev method with $N_\theta = 256$ (left) and $N_\theta = 2048$ (right).

Both pictures in Figure 3.11 are in the same scale. We can check that the error discontinuity at time $\hat{t}_1$, "Error B" and the size of the oscillations for $t \in [\hat{t_0}, T]$ reduce as we increase the number of spatial nodes.

Now we proceed to check the rate of error convergence. We define the Root of the Mean Square Error as

$$\text{RMSE}_{\{N_\theta, N_t\}}\left(v^{\mathbf{N}}\right) = \sqrt{\frac{1}{N_t+1}\sum_{l=0}^{N_t}\left(v^{\mathbf{N}}(0,t_l) - v(0,t_l)\right)^2}. \tag{3.95}$$

The next figure shows the convergence of spatial error for $\Delta t = 3.9 \cdot 10^{-4}$ and different number of spatial nodes N_θ.

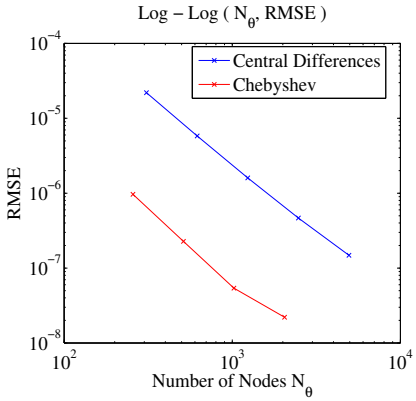

Figure 3.12: Spatial Error convergence of $v^{\mathbf{N}}$ in logarithmic scale of the FD (blue) and Chebyshev (red) methods.

On Figure 3.12, we have plotted, in logarithmic scale, the number N_θ of spatial nodes versus the value $\mathrm{RMSE}_{\{N_\theta,N_t\}}\left(v^{\mathbf{N}}\right)$. The slope of the regression line of the FD method (plotted in blue) is -1.80 and of the Chebyshev method (plotted in red) is -1.85.

The spectral convergence that we could expect in the Chebyshev method probably does not occur due to both the Error discontinuity at time $\hat{t}_1$ and the imposed Neumann boundary condition (see Subsection 3.6.3).

We proceed now to check the temporal error convergence. We fix $N_\theta = 4960$ for the Central Differences method and $N_\theta = 2048$ for the Chebyshev method. We compute the RMSE for different number of time partitions N_t.

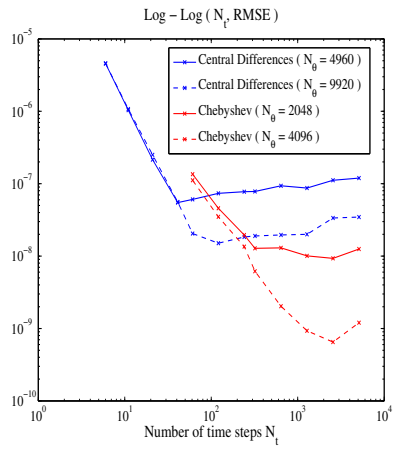

Figure 3.13: Temporal Error convergence of $v^{\mathbf{N}}$ in logarithmic scale of the FD (blue) and Chebyshev (red) methods.

In Figure 3.13, we have plotted, in logarithmic scale, the number N_t versus the value $\mathrm{RMSE}_{\{N_\theta,N_t\}}\left(v^{\mathbf{N}}\right)$. The slope of the regression line of the FD method (solid-blue) is -2.31 as it could be expected from an order 2 method.

The slope of the Chebyshev method (solid-red) is -1.4. We point out that in the Chebyshev method, for $t_l \in [\hat{t}_1, T]$, the lower limit of the computational domain $I(t_l)$, given by (3.74) or (3.75), is much closer to $\theta = \frac{\pi}{2}$ than in the FD method. Therefore, the boundary error due to the imposition of Neumann boundary conditions is probably bigger in the Chebyshev method. Furthermore, the smallest values of N_t in the Chebyshev method are near the empirical constraints (3.92) and for bigger values we reach very soon the error limit marked by the size of N_θ. Probably this is the reason why we cannot see an order 2 in time for the Chebyshev method.

We carry out a second experiment doubling the value of N_θ (dashed-blue/red) to check that the lowest value reached by the error was given by the size of the spatial mesh.

Depending on the error tolerance, we might need a big value for N_θ in the FD method but much smaller in the Chebyshev method. This makes that, depending on the required precision, Chebyshev performs better in computational cost than FD. This will be studied in Subsection 3.7.4.

3.7.2 Location of the Buying Region frontier at time $\hat{t}_1$

From Property c) of Subsection 3.3.1 we know that in polar coordinates $\mathrm{BR}_F(\hat{t}_1) = \frac{\pi}{2}$.

Given a number of time steps N_t, we look for $t_{l_1} \in \{t_l\}_{l=0}^{N_t}$ which is nearest to $\hat{t}_1$ and define the Absolute Error (just for this experiment) as:

$$\text{Absolute Error}_{\mathbf{N}}(\hat{t}_1) = \left| \mathrm{BR}_F^{\mathbf{N}}(t_{l_1}) - \frac{\pi}{2} \right|.$$

Another option to numerically compute the value $\mathrm{BR}_F^{\mathbf{N}}(\hat{t}_1)$ is to interpolate $\left\{\mathrm{BR}_F^{\mathbf{N}}(t_l)\right\}_{l=0}^{N_t}$. Although this would give us more precision in all the cases (1-2 digits more), we have not employed it because the error discontinuity at $\hat{t}_1$ impedes us to see any error convergence (the error oscillates between $10^{-5} - 10^{-7}$ for the Chebyshev method).

Fixed $\Delta t = 3.9 \cdot 10^{-4}$, we compute the Absolute Error for different number of spatial nodes N_θ. We check the Spatial Error convergence plotting, in semilogarithmic scale, the value of N_θ versus the absolute error for both methods:

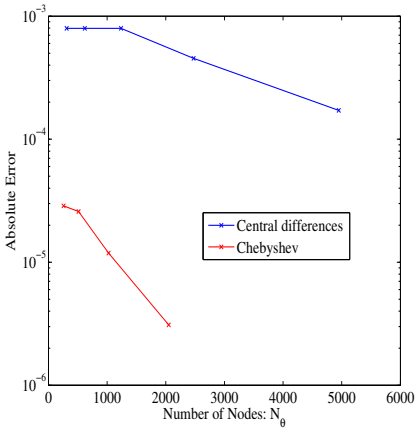

Figure 3.14: Spatial Error convergence for instant $BF_R = \frac{\pi}{2}$ of the FD (blue) and Chebyshev (red) methods in semilogarithmic scale.

We recall that in the FD method, the Buying and Region frontiers were not obtained by interpolation, but they were points from the spatial mesh (see Subsection 3.5.3). This is the reason why the error of FD method on Figure 3.14 is step shaped ($N_\theta = \{310, 620, 1240\}$ give the same value).

The spatial error reduces as we increase the value of N_θ. At equal number of nodes, the Chebyshev method gives much smaller errors than the FD method.

Concerning the temporal error, we fix $N_\theta = 4960$ for the Central Differences method and $N_\theta = 2048$ for the Chebyshev method. We compute the Absolute Error for different number of time partitions $N_t = \{640, 1280,\ 2560,\ 5120,\ 10240\}$. On the following picture, we plot in semilogarithmic scale the value of N_t versus the absolute error.

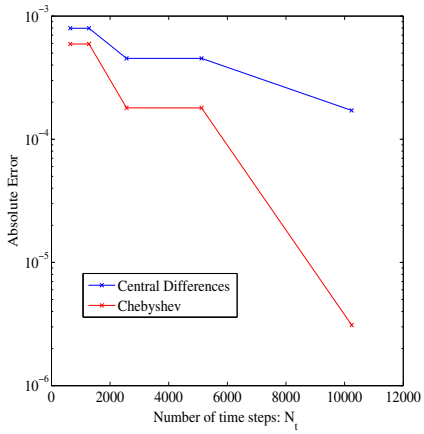

Figure 3.15: Temporal Error convergence for instant $BF_R = \frac{\pi}{2}$ of the FD (blue) and Chebyshev (red) methods in semilogarithmic scale.

In this case, both results are step shaped because of the definition of Absolute Error and the time partition when Δt is halved. Each time partition is included in the following one and t_{i_1} sometimes changes and sometimes not.

The temporal error reduces as we increase the value of N_t. As in the spatial error, the Chebyshev method outperforms the FD method.

3.7.3 First instant when is optimal to have a positive amount of the stock.

From Property b) of Subsection 3.3.1 we know that this time is

$$\hat{t}_0 = T - \frac{1}{\alpha - r} \log\left(\frac{1+\lambda}{1-\mu}\right) \quad \text{and that} \quad \begin{cases} \mathrm{BR}_F(t) = 0, & t \geq \hat{t}_0 \\ \mathrm{BR}_F(t) > 0, & t < \hat{t}_0 \end{cases}$$

Given a number of time steps N_t, we look for $t_{l_0} \in \{t_l\}_{l=0}^{N_t}$ such that

$$t_{l_0} \geq \hat{t}_0 > t_{l_0+1}$$

For this experiment, the error behaviour of each method has to be studied independently. In the case of the FD method, once fixed N_t, we have found that

$$\mathrm{BR}_F^{N_\theta}(t_l) = 0, \quad l = N_t,\ N_t - 1,\ ..., l_0 + 1$$

and the error is due to that there might exist $k > 0$ such that

$$\mathrm{BR}_F^{N_\theta}(t_l) = 0, \quad l = l_0,\ l_0 - 1, ..., l_0 - k$$

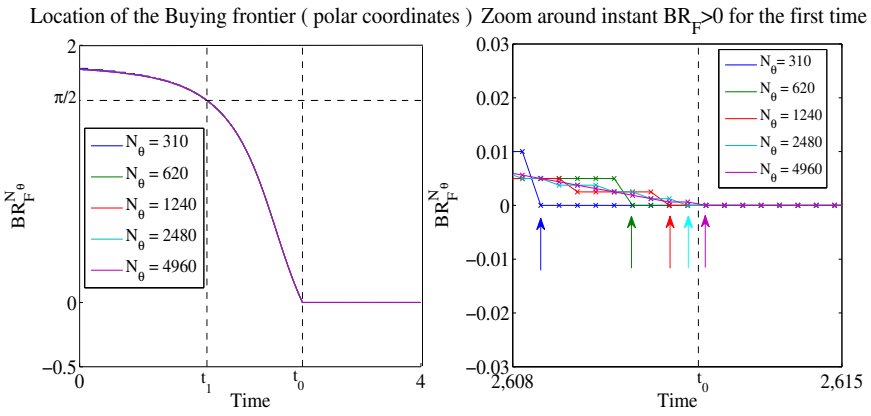

Figure 3.16: Numerical estimation of the Buying Frontier with the FD method for $t \in [0,4]$ (left) and zoom around $\hat{t}_0$ (right). Arrows mark the last instant when $\mathrm{BR}_F^{\mathbf{N}} = 0$ for each N_θ.

In left picture of Figure 3.16, we plot the numerical estimation of the Buying Frontier with the FD method for $N_\theta = 310$ (blue), $N_\theta = 620$ (red), $N_\theta = 1240$ (green) ,$N_\theta = 2480$ (celest) $N_\theta = 4960$ (violet). On the right picture we zoom around $\hat{t}_0$ and the arrows mark the last instant when $\mathrm{BR}_F^{\mathbf{N}} = 0$ for each N_θ.

In the Central Finite Differences method, we search for:

$$t^{FD} = \max\left\{ t \in \{t_l\}_{l=0}^{N_t} / \mathrm{BR}_F^{\mathbf{N}}(t) > 0 \right\},$$

and define the absolute error (for this method and experiment)

$$\text{Absolute Error}^{FD} = \left| t^{FD} - \hat{t}_0 \right|.$$

We check the spatial ($\Delta t = 3.9 \cdot 10^{-4}$ and several values for N_θ) and temporal ($N_\theta = 4960$ and several values for N_t) error convergence. On Figure 3.17, we plot the errors in logarithmic scale.

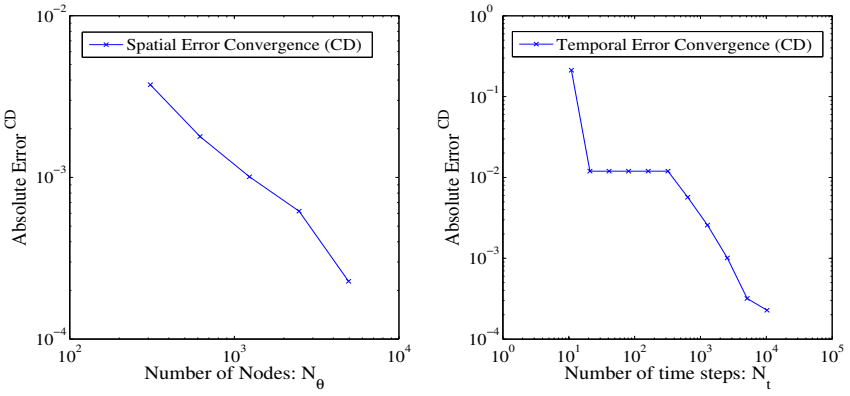

Figure 3.17: Spatial (left) and temporal (right) error convergence of the first instant when it is optimal to have a positive amount of stock (FD method).

The left side picture of Figure 3.17 represents the spatial error and the right side picture the temporal error, both in logarithmic scale. The right side picture is step-shaped again due to the definition of the error and the choice of the time partitions when Δt is halved.

In the case of the Chebyshev method, the error behaves differently. For this method, the $\mathrm{BR}_F^{\mathbf{N}}$ may be bigger than 0 a few time steps prior to l_0. We note that in the Chebyshev method, the lower limit of $I(t_l),\ t_l \in [\hat{t}_0, T]$ is the Buying frontier. The boundary error due to the imposition of Neumann conditions is probably more relevant in this method and the cause of this behaviour.

In left picture of Figure 3.18, we have plotted the numerical estimation of the Buying Frontier with the Chebyshev method for $N_\theta = 310$ (blue), $N_\theta = 256$ (blue), $N_\theta = 512$ (red), $N_\theta = 1024$ (green) $N_\theta = 2048$ (black). In the right picture we zoom around $\hat{t}_0$.

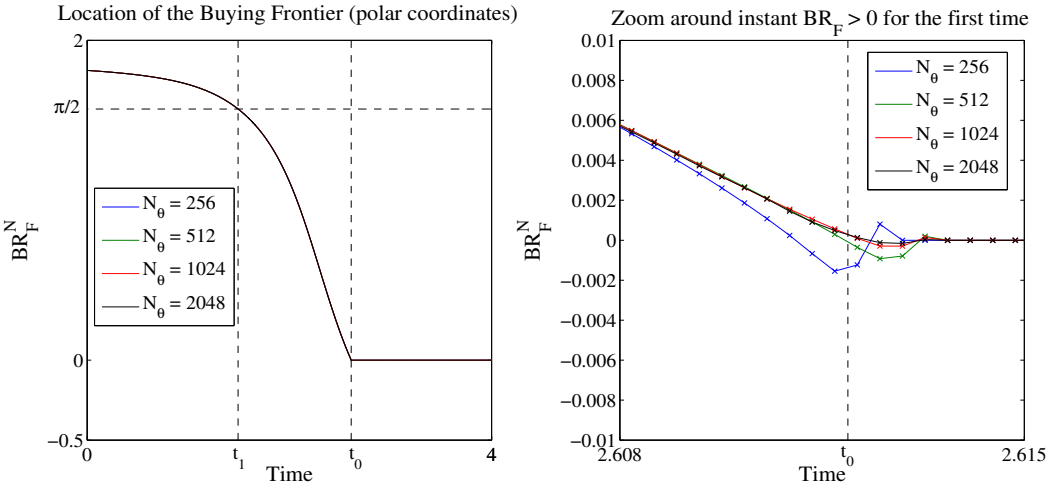

Figure 3.18: Numerical estimation of the Buying Frontier with the Chebyshev method for $t \in [0, 4]$ (left) and zoom around $\hat{t}_0$ (right). Arrows mark the last instant when $\mathrm{BR}_F^{\mathbf{N}} = 0$ for each N_θ.

Let $k \geq 0$ be the biggest value such that

$$\mathrm{BR}_F^{\mathbf{N}}(t_{l_0+k}) > 0.$$

Remark 3.7.1. We recall that in the implementation of the Numerical Algorithm, it is at time step t_{l_0+k}, where we change the kind of adaptive interval $I(t_l)$.

If $k > 0$, the location of the Buying Frontier oscillates around 0 for $t_l \in \{t_{l_0+k}, ..., t_{l_0+1}\}$ and it is for $t_l < t_{l_0}$ when it behaves as we could expect from Property a) of Subsection 3.3.1.

Numerical experiments show that it is better to let $\mathrm{BR}_F^{\mathbf{N}}(t_l)$ oscillate around 0 rather than imposing $\mathrm{BR}_F^{\mathbf{N}}(t_l) = \max\{\mathrm{BR}_F^{\mathbf{N}}(t_l),\ 0\}$.

As mentioned, the oscillations observed in Figure 3.18 are probably generated by the imposition of the Neumann conditions. The boundary error is controlled by N_t and N_θ, but probably the spatial error is dominant. The instant when the numerical solution begins to

oscillate is always very close to $\hat{t}_0$ $\left(\left|t_{l_0-k} - \hat{t}_0\right| \leq 1.5 \cdot 10^{-3}\right)$ and the size of the oscillations reduces as N_θ increases.

These oscillations are the error that we are going to study. They include all the negative values (since the Buying Frontier must be always positive) and any positive value for time steps bigger than $\hat{t}_0$. Thus, we define the absolute error (for this method and experiment)

$$\text{Absolute Error}^{Ch} = \max\left\{\left|\min_{l=0,1,\ldots,N_t}\left\{\text{BR}_F^{\mathbf{N}}(t_l)\right\}\right| , \left|\max_{l=l_0+1,l=l_0+2,\ldots,N_t}\left\{\text{BR}_F^{\mathbf{N}}(t_l)\right\}\right|\right\}.$$

We fix $\Delta t = 3.9 \cdot 10^{-4}$ and compute the absolute error for several values for N_θ). In Figure we plot, in logarithmic scale, the value of N_θ versus the absolute error.

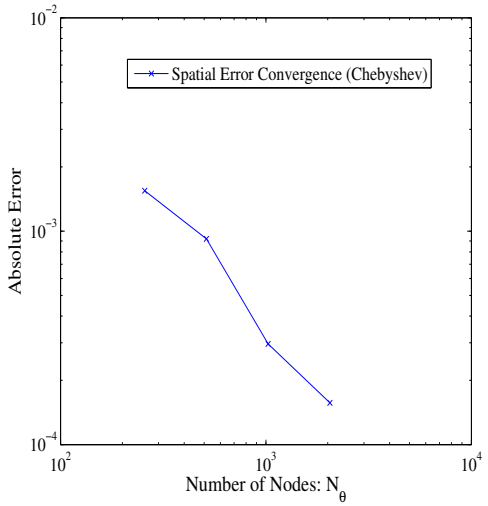

Figure 3.19: Spatial error convergence of the first instant when it is optimal to have a positive amount of stock (Chebyshev method).

Remark 3.7.2. This error is also the origin of the bounds (3.92). If Δt is very small and N_θ is not big enough, these oscillations may be too big and complicate the location of the frontiers for the rest of the time steps.

3.7.4 Performance Analysis

We are going to carry out a performance comparison between both numerical methods. First of all, we fix several time / spatial discretizations:

(i) $\Delta t \in [0.02,\ 3.9^{-4}]$

(ii) $N \in [141,\ 1024]$ (Chebyshev)

(iii) $N \in [300,\ 6000]$ (Crank-Nicholson)

and solve the problem with all the combinations of the different discretizations for both methods. We store the error and the computational time employed in each of them.

We plot in logarithmic scale the value of $\text{RMSE}_{\{N_\theta, N_t\}}\left(v^{\mathbf{N}}(0,t)\right)$ versus the computational time employed in computing $v^{\mathbf{N}}$ for each different spatial and temporal meshes.

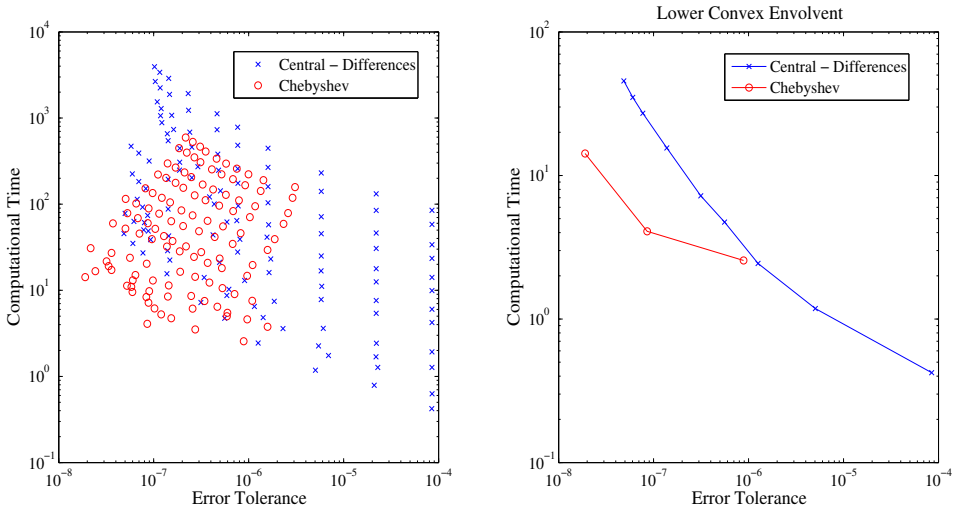

Figure 3.20: Performance comparison of the Error at $v^{\mathbf{N}}(0,t)$. In logarithmic scale, we plot (left), the value of RMSE versus the total computational costs of CFD (blue) and Chebyshev (red) methods and their respective lower enveloping curves (right).

The left-side picture of Figure 3.20 represents the cloud of results for the different discretizations of each method. The right-side, which is more visual, represents the lower convex enveloping curve.

With the right-side picture, we can obtain an approximate behaviour of the evolution of the error versus the required computational time to reach that precision. We fix the error tolerance that we require for our problem and find which method and spatial/time discretization reaches it first.

As we can see, the FD method (blue in Figure 3.20) performs better if we do not require a high precision. This is due to the bounds over Δt, N_θ (3.92) imposed for the Chebyshev method (red in Figure 3.20). If a higher precision is required, Chebyshev performs better.

The behaviour of the value of the Buying frontier at $\hat{t}_1$ is also very important. It gives the optimal investment strategy that we must follow. In this case, we plot in Figure 3.21, in logarithmic scale, the absolute error obtained versus the computational time employed for each different spatial/temporal meshes.

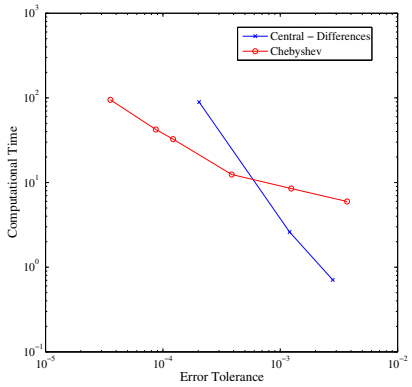

Figure 3.21: Performance comparison (lower convex envolvent in logarithmic scale) of the Error $\mathrm{BR}_F^{\mathbf{N}}(\hat{t}_1) = \frac{\pi}{2}$ versus the total computational costs of the CFD (blue) and Chebyshev (red) methods.

The conclusion of this experiment is the same as in the previous one. If more precision is required, time partition must be refined for both methods, but the Central Differences method requires more refined space meshes than the Chebyshev method, something that increases its computational cost.

3.7.5 Stationary state

BR_F and SR_F tend to a stationary state as $T \to \infty$ that can also be computed explicitly (see Subsection 3.3.1).

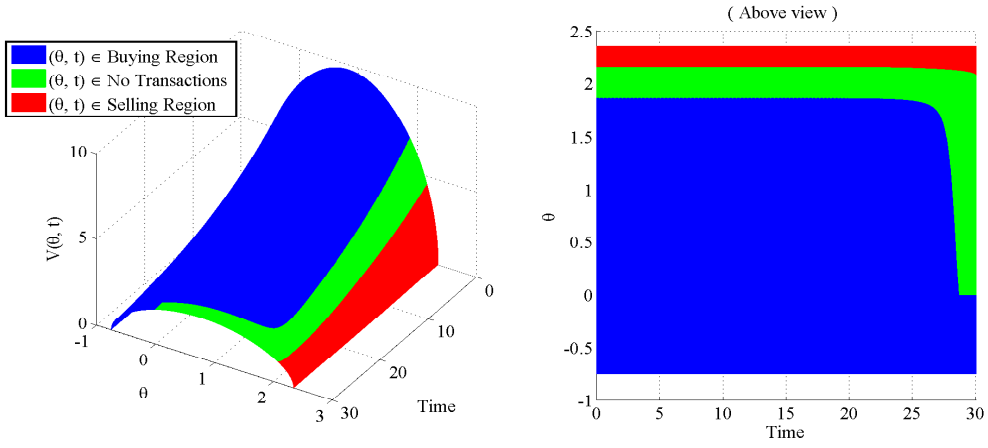

Figure 3.22: Value function (Chebyshev) for $(\theta, t) \in [\beta_1, \beta_2] \times [0, 30]$ colored if (θ, t) is in the Buying(blue), No Transactions (green) and Selling Region (Red).

In the example, computed for $T = 30$ years with the Chebyshev method ($\Delta t = 10^{-4}$,

$N_\theta = 512$), frontiers have stabilized a few years before reaching $t = 0$ at:

$$\text{Buying Frontier: } 1.8626 \quad (1.8622 \text{ exact value})$$
$$\text{Selling Frontier: } 2.1559 \quad (2.1561 \text{ exact value})$$

In this experiment, and for the Chebyshev method, temporal error is dominant if we compare it with respect to the spatial error. In the case of the FD method, the error depends more in both the spatial and temporal discretizations.

We define the absolute error (for this experiment) as

$$\text{Absolute Error} = \left|\text{BR}_F^{\mathbf{N}}(0) - BR_s\right|$$

We study the spatial ($N_t = 10^{-3}$ and several values for N_θ) and temporal ($N_\theta = 4960$ for the FD, $N_\theta = 512$ for the Chebyshev method, and several values for N_t) error convergence. In Figure 3.23 we plot, in logarithmic scale, the value of N_θ (left) versus the absolute value of the error and the value of N_t (right) versus the absolute value of the error for both methods.

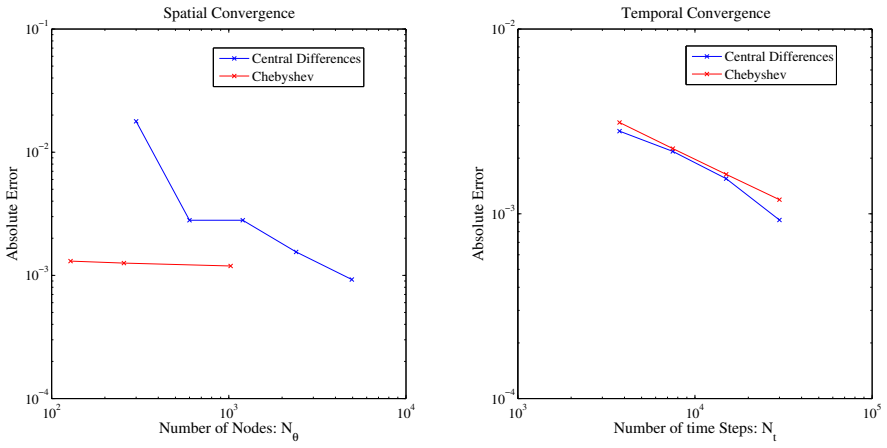

Figure 3.23: Spatial (left) and Temporal (right) error convergence, in logarithmic scale, of the Stationary State of the Buying Frontier for the CFD(blue) and Chebyshev (red) methods.

On the left side picture, we can see that the Chebyshev method reaches the error marked by the time discretization with the smallest number of nodes (as mentioned before, the temporal error is dominant). Therefore, if a high precision is required, Chebyshev will perform better than the Central Finite Differences method.

The error behaviour of the Selling Frontier is similar to the one of the Buying Frontier.

Chapter 4

Option Pricing with Transaction Costs under Exponential Utility

4.1 Introduction

When pricing a derivative, the portfolio replication technique is based on the possibility of building a hedging portfolio that mimics the behaviour of the derivative. In the case of an European Option, the replicating portfolio is formed by the bond and the stock and it will be necessary to rebalance it after each change in the stock price. Since the stock prices change continuously, negligible transaction costs are needed. Otherwise, the replication technique will not be feasible.

In presence of transaction costs, one can try a dominating, rather than a hedging strategy. For the European Option, Soner et al. proved in [58] that the least expensive method of dominate the Call under transaction costs is to buy a share of the underlying stock and hold it until maturity.

An alternative to the construction of replicating portfolios or dominating strategies is to price derivatives using the technique called "Indifference Pricing". The basics of the technique in option pricing, from the point of view of the seller, are the following. We define an adequate function (strictly increasing and concave) that allows us to measure the utility of the wealth and we build two scenarios for a fixed initial amount of money.

In the first one, only the stock and the bond are considered and we need to solve an Optimal Investment problem under transaction costs. In the second one, we receive a certain amount p_w for selling an option and, with the total amount of money, we solve again an Optimal Investment problem including this time the obligation acquired when selling the option. The quantity p_w that equals the expected terminal utility of both scenarios will be the price of the contract.

Besides modeling transaction costs, this model is also interesting due to the following

empirically observed property: "the no-linearity of the price in relation with the number of contracts". The no-linearity towards risk is reflected by the market when we observe the price of the contracts in a trade panel. The price depends on the number of the contracts offered but, if all risks were hedgeable, all the contracts should have the same price.

In [12], a full description of the "Indifference Pricing" technique and its latest applications to several different models can be found. Furthermore, closed solutions for certain specific cases also are included but, in general, numerical methods will have to be employed.

In this work we are going to present a numerical method specifically designed for the model derived by Davis, Panas and Zaripopoulos in [22] where they price European Options with transaction costs under Exponential Utility. The Exponential Utility is among the most used utility functions and has several advantages. It usually gives quite tractable equations and, in this case, it will also allow us to reduce one of the dimensions of the problem. But it also has its drawbacks, since it gives numerical difficulties in lognormal models, as pointed out in [12], due to the behaviour of the exponential utility function.

The outline of the chapter is as follows. In Section 4.2 a description of the model presented in [22] will be done and it will be equivalently reformulated for technical reasons. In Section 4.3, we propose two changes of variables that reduce the numerical difficulties related with the Exponential Utility. The associated partial differential equation that we obtain results to be non-linear and a Fourier pseudospectral method is applied to solve it. Results that guarantee the convergence and stability of the numerical solution of the pseudospectral method will be included. Section 4.4 will be devoted to the numerical analysis. When transaction costs disappear, and all risks become again hedgeable, the replication price, i.e. the Black-Scholes price must be recovered. Theoretical results both in [12] and [22] guarantee it, and this will allow us to employ explicit formulas to check the convergence error of the pseudospectral method. The effect of incorporating transaction costs will also be studied.

4.2 The original model

4.2.1 Pricing options via utility maximization.

Let $(\Omega, \mathcal{F}, P)$ be a filtered probability space. Let us suppose that the market consists of a bank account and a stock whose dynamics are respectively given by:

$$\begin{cases} d\bar{X}(t) = r\bar{X}(t)dt, \\ d\bar{S}(t) = \alpha\bar{S}(t)dt + \sigma\bar{S}(t)d\bar{z}_t, \end{cases} \tag{4.1}$$

where r denotes the constant risk-free rate, α is the constant expected rate of return of the stock, $\sigma > 0$ is the constant volatility of the stock, and $\bar{z}_t$ denotes the standard brownian motion.

Similar to Chapter 3, $\bar{X}(t)$ represents the amount of money invested in the bank account. In this Chapter, the amount of money invested in the stock will be controlled by the number of shares of the stock that the investor holds, which will be denoted by a new variable $\bar{y}(t)$.

Although the utility maximization problems that we are going to propose will be solved for any initial position, for simplicity reasons, we will assume that when we want to price an option, and prior to enter into the market, the position of an investor is always a certain amount of money in the bank account and no holdings in the stock.

Definition 4.2.1. *The set of all admissible trading strategies available for an investor who starts at $t = 0^-$ with an amount $\bar{X}(0^-) = X_0$ in the bank account and $\bar{y}(0^-) = 0$ in the stock will be denoted by $\tau(X_0)$.*

In this Chapter, as in Chapter 3, we assume that the transaction costs are a fixed percentage of the transacted amount (proportional transaction costs). These percentages will be given by:

(a) $\lambda \in [0, 1)$: For buying shares of the stock.

(b) $\mu \in [0, 1)$: For selling shares of the stock.

Definition 4.2.2. *We define $\pi \in \tau(X_0)$ as an adapted stochastic process $(X^\pi(t),\ y^\pi(t)),\ t \in [0,\ T]$, where $X^\pi(t)$ denotes the amount of money held in the bank account and $y^\pi(t)$ denotes the number of shares of the stock held by the investor at time t.*

We point out that the investor may borrow from the bank at interest rate r and that $\bar{y} \in \mathbb{R}$, so that long and short positions are both accepted.

We also point out that we are allowed to buy from the first moment that we enter into the market at $t = 0$. Let $\bar{S}(0) = S_0$ and our position $(\bar{X}(0^-), \bar{y}(0^-)) = (X_0, 0)$. Formally, it may occur:

$$(X^\pi(0^+),\ y^\pi(0^+)) = (X_0 - (1+\lambda)S_0\epsilon, \epsilon),$$

or

$$(X^\pi(0^+),\ y^\pi(0^+)) = (X_0 + (1-\mu)S_0\epsilon, -\epsilon),$$

where $\epsilon \geq 0$. We define $(X^\pi(0),\ y^\pi(0)) = (X^\pi(0^+),\ y^\pi(0^+))$.

The liquidated cash value of a portfolio, denoted by $c(\bar{y}, \bar{S})$, is given by:

$$c(\bar{y}, \bar{S}) = \begin{cases} (1+\lambda)\bar{S}\bar{y}, & \bar{y} < 0, \\ (1-\mu)\bar{S}\bar{y}, & \bar{y} \geq 0. \end{cases} \tag{4.2}$$

We consider two different optimal investment problems.

1. Investments are realized only in the bank account and in the stock.

2. Before entering into the market, the investor sells one European Option.

Scenario 1:

In this scenario, the investor may hold money in the bank account and in shares, but he/she has not sold an option. The net wealth of the investor at maturity, $W_1(T)$, is given by:

$$W_1(T) = X^\pi(T) + c(y^\pi(T), \bar{S}(T)). \tag{4.3}$$

The Optimal Investment problem in this scenario consists in finding, for an initial amount of money $\bar{X}(0^-) = X$ held in the bank account and $\bar{y}(0^-) = 0$, an admissible strategy that maximizes the Expected Utility of the terminal wealth :

$$V_1(X) = \sup_{\pi \in \tau(X)} \mathbb{E}\left\{U\left(W_1(T)\right)\right\}, \tag{4.4}$$

where $\tau(X)$ is the set of admissible trading strategies for $t \in [0,\ T]$ and U is a Utility function (a function with continuous second order derivatives, strictly increasing and strictly concave). In this Chapter we also impose that $U(0) = 0$.

Scenario 2:

Suppose that the investor has sold an European Option with strike K. At maturity, the net wealth of the investor, $W_w(T)$ is given by:

$$W_w(T) = \begin{cases} X^\pi(T) + c(y^\pi(T), \bar{S}(T)), & \text{if } \bar{S}(T) < K, \\ X^\pi(T) + K + c(y^\pi(T) - 1, \bar{S}(T)), & \text{if } \bar{S}(T) \geq K, \end{cases} \tag{4.5}$$

or, equivalently, what it is held in the bank plus

(a) The net value of the portfolio if the option is not exercised.

(b) The net value of the portfolio minus one share plus the strike value.

The Optimal Investment problem in this scenario consists in finding, for an initial amount of money $\bar{X}(0^-) = X$ held in the bank account and $\bar{y}(0^-) = 0$, an admissible strategy that maximizes the Expected Utility of the terminal wealth :

$$V_w(X) = \sup_{\pi \in \tau(X)} \mathbb{E}\left\{U\left(W_w(T)\right)\right\}, \tag{4.6}$$

where $\tau(X)$ is the set of admissible trading strategies for $t \in [0,\ T]$ and U is the same Utility function as in (4.4).

The indifferent price $p_w(X)$ of one European Option for an investor with an initial amount of money $\bar{X}(0^-) = X$ in the bank account and $\bar{y}(0^-) = 0$ is the price which leaves him indifferent between:

1. Enter directly into the market without selling an option
2. Sell one European option, receive the amount $p_w(X)$ and enter into the market.

Remark 4.2.1. Before entering into the market, the investor may sell one or n European Options. Although the option price is non linear in the number of contracts, for simplicity, the problem and the numerical examples will be solved for just one contract.

The development is identical substituting 1 by n in the definition of $W_w(T)$ (formula (4.5)).

We assume that a solution for both problems exists and that for $j \in \{1, w\}$ functions V_j are continuous and concave (concavity is inherited from the Utility function and continuity is proved in [22]). The following result is also needed.

Proposition 4.2.1. *The functions $V_j(X),\ j \in \{1, w\}$ are strictly increasing.*

Proof. Suppose that the initial amount of money of the investor is $X_0 = C \in \mathbb{R}$.

For $j \in \{1, w\}$, let π_j^C be an optimal trading strategy which solves:

$$V_j(C) = \sup_{\pi \in \tau(C)} \mathbb{E}\left\{U\left(W_j(T)\right)\right\}.$$

Let $W_j^{\pi_j^C}(T)$ be the expected terminal wealth when strategy π_j^C is followed. The value function V_j is given by

$$V_j(C) = U\left(W_j^{\pi_j^C}(T)\right).$$

Now, suppose that the initial position is $C + \epsilon_0$ where $\epsilon_0 > 0$.

Consider the, a priori suboptimal, trading strategy π_j^s which consists in keeping ϵ_0 in the bank account until maturity while we independently follow strategy π_j^C with the rest of the assets.

The expected terminal wealth is

$$W_j^{\pi_j^s}(T) = \epsilon_0 \cdot e^{rT} + W_j^{\pi_j^C}(T).$$

Therefore, by the suboptimality of the strategy, it holds that

$$V_j(C+\epsilon_0) = \sup_{\pi \in \tau(C+\epsilon_0)} \mathbb{E}\left\{U\left(W_j(T)\right)\right\} \geq U\left(W_j^{\pi_j^s}(T)\right) = U\left(\epsilon_0 \cdot e^{r(T-0)} + W_j^{\pi_j^C}(T)\right) > V_j(C),$$

because the Utility function is a strictly increasing function. □

Definition 4.2.3. *We define the indifferent price $p_w(X)$ as the quantity which equals the functions*

$$V_1(X) = V_w\left(X + p_w(X)\right). \tag{4.7}$$

Remark 4.2.2. The definition of the indifferent price makes the option price dependent of the initial wealth of the investor X. The merit of the particular choice of Utility function made by Davis et al. in [22] (Exponential Utility) is that the indifferent price becomes wealth-independent and can be globally defined for all $X \in \mathbb{R}$.

For finishing this Subsection and prior to the development of the equations of the model, let us study a particular interesting case presented in [22]. There, a slightly different reasoning, but consistent with definition 4.2.3, is employed to arrive to the indifferent price.

Suppose that the investor has no holdings at all (neither stock shares nor money in the bank account). If he follows the, a priori suboptimal, trading strategy of not investing at all, it is clear that the terminal utility is 0 ($U(0) = 0$ by hypothesis). On the other hand, let X_0^1 be such that:

$$V_1(X_0^1) = 0, \tag{4.8}$$

which exists and satisfies $X_0^1 \leq 0$, due to the continuity, concavity and strictly increasing properties of function $V_1(X)$ and the fact that $V_1(0) \geq 0$ (it is easy to check that, starting from $X = 0$, function $V_1(X)$ cannot be lower bounded by the left).

The physical interpretation of quantity X_0^1 in their setting is: "An investor (without holdings) is indifferent between (a) do nothing and (b) "pay" X_0^1 as an entry fee and enter into the market to buy and sell the stock".

Similarly, if the investor has no holdings at all, let X_0^w be such that:

$$V_w(X_0^w) = 0. \tag{4.9}$$

The physical interpretation of the quantity X_0^w is: "An investor (without holdings) is indifferent between (a) do nothing and (c) sell the option, receive X_0^w and enter into the market to invest in the stock and in the bank account since both strategies provide the same expected terminal utility".

Since scenarios (a), (b) and (c) are indifferent to an investor with no holdings in this setting, Davis et al. define the indifferent price p_w^* of the option as

$$p_w^* = X_0^w - X_0^1.$$

Davis et al. give this definition of indifference price since the Exponential Utility function that they later employ leads to an option price which is wealth-independent, thus the value of X does not affect the option price.

Note that in their reasoning, in scenario (a) the investor is not allowed to enter the market at all. To enter into the market he has to "pay" X_0^1 as an entry fee in scenario (b) or he is forced to sign the option in scenario (c).

If we employ Definition 4.2.3, $p_w^* = p_w(X_0^1)$ which corresponds to the particular initial condition $\bar{X}(0) = X_0^1$ (the paid fee)

$$V_1(X_0^1) = 0 = V_w(X_0^w) = V_w(X_0^1 + p_w(X_0^1)).$$

We point out that it is Definition 4.2.3 the general one. Moreover, it is implicitly employed to derive the indifferent option price in [22] and to check that it becomes wealth-independent under the Exponential Utility.

The importance of this particular case is that, if no transaction costs are present ($\lambda = \mu = 0$), $p_w^* = p_w(X_0^1)$ is indeed the Black-Scholes price of the option. The following result, shown in [22], guarantees this statement.

Definition 4.2.4. *Given and option negotiated over $\bar{S}$, a replicating portfolio for the seller of the option is and element $\hat{\pi} \in \tau(\hat{X}_0)$ for an initial endowment $\hat{X}_0$, such that:*

$$(X^{\hat{\pi}}(T),\ y^{\hat{\pi}}(T)) = (-K, 1) I_{\bar{S}(T)\geq K}.$$

where $I_{\bar{S}(T)\geq K}$ is the indicator function.

Equivalently, the replicating portfolio has the same value as the option at maturity.

If no transaction costs are present, wealth $W(t)$ obeys the following stochastic differential equation

$$\begin{aligned} dW(t) &= d\bar{X}(t) + \bar{y}(t) d\bar{S}(t) \\ &= r d\bar{X}(t) + \bar{y}(t)\bar{S}(t)\alpha dt + \bar{y}(t)\bar{S}(t)\sigma dz(t), \end{aligned}$$

which can be rewritten as

$$dW(t) = rW(t)dt + \bar{y}(t)\bar{S}(t)\sigma d\tilde{z}(t), \tag{4.10}$$

where $\tilde{z}(t)$ is a brownian motion with drift.

From the previous equation, we infer that $\tau(X)$ is a linear space, i.e. that if $\pi_i \in \tau(X_0^i),\ i \in \{i_1, i_2\}$, then $\forall a, b \in \mathbb{R}$ we have that $a\pi_{i_1} + b\pi_{i_2} \in \tau(aX_0^{i_1} + bX_0^{i_2})$ where

$$a\pi_{i_1} + b\pi_{i_2} = (aX^{\pi_{i_1}} + bX^{\pi_{i_2}}, ay^{\pi_{i_1}} + by^{\pi_{i_2}}).$$

Theorem 4.2.1. *Suppose that both $V_w(X)$ and $V_1(X)$ are continuous and strictly increasing functions of X. Then $p_w^* = \hat{X}_0$ if a replicating portfolio $\hat{\pi} \in \tau(\hat{X}_0)$ exists.*

Proof. From the linearity of τ, any arbitrary trading strategy $\pi \in \tau(X_0)$ can be written as $\pi = \hat{\pi} + \tilde{\pi}$ where $\hat{\pi} \in \tau(\hat{X}_0),\ \tilde{\pi} \in \tau(\tilde{X}_0)$ and $X_0 = \hat{X}_0 + \tilde{X}_0$.

Then it holds that

$$\begin{aligned} 0 &= V_w(X_0^w) \\ &= \sup_{\pi\in\tau(X_0^w)} \mathbb{E}\left\{U\left(X^{\pi}(T) + I_{(\bar{S}(T)<K)} c(y^{\pi}(T), \bar{S}(T)) + I_{(\bar{S}(T)\geq K)}\left[K + c(y^{\pi}(T) - 1, \bar{S}(T))\right]\right)\right\} \\ &= \sup_{\tilde{\pi}\in\tau(X_0^w - \hat{X}_0)} \mathbb{E}\left\{U\left(X^{\tilde{\pi}}(T) + X^{\hat{\pi}}(T) + I_{(\bar{S}(T)<K)} c(y^{\tilde{\pi}}(T) + y^{\hat{\pi}}(T), \bar{S}(T))\right.\right. \\ &\qquad \left.\left. + I_{(\bar{S}(T)\geq K)}\left[K + c(y^{\tilde{\pi}}(T) + y^{\hat{\pi}}(T) - 1, \bar{S}(T))\right]\right)\right\} \\ &= \sup_{\tilde{\pi}\in\tau(X_0^w - \hat{X}_0)} \mathbb{E}\left\{U\left(X^{\tilde{\pi}}(T) - KI_{(\bar{S}(T)\geq K)} + I_{(\bar{S}(T)<K)} c(y^{\tilde{\pi}}(T), \bar{S}(T))\right.\right. \\ &\qquad \left.\left. + I_{(\bar{S}(T)\geq K)}\left[K + c(y^{\tilde{\pi}}(T), \bar{S}(T))\right]\right)\right\} \\ &= \sup_{\tilde{\pi}\in\tau(X_0^w - \hat{X}_0)} \mathbb{E}\left\{U\left(X^{\tilde{\pi}}(T) + c(y^{\tilde{\pi}}(T), \bar{S}(T))\right)\right\} \\ &= V_1(X_0^w - \hat{X}_0). \end{aligned}$$

By definition of X_0^1, it is straightforward that $\hat{X}_0 = X_0^w - X_0^1 = p_w^*$. □

This result will be employed in the error analysis of the numerical method proposed in Subsection 4.3.

4.2.2 The Bellman equation.

Let us suppose now that the investors have to pay transaction cost ($\lambda + \mu > 0$) when money is transferred from the bank account to the stock or viceversa.

Based on the model outlined in the previous Subsection, our objective now is to derive formally a market model and the partial differential equation which is satisfied by the value functions introduced in the previous Subsection.

Let $(\Omega, \mathcal{F}, P)$ be a filtered probability space. The market model equations are:

$$\begin{cases} d\bar{X}(t) = r\bar{X}(t)dt - (1+\lambda)\bar{S}(t)dL(t) + (1-\mu)\bar{S}(t)dM(t), \\ d\bar{y}(t) = dL(t) - dM(t), \\ d\bar{S}(t) = \bar{S}(t)\alpha dt + \bar{S}(t)\sigma d\bar{z}_t, \end{cases} \tag{4.11}$$

where $L(t)$ and $M(t)$ are cumulative processes of the number of shares bought and sold respectively, $\bar{z}_t$ denotes the standard brownian motion and $\lambda,\ \mu$ are the percentages of the proportional transaction costs. The rest of parameters are those introduced in equation (4.1).

Definition 4.2.5. *The set of admissible strategies $\tau_E(X_{t_0}, y_{t_0})$ consists of the two dimensional, right-continuous, measurable processes $(X^\pi(t), y^\pi(t))$ which are the solution of equation (4.11), corresponding to some pair of right-continuous, measurable $\mathcal{F}_t$-adapted, increasing processes $(L(t), M(t))$ such that*

$$\begin{cases} \bar{X}(t_0^-) = X_{t_0},\ \bar{y}(t_0^-) = y_{t_0}, \\ (X^\pi(t), y^\pi(t), \bar{S}(t)) \in \mathscr{E}_E, \quad \forall t \in [t_0, T] \end{cases}$$

where $E > 0$ is a constant which may depend on the policy π and

$$\mathscr{E}_E = \left\{ (X, y, S) \in \mathbb{R} \times \mathbb{R} \times \mathbb{R}^+ : (x + c(y-1, S))\, e^{r(T-t)} > -E,\ t \in [t_0, T] \right\}, \tag{4.12}$$

where X, y and S respectively denote the money in the bank account, the number of shares and the stock price.

By convention, $L(t_0^-) = M(t_0^-) = 0$ but $L(t_0)$ or $M(t_0)$ may be positive.

We also consider the two wealth functions W_1 and W_w given in (4.3) and (4.5), which respectively correspond to the two possible scenarios introduced in the previous Subsection.

Remark 4.2.3. $\mathscr{E}_E$ was originally defined in [22] by:

$$\mathscr{E}_E^* = \left\{ (X, y, S) \in \mathbb{R} \times \mathbb{R} \times \mathbb{R}^+ : (X + c(y, S)) > -E,\ t \in [t_0, T] \right\}.$$

We have been a bit more restrictive (it is easy to check that $\mathscr{E}_E \subset \mathscr{E}_E^*$), just to ensure that the trading strategies

$$\begin{cases} y^\pi(t) \equiv 0, & \text{(no option was sold)}, \\ y^\pi(t) \equiv 1, & \text{(one option was sold)}, \end{cases}$$

are both admissible for any initial position $(t, X_t, y_t, S_t) \in [t_0, T] \times \mathscr{E}_E$, i.e. we have explicitly found a trading strategy which lower bounds our wealth for each scenario.

The lower bound of the wealth is needed for technical reasons (existence and uniqueness) in Subsection 4.2.3.

Definition 4.2.6. *Fix a Utility function U. For $(t, X, y, S) \in [t_0, T] \times \mathscr{E}_E$, we define the two value functions:*

$$V_j^{\mathscr{E}_E}(t, X, y, S) = \sup_{\pi \in \tau_E(X,y)} \mathbb{E}\left\{ U(W_j(T, X^\pi(T), y^\pi(T), S(T)))| \left(\bar{X}(t), \bar{y}(t), \bar{S}(t)\right) = (X, y, S)\right\}, \tag{4.13}$$

where $j \in \{1, w\}$.

We assume, as in [22], that fixed an initial position (t, X, y, S), the value of $V_j^{\mathscr{E}_E}(t, X, y, S)$ does not depend on the particular choice of E for $E \geq E_0$ big enough. This means that, although the set of allowed trading strategies increases with the value of E, we obtain the same result. In [22] it was argued that this occurred because constraint $\mathscr{E}_E$ only ruled out suboptimal trading strategies.

As we will see below, when there are no transaction costs, the optimal trading strategy can be explicitly computed and only depends on the stock price. This is a consequence of the particular choice of Exponential Utility, which makes strategies wealth-independent. When there are transaction costs, optimal trading strategies still depend only on the stock price. Furthermore, in Subsection 4.2.3 we prove that for (t_0, X_0, y_0, S_0) fixed, the value of $V_j^{\mathscr{E}_E}(t_0, X_0, y_0, S_0)$ is bounded, no matter how big is E. This strongly suggest that the assumption is correct.

For simplicity in the notation, we drop the dependance on $\mathscr{E}_E$ in the definition (4.13) of the value function and denote $V_j(t, X, y, S)$. We assume for the rest of the Chapter that $E > E_0$ is big enough. The notation employed in (4.13) is recovered for the existence and uniqueness theorems in Subsection 4.2.3 and below in the development, when we consider a subset of the allowed trading strategies.

We note that with this assumption, if E is big enough, $V_j(t, X, y, S)$ can be defined for any $(t, X, y, S) \in [t_0, T] \times \mathbb{R} \times \mathbb{R} \times \mathbb{R}^+$.

Prior to the development of the equations, we present the following result.

Proposition 4.2.2. *The value functions V_j, $j \in \{1, w\}$ are strictly increasing functions of X and y.*

Proof. For any fixed initial position $(t_0, X_{t_0}, y_{t_0}, S_{t_0})$ consider an associated optimal trading strategy π^o.

For any initial position $(t_0, X_{t_0} + \Delta x, y_{t_0}, S_{t_0})$, where $\Delta x > 0$, consider the, a priori suboptimal, trading strategy which consists in retain Δx in the bank account until maturity while we independently follow strategy π^o with the rest of the holdings.

For any initial position $(t_0, X_{t_0}, y_{t_0} + \Delta y, S_{t_0})$, where $\Delta y > 0$, consider the, a priori sub-optimal, trading strategy which consists in selling Δy stocks and then retain $(\Delta y)(1-\mu)S_{t_0}$ in the bank account until maturity while we independently follow strategy π^o with the rest of the holdings.

In both cases, the same argument employed in Proposition 4.2.1 is applicable and the result is straightforward.

□

Now, following the arguments in [22], we give the Hamilton-Jacobi-Bellman equations associated with the two stochastic control problems $j \in \{1, w\}$.

Given a constant $k > 0$, let $\mathbb{B}^k([0,T])$ denote the set of nonnegative functions such that are uniformly bounded by k. Consider a subclass of strategies $\tau'_k \subset \tau_E(X,y)$, such that $L(t)$ y $M(t)$ are absolutely continuous processes given by:

$$L(t) = \int_0^t l(\psi)d\psi, \quad M(t) = \int_0^t m(\psi)d\psi, \tag{4.14}$$

where $l(t), m(t) \in \mathbb{B}^k([0,T])$. Consider, for $j \in \{1, w\}$, the value functions given by:

$$V_j^{\mathscr{E}_E,k}(t,X,y,S) = \sup_{\pi\in\tau'_k} \mathbb{E}\left\{ U(W_j(T, X^\pi(T), y^\pi(T), S^\pi(T)))| \left(\bar{X}(t), \bar{y}(t), \bar{S}(t)\right) = (X,y,S)\right\}. \tag{4.15}$$

The Bellman equation for $j \in \{1, w\}$ and $k > 0$ is (see [22]):

$$\begin{aligned} \max_{0\le l(t), m(t)\le k} &\left\{ \left(\frac{\partial V_j^{\mathscr{E}_E,k}}{\partial y} - (1+\lambda) S \frac{\partial V_j^{\mathscr{E}_E,k}}{\partial X} \right) l(t) - \left(\frac{\partial V_j^{\mathscr{E}_E,k}}{\partial y} - (1-\mu) S \frac{\partial V_j^{\mathscr{E}_E,k}}{\partial X} \right) m(t) \right\} \\ &+ \frac{\partial V_j^{\mathscr{E}_E,k}}{\partial t} + rX \frac{\partial V_j^{\mathscr{E}_E,k}}{\partial X} + \alpha S \frac{\partial V_j^{\mathscr{E}_E,k}}{\partial S} + \frac{1}{2}\sigma^2 S^2 \frac{\partial^2 V_j^{\mathscr{E}_E,k}}{\partial S^2} = 0, \end{aligned} \tag{4.16}$$

where $(t,X,y,S) \in [0,T] \times \mathbb{R} \times \mathbb{R} \times \mathbb{R}^+$.

The optimal trading strategy can be found considering the following three possible cases:

$$\frac{\partial V_j^{\mathscr{E}_E,k}}{\partial y} - (1+\lambda) S \frac{\partial V_j^{\mathscr{E}_E,k}}{\partial X} \ge 0, \quad \frac{\partial V_j^{\mathscr{E}_E,k}}{\partial y} - (1-\mu) S \frac{\partial V_j^{\mathscr{E}_E,k}}{\partial X} > 0, \tag{4.17}$$

where the maximum is achieved by $m(t) = 0$ and $l(t) = k$;

$$\frac{\partial V_j^{\mathscr{E}_E,k}}{\partial y} - (1+\lambda) S \frac{\partial V_j^{\mathscr{E}_E,k}}{\partial X} < 0, \quad \frac{\partial V_j^{\mathscr{E}_E,k}}{\partial y} - (1-\mu) S \frac{\partial V_j^{\mathscr{E}_E,k}}{\partial X} \le 0, \tag{4.18}$$

where the maximum is achieved by $m(t) = k$ and $l(t) = 0$;

$$\frac{\partial V_j^{\mathscr{E}_E,k}}{\partial y} - (1+\lambda) S \frac{\partial V_j^{\mathscr{E}_E,k}}{\partial X} \le 0, \quad \frac{\partial V_j^{\mathscr{E}_E,k}}{\partial y} - (1-\mu) S \frac{\partial V_j^{\mathscr{E}_E,k}}{\partial X} \ge 0, \tag{4.19}$$

where the maximum is achieved by $m(t) = 0$ and $l(t) = 0$ (do nothing).

The rest of the casuistics for the inequalities are impossible since the value functions are strictly increasing functions of X and y (Proposition 4.2.2). For example, if it holds that

$$\frac{\partial V_j^{\mathscr{E}_E,k}}{\partial y} - (1+\lambda)S\frac{\partial V_j^{\mathscr{E}_E,k}}{\partial X} \geq 0, \quad \frac{\partial V_j^{\mathscr{E}_E,k}}{\partial y} - (1-\mu)S\frac{\partial V_j^{\mathscr{E}_E,k}}{\partial X} \leq 0,$$

and since $S, \lambda \geq 0$ and $\mu \in [0,1)$, this implies that

$$(1+\lambda)S\frac{\partial V_j^{\mathscr{E}_E,k}}{\partial X} \leq (1-\mu)S\frac{\partial V_j^{\mathscr{E}_E,k}}{\partial X} \Rightarrow \frac{\partial V_j^{\mathscr{E}_E,k}}{\partial X} \leq 0,$$

which is a contradiction.

These results suggest that the optimization problem is a free boundary problem where, if the value function is known in the four dimensions (t, X, y, S), the optimal trading strategy is determined by the previous inequalities.

We conjecture, as in [22], that the space is divided in three regions, The Buying Region (**BR**), The Selling Region (**SR**) and The No Transactions Region (**NT**). The Buying and Selling regions do not intersect since it is not optimal to buy and sell shares at the same time.

Definition 4.2.7. *The frontiers between the No Transactions Region and the Buying/Selling Regions will be respectively denoted by* $y_j^{\mathscr{B}}$ *and* $y_j^{\mathscr{S}}$, $j \in \{1, w\}$.

As $k \to \infty$, the class of admissible strategies approaches to the one given in Definition 4.2.6. Therefore, $V_j^{\mathscr{E}_E,k}$, $j \in \{1, w\}$ converges to $V_j^{\mathscr{E}_E} = V_j$ assuming that $E > E_0$, E_0 big enough.

Complementary to the previous assertion that the value of $E > E_0$ does not affect the function value, Davis et al. conjecture that the buying/selling frontiers of functions $V_j^{\mathscr{E}_E}$ do not depend on the particular choice of $E > E_0$.

The optimal trading strategy is always to immediately buy/sell shares until reaching the corresponding frontier if we are located inside the **BR**/**SR** respectively.

When we respectively approximate the Buying (respectively Selling) frontiers from the Buying (respectively Selling) regions, the limit argument employed in [22] leads to the following equations:

$$\begin{cases} \dfrac{\partial V_j}{\partial y} - (1+\lambda)S\dfrac{\partial V_j}{\partial X} = 0, & (t,X,y,S) \in \mathbf{BR}, \\ \dfrac{\partial V_j}{\partial y} - (1-\mu)S\dfrac{\partial V_j}{\partial X} = 0, & (t,X,y,S) \in \mathbf{SR}, \\ \dfrac{\partial V_j}{\partial t} + rX\dfrac{\partial V_j}{\partial X} + \alpha S\dfrac{\partial V_j}{\partial S} + \dfrac{1}{2}\sigma^2 S^2\dfrac{\partial V_j}{\partial S^2} = 0, & (t,X,y,S) \in \mathbf{NT}, \end{cases} \tag{4.20}$$

which can be written in the form:

$$\begin{aligned}\max\Bigg\{&\frac{\partial V_j}{\partial y}-(1+\lambda)S\frac{\partial V_j}{\partial X},-\left(\frac{\partial V_j}{\partial y}-(1-\mu)S\frac{\partial V_j}{\partial X}\right),\\&\frac{\partial V_j}{\partial t}+rX\frac{\partial V_j}{\partial X}+\alpha S\frac{\partial V_j}{\partial S}+\frac{1}{2}\sigma^2S^2\frac{\partial V_j}{\partial S^2}\Bigg\}=0,\end{aligned}\tag{4.21}$$

where $(t,X,y,S)\in[0,T]\times\mathbb{R}\times\mathbb{R}\times\mathbb{R}^+$.

In the rest of the Chapter, we will use the following Utility function.

Definition 4.2.8. *Let $U(x)$ be the Exponential Utility function*

$$U(x)=1-\exp(-\gamma x).\tag{4.22}$$

Note that $\gamma=-\frac{U''(x)}{U'(x)}$, the index of risk aversion, is independent of the investor's wealth.

Under the Exponential Utility, the value function given in (4.13) can be rewritten as:

$$\begin{aligned}V_j(t,X,y,S)&=\sup_{\pi\in\tau(X,y)}\mathbb{E}\left\{U(W_j(T,X^\pi(T),y^\pi(T),\bar{S}(T)))\right\}\\&=1-\inf_{\pi\in\tau(X,y)}\mathbb{E}\left\{\exp(-\gamma W_j)\right\}\\&=1-\inf_{\pi\in\tau(X,y)}\mathbb{E}\left\{\exp(-\gamma X^\pi(T))\exp(-\gamma(W_j-X^\pi(T))\right\},\end{aligned}\tag{4.23}$$

where:

$$W_j-X^\pi(T)=\begin{cases}c(y(T),S(T)), & j=1,\\ I_{S(T)<K}c(y(T),S(T))+I_{S(T)\geq K}\left[c(y(T)-1,S(T))+K\right], & j=w.\end{cases}\tag{4.24}$$

On the other hand (see [22]), $X^\pi(T)$ is given by the following integral version of the state equation (4.11):

$$\bar{X}(T)=\frac{X}{\delta(T,t)}-\int_t^T\frac{(1+\lambda)\bar{S}(t)}{\delta(T,t)}dL(t)+\int_t^T\frac{(1-\mu)\bar{S}(t)}{\delta(T,t)}dM(t),$$

where, for homogeneity with the notation in [22], $\delta(T,t)$ is the discount factor:

$$\delta(T,t)=\exp(-r(T-t)).\tag{4.25}$$

Therefore, we can write the value functions as:

$$V_j(t,X,y,S)=1-\exp\left(-\gamma\frac{X}{\delta(T,t)}\right)Q_j(t,y,S),\tag{4.26}$$

where $Q_j(t,y,S)$ is a convex nonincreasing continuous function in y and S given by

$$Q_j(t,y,S)=1-V_j(t,0,y,S).\tag{4.27}$$

Remark 4.2.4. This result has a very important interpretation: "The amount invested in the risky asset is independent of the total wealth."

The indifferent price $p_w(X,t,S)$ was introduced in Definition 4.2.3 as:

$$V_1(t,X,0,S) = V_w(t,X+p_w(X,t,S),0,S), \tag{4.28}$$

which leads to

$$1-\exp\left(-\gamma\frac{X}{\delta(T,t)}\right)Q_1(t,0,S) = 1-\exp\left(-\gamma\frac{X+p_w(X,t,S)}{\delta(T,t)}\right)Q_w(t,0,S).$$

The indifferent price is explicitly computable:

$$p_w(X,t,S) = \frac{\delta(T,t)}{\gamma}\log\left(\frac{Q_w(t,0,S)}{Q_1(t,0,S)}\right). \tag{4.29}$$

We remark that it is independent of the initial wealth $p_w(X,t,S) = p_w(t,S)$.

Substituting the value V_j into the partial differential equation, we obtain:

$$\min\left\{\frac{\partial Q_j}{\partial y}+\frac{\gamma(1+\lambda)S}{\delta(T,t)}Q_j, -\left(\frac{\partial Q_j}{\partial y}+\frac{\gamma(1-\mu)S}{\delta(T,t)}Q_j\right), \frac{\partial Q_j}{\partial t}+\alpha S\frac{\partial Q_j}{\partial S}+\frac{1}{2}\sigma^2S^2\frac{\partial Q_j}{\partial S^2}\right\} = 0, \tag{4.30}$$

defined in $[0,T]\times\mathbb{R}\times\mathbb{R}^+$. The terminal conditions are given by:

$$Q_1(T,y,S) = \exp(-\gamma c(y,S)), \tag{4.31}$$

and

$$Q_w(T,y,S) = \exp\left(-\gamma\left(I_{(S<K)}c(y,S)+I_{(S\geq K)}\left[c(y-1,S)+K\right]\right)\right). \tag{4.32}$$

If the value of functions $Q_j,\ j\in\{1,w\}$ is known when the functions lay inside the No Transactions Region and we know the location of the Buying/Selling frontiers for each value of S, we can employ two equations from (4.30) in order to obtain its explicit value in these regions. In the Buying region:

$$Q_j(t,y,S) = Q_j(t,y_j^{\mathscr{B}}(t,S),S)\exp\left(-\frac{\gamma(1+\lambda)S}{\delta(T,t)}(y-y_j^{\mathscr{B}}(t,S))\right),\quad y\leq y_j^{\mathscr{B}}(t,S), \tag{4.33}$$

and in the Selling region:

$$Q_j(t,y,S) = Q_j(t,y_j^{\mathscr{S}}(t,S),S)\exp\left(\frac{\gamma(1-\mu)S}{\delta(T,t)}(y_j^{\mathscr{S}}(t,S)-y)\right),\quad y\geq y_j^{\mathscr{S}}(t,S). \tag{4.34}$$

Therefore, the problem is reduced to solve equation (4.30) subject to the maturity conditions (4.31)-(4.32), computing the function value in the No Transactions region and finding the location of the frontiers.

To finish this Subsection, we mention (see [22] and [42]) that when no transaction costs are present ($\lambda = \mu = 0$) and there are no budget constraints (E arbitrary big), the problem is explicitly solvable. In this case, we denote the value function by $\mathbb{Q}_j,\ j \in \{1, w\}$. For $j = 1$ we have:

$$\begin{aligned} y_1^{\mathscr{B}}(t,S) = y_1^{\mathscr{S}}(t,S) &= \frac{\delta(T,t)}{\gamma S}\frac{\alpha - r}{\sigma^2}, \\ \mathbb{Q}_1(t,y,S) &= \exp\left(-\frac{(\alpha-r)^2}{2\sigma^2}(T-t)\right)\exp\left(-\frac{\gamma y S}{\delta(T,t)}\right). \end{aligned} \tag{4.35}$$

For $j = w$, the value function and the optimal trading strategy can be obtained from the results of Theorem 4.2.1 employing first formulas (4.29), (4.35) and then formula (4.33):

$$\begin{aligned} y_w^{\mathscr{B}}(t,S) = y_w^{\mathscr{S}}(t,S) &= \frac{\delta(T,t)}{\gamma S}\frac{\alpha - r}{\sigma^2} + \frac{\partial \mathscr{C}(t,T;S)}{\partial S}, \\ \mathbb{Q}_w(t,y,S) &= \exp\left(-\frac{(\alpha-r)^2}{2\sigma^2}(T-t)\right)\exp\left(-\frac{\gamma}{\delta(T,t)}\left[yS - \mathscr{C}(t,T;S)\right]\right), \end{aligned} \tag{4.36}$$

where $\mathscr{C}(t,T;S)$ and $\frac{\partial \mathscr{C}(t,T;S)}{\partial S}$ respectively denote the price and the Delta of the European Option.

Remark 4.2.5. We point out that if $\alpha > r$, the previous formulas imply that, when there are no transaction costs, $y_j^{\mathscr{B}}(t,S) > 0,\ j \in \{1, w\}$, i.e., shortselling is always a suboptimal strategy.

Numerical experiments (see Subsection 4.4.2) suggest that this also holds when transaction cost appear.

We also note that in the previous formulas, $y_w^{\mathscr{B}}(t,S)$ has a jump discontinuity at $t = T$.

4.2.3 Existence and uniqueness of the solution. Comments about constraint $\mathscr{E}_E$

In this Subsection, we present all the results included in [22] that characterise the value functions $V_j^{\mathscr{E}_E},\ j \in \{1, w\}$ given by (4.13) as weak (viscosity) solutions of the variational inequality (4.21). The proofs can be found in [22] and in [62].

The notion of viscosity solutions was introduced by Crandall and Lions [18]. We also refer to [19] and [44]. The notion of constrained viscosity solution was introduced by Soner [57] and by Capuzzo-Dolcetta and Lions [11]. Some technical results employed can be found in [37] and [43].

Definition 4.2.9. *Let*

$$F(Z, \Theta, D\Theta, D^2\Theta) = 0, \quad [0,T] \times \mathscr{E}, \tag{4.37}$$

be a nonlinear second order p.d.e. where $\mathscr{E} \subseteq \mathbb{R}^3$ is an open set and such that

$$F(Z,p,q,A+N) \leqq F(Z,p,q,A) \quad \textit{if} \quad N \geqq 0.$$

A continuous function $\Theta : [0,T] \times \bar{\mathscr{E}} \to \mathbb{R}$ is a constrained viscosity solution of (4.37) if:

1. *Θ is a viscosity subsolution of (4.37) in $[0,T]\times\bar{\mathscr{E}}\to\mathbb{R}$, i.e., $\forall\phi\in\mathcal{C}^{1,2}([0,T]\times\bar{\mathscr{E}})$ and for any local maximum point $Z_0\in[0,T]\times\bar{\mathscr{E}}$ of $\Theta-\phi$ we have that:*

$$F(Z_0,\Theta(Z_0),D\phi(Z_0),D^2\phi(Z_0))\leqq 0.$$

2. *Θ is a viscosity supersolution of (4.37) in $[0,T]\times\mathscr{E}\to\mathbb{R}$, i.e., $\forall\phi\in\mathcal{C}^{1,2}([0,T]\times\bar{\mathscr{E}})$ and for any local minimum point $Z_0\in[0,T]\times\mathscr{E}$ of $\Theta-\phi$ we have that:*

$$F(Z_0,\Theta(Z_0),D\phi(Z_0),D^2\phi(Z_0))\geqq 0.$$

The notion of constrained viscosity solution has some technical difficulties when we have to deal with the boundary of the domain. The complete development of the results included in the references mentioned at the beginning of this Subsection is too extensive to be included. Nevertheless, we make a summary of the key concepts that are employed in the results presented in [22].

In order to prove that the function value is a constrained viscosity solution, we need to prove that it can be extended continuously to the frontier when needed, so that, the standard arguments (see [57] or [37]) can be employed.

The are also some difficulties in the uniqueness result. The proof relies in a technique presented in [37], which we sketch without entering into the details. Suppose that u_1 and u_2 are respectively sub and super solutions of $F=0$ in an open set Ω. Suppose also that $u_1\leq u_2$ in $\partial\Omega$ and that we can find a perturbed supersolution $u_2^\epsilon=\epsilon u_2+(1-\epsilon)h$ such that for any $\epsilon\in(0,1)$ it holds that $u_1\leq u_2^\epsilon$ in $\partial\Omega$ and u_2^ϵ is a supersolution of $F=0$ and of $F-(1-\epsilon)g=0$ with $g>0$. Then it can be proved, with limit arguments, that $u_1\leq u_2$ in $\bar{\Omega}$.

The value function $V_j^{\mathscr{E}_E}(t,X,y,S),\ j\in 1,w$ given in (4.13) is continuous in $[0,T]\times\mathscr{E}_E$ (see [22]) and can be extended continuously to be defined in $[0,T]\times\bar{\mathscr{E}}$. We note that the function value is already defined in $t=0$ and $t=T$. Furthermore, it can be explicitly computed for $t=T$ and/or $S=0$ (the money is only in the bank account).

On the other side, with the particular choice of the Exponential Utility, the value function $V_j^{\mathscr{E}_E}(t,X,y,S)$ defined in (4.13) is upper bounded for positive wealth (see (4.22)) and lower bounded for negative wealth (see Proposition 4.2.3 below). For $t\in[0,T)$, the frontier defined by $\mathscr{E}_E$ is reached only for negative wealth and the strictly increasing property in y and x allows to extend the function continuously in the remaining frontier.

In order to prove that $V_j^{\mathscr{E}_E}(t,X,y,S)$ is the only constrained viscosity solution, Davis et al. prove that if u is a constrained viscosity solution such that u is upper and lower bounded and

$$u(t,X,y,0)=V_j^{\mathscr{E}_E}(t,X,y,0),\quad u(T,X,y,S)=V_j^{\mathscr{E}_E}(T,X,y,S),$$

which are explicitly computable, then it holds $u(t,X,y,S)=V_j^{\mathscr{E}_E}(t,X,y,S),\ (t,X,y,S)\in[0,T]\times\bar{\mathscr{E}}_E$.

The arguments employed by Davis et al. are based in the technique of [37] previously described. If u_1 and u_2 are respectively (bounded) sub and supersolutions of our problem

and $u_1 \leq u_2$ for $S = 0$ and/or $t = T$, then $u_1 \leq u_2$ in $[0,T] \times \bar{\mathscr{E}}_E$. The proof relies in the construction of the perturbed solution $u_2^\epsilon = \epsilon u_2 + (1-\epsilon)h$ where h is explicitly given and u_2^ϵ is a supersolution of $F = 0$ and $F - (1-\epsilon)g = 0$ with $g > 0$.

We remark that the hypothesis of bounded functions is essential to define h and the reason why $\mathscr{E}_E$ was introduced. The following results can be found in [22].

Theorem 4.2.2. *For any $(t_0, X_0, y_0, S_0) \in [0,T] \times \bar{\mathscr{E}}_E$ it exists an optimal trading strategy which solves $V_j^{\bar{\mathscr{E}}_E}$, $j \in \{1, w\}$.*

Theorem 4.2.3. *The value function $V_j^{\bar{\mathscr{E}}_E}(s, X, y, S)$ is a constrained viscosity solution of*

$$\begin{aligned} \min \Bigg\{ &- \left(\frac{\partial \Theta}{\partial y} - (1+\lambda) S \frac{\partial \Theta}{\partial X} \right), \left(\frac{\partial \Theta}{\partial y} - (1-\mu) S \frac{\partial \Theta}{\partial X} \right), \\ &- \left(\frac{\partial \Theta}{\partial s} + rX \frac{\partial \Theta}{\partial X} + \alpha S \frac{\partial \Theta}{\partial S} + \frac{1}{2} \sigma^2 S^2 \frac{\partial^2 \Theta}{\partial S^2} \right) \Bigg\} = 0 \end{aligned} \tag{4.38}$$

in $[0,T] \times \bar{\mathscr{E}}_E$

Theorem 4.2.4. *Let u be a bounded upper semicontinuous viscosity subsolution of (4.38) on $[0,T] \times \bar{\mathscr{E}}_E$, and let v be a bounded from below lower semicontinuous viscosity supersolution of (4.38) on $[0,T] \times \bar{\mathscr{E}}_E$ such that:*

(i) $u(t, X, y, 0) \leqq v(t, X, y, 0)$ *on* $[0,T] \times \bar{\mathscr{E}}_E$,

(ii) $u(T, z) \leqq v(T, z)$, $\forall z \in \bar{\mathscr{E}}_E$,

where $u(t, X, y, 0) = 1 - \exp(-\gamma X)$ and $u(T, z) = 1 - \exp(-\gamma(X + c(y, S)))$.

Then $u \leqq v$ on $[0,T] \times \bar{\mathscr{E}}_E$.

Comments about constraint $\mathscr{E}_E$.

Constraint $\mathscr{E}_E$ has been employed, as we have seen, to prove the existence and uniqueness of the variational inequalities that characterize the value functions $V_j^{\mathscr{E}_E}(t, X, y, S)$ when $(t, X, y, S) \in [0,T] \times \mathscr{E}_E$.

In [22] it was argued that this constraint is needed just for technical reasons and that it does not affect the value functions (for E big enough) because it only ruled out suboptimal strategies.

When we numerically solve the problem, for a fixed initial position and a bound $E = E_0 > 0$ big enough, whether we are in a scenario with or without transaction costs, the results suggest that the option price/value functions do not change for $E > E_0$ (or that the values quickly converge to a certain value as $E \to \infty$).

We are going to prove that (at least punctually) the stochastic control problem converges as $E \to \infty$ for any fixed initial position $(t_0, X_{t_0}, y_{t_0}, S_{t_0})$.

We introduce the following value functions.

Definition 4.2.10. *Let $\mathbb{V}_j^{\mathscr{E}_E},\ j \in \{1, w\}$ denote the value functions (4.13) when there are no transaction costs present ($\lambda = \mu = 0$).*

Let also $\mathbb{V}_j,\ j \in \{1, w\}$ denote the value function when there are no transaction costs and E can be arbitrary big, i.e. .

$$\mathbb{V}_j(t, X, y, S) = 1 - \exp\left(-\gamma \frac{X}{\delta(T,t)}\right) \mathbb{Q}_j(t, y, S), \quad j \in \{1, w\}, \tag{4.39}$$

where functions $\mathbb{Q}_j,\ j \in \{1, w\}$ are given in (4.35) and (4.36).

Consider a fixed initial position $(t_0, X_{t_0}, y_{t_0}, S_{t_0})$ and let $N_0 = N_0(t_0, X_{t_0}, y_{t_0}, S_{t_0}) \in \mathbb{N}$ be such that

$$\max\left\{(X_{t_0} + c(y_{t_0}, S_{t_0}))\, e^{r(T-t_0)}, (X_{t_0} + c(y_{t_0} - 1, S_{t_0}))\, e^{r(T-t_0)}\right\} > -N_0. \tag{4.40}$$

Remark 4.2.6. For $N \geq N_0$, the (suboptimal) trading strategies

(a) $y^\pi(t) = 0, \quad t \in (t_0, T)$ if $j = 1$ (no option was sold).

(b) $y^\pi(t) = 1, \quad t \in (t_0, T)$ if $j = w$ (one option was sold).

are both admissible in $\tau_{N_0}(X_0, y_0)$ because they limit our losses by less than $-N_0$ for $t \in [t_0, T]$.

Therefore, for $(t_0, X_{t_0}, y_{t_0}, S_{t_0})$ we have explicitly found an admissible strategy for $N \geq N_0$ and, by a suboptimality argument, all the value functions $V_j^{\mathscr{E}_N},\ \mathbb{V}_j^{\mathscr{E}_N},\ V_j,\ \mathbb{V}_j,\ j \in \{1, w\}$ will be lower bounded at point $(t_0, X_{t_0}, y_{t_0}, S_{t_0})$ by

$$1 - \exp(\gamma N_0).$$

Lemma 4.2.1. *For any $N, N' \in \mathbb{N}$ such that $N_0 \leq N < N'$ it holds for $j \in \{1, w\}$ that*

$$\begin{cases} V_j^{\mathscr{E}_N}(t_0, X_{t_0}, y_{t_0}, S_{t_0}) \leq V_j^{\mathscr{E}_{N'}}(t_0, X_{t_0}, y_{t_0}, S_{t_0}), \\ \mathbb{V}_j^{\mathscr{E}_N}(t_0, X_{t_0}, y_{t_0}, S_{t_0}) \leq \mathbb{V}_j^{\mathscr{E}_{N'}}(t_0, X_{t_0}, y_{t_0}, S_{t_0}). \end{cases}$$

Proof. Since all the admissible trading strategies in $\tau_N(X, y)$ are included in $\tau_{N'}(X, y)$,

$$\tau_N(X, y) \subset \tau_{N'}(X, y),$$

the result of the maximization problem will always be equal or better. □

Corollary 4.2.1. *The previous result also implies that*

$$\mathbb{V}_j^{\mathscr{E}_N}(t_0, X_{t_0}, y_{t_0}, S_{t_0}) \leq \mathbb{V}_j(t_0, X_{t_0}, y_{t_0}, S_{t_0}), \quad j \in \{1, w\}.$$

because for the stochastic control problem $\mathbb{V}_j,\ j \in \{1, w\}$ there are no constraints upon the set of optimal trading strategies.

We also remark that $\mathbb{V}_j(t_0, X_{t_0}, y_{t_0}, S_{t_0}) < \infty,\ j \in \{1, w\}$ since we already know that, when there are no transaction costs, the problem has a solution which is explicitly computable.

Lemma 4.2.2. *For any $N > N_0$ it holds that*

$$V_j^{\mathscr{E}_N}(t_0, X_{t_0}, y_{t_0}, S_{t_0}) \leq \mathbb{V}_j^{\mathscr{E}_N}(t_0, X_{t_0}, y_{t_0}, S_{t_0}).$$

Proof. This result is derived from the fact that the effect of transaction costs is to decrease by $\Delta y(\lambda S)$ or by $\Delta y(\mu S)$ our total wealth each time a transaction Δy is realized.

Consider the optimal trading strategy π^o obtained for the case where transaction costs ($\lambda = \lambda_0 \geq 0,\ \mu = \mu_0 \geq 0$) are present.

For the case where there are no transaction costs, consider the (suboptimal) trading strategy which consist in, each time a transaction is performed, retain $\Delta y(\lambda_0 S)$ or $\Delta y(\mu_0 S)$ in the bank account until maturity while we independently follow π^o with the rest of the money and assets.

The proof ends using the same argument of Proposition 4.2.1. □

We note that for any value $E > 0$, we can always find $N \in \mathbb{N}$, $N > E$ which implies that $\tau_E(X, y) \subset \tau_N(X, y)$. The argument finishes constructing and increasing and upper bounded sequence.

Proposition 4.2.3. *For $j \in \{1, w\}$, we have that*

$$\lim_{N \to \infty} V_j^{\mathscr{E}_N}(t_0, X_{t_0}, y_{t_0}, S_{t_0}) < \infty. \tag{4.41}$$

Proof. By the previous results, for $N \geq N_0$, it holds that

$$\begin{aligned} 1 - \exp(\gamma N_0) &\leq V_j^{\mathscr{E}_N}(t_0, X_{t_0}, y_{t_0}, S_{t_0}) \leq V_j^{\mathscr{E}_{N'}}(t_0, X_{t_0}, y_{t_0}, S_{t_0}) \\ &\leq \mathbb{V}_j^{\mathscr{E}_{N'}}(t_0, X_{t_0}, y_{t_0}, S_{t_0}) \leq \mathbb{V}_j(t_0, X_{t_0}, y_{t_0}, S_{t_0}) < \infty. \end{aligned}$$

where $N' > N$.

Consider the sequence

$$\left\{ V_j^{\mathscr{E}_N}(t_0, X_{t_0}, y_{t_0}, S_{t_0}) \right\}_{N=N_0}^{\infty},$$

which is increasing and bounded above. Therefore, it has a limit. □

The previous Proposition implies that the value of function $V_j^{\mathscr{E}_E}$ converges, at least punctually, as E tends to ∞.

4.2.4 Restatement of the problem: Bankruptcy state

A priori, the model is not linear in the relation $\frac{S}{K}$, so we cannot use the technique employed in Chapter 1 of fixing the strike $K = 1$ and a domain $S \in [S_{\min}, S_{\max}]$, solving the problem there and computing the option price for other values of S/K by interpolation. The problem has to be solved for each strike K and each stock price S.

Furthermore, the model is not linear in the number of European Options sold. If we negotiate n options instead of one, we have to compute, for $y = 0$ and $S > K$:

$$Q_w(T, 0, S) = \exp\left(\gamma n \left[(1+\lambda)S - K\right]\right),$$

which grows very fast.

Market data may take big values. For example, in Chapter 1, the index S&P (around 350 points) negotiates options with strike $K = 300$. This means that we have to work with values equivalent to exp(50). Therefore, there is a scaling problem that must be handled.

When an European option is signed (or other derivative), the market (Clearing House), acts as a central counterparty which mediates between the seller and the buyer of the option. Furthermore, the market demands some type of guaranty to the seller of the option.

Let $t \in [0, T]$ and suppose that the European option has been signed at time $t = 0$ and expires at $t = T$. The objective of the guaranty is to ensure that, at any moment $0 \leq t \leq T$, the seller of the option can afford all the potential loses that he might have incurred between $[0, t]$, even if the option cannot be exercised prior to time T.

This guaranty can take different forms like money or other stocks or goods. Formally, the seller of the option may not have to give anything out while he is solvent (he does not need to alter his investment strategies), but the Clearing House can confiscate the guaranty and expel the seller of the option from the market if he goes into theoretical bankruptcy at any time $t \in [0, T]$ (see, for example, [5]).

Simplifying the situation, the constraint $\mathscr{E}_E$ could be understood as a bankruptcy constraint. We allow any trading strategy to the seller of the option, but, if at any time t his strategy has led him out outside $\mathscr{E}_E$, he is automatically expelled from the market (not allowing him to return) and he remains with a residual bankruptcy utility forever.

Retaining the previous definitions, we introduce two new value functions.

Definition 4.2.11. *Let $E > 0$. For $t \in [0, T]$ and $j \in \{1, w\}$, we define the value functions*

$$V_j^{B_E}(t,X,y,S) = \begin{cases} \sup\limits_{\pi \in \tau(X,y)} \mathbb{E}\left\{ U(W_j(T, X^\pi(T), y^\pi(T), S(T)))| \left(\bar{X}(t), \bar{y}(t), \bar{S}(t)\right) = (X, y, S)\right\}, & (X, y, S) \in \mathscr{E}_E, \\ 1 - \exp(\gamma E), & (X, y, S) \notin \mathscr{E}_E, \end{cases} \tag{4.42}$$

where $\tau(X, y)$ denotes that we allow any trading strategy.

These new value functions are defined in $[0, T] \times \mathbb{R} \times \mathbb{R} \times \mathbb{R}^+$ and they do not alter the model thanks to the following result.

Proposition 4.2.4. *If $(t, X, y, S) \in [0, T] \times \mathscr{E}_E$, it holds that*

$$V_j^{B_E}(t, X, y, S) = V_j^{\mathscr{E}_E}(t, X, y, S).$$

Proof. By the definition of $\mathscr{E}_E$, we knew that the trading strategies

$$\begin{cases} y^{\pi^s} \equiv 0, & j = 1, \\ y^{\pi^s} \equiv 1, & j = w, \end{cases}$$

where admissible in $\tau_E(X, y)$, so they are in $\tau(X, y)$. Under these strategies, the final wealth satisfies

$$W_j((T, X^{\pi^s}(T), y^{\pi^s}(T), \bar{S}(T)) > -E, \quad j \in \{1, w\}.$$

Any trading strategy $\pi \in \tau$ that lies outside $\mathscr{E}_E$ for any $t \in [0, T]$, leads automatically to the residual utility $1 - \exp(\gamma E)$, which is always suboptimal.

Therefore, the optimal trading strategy must belong to $\tau_E(X, y)$. Consequently,

$$V_j^{B_E}(t, X, y, S) = V_j^{\mathscr{E}_E}(t, X, y, S).$$

□

Proposition 4.2.5. *The functions $V_j^{B_E}$, $j \in \{1, w\}$ satisfy for $t \in [0, T]$ that:*

$$\begin{aligned} V_j^{B_E}(t, X, y, S) &\geq 1 - \exp(\gamma E), \quad (X, y, S) \in \mathscr{E}_E, \\ V_j^{B_E}(t, X, y, S) &= 1 - \exp(\gamma E), \quad (X, y, S) \notin \mathscr{E}_E, \end{aligned}$$

Proof. The first inequality is obtained by a suboptimality argument employing strategy π^s of the previous proof and the second one comes from the definition of function $V_j^{B_E}$, $j \in \{1, w\}$. □

Thanks to Proposition 4.2.4, we inherit all the existence and uniqueness results of the original development of the model in [22]. For the shake of completeness, we present now the two differences with the original development of the model.

Proposition 4.2.6. *Functions $V_j^{B_E}$, $j \in \{1, w\}$ are not decreasing functions of X and y.*

Proof. In $[0, T] \times \mathscr{E}_E$, functions $V_j^{B_E}$ match with functions $V_j^{\mathscr{E}_E}$, which are strictly growing functions of X and y (see Proposition 4.2.2).

Outside that domain, functions $V_j^{B_E}$ are constant and smaller than the function values of any point which belongs to $[0, T] \times \mathscr{E}_E$.

Due to the definition of $\mathscr{E}_E$, for any fixed (t_0, y_0, S_0), it exists X_0 such that

$$\begin{cases} (t_0, X, y_0, S_0) \in [0, T] \times \mathscr{E}_E, & X > X_0, \\ (t_0, X, y_0, S_0) \notin [0, T] \times \mathscr{E}_E, & X \leq X_0, \end{cases}$$

and a similar argument can be obtained for y and any fixed (t_0, X_0, S_0). Therefore, the value functions are constant or strictly growing functions of X and y. □

In Subsection 4.2.2, we gave the possible optimal trading strategies, see equations (4.17)-(4.19), that were obtained in [22]. There were only three possibilities (Buying/Selling/No Transactions) thanks to the strictly growing property of functions $V_j^{\mathscr{E}_E},\ j \in \{1, w\}$.

Now, due to the non-decreasing property of functions $V_j^{B_E},\ j \in \{1, w\}$, a fourth case appears:

$$\frac{\partial V_j^k}{\partial y} - (1+\lambda) S \frac{\partial V_j^k}{\partial X} = 0, \quad \frac{\partial V_j^k}{\partial y} - (1-\mu) S \frac{\partial V_j^k}{\partial X} = 0, \tag{4.43}$$

which corresponds to the Bankruptcy state. Since in this case, the investor has been expelled from the market, no trading strategy has to be obtained.

Similar to the model presented in [22], we are interested in the limit value of the functions when $E \to \infty$. Again, thanks to Proposition 4.2.4, we inherit the results presented in Subsection 4.2.3.

Since the option price is independent of the initial wealth, we will work numerically with a function $Q_j(t, y, S)$ derived by formula (4.26) from $V_j = V_j^{\mathscr{E}_E} = V_j^{B_E},\ j \in \{1, w\}$, when E is considered big enough.

Retaining the definitions from Subsection 4.2.2, let us fix $X = X_0$. We apply formula (4.26) to functions $V_j^{B_E}$ in order to obtain functions that we will denote by $Q_j^{B_{E,X_0}}$.

It is clear that $Q_j = Q_j^{\mathscr{E}_{E,X_0}} = Q_j^{B_{E,X_0}},\ j \in \{1, w\}$ when E is considered big enough.

For finishing this Subsection, we give the following result.

Proposition 4.2.7. *For $X = X_0$ and $E = E_0$ fixed, it exists $M = M(X_0, E_0) \geq 0$ such that $\forall (t, y, S), \in [0, T] \times \mathbb{R} \times \mathbb{R}^+$ it holds*

$$0 < Q_j^{B_{E_0,X_0}} \leq M, \quad j \in \{1, w\}.$$

Proof. If we substitute formula (4.26) into formula (4.23) it directly implies that $Q_j^{B_{E_0,X_0}} > 0, \quad j \in \{1, w\}$.

The second statement is a consequence of formula (4.26) and Proposition 4.2.5. □

4.3 Numerical Method

In this Section we introduce two changes of variables that drastically reduce the impact of the exponential growth of functions $Q_j,\ j \in \{1, w\}$ and we propose a Fourier pseudospectral method to solve the partial differential equation that we will obtain.

The procedure is as follows: First, we perform two changes of variables and compute the corresponding variational inequality.

The second step is the localization of the problem. We fix a finite domain and perform an odd-even extension, imposing periodic boundary conditions.

Finally, we employ a Fourier Pseudospectral method to solve the partial differential equation. We will summarize all the steps in the numerical algorithm in Subsection 4.3.4

For finishing the Section, we will include a theoretical analysis of the stability and convergence of the numerical method as well as an analysis of the localization error.

4.3.1 Change of variables.

The following two changes of variables reduce the impact of the exponential growth.

We change the stock price to logarithmic scale.

$$\hat{x} = \log(S). \tag{4.44}$$

so that, variational inequality (4.30) is transformed into

$$\begin{aligned} \min \left\{ \frac{\partial Q_j}{\partial y} + \frac{\gamma(1+\lambda)\exp(\hat{x})}{\delta(T,t)} Q_j, - \left(\frac{\partial Q_j}{\partial y} + \frac{\gamma(1-\mu)(\hat{x})}{\delta(T,t)} Q_j \right), \right. \\ \left. \frac{\partial Q_j}{\partial t} + \left(\alpha - \frac{\sigma^2}{2} \right) \frac{\partial Q_j}{\partial \hat{x}} + \frac{1}{2}\sigma^2 \frac{\partial^2 Q_j}{\partial \hat{x}^2} \right\} = 0, \quad j \in \{1, w\}. \end{aligned} \tag{4.45}$$

The second stage consists in consider a new function $H_j(t, y, \hat{x})$ defined by:

$$H_j(t, y, \hat{x}) = \log\left(Q_j(t, y, \hat{x})\right), \quad j \in \{1, w\}, \tag{4.46}$$

which is admissible after Proposition 4.2.7.

In Figure 4.1 we plot the values of function $H_1(T, y, \hat{x})$ (left) and function $H_w(T, y, \hat{x})$ (right) for $\hat{x} \in [-5, 5]$, $y \in [0, 2]$, $\lambda = \mu = 0.002$, $\gamma = 1$ and log(Strike) $= 3$. The benefit of working with function $H_w(T, y, \hat{x})$ is that it takes much smaller values (absolute value) than function $Q_w(T, y, x) = \exp(H_w(T, y, \exp(\hat{x})))$.

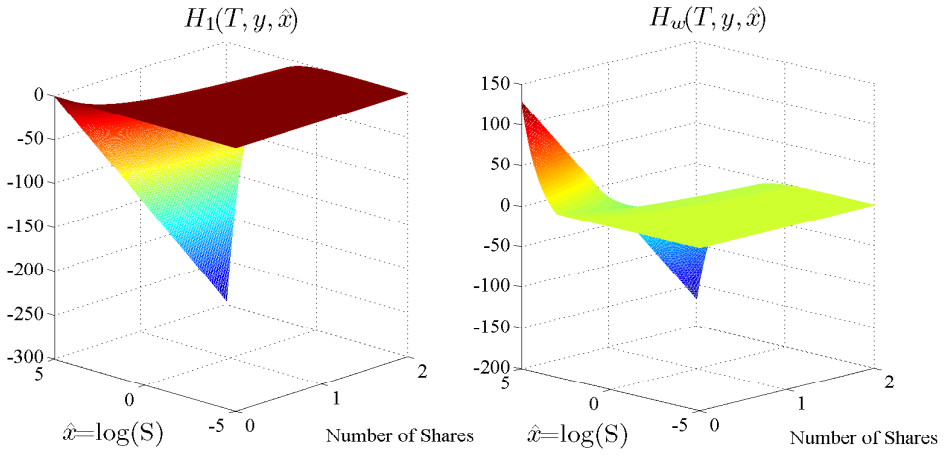

Figure 4.1: Graph of $H_1(T, y, \hat{x})$ (left) and $H_w(T, y, \hat{x})$ (right), $\hat{x} \in [-5, 5]$, $y \in [0, 2]$, $\lambda = \mu = 0.002$, $\gamma = 1$, log(Strike) $= 3$.

With the second change, the variational inequality (4.30) becomes

$$\begin{aligned}\min\Bigg\{&\frac{\partial H_j}{\partial y}+\frac{\gamma(1+\lambda)\exp(\hat{x})}{\delta(T,t)},\ -\left(\frac{\partial H_j}{\partial y}+\frac{\gamma(1-\mu)\exp(\hat{x})}{\delta(T,t)}\right),\\ &\frac{\partial H_j}{\partial t}+\left(\alpha-\frac{\sigma^2}{2}\right)\frac{\partial H_j}{\partial \hat{x}}+\frac{1}{2}\sigma^2\frac{\partial^2 H_j}{\partial \hat{x}^2}+\frac{1}{2}\sigma^2\left(\frac{\partial H_j}{\partial \hat{x}}\right)^2\Bigg\}=0,\quad j\in\{1,w\},\end{aligned}\tag{4.47}$$

subject to

$$H_1(T,y,\hat{x})=-\gamma c(y,\exp(\hat{x})),\tag{4.48}$$

and

$$H_w(T,y,\hat{x})=-\gamma\left(I_{(\exp(\hat{x})<K)}c(y,\exp(\hat{x}))+I_{(\exp(\hat{x})\geq K)}\left[c(y-1,\exp(\hat{x}))+K\right]\right).\tag{4.49}$$

If the value of functions $H_j,\ j\in\{1,w\}$ is known when $(t,y,\hat{x})\in\mathbb{R}\times\mathbb{R}\times\mathbb{R}^+$ lays inside the No Transactions Region and the location of the Buying/Selling frontiers is also known for each value of $(t,\hat{x})\in\mathbb{R}\times\mathbb{R}^+$, we can explicitly compute the value of the function in the other two regions. In the Buying region:

$$H_j(t,y,\hat{x})=H_j(t,y_j^{\mathscr{B}}(t,\hat{x}),\hat{x})+\left(-\frac{\gamma(1+\lambda)\exp(\hat{x})}{\delta(T,t)}(y-y_j^{\mathscr{B}}(t,\hat{x}))\right),\quad y\leq y_j^{\mathscr{B}}(t,\hat{x}),\tag{4.50}$$

and in the Selling region:

$$H_j(t,y,\hat{x})=H_j(t,y_j^{\mathscr{S}}(t,\hat{x}),\hat{x})+\left(\frac{\gamma(1-\mu)\exp(\hat{x})}{\delta(T,t)}(y_j^{\mathscr{S}}(t,\hat{x})-y)\right),\quad y\geq y_j^{\mathscr{S}}(t,\hat{x}),\tag{4.51}$$

Formulas (4.50) and (4.51) correspond to formulas (4.33) and (4.34) in the new variables.

Therefore, the problem is reduced to numerically solve equation

$$\frac{\partial H_j}{\partial t}+\left(\alpha-\frac{\sigma^2}{2}\right)\frac{\partial H_j}{\partial \hat{x}}+\frac{1}{2}\sigma^2\frac{\partial^2 H_j}{\partial \hat{x}^2}+\frac{1}{2}\sigma^2\left(\frac{\partial H_j}{\partial \hat{x}}\right)^2=0,\quad j\in\{1,w\},\tag{4.52}$$

subject to proper terminal conditions (see Subsection 4.3.2), computing the function value in the No Transactions region and finding the location of the frontiers.

It should be remarked that, although the exponential grow is still present, working in the logarithmic scale allows us to compute option prices very deep in the money and to use higher values for the stock and the strike.

4.3.2 Localization of the problem

Our objective is to implement a Fourier pseudospectral method. The procedure of the localization of the problem is similar to the one found in [9].

We denote by $[L_{\min}, L_{\max}] \subset \mathbb{R}$ the *approximation domain*, which is a finite interval such that it covers all the logarithmic stock prices in which we are interested to compute the function values.

We denote by $[\hat{x}_{\min}, \hat{x}_{\max}] \subset \mathbb{R}$ the *computational domain*, which is a finite interval such that $L_{\min} > \hat{x}_{\min}$ and $L_{\max} < \hat{x}_{\max}$.

The truncation of the domain that we are going to propose induces the so called localization error. This error is due to the extension of the function and the imposition of periodic boundary conditions, since the original function is not periodic.

In Subsection 4.3.5, we will prove that the localization error can be made arbitrary small in a fixed approximation domain $[L_{\min}, L_{\max}]$ taking the computational domain large enough.

Although periodic boundary conditions could be directly imposed, in order to avoid the Gibbs effect, it is better to perform first an odd-even extension and then impose periodic conditions. We define $H_j^e(t, y, \hat{x}),\ j \in \{1, w\}$ by:

$$
\begin{array}{ll}
H_j(t, y, \hat{x}), & \text{if } \hat{x} \in [\hat{x}_{\min}, \hat{x}_{\max}], \\
2H_j(t, y, \hat{x}_{\max}) - H_j(t, y, 2\hat{x}_{\max} - \hat{x}), & \text{if } \hat{x} \in [\hat{x}_{\max}, 2\hat{x}_{\max} - \hat{x}_{\min}], \\
H_j^e(t, y, (4\hat{x}_{\max} - 2\hat{x}_{\min}) - \hat{x}), & \text{if } \hat{x} \in [2\hat{x}_{\max} - \hat{x}_{\min}, 4\hat{x}_{\max} - 3\hat{x}_{\min}], \\
H_j^e(t, y, z), \quad \begin{cases} \hat{x} = z + \hat{x}_{\min} + k(4\hat{x}_{\max} - 4\hat{x}_{\min}) \\ z \in [\hat{x}_{\min}, 4\hat{x}_{\max} - 3\hat{x}_{\min}],\ k \in \mathbb{Z} \end{cases} & \text{if } \hat{x} \notin [\hat{x}_{\min}, 4\hat{x}_{\max} - 3\hat{x}_{\min}].
\end{array}
\tag{4.53}
$$

In Figure 4.2 we plot function $H_1^e(T, y, \hat{x})$ (left) and function $H_w^e(T, y, \hat{x})$ (right) for $\hat{x} \in [-5, 35]$, $y \in [0, 2]$, $\lambda = \mu = 0.002$, $\gamma = 1$ and log(Strike) $= 3$. Functions $H_j^e(T, y, \hat{x}),\ j \in \{1, w\}$ correspond to those of Figure 4.1 after the odd-even extension defined by (4.53).

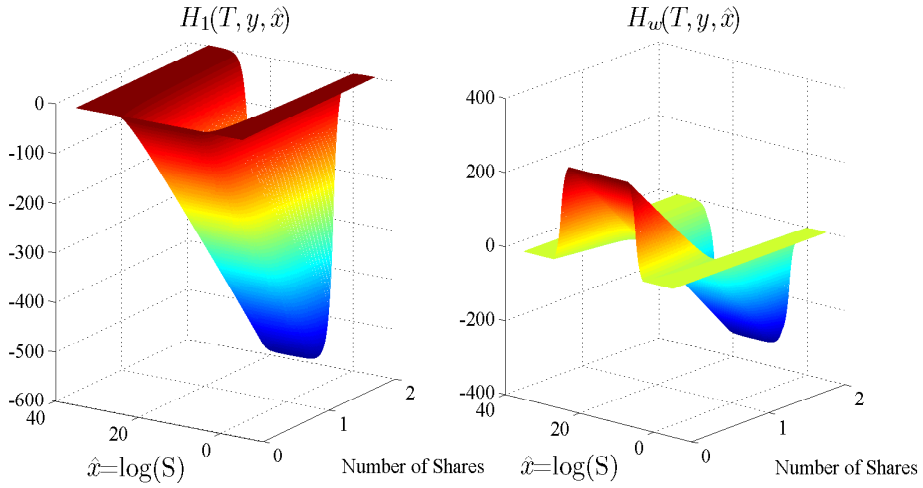

Figure 4.2: Graph of $H_1^e(T, y, \hat{x})$ (left) and $H_w^e(T, y, \hat{x})$ (right), $\hat{x} \in [-5, 35]$, $y \in [0, 2]$, $\lambda = \mu = 0.002$, $\gamma = 1$, log(Strike) $= 3$.

Fix a grid $\bar{t} = \{t_m\}_{m=0}^{N},\ 0 = t_0 < ... < t_m < t_{m+1} < ... < t_N = T$.

For $t \in [t_m, t_{m+1}]$, $\hat{x} \in [\hat{x}_{\min}, 4\hat{x}_{\max} - 3\hat{x}_{\min}]$, we define an approximate function $H_j^p,\ j \in \{1, w\}$ as the solution of equation (4.52) supplemented with periodic boundary conditions:

$$\begin{aligned} H_j^p(t, y, \hat{x}_{\min}) &= H_j^p(t, y, 4\hat{x}_{\max} - 3\hat{x}_{\min}), \\ \frac{\partial H_j^p}{\partial x}(t, y, \hat{x}_{\min}) &= \frac{\partial H_j^p}{\partial x}(t, y, 4\hat{x}_{\max} - 3\hat{x}_{\min}), \end{aligned}$$

and with the final condition

$$H_j^p(t_{m+1}, y, \hat{x}) = H_j^e(t_{m+1}, y, \hat{x}).$$

We remark that in the numerical procedure (see Subsection 4.3.4), the value function $H_j(t_{m+1}, y, \hat{x}),\ \hat{x} \in [x_{\min}, x_{\max}]$ employed in (4.53) is substituted by an approximation computed in the previous step of the numerical procedure.

Finally, and for notational convenience, we are going to change the spatial domain to $x \in [0, 2\pi]$ defining:

$$u_j(t, y, x) = H_j^p\left(t, y, \hat{x}_{\min} + \frac{4\hat{x}_{\max} - 4\hat{x}_{\min}}{2\pi} x\right). \tag{4.54}$$

Therefore, equation (4.52) becomes

$$\frac{\partial u_j}{\partial t} + A\frac{\partial u_j}{\partial x} + B\frac{\partial^2 u_j}{\partial x^2} + C\left(\frac{\partial u_j}{\partial x}\right)^2 = 0, \quad j \in \{1, w\}, \tag{4.55}$$

supplemented with periodic boundary conditions:

$$\begin{aligned} u(0, t) &= u(2\pi, t), \\ u_x(0, t) &= u_x(2\pi, t), \end{aligned}$$

where

$$\begin{aligned} A &= \left(\frac{2\pi}{4\hat{x}_{\max} - 4\hat{x}_{\min}}\right)\left(\alpha - \frac{\sigma^2}{2}\right), \\ B &= \left(\frac{2\pi}{4\hat{x}_{\max} - 4\hat{x}_{\min}}\right)^2 \frac{1}{2}\sigma^2, \\ C &= \left(\frac{2\pi}{4\hat{x}_{\max} - 4\hat{x}_{\min}}\right)^2 \frac{1}{2}\sigma^2. \end{aligned} \tag{4.56}$$

4.3.3 A Pseudospectral method.

For $N \in \mathbb{N}$, let S_N be the space of trigonometric polynomials

$$S_N = \operatorname{span}\left\{e^{ikx} \;\middle|\; -N \le k \le N - 1\right\}. \tag{4.57}$$

Definition 4.3.1. *Let $u(x,t)$ defined in $[0,2\pi]\times[0,T]$ be a continuous function. We define the set of nodes $\{x_j\}_{j=0}^{2N-1}$ by*

$$x_j = j\frac{\pi}{N},\ j = 0,1,...,2N-1, \tag{4.58}$$

The Discrete Fourier Transform (DFT) coefficients $\{\hat{u}_k(t)\}_{k=-N}^{N-1}$ are defined by

$$\hat{u}_k(t) = \frac{1}{2N}\sum_{j=0}^{2N-1} u(x_j,t)e^{-ikx_j}, \quad k = -N,...,N-1. \tag{4.59}$$

The trigonometric interpolant of the function $u(x,t)$ at the nodes $\{x_j\}_{j=0}^{2N-1}$ is given by

$$I_N(u(x,t)) = \sum_{k=-N}^{N-1}\hat{u}_k(t)e^{ikx} \tag{4.60}$$

where the $\{\hat{u}_k(t)\}_{k=-N}^{N-1}$ are given by (4.59).

Let $u^N \in S_N$. The polynomial u^N is unambiguously defined by its values at the nodes $\{x_j\}_{j=0}^{2N-1}$ given by (4.58). We denote

$$\boldsymbol{U}_N = \left[u^N(x_0),...,u^N(x_{2N-1})\right]^T. \tag{4.61}$$

The Discrete Fourier Transform (DFT) is an invertible, linear transformation:

$$\mathfrak{F}_N : \mathbb{C}^{2N} \longrightarrow \mathbb{C}^{2N},$$

where it holds that $\mathfrak{F}_N^{-1} = 2N\mathfrak{F}_N^* = 2N\left(\bar{\mathfrak{F}}_N^T\right)$. We define

$$\hat{\boldsymbol{U}}_N = [\hat{u}_{-N}^N,...,\hat{u}_0^N,...,\hat{u}_{N-1}^N] = \mathfrak{F}_N\boldsymbol{U}_N, \tag{4.62}$$

The inverse operator $\mathfrak{F}_N^{-1}$ is explicitly computable $\boldsymbol{U}_N = \mathfrak{F}_N^{-1}\hat{\boldsymbol{U}}_N$ by the inversion formula

$$u^N(x_j) = \sum_{k=-N}^{N-1}\hat{u}_k^N e^{ikx_j}, \quad j = 0,...,2N-1. \tag{4.63}$$

We define a diagonal matrix Δ_N whose elements are given by

$$\Delta_N = \mathrm{diag}(in : -N \le n \le N-1) = \begin{pmatrix} -iN & 0 & ... & 0 & 0 \\ 0 & i(-N+1) & ... & 0 & 0 \\ ... & ... & ... & ... & ... \\ 0 & 0 & ... & i(N-2) & 0 \\ 0 & 0 & ... & 0 & i(N-1) \end{pmatrix}. \tag{4.64}$$

The spectral derivative is given by:

$$D_N \boldsymbol{U}_N = \mathfrak{F}_N^{-1} \Delta_N \mathfrak{F}_N \boldsymbol{U}_N,$$

and recursively for higher order derivatives $D_N^k = \mathfrak{F}_N^{-1} \Delta_N^k \mathfrak{F}_N$.

For the rest of the Chapter, given a complex function $u(x,t)$ defined in $[0,2\pi] \times [0,T]$, the notation $u(t)$ refers to a function $u(\cdot,t) \in L^2([0,2\pi],\mathbb{C})$.

Let $u_T(x)$ be a given function. The Fourier collocation method for equation (4.55) supplemented with periodic boundary conditions and subject to $u(x,T) = u_T(x)$ consists in finding a trigonometric polynomial $u^N(t) \in S_N$ such that $\forall j = 0,1,...,2N-1$:

$$\begin{aligned} \frac{\partial u^N(x_j,t)}{\partial t} + A\frac{\partial u^N(x_j,t)}{\partial x} + B\frac{\partial^2 u^N(x_j,t)}{\partial x^2} + C\left(\frac{\partial u^N(x_j,t)}{\partial x}\right)^2 = 0, \\ u^N(x_j,T) = u_T(x_j). \end{aligned} \tag{4.65}$$

The partial differential equation can be written as

$$\frac{\partial \boldsymbol{U}_N}{\partial t} + AD_N \boldsymbol{U}_N + BD_N^2 \boldsymbol{U}_N + C\left(D_N \boldsymbol{U}_N \circ D_N \boldsymbol{U}_N\right) = 0,$$

where $\circ$ denotes the Hadamard (entrywise) product.

Alternatively, using that $\hat{\boldsymbol{U}}_N = \mathfrak{F}_N \boldsymbol{U}_N$,

$$\frac{\partial \hat{\boldsymbol{U}}_N}{\partial t} + A\Delta_N \hat{\boldsymbol{U}}_N + B\Delta_N^2 \hat{\boldsymbol{U}}_N + C\mathfrak{F}_N\left(\mathfrak{F}_N^{-1}\Delta_N \hat{\boldsymbol{U}}_N \circ \mathfrak{F}_N^{-1}\Delta_N \hat{\boldsymbol{U}}_N\right) = 0, \tag{4.66}$$

which is condensed as

$$\frac{\partial \hat{\boldsymbol{U}}_N}{\partial t} = \mathrm{L}\left(\hat{\boldsymbol{U}}_N\right) + \mathrm{NL}\left(\hat{\boldsymbol{U}}_N\right), \tag{4.67}$$

where

$$\begin{aligned} \mathrm{L}\left(\hat{\boldsymbol{U}}_N\right) &= -\left[A\Delta_N + B\Delta_N^2\right]\hat{\boldsymbol{U}}_N, \\ \mathrm{NL}\left(\hat{\boldsymbol{U}}_N\right) &= -C\mathfrak{F}_N\left(\mathfrak{F}_N^{-1}\Delta_N \hat{\boldsymbol{U}}_N \circ \mathfrak{F}_N^{-1}\Delta_N \hat{\boldsymbol{U}}_N\right). \end{aligned} \tag{4.68}$$

Expression (4.67) is equivalent to the collocation equation (4.65). For recovering the function values at the nodes we just apply the inverse operator $\boldsymbol{U}_N = \mathfrak{F}_N^{-1}\hat{\boldsymbol{U}}_N$ when necessary.

The numerical solution of (4.55) subject to $u(x,T) = u_T(x)$ is the polynomial $u^N(x,t)$ such that

$$\boldsymbol{U}_N(t) = \left[u^N(x_0,t),...,u^N(x_{2N-1},t)\right]^T, \tag{4.69}$$

which satisfies

$$\begin{aligned} \frac{\partial \hat{\boldsymbol{U}}_N}{\partial t} &= \mathrm{L}\left(\hat{\boldsymbol{U}}_N\right) + \mathrm{NL}\left(\hat{\boldsymbol{U}}_N\right), \\ \boldsymbol{U}_N(T) &= \left[u_T(x_0),...,u_T(x_{2N-1})\right]^T. \end{aligned} \tag{4.70}$$

We refer to Subsection 4.3.5 for the theoretical analysis of the stability and convergence of the pseudospectral method. We now proceed to give the computational algorithm.

4.3.4 Numerical algorithm

Suppose that we want to compute option prices for $\hat{x}$ in the *approximation domain*, $\hat{x} \in [L_{\min}, L_{\max}]$.

Therefore, we want to obtain a numerical solution for:

$$H_j(t, y, \hat{x}) : [0, T] \times [y_{\min}, y_{\max}] \times [\hat{x}_{\min}, \hat{x}_{\max}] \longrightarrow \mathbb{R}.$$

where $y_{\min}$, $y_{\max}$, $\hat{x}_{\min}$ and $\hat{x}_{\max}$ are chosen to be big enough. We refer to Subsection 4.4.1 for the empirical error analysis (localization error/ number of shares).

Definition 4.3.2. *Given* $\boldsymbol{N} = (N_t,\ N_y,\ N_{\hat{x}}) \in \mathbb{N}^3$*, we define:*

$$\Delta y = \frac{y_{\max} - y_{\min}}{N_y}, \quad \Delta\hat{x} = \frac{\hat{x}_{\max} - \hat{x}_{\min}}{N_{\hat{x}}}, \quad \Delta t = \frac{T}{N_t}, \tag{4.71}$$

and the sets of points

$$\begin{aligned} &\{y_l\}_{l=0}^{N_y}, \quad && y_l = y_{\min} + l\Delta y, \\ &\{\hat{x}_k\}_{k=0}^{N_{\hat{x}}}, \quad && \hat{x}_k = \hat{x}_{\min} + k\Delta\hat{x}, \\ &\{t_m\}_{m=0}^{N_t}, \quad && t_m = m\Delta t. \end{aligned} \tag{4.72}$$

For the localization procedure, we define two auxiliary sets of points.

Definition 4.3.3. *We define* $N_x = 4N_{\hat{x}}$ *and denote* $\boldsymbol{N}_e = (N_t,\ N_y,\ N_x) \in \mathbb{N}^3$*. We define:*

$$\Delta\hat{x}^e = \frac{4\hat{x}_{\max} - 3\hat{x}_{\min}}{N_x} = (\Delta\hat{x}), \quad \Delta x = \frac{2\pi}{N_x}, \tag{4.73}$$

and the sets of points

$$\begin{aligned} &\{\hat{x}_s^e\}_{s=0}^{N_x}, \quad && \hat{x}_s^e = \hat{x}_{\min} + s\Delta\hat{x}^e, \\ &\{x_s\}_{s=0}^{N_x}, \quad && x_s = s\Delta x. \end{aligned} \tag{4.74}$$

We note that $\hat{x}_k = \hat{x}_k^e,\ k = 0, 1, ..., N_{\hat{x}}$. The set of spatial nodes $\{\hat{x}_s^e\}_{s=0}^{N_x}$ is needed in order to define the odd-even extension given by (4.53).

The numerical solution is denoted by $H_j^{\mathbf{N}}, \quad j \in \{1, w\}$. This solution is only computed for the discrete values included in $\{y_l\}_{l=0}^{N_y}$ and $\{t_m\}_{m=0}^{N_t}$.

We remark that $H_j^{\mathbf{N}},\ j \in \{1, w\}$ is the numerical approximation to the function value just in $[\hat{x}_{\min}, \hat{x}_{\max}]$ but, for a particular choice of y_{l_0} and t_{m_0}, the functions $H_j^{\mathbf{N}}(t_{m_0}, y_{l_0}, \hat{x}), \quad j \in \{1, w\}$ are a $N_x = 4N_{\hat{x}}$ degree trigonometric polynomial defined in $[\hat{x}_{\min}, 4\hat{x}_{\max} - 3\hat{x}_{\min}]$ by its values at $\{\hat{x}_s^e\}_{s=0}^{N_x}$ after performing the odd-even extension given in (4.53).

Let S_k be defined by

$$S_k = \exp(\hat{x}_k). \tag{4.75}$$

The algorithm is:

Step 0: Set $m = N_t$ ($t_{N_t} = T$).

For each $y_l \in \{y_l\}_{l=0}^{N_y}$ and for each $\hat{x}_k \in \{\hat{x}_k\}_{k=0}^{N_{\hat{x}}}$ compute

$$H_j^{\mathbf{N}}(T, y_l, \hat{x}_k) = H_j(T, y_l, \hat{x}_k),\ j \in \{1, w\}$$

with formulas (4.48) or (4.49).

Step 1: For each $y_l \in \{y_l\}_{l=0}^{N_y}$, extend the function $H_j^{\mathbf{N}}(t_m, y_l, \hat{x})$ defined in $[\hat{x}_{\min}, \hat{x}_{\max}]$ to the trigonometric polynomials $\mathbb{H}_j^{\mathbf{N}_e}(t_m, y_l, \hat{x})$ defined in $[\hat{x}_{\min}, 4\hat{x}_{\max} - 3\hat{x}_{\min}]$ as in Subsection 4.3.2.

For each $y_l \in \{y_l\}_{l=0}^{N_y}$ and for $s = 0, 1, ..., 4N_{\hat{x}} - 1$ define $\mathbb{H}_j^{\mathbf{N}_e}(t_m, y_l, \hat{x}_s^e) =$

$$\begin{array}{ll}
H_j^{\mathbf{N}}(t_m, y_l, \hat{x}_s^e), & \text{if } \hat{x}_s^e \in [\hat{x}_{\min}, \hat{x}_{\max}], \\
2H_j^{\mathbf{N}} t_m, y_l, \hat{x}_{\max}) - H_j^{\mathbf{N}}(t_m, y_l, 2\hat{x}_{\max} - \hat{x}_s^e), & \text{if } \hat{x}_s^e \in [\hat{x}_{\max}, 2\hat{x}_{\max} - \hat{x}_{\min}], \\
\mathbb{H}_j^{\mathbf{N}}(t_m, y_l, (4\hat{x}_{\max} - 2\hat{x}_{\min}) - \hat{x}_s^e), & \text{if } \hat{x}_s^e \in [2\hat{x}_{\max} - \hat{x}_{\min}, 4\hat{x}_{\max} - 3\hat{x}_{\min}], \\
\mathbb{H}_j^{\mathbf{N}}(t_m, y_l, z), \begin{cases} \hat{x} = z + \hat{x}_{\min} + k(4\hat{x}_{\max} - 4\hat{x}_{\min}) \\ z \in [\hat{x}_{\min}, 4\hat{x}_{\max} - 3\hat{x}_{\min}],\ k \in \mathbb{Z}, \end{cases} & \text{if } \hat{x}_s^e \notin [\hat{x}_{\min}, 4\hat{x}_{\max} - 3\hat{x}_{\min}],
\end{array}$$

For each $y_l \in \{y_l\}_{l=0}^{N_y}$ and each $x_s \in \{x_s\}_{s=0}^{N_x}$ write

$$u_j^{N_x}(t_m, y_l, x_s) = \mathbb{H}_j^{\mathbf{N}_e}\left(t_m, y_l, \hat{x}_{\min} + \frac{4\hat{x}_{\max} - 4\hat{x}_{\min}}{2\pi} x_s\right)$$

to obtain trigonometric polynomials defined for $x \in [0, 2\pi]$. Set:

$$\boldsymbol{U}_{N_x}^{y_l} = \left[u_j^{N_x}(t_m, y_l, x_0), u_j^{N_x}(t_m, y_l, x_1), ..., u_j^{N_x}(t_m, y_l, x_{N_x - 1})\right]^T.$$

Then, for each $y_l \in \{y_l\}_{l=0}^{N_y}$ compute the approximated No Transactions function value $u_j^{N_x}(t_{m-1}, y_l, x)$ as the numerical solution of the Fourier pseudospectral method:

$$\begin{cases} \dfrac{\partial \hat{\boldsymbol{U}}}{\partial t} + A\Delta\hat{\boldsymbol{U}} + B\Delta^2\hat{\boldsymbol{U}} + C\mathfrak{F}\left(\mathfrak{F}^{-1}\Delta\hat{\boldsymbol{U}} \circ \mathfrak{F}^{-1}\Delta\hat{\boldsymbol{U}}\right) = 0, \\ \hat{\boldsymbol{U}}(t_m) = \mathfrak{F}\left(u_j^N(t_m, y_l, \bar{\mathrm{x}})\right), \end{cases}$$

where $\hat{\boldsymbol{U}} = \hat{\boldsymbol{U}}_{N_x}^{y_l}$, $\Delta\hat{\boldsymbol{U}} = \Delta_{N_x}\hat{\boldsymbol{U}}_{N_x}^{y_l}$, $\mathfrak{F} = \mathfrak{F}_{N_x}$, constants A, B, C are given by formula (4.56).

For each $y_l \in \{y_l\}_{l=0}^{N_y}$, and each $\hat{x}_k \in \{\hat{x}_k\}_{k=0}^{N_{\hat{x}}}$ define

$$H_j^p(t_{m-1}, y_l, \hat{x}_k) = u_j^N(t_{m-1}, y_l, x_k),$$

which corresponds to the function values if no transactions are realized. We remark that $\hat{x}_k \in [\hat{x}_{\min}, \hat{x}_{\max}]$, the values that correspond to the computational domain.

Step 2: Search the location of the buying/selling frontiers for each $\hat{x}_k \in \{\hat{x}_k\}_{k=0}^{N_{\hat{x}}}$ at $t = t_{m-1}$.

We assume that the state space remains divided in three Regions (Buying/Selling/No Transactions).

The location of the frontiers is done through the discrete counterpart of equation (4.47) searching the biggest/smallest values for which it is not optimal to respectively buy/sell shares. The numerical approximation to the Buying frontier is

$$y_j^{\mathscr{B}}(t_{m-1},\hat{x}_k) = \min_{y\in\{y_l\}_{l=0}^{N_y}} \left\{ \frac{\gamma(1+\lambda)\exp(\hat{x}_k)}{\delta(T,t_{m-1})}\Delta y + H_j^p(t_{m-1},y_l+\Delta y,\hat{x}_k) - H_j^p(t_{m-1},y_l,\hat{x}_k) > 0 \right\},$$

and to the Selling frontier is

$$y_j^{\mathscr{S}}(t_{m+1},\hat{x}_k) = \max_{y\in\{y_l\}_{l=0}^{N_y}} \left\{ -\frac{\gamma(1-\mu)\exp(\hat{x}_k)}{\delta(T,t_{m-1})}\Delta y + H_j^p(t_{m-1},y_l-\Delta y,\hat{x}_k) - H_j^p(t_{m-1},y_l,\hat{x}_k) > 0 \right\}.$$

We remark that with this definition, the discrete frontier is a point of the mesh $\{y_l\}_{l=0}^{N_y}$, so that the time evolution is piecewise constant.

Step 3: Obtain, for each $\hat{x}_k \in \{\hat{x}_k\}_{k=0}^{N_{\hat{x}}}$ and each $y_l \in \{y_l\}_{l=0}^{N_y}$ the value of $H_j^{\mathbf{N}}(t_{m-1},y_l,\hat{x}_k)$ employing the explicit formulas (4.50) and (4.51).

If $(t_{m-1},y_l,\hat{x}_k)$ belongs to the Buying Region $\left(y_l < y_j^{\mathscr{B}_{\mathbf{N}}}(t_{m-1},\hat{x}_k)\right)$

$$H_j^{\mathbf{N}}(t_{m-1},y_l,\hat{x}_k) = H_j^p(t_{m-1},y_j^{\mathscr{B}_{\mathbf{N}}}(t_{m-1},\hat{x}_k),\hat{x}_k) + \left(-\frac{\gamma(1+\lambda)\exp(\hat{x}_k)}{\delta(T,t_{m-1})}(y_l - y_j^{\mathscr{B}_{\mathbf{N}}}(t_{m-1},\hat{x}_k,)) \right),$$

If $(t_{m-1},y_l,\hat{x}_k)$ belongs to the No Transactions $\left(y_j^{\mathscr{B}_{\mathbf{N}}}(t_{m-1},\hat{x}_k) \le y_l \le y_j^{\mathscr{S}_{\mathbf{N}}}(t_{m-1},\hat{x}_k)\right)$

$$H_j^{\mathbf{N}}(t_{m-1},y_l,\hat{x}_k) = H_j^p(t_{m-1},y_l,\hat{x}_k),$$

If $(t_{m-1},y_l,\hat{x}_k)$ belongs to the Selling Region $\left(y_l > y_j^{\mathscr{S}_{\mathbf{N}}}(t_{m-1},\hat{x}_k)\right)$

$$H_j^{\mathbf{N}}(t_{m-1},y,\hat{x}_k) = H_j^p(t_{m-1},y_j^{\mathscr{S}_{\mathbf{N}}}(t_{m-1},\hat{x}_k,),\hat{x}_k) + \left(\frac{\gamma(1-\mu)\exp(\hat{x}_k)}{\delta(T,t_{m-1})}(y_j^{\mathscr{S}_{\mathbf{N}}}(t_{m-1},\hat{x}_k,) - y) \right).$$

Step 4: If $t_{m-1}=0$ end. Otherwise, $m=m-1$ and proceed to **Step 1**.

For each $y_l \in \{y_l\}_{l=0}^{N_y}$ and each $t_m \in \{t_m\}_{m=0}^{N_t}$, redefine $H_j^{\mathbf{N}}(t_m,y_l,\hat{x})$ as the trigonometric polynomial defined $[\hat{x}_{\min}, 4\hat{x}_{\max} - 3\hat{x}_{\min}]$ by its values at $\hat{x}_s^e \in \{\hat{x}_s^e\}_{s=0}^{N_x}$ with the odd-even extension given by (4.53).

The numerical approximation to the option price $\forall \hat{x} \in [\hat{x}_{\min},\hat{x}_{\max}]$ and for each $t_m \in \{t_m\}_{m=0}^{N_t}$ is computed through

$$p_w^{\mathbf{N}}(t_m,\hat{x}) = \frac{\delta(T,t_m)}{\gamma}\left(H_w^{\mathbf{N}}(t_m,0,\hat{x}) - H_1^{\mathbf{N}}(t_m,0,\hat{x})\right), \tag{4.76}$$

4.3.5 Stability, consistency and convergence. Localization error.

First, we are going to study the stability and convergence of the Fourier pseudospectral method following the lines presented in [30] or [32]. Finally, we will analyze the *localization error*.

Since partial differential equation (4.55) is solved backwards, for simplicity, we perform the change of variable $\tau = T - t$, so that we deal with the non-linear periodic problem:

$$\begin{aligned} &\frac{\partial u}{\partial \tau} = A\frac{\partial^2 u}{\partial x^2} + B\frac{\partial u}{\partial x} + C\left(\frac{\partial u}{\partial x}\right)^2, \\ &u(0,\tau) = u(2\pi,\tau), \quad u_x(0,\tau) = u_x(2\pi,\tau), \\ &u(x,0) = u_0(x) \end{aligned} \tag{4.77}$$

where $u_0(x)$ is given and constants A, B, C are the same as in (4.56).

For the analysis, we assume that the regularity conditions upon $u_0(x)$ are the same regularity conditions required upon u in the different Theorems and Propositions. The particular initial conditions of the financial problem that we are dealing with will be discussed after the theoretical development.

Let $L^2 = L^2(0, 2\pi)$ denote the space of the Lebesgue-measurable functions $u : (0, 2\pi) \to \mathbb{C}$ such that

$$\int_0^{2\pi} |u|^2 dx < +\infty.$$

We denote by $(\cdot, \cdot)$ the usual L^2 scalar product and by $\|.\|$ the usual L^2 norm which, $\forall u, v \in L^2$, are given by:

$$(u, v) = \int_0^{2\pi} u(x)\overline{v(x)}dx, \quad \|u\| = \left(\int_0^{2\pi} |u(x)|^2 dx\right)^{\frac{1}{2}}.$$

Let $H^s = H^s(0, 2\pi)$ denote the usual Sobolev space of order s (see [10, A.11]) and $||.||_{H^s}$ denote its norm:

$$||u||_{H^s} = \left(\sum_{k=0}^{s} \left\|\frac{\partial^k u}{\partial x^k}\right\|^2\right)^{\frac{1}{2}}.$$

We define the norm $||u||_\infty$ (see [10, 5.1.3]) by $||u||_\infty = \sup_{0\le x\le 2\pi} |u(x)|$.

For any function $u(\tau) \in L^2([0, 2\pi])$, we denote by

$$\tilde{u}_k(\tau) = \frac{1}{2\pi}\int_0^{2\pi} u(x,\tau)e^{-ikx}dx, \quad k = 0, \pm 1, \pm 2, ...,$$

the n$^{\text{th}}$ coefficient in the Fourier expansion of u:

$$u(x,\tau) = \sum_{k=-\infty}^{\infty} \tilde{u}_k(\tau)e^{ikx}.$$

We denote by $P_N u(\tau) \in S_N$ the orthogonal projection of $u(\tau)$ over S_N, i.e.

$$P_N u(\tau) = \sum_{k=-N}^{N-1} \tilde{u}_k(\tau) e^{ikx}.$$

For $u, v \in S_N$, we denote by $(u, v)_N$ the usual discrete scalar product in S_N, given by

$$(u, v)_N = \frac{\pi}{N} \sum_{j=0}^{2N-1} u(x_j)\overline{v(x_j)},$$

and by $||u||_N = [(u, u)_N]^{\frac{1}{2}}$ the discrete norm in S_N induced by $(\cdot, \cdot)_N$.

For any pair of functions $u, v \in S_N$, it holds (see [10, (2.1.33)]):

$$(u, v)_N = (u, v). \tag{4.78}$$

We consider the subspace $H_p^s \subset H^s$ defined by (see [10]):

$$H_p^s(0, 2\pi) = \left\{ v \in L^2(0, 2\pi) : \text{for } 0 \le k \le s, \text{ the derivative } \frac{\mathrm{d}^k v}{\mathrm{d}x^k} \text{ in the sense of periodic distributions belongs to } L^2(0, 2\pi) \right\}.$$

Stability, consistency and convergence.

We recall that in the proposed collocation method, we search for a function $u^N(\tau) \in S_N$ such that $\forall j = 0, \dots, 2N-1$:

$$\begin{aligned} &\frac{\partial u^N}{\partial \tau}(x_j, \tau) = A\frac{\partial^2 u^N}{\partial x^2}(x_j, \tau) + B\frac{\partial u^N}{\partial x}(x_j, \tau) + C\left(\frac{\partial u^N}{\partial x}(x_j, \tau)\right)^2, \\ &u^N(0, \tau) = u^N(2\pi, \tau), \\ &u^N(x_j, 0) = u_0(x_j). \end{aligned} \tag{4.79}$$

Fixed T>0. Let $V(x, \tau), W(x, \tau)$ be two 2π-periodic and smooth functions defined in $[0,\ 2\pi] \times [0,\ T]$. This functions will be seen as perturbed solutions of equation (4.77).

Let $V^N(\tau) = I_N(V(\tau))$ and $W^N(\tau) = I_N(W(\tau))$. We define the residuals $F^N(x, \tau)$, $G^N(x, \tau) \in S_N$, as the trigonometric polynomials such that for $j = 0, \dots, 2N-1$ satisfy:

$$\begin{aligned} F^N(x_j, \tau) &= \frac{\partial V^N}{\partial \tau}(x_j, \tau) - A\frac{\partial^2 V^N}{\partial x^2}(x_j, \tau) - B\frac{\partial V^N}{\partial x}(x_j, \tau) - C\left(\frac{\partial V^N}{\partial x}(x_j, \tau)\right)^2, \\ G^N(x_j, \tau) &= \frac{\partial W^N}{\partial \tau}(x_j, t) - A\frac{\partial^2 W^N}{\partial x^2}(x_j, \tau) - B\frac{\partial W^N}{\partial x}(x_j, \tau) - C\left(\frac{\partial W^N}{\partial x}(x_j, \tau)\right)^2. \end{aligned}$$

Theorem 4.3.1. *(Stability) Let $T>0$ be fixed and $V^N,\ W^N,\ F^N,\ G^N$ defined above. Let $M \geq 0$ such that:*

$$\|(V^N)_x\|_\infty, \|(W^N)_x\|_\infty \leq M, \quad \tau \in [0,T]. \tag{4.80}$$

Then, it exists a constant $R = R(M)$ such that

$$\max_{0\leq\tau\leq T}\|e^N(\tau)\|^2 + \frac{A}{2}\int_0^T \|e_x^N(\tau)\|^2 d\tau \leq R\left(\|e^N(0)\|^2 + \int_0^T \|F^N(\tau) - G^N(\tau)\|^2 d\tau\right),$$

where $e^N(\tau) = V^N(\tau) - W^N(\tau)$.

Proof. By definition, we have for $j = 0, 1, ..., 2N-1$,

$$\frac{\partial V^N}{\partial \tau}(x_j,\tau) = A\frac{\partial^2 V^N}{\partial x^2}(x_j,\tau) + B\frac{\partial V^N}{\partial x}(x_j,\tau) + C\left(\frac{\partial V^N}{\partial x}(x_j,\tau)\right)^2 + F^N(x_j,\tau),$$
$$\frac{\partial W^N}{\partial \tau}(x_j,\tau) = A\frac{\partial^2 W^N}{\partial x^2}(x_j,\tau) + B\frac{\partial W^N}{\partial x}(x_j,\tau) + C\left(\frac{\partial W^N}{\partial x}(x_j,\tau)\right)^2 + G^N(x_j,\tau).$$

Subtracting both expressions, we obtain for $j = 0, \dots, 2N-1$ and $\forall \tau \in [0,T]$:

$$\frac{\partial e^N}{\partial \tau}(x_j) = A\frac{\partial^2 e^N}{\partial x^2}(x_j) + B\frac{\partial e^N}{\partial x}(x_j) + C\left[\left(\frac{\partial V^N}{\partial x}(x_j)\right)^2 - \left(\frac{\partial W^N}{\partial x}(x_j)\right)^2\right] + \left(F^N(x_j) - G^N(x_j)\right),$$

where $e^N = V^N - W^N$. Equivalently,

$$\frac{\partial e^N}{\partial \tau} = A\frac{\partial^2 e^N}{\partial x^2} + B\frac{\partial e^N}{\partial x} + C\left(I_N\left[\left(\frac{\partial V^N}{\partial x}\right)^2 - \left(\frac{\partial W^N}{\partial x}\right)^2\right]\right) + \left(F^N - G^N\right),$$

since, by definition, $e^N,\ F^N,\ G^N \in S_N$.

For $\phi \in S_N$, taking the scalar product of the previous expression with respect to ϕ, we obtain:

$$\begin{aligned}\left(\frac{\partial e^N}{\partial \tau},\ \phi\right) =& A\left(\frac{\partial^2 e^N}{\partial x^2},\ \phi\right) + B\left(\frac{\partial e^N}{\partial x},\ \phi\right) + C\left(I_N\left[\left(\frac{\partial V^N}{\partial x}(x_j)\right)^2 - \left(\frac{\partial W^N}{\partial x}(x_j)\right)^2\right],\ \phi\right) \\ &+ \left(F^N - G^N, \phi\right).\end{aligned}$$

Taking $\phi = e^N$ and noting that the periodic boundary conditions imply that $\left(\frac{\partial e^N}{\partial x}, e^N\right) = 0$ and $\left(\frac{\partial^2 e^N}{\partial x^2}, e^N\right) = -\left(\frac{\partial e^N}{\partial x}, \frac{\partial e^N}{\partial x}\right)$ we get:

$$\frac{1}{2}\frac{d}{d\tau}||e^N(\tau)||^2 + A||(e^N)_x(\tau)||^2 = C\left(I_N\left[\left(\frac{\partial V^N}{\partial x}\right)^2 - \left(\frac{\partial W^N}{\partial x}\right)^2\right],\ e^N\right) + \left(F^N - G^N, e^N\right).$$

Using (4.78)

$$\begin{aligned}
&\left|\left(I_N\left[\left(\frac{\partial V^N}{\partial x}\right)^2-\left(\frac{\partial W^N}{\partial x}\right)^2\right],\ e^N\right)\right| \\
&\quad=\left|\sum_{j=0}^{2N-1}\left[\left(\frac{\partial V^N}{\partial x}(x_j)\right)^2-\left(\frac{\partial W^N}{\partial x}(x_j)\right)^2\right]e^N(x_j)\right| \\
&\quad\le\sum_{j=0}^{2N-1}\left|\left[\left(\frac{\partial V^N}{\partial x}(x_j)\right)^2-\left(\frac{\partial W^N}{\partial x}(x_j)\right)^2\right]\right|\left|e^N(x_j)\right| \\
&\quad\le\sum_{j=0}^{2N-1}\left|\left(\frac{\partial V^N}{\partial x}(x_j)\right)+\left(\frac{\partial W^N}{\partial x}(x_j)\right)\right|\left|\left(\frac{\partial V^N}{\partial x}(x_j)\right)-\left(\frac{\partial W^N}{\partial x}(x_j)\right)\right|\left|e^N(x_j)\right| \\
&\quad\le 2M\sum_{j=0}^{2N-1}\left|(e^N)_x(x_j)\right|\left|e^N(x_j)\right| \\
&\quad\le 2M\|(e^N)_x\|_N\|e^N\|_N=2M\|(e^N)_x\|\|e^N\|,
\end{aligned}$$

where we have employed:

$$\left\|\frac{\partial V^N}{\partial x}+\frac{\partial W^N}{\partial x}\right\|_\infty\le\left\|\frac{\partial V^N}{\partial x}\right\|_\infty+\left\|\frac{\partial W^N}{\partial x}\right\|_\infty\le 2M,$$

from the hypothesis of the theorem. Therefore, we can bound

$$\left|C\left(I_N\left[\left(\frac{\partial V^N}{\partial x}\right)^2-\left(\frac{\partial W^N}{\partial x}\right)^2\right],\ e^N\right)\right|\le 2M|C|\|(e^N)_x\|\|e^N\|.$$

Using Cauchy Schwartz's inequality to bound $\left(F^N-G^N,e^N\right)$, we get

$$\frac{1}{2}\frac{d}{d\tau}||e^N(\tau)||^2+A||(e^N)_x(\tau)||^2\le 2M|C|\|(e^N)_x(\tau)\|\|e^N(\tau)\|+\|F^N(\tau)-G^N(\tau)\|\|e^N(\tau)\|.$$

We apply to both terms on the right side the inequality $ab\le\left(\epsilon a^2+\frac{1}{4\epsilon}b^2\right),\ \ a,b>0$ with $\epsilon=\frac{A}{4M|C|}$ and $\epsilon=1$ respectively.

$$\begin{aligned}
\frac{1}{2}\frac{d}{d\tau}||e^N(\tau)||^2+A\|(e^N)_x(\tau)||^2\le&\frac{A}{2}\|(e^N)_x(\tau)\|^2+\frac{2M^2C^2}{A}\|e^N(\tau)\|^2 \\
&+\|F^N(\tau)-G^N(\tau)\|^2+\frac{1}{4}\|e^N(\tau)\|^2,
\end{aligned}$$

so that

$$\frac{1}{2}\frac{d}{d\tau}||e^N(\tau)||^2+\frac{A}{2}\|(e^N)_x(\tau)\|^2\le K\|e^N(\tau)\|^2+\|F^N(\tau)-G^N(\tau)\|^2,$$

where $K=\frac{2M^2C^2}{A}+\frac{1}{4}$.

Using Gronwall's lemma (see [10, A.15]),

$$\max_{0\le\tau\le T}\|e^N(\tau)\|^2+\frac{A}{2}\int_0^T\|(e^N)_x(\tau)\|^2d\tau\le R\left(\|e^N(0)\|^2+\int_0^T\|F^N(\tau)-G^N(\tau)\|^2d\tau\right),$$

with $R=\exp(KT)$.

□

Proposition 4.3.1. *Let $u(\tau)\in H_p^{s+r}$, $s,r\ge 1$ for $\tau\in[0,T]$ continuous.*

Then it exists a constant $M=M\left(\max_{0\le\tau\le T}\left\|\frac{\partial^{s+1}u}{\partial x^{s+1}}\right\|\right)\ge 0$ such that for any $N\in\mathbb{N}$, it holds:

$$\left\|\frac{\partial^s P_N(u(\tau))}{\partial x^s}\right\|_\infty\le M,\quad \left\|\frac{\partial^s I_N(u)}{\partial x^s}\right\|_\infty\le M,\quad \tau\in[0,T].$$

Proof. For any $\tau\in[0,T]$, we decompose:

$$\begin{aligned}\left\|\frac{\partial^s P_N(u)}{\partial x^s}\right\|_\infty&\le\left\|\frac{\partial^s P_N(u)}{\partial x^s}-\frac{\partial^s u}{\partial x^s}\right\|_\infty+\left\|\frac{\partial^s u}{\partial x^s}\right\|_\infty,\\ \left\|\frac{\partial^s I_N(u)}{\partial x^s}\right\|_\infty&\le\left\|\frac{\partial^s I_N(u)}{\partial x^s}-\frac{\partial^s u}{\partial x^s}\right\|_\infty+\left\|\frac{\partial^s u}{\partial x^s}\right\|_\infty.\end{aligned}\tag{4.81}$$

Inequality [10, (A.12)] implies that

$$\left\|\frac{\partial^s u}{\partial x^s}\right\|_\infty\le C_1\left\|\frac{\partial^{s+1}u}{\partial x^{s+1}}\right\|_{L^2},$$

and

$$\begin{aligned}\left\|\frac{\partial^s P_N(u)}{\partial x^s}-\frac{\partial^s u}{\partial x^s}\right\|_\infty&\le C_1\left\|\frac{\partial^s P_N(u)}{\partial x^s}-\frac{\partial^s u}{\partial x^s}\right\|_{H^1},\\ \left\|\frac{\partial^s I_N(u)}{\partial x^s}-\frac{\partial^s u}{\partial x^s}\right\|_\infty&\le C_1\left\|\frac{\partial^s I_N(u)}{\partial x^s}-\frac{\partial^s u}{\partial x^s}\right\|_{H^1},\end{aligned}$$

Applying [10, (5.1.5)] (Bernstein's inequality), standard approximation results of projection [10, (5.1.10)] and aliasing error ($\|I_N(u)-P_N(u)\|_{L^2}$) result [10, (5.1.18)], we can bound

$$\begin{aligned}\left\|\frac{\partial^s P_N(u)}{\partial x^s}-\frac{\partial^s u}{\partial x^s}\right\|_{H^1}&\le K_1N^{1-r}\left\|\frac{\partial^{s+r}u}{\partial x^{s+r}}\right\|_{L^2},\\ \left\|\frac{\partial^s I_N(u)}{\partial x^s}-\frac{\partial^s u}{\partial x^s}\right\|_{H^1}&\le\left\|\frac{\partial^s I_N(u)}{\partial x^s}-\frac{\partial^s P_N(u)}{\partial x^s}\right\|_{H^1}+\left\|\frac{\partial^s P_N(u)}{\partial x^s}-\frac{\partial^s u}{\partial x^s}\right\|_{H^1}\\ &\le N^s\|I_N(u)-P_N(u)\|_{H^1}+K_1N^{1-r}\left\|\frac{\partial^{s+r}u}{\partial x^{s+r}}\right\|_{L^2}\\ &\le N^{s+1}\|I_N(u)-P_N(u)\|_{L^2}+K_1N^{1-r}\left\|\frac{\partial^{s+r}u}{\partial x^{s+r}}\right\|_{L^2}\\ &\le K_1N^{1-r}\left\|\frac{\partial^{s+r}u}{\partial x^{s+r}}\right\|_{L^2}+K_1N^{1-r}\left\|\frac{\partial^{s+r}u}{\partial x^{s+r}}\right\|_{L^2}=2K_1N^{1-r}\left\|\frac{\partial^{s+r}u}{\partial x^{s+r}}\right\|_{L^2},\end{aligned}$$

if $u \in H_p^{s+r},\ r \geq 1$.

The choice of

$$M = (2K_1 + C_1) \max_{0 \leq \tau \leq T} \left\| \frac{\partial^{s+1} u}{\partial x^{s+1}} \right\|,$$

completes the proof. □

Proposition 4.3.2. *(Consistency) Let $u(x,\tau)$ be the solution of equation (4.77). Suppose that $\forall \tau \in [0,T]$, function $u(\tau) \in H_p^{s+2}$ and $u_\tau(\tau) \in H_p^s$.*

Define $F^N(\tau) \in S_N,\ \forall \tau \in [0,T]$ by

$$F^N(x_j,\tau) = \left[\frac{\partial I_N(u)}{\partial \tau} - A \frac{\partial^2 I_N(u)}{\partial x^2} - B \frac{\partial I_N(u)}{\partial x} - C \left(\frac{\partial I_N(u)}{\partial x} \right)^2 \right] \Bigg|_{(x_j,\tau)}, \quad j = 0, \dots, 2N-1. \tag{4.82}$$

Then it exists a constant

$$M = M \left(\max_{0 \leq \tau \leq T} \left\{ \left\| \frac{\partial^{s+1} u}{\partial x^{s+1}} \right\|, \left\| \frac{\partial^{s+2} u}{\partial x^{s+2}} \right\|, \left\| \frac{\partial^s u_\tau}{\partial x^s} \right\| \right\} \right),$$

such that

$$\max_{0 \leq \tau \leq T} \|F^N\| \leq M N^{-s}.$$

Proof. Let us define the function:

$$J^{2N} = \frac{\partial I_N(u(x,\tau))}{\partial \tau} - A \frac{\partial^2 I_N(u(x,\tau))}{\partial x^2} - B \frac{\partial I_N(u(x,\tau))}{\partial x} - C \left[\left(\frac{\partial I_N(u(x,\tau))}{\partial x} \right)^2 \right], \tag{4.83}$$

and note that:

$$J^{2N} \in S_{2N},$$
$$F^N = I_N \left(J^{2N} \right).$$

The function $u(x,\tau)$ satisfies:

$$0 = \frac{\partial u(x,\tau)}{\partial \tau} - A \frac{\partial^2 u(x,\tau)}{\partial x^2} - B \frac{\partial u(x,\tau)}{\partial x} - C \left[\left(\frac{\partial u(x,\tau)}{\partial x} \right)^2 \right]. \tag{4.84}$$

Subtracting (4.83) and (4.84):

$$J^{2N} = J_1^{2N} - A J_2^{2N} - B J_3^{2N} - C J_4^{2N},$$

with

$$J_1^{2N} = \frac{\partial I_N(u(x,\tau))}{\partial \tau} - \frac{\partial u(x,\tau)}{\partial \tau},$$
$$J_2^{2N} = \frac{\partial^2 I_N(u(x,\tau))}{\partial x^2} - \frac{\partial^2 u(x,\tau)}{\partial x^2},$$
$$J_3^{2N} = \frac{\partial I_N(u(x,\tau))}{\partial x} - \frac{\partial u(x,\tau)}{\partial x},$$
$$J_4^{2N} = \left(\frac{\partial I_N(u(x,\tau))}{\partial x} \right)^2 - \left(\frac{\partial u(x,\tau)}{\partial x} \right)^2,$$

for all $\tau \in [0, T]$.

The no linear term J_4^{2N} is bounded by:

$$\left\| \left(\frac{\partial I_N(u)}{\partial x} \right)^2 - \left(\frac{\partial u}{\partial x} \right)^2 \right\| \leq \left\| \frac{\partial I_N(u)}{\partial x} + \frac{\partial u}{\partial x} \right\|_\infty \left\| \frac{\partial I_N(u)}{\partial x} - \frac{\partial u}{\partial x} \right\|.$$

From Proposition 4.3.1, it exists a constant $M_1 = M_1 \left(\max_{0 \leq \tau \leq T} \left\| \frac{\partial^2 u}{\partial x^2} \right\| \right)$ such that

$$\max_{0 \leq \tau \leq T} \left\{ \left\| \frac{\partial I_N(u)}{\partial x}(\tau) \right\|_\infty, \left\| \frac{\partial u}{\partial x}(\tau) \right\|_\infty \right\} \leq M_1,$$

The second term is bounded by

$$\|u_x - (I_N u)_x\|_{L^2} \leq K_1 N^{-s} \left\| \frac{\partial^{s+1} u(x, \tau)}{\partial x^{s+1}} \right\|_{L^2},$$

due to the approximation result [10, (5.1.20)].

Therefore, the no linear term J_4^{2N} is bounded by

$$\left\| \left(\frac{\partial I_N(u)}{\partial x} \right)^2 - \left(\frac{\partial u}{\partial x} \right)^2 \right\| \leq K_1 M_1 N^{-s} \left\| \frac{\partial^{s+1} u}{\partial x^{s+1}} \right\|.$$

Obviously, term J_3^{2N} can also be bounded by [10, (5.1.20)]:

$$\left\| J_3^{2N} \right\| \leq K_1 N^{-s} \left\| \frac{\partial^{s+1} u}{\partial x^{s+1}} \right\|.$$

Using again approximation result [10, (5.1.9)], Bernstein's inequality [10, (5.1.5)] and aliasing error result [10, (5.1.18)], term J_2^{2N} can be bounded by

$$\begin{aligned} \|J_2^{2N}\| &\leq \left\| \frac{\partial^2 I_N(u)}{\partial x^2} - \frac{\partial^2 P_N(u)}{\partial x^2} \right\| + \left\| \frac{\partial^2 P_N(u(x,t))}{\partial x^2} - \frac{\partial^2 u(x,t)}{\partial x^2} \right\| \\ &\leq N^2 \|I_N(u) - P_N(u)\| + \|P_N(u_{xx}) - u_{xx}\| \\ &\leq K_1 N^{-s} \left\| \frac{\partial^s u_{xx}}{\partial x^s} \right\| + K_1 N^{-s} \left\| \frac{\partial^s u_{xx}}{\partial x^s} \right\| = 2K_1 N^{-s} \left\| \frac{\partial^s u_{xx}}{\partial x^s} \right\|. \end{aligned}$$

For the last term, using [10, (5.1.16)]:

$$\|J_1^{2N}\| = \left\| I_N \left(\frac{\partial u(x, \tau)}{\partial \tau} \right) - \frac{\partial u(x, \tau)}{\partial \tau} \right\| \leq K_1 N^{-s} \left\| \frac{\partial^s u_\tau}{\partial x^s} \right\|,$$

since interpolation does commute with derivation with respect the temporal variable.

Thus, there exists a constant $M_2 \geq 0$, which depends on $\max_{0\leq\tau\leq T}\left\{\left\|\frac{\partial^{s+1}u}{\partial x^{s+1}}\right\|, \left\|\frac{\partial^{s+2}u}{\partial x^{s+2}}\right\|, \left\|\frac{\partial^{s}u_\tau}{\partial x^{s}}\right\|\right\}$, such that:

$$\|J^{2N}\| \leq M_2 N^{-s}.$$

Finally, using again Bernstein's inequality [10, (5.1.5)] and the approximation result [10, (5.1.16)], since $J^{2N} \in S_{2N}$ we can bound

$$\begin{aligned}\left\|F^N\right\| \leq \left\|F^N - J^{2N}\right\| + \left\|J^{2N}\right\| = \left\|I_N\left(J^{2N}\right) - J^{2N}\right\| + \left\|J^{2N}\right\| \leq K_1 N^{-s}\left\|\frac{\partial^s J^{2N}}{\partial x^s}\right\| + \left\|J^{2N}\right\| \leq \\ \leq K_1 2^s \left\|J^{2N}\right\| + \left\|J^{2N}\right\| \leq \left(K_1 \cdot 2^s + 1\right)\left\|J^{2N}\right\| \leq M N^{-s},\end{aligned}$$

where $M = (K_1 2^s + 1)\, M_2$.

□

We prove now that the threshold condition (4.80) holds for u^N.

Proposition 4.3.3. *Fix $T>0$. Let u be the solution of equation (4.77). Suppose that $\forall\tau \in [0,T]$, functions $u(\tau)$ and $u_\tau(\tau)$ are functions in H_p^{s+2} and H_p^s respectively.*

Then, it exists a constant M and $N_0 \in \mathbb{N}$, such that $\forall N \geq N_0$ it holds that

$$\|(u^N)_x(\tau)\|_\infty \leq M, \quad \tau \in [0,T]. \tag{4.85}$$

Proof. Let

$$M_1 = \max_{0\leq\tau\leq T}\left\|(I_N u(\tau))_x\right\|_\infty,$$

which exists from Proposition 4.3.1 under the regularity hypothesis of u.

For $\tau = 0$ we have that $\|(u^N)_x(0)\|_\infty = \|(I_N u(0))_x\|_\infty \leq M_1$.

By a continuity argument, it must exist $\epsilon > 0$ and N_1 big enough such that $\forall N \geq N_1$ it holds that

$$\|u_x^N(\tau)\|_\infty \leq 2M_1, \quad t \in [0,\epsilon]. \tag{4.86}$$

We argue by contradiction. For any $N \in \mathbb{N}$, we define:

$$\epsilon_N = \sup_\tau\left\{0 < \tau \leq T : \|u_x^N(s)\|_\infty < 2M_1,\ s \in [0,\tau]\right\}.$$

where it holds that $\epsilon_N > 0$ because u^N is the solution of an ODE system.

If (4.86) does not hold, we can find a strictly increasing sequence $N_1, N_2, ... \to \infty$ and a strictly decreasing sequence $\epsilon_{N_1}, \epsilon_{N_2} ... \to 0$ such that

$$\lim_{n\to\infty}\max_{0\leq\tau\leq\epsilon_{N_n}}\|u_x^{N_n}(\tau)\|_\infty = 2M_1. \tag{4.87}$$

Applying Nicholsky and Bernstein inequalities,

$$\begin{aligned}\|u_x^{N_n}(\tau)\|_\infty &\leq \|u_x^{N_n}(\tau) - (I_N(u(\tau)))_x\|_\infty + \|(I_{N_n}u)_x(\tau)\|_\infty \\ &\leq K_1 N_n^{\frac{3}{2}} \left\|u^{N_n}(\tau) - I_{N_n}u(\tau)\right\| + \|(I_{N_n}u)_x(\tau)\|_\infty \\ &\leq K_1 N_n^{\frac{3}{2}} \left\|u^{N_n}(\tau) - I_{N_n}u(\tau)\right\| + M_1.\end{aligned}$$

By construction, $\|u_x^{N_n}(\tau)\| \leq 2M_1,\ \tau \in [0, \epsilon_{N_n}]$, therefore, employing the arguments used in the proof of the stability Theorem 4.3.1 with $V^{N_n} = I_{N_n}u$ and $W^{N_n} = u^{N_n}$, it holds:

$$\max_{0\leq\tau\leq\epsilon_{N_n}} \left\|u^{N_n}(\tau) - I_{N_n}u(\tau)\right\|^2 \leq R\left(\|I_{N_n}(u(0)) - u^{N_n}(0)\|^2 + \int_0^{\epsilon_{N_n}} \|F^{N_n}(\tau)\|^2 d\tau\right),$$

where $\|I_{N_n}(u(0)) - u^{N_n}(0)\|^2 = 0$ by definition of the collocation method and term $\|F^{N_n}(\tau)\|$ is given by (4.82).

Term $\|F^{N_n}(\tau)\|$ can be globally bounded in $[0, T]$. Therefore in $[0, \epsilon_{N_n}]$, by Proposition 4.3.2 and the regularity hypothesis over u

$$\|F^{N_n}(\tau)\| \leq M_2 N_n^{-s} \leq M_2 N_n^{-2},$$

This implies, rearranging terms, that for any $\tau \in [0, \epsilon_{N_n}]$

$$\max_{0\leq\tau\leq\epsilon_{N_n}} \|u_x^{N_n}(\tau)\|_\infty \leq K N_n^{-\frac{1}{2}} + M_1, \tag{4.88}$$

where K is a constant that depends on M_2 and R. This is a contradiction with (4.87) since

$$\lim_{n\to\infty} \max_{0\leq\tau\leq\epsilon_{N_n}} \|u_x^{N_n}(\tau)\|_\infty \leq M_1 < 2M_1. \tag{4.89}$$

Now, let $\epsilon^* > 0$ be the maximum value for which it exists a value N_0 big enough such that $\forall N \geq N_0$ it holds that

$$\|u_x^N(\tau)\|_\infty < 2M_1, \quad \tau \in [0, \epsilon^*].$$

Suppose $\epsilon^* < T$. We argue as before, so that

$$\|u_x^N(\tau)\|_\infty \leq K_1 N_n^{\frac{3}{2}} \left\|u^{N_n}(\tau) - I_{N_n}u(\tau)\right\| + M_1.$$

and noting that $\forall N \geq N_0$, by Stability Theorem 4.3.1 on $[0, \epsilon^*]$

$$\max_{0\leq\tau\leq\epsilon^*} \|u_x^{N_n}(\tau)\|_\infty \leq K N^{-\frac{1}{2}} + M_1, \tag{4.90}$$

Again, by a continuity argument, there must exist $\epsilon_1^* > \epsilon^*$ and a value $N_0^{\epsilon^*} >$ big enough, such that $\forall N \geq N_0^{\epsilon^*}$ it holds that $\|(u^N)_x\|_\infty < 2M_1, \quad \tau \in [0, \epsilon_1^*]$. Otherwise we could find a strictly increasing sequence $N_1^{\epsilon^*}, N_2^{\epsilon^*}, ... \to \infty$ and a strictly decreasing sequence $\epsilon_{N_1^{\epsilon^*}}, \epsilon_{N_2^{\epsilon^*}} ... \to \epsilon^*$ such that

$$\lim_{n\to\infty} \max_{0\leq\tau\leq\epsilon_{N_n^{\epsilon^*}}} \|u_x^{N_n^{\epsilon^*}}(\tau)\|_\infty = 2M_1,$$

which would lead to a contradiction with (4.90) exactly with same arguments as before.

□

Theorem 4.3.2. *(Convergence)*

Let $u(\tau)$ be the solution of (4.77). Suppose that $u(\tau)$, $u_\tau(\tau)$ are respectively functions in H_p^{s+2} and H_p^s and continuous with respect $\tau \in [0,T]$.

Then, if $u^N(x,\tau)$ is the approximation obtained by the collocation method (4.79), it exists a constant

$$M = M\left(\max_{0\le\tau\le T}\left\{\left\|\frac{\partial^{s+1}u}{\partial x^{s+1}}\right\|, \left\|\frac{\partial^{s+2}u}{\partial x^{s+2}}\right\|, \left\|\frac{\partial^s u_\tau}{\partial x^s}\right\|\right\}\right),$$

and $N_0 \in \mathbb{N}$ such that $\forall N \ge N_0$ it holds

$$\max_{0\le\tau\le T}\left\{\|u(\tau) - u^N(\tau)\|\right\} \le MN^{-s}.$$

Proof. We decompose:

$$\|u(\tau) - u^N(\tau)\| \le \|u(\tau) - I_N(u(\tau)\| + \|I_N(u(\tau)) - u^N(\tau)\|.$$

The term $\|u(\tau) - I_N(u(\tau)\|$ is bounded by the estimate [10, (5.1.16)]

$$\max_{0\le\tau\le T}\|u(\tau) - I_N(u(\tau))\| \le K_1 N^{-s} \max_{0\le\tau\le T}\left\|\frac{\partial^s u}{\partial x^s}(\tau)\right\|.$$

We apply Theorem 4.3.1 to the second term $\|I_N(u(\tau)) - u^N(\tau)\|$, taking $V^N = I_N(u)$ and $W^N = u^N$. Note that the definition of the collocation method (4.65) implies that $G^N \equiv 0$ and that the threshold condition (4.80) holds for $N \ge N_0$ big enough from Proposition 4.3.3. Therefore,

$$\max_{0\le\tau\le T}\|I_N(u(\tau)) - u^N(\tau)\|^2 \le R\left(\|I_N(u(0)) - u^N(0)\|^2 + \int_0^T \|F^N(\tau)\|^2 d\tau\right).$$

We apply Proposition 4.3.2 to bound

$$\|F^N(\tau)\| \le M_1 N^{-s}.$$

For completing the proof, note that in the collocation method $u^N(0) = I_N(u_0)$. Therefore, we can bound

$$\max_{0\le\tau\le T}\left\{\|u(\tau) - u^N(\tau)\|\right\} \le K_1 N^{-s} \max_{0\le\tau\le T}\left\|\frac{\partial^s u}{\partial x^s}(\tau)\right\| + \sqrt{R} M_1 N^{-s},$$

by the regularity hypothesis over u.

□

In this Subsection we have given general regularity conditions that guarantee the results of stability, consistency and convergence.

Comments about threshold condition in our financial problem.

In the theoretical analysis, we implicitly assumed that the initial condition, $u_0(x)$, was smooth enough. The numerical analysis of the pseudospectral method when we apply it to the financial problem is postponed to Section 4.4. Nevertheless, we study now the regularity of the initial condition.

Note that $u(0) = u_0$ is explicitly given. This is relevant in Proposition 4.3.3 (Threshold condition)

$$\|(u^N)_x(0)\|_\infty = \|(I_N(u_0))_x\|_\infty \leq M_1$$

where M_1 is independent of N. We have also to check in Theorem 4.3.2 (Convergence)

$$\max_{0\leq\tau\leq T} \left\{\|u(\tau) - u^N(\tau)\|\right\} \leq MN^{-s}.$$

which implies that we have to study $\|u(0) - u^N(0)\| = \|u_0 - I_N(u_0)\|$.

In our problem, we invoke the pseudospectral method in different time steps (see Subsection 4.3.4). We solve equation (4.77) with different initial conditions which correspond to a certain function

$$u_0 = u_j(t_m, y_k, x),\ j \in \{1, w\},$$

where t_m and y_m are values from the time and number of shares meshes respectively and functions $u_j(t, y, x),\ j \in \{1, w\}$ were defined in (4.54).

We recall that functions $u_j(t, y, x),\ j \in \{1, w\}$ were constructed from $H_j(t, y, \hat{x}), j \in \{1, w\}$ after performing the odd-even extension, imposing periodic boundary conditions and a change of variable to $[0, 2\pi]$.

For $t_m = T$, we know that $H_w(T, y_k, x)$ is a continuous but not differentiable function and, in general, the odd-even extension procedure does not give differentiable functions, even when applied to differentiable functions.

1. Cases $u_0 = u_j(t_m, y_k, x),\ j \in \{1, w\},\ t_m \neq T$ and $u_0 = u_1(T, y_k, x)$:

For $t_m \in [0, T),\ j \in \{1, w\}$, the conditions

$$\|u_0 - I_N(u_0)\| \leq MN^{-2}, \quad \|(I_N(u_0))_x\|_\infty \leq M_1 \tag{4.91}$$

have a justification based in the following result.

Proposition 4.3.4. *Let $f(x),\ x \in \left(0, \frac{\pi}{2}\right)$ be a twice derivable function such that $f'(0^+) = 0$ and $f'\left(\frac{\pi^-}{2}\right),\ f''(0^+),\ f''\left(\frac{\pi^-}{2}\right)$ exist.*

We define the function:

$$f^e(x) = \begin{cases} f(x), & x \in \left(0, \frac{\pi}{2}\right], \\ 2f\left(\frac{\pi}{2}\right) - f\left(\pi - x\right), & x \in \left(\frac{\pi}{2}, \pi\right], \\ 2f\left(\frac{\pi}{2}\right) - f\left(x - \pi\right), & x \in \left(\pi, \frac{3\pi}{2}\right], \\ f\left(2\pi - x\right), & x \in \left(\frac{3\pi}{2}, 2\pi\right). \end{cases}$$

It holds that:

$$\|f^e - I_N(f^e)\| \leq K_1 N^{-s}, \ s = 2.$$

Proof. Function f^e admits a classical derivative in $(0, 2\pi)$

$$(f^e(x))' = \begin{cases} f'(x), & x \in \left(0, \frac{\pi}{2}\right], \\ f'\left(\pi - x\right), & x \in \left(\frac{\pi}{2}, \pi\right], \\ -f'\left(x - \pi\right), & x \in \left(\pi, \frac{3\pi}{2}\right], \\ -f'\left(2\pi - x\right), & x \in \left(\frac{3\pi}{2}, 2\pi\right), \end{cases}$$

because $f'(0^-) = 0 \Rightarrow (f^e)'(\pi - \pi^-) = -(f^e)'(\pi^+ - \pi) = 0$. It also admits a second derivative (in distributional sense)

$$(f^e(x))'' = \begin{cases} f''(x), & x \in \left(0, \frac{\pi}{2}\right), \\ -f''\left(\pi - x\right), & x \in \left(\frac{\pi}{2}, \pi\right), \\ -f''\left(x - \pi\right), & x \in \left(\pi, \frac{3\pi}{2}\right), \\ f''\left(2\pi - x\right), & x \in \left(\frac{3\pi}{2}, 2\pi\right), \end{cases}$$

defined everywhere but for $x = \left\{\frac{\pi}{2}, \pi, \frac{3\pi}{2}\right\}$.

Therefore, $f^e \in H_p^2$ and the standard approximation result for interpolation and Proposition 4.3.1 can be applied. □

Up to the change of variable

$$x = \hat{x}_{\min} + \frac{4\hat{x}_{\max} - 4\hat{x}_{\min}}{2\pi} x,$$

note that for $t_m \neq T$, function $H_j(t_m, y_k, \hat{x}),\ j \in \{1, w\}$ defined in $\hat{x} \in [\hat{x}_{\min}, \hat{x}_{\max}]$ plays the role of $f(x)$ and $u_j(t_m, y_k, x) = H_j^e(t_m, y_k, \hat{x})$ plays the role of $f^e(x)$ of the previous Proposition.

The result has to be applied in the limit $\hat{x}_{\min} \to -\infty$ and for H_j regular enough.

For the case when there are no transaction costs, the regularity and that

$$\lim_{\hat{x}\to-\infty} \frac{\partial H_j}{\partial \hat{x}}(t_m, y_k, \hat{x}) = 0$$

can be explicitly checked. We conjecture that the conditions hold when transaction costs appear.

For function $u_0 = u_1(T, y_k, x)$ the same argument can be applied.

2. Case $u_0 = u_w(T, y_k, x)$:

This initial condition has to be studied independently. It is easy to check that in this case, $u_0 \in H_p^1$, that we will denote by $u_{0,x}$. Function $u_{0,x}$ is of finite variation, derivable everywhere except at two points where it presents two jump discontinuities and which correspond to the strike value up to the odd-even extension and the change of variable.

In this case, we know that the truncated Fourier series $P_N(u_{0,x})$ converges pointwise to $\frac{u_{0,x}(x^-)+u_{0,x}(x^+)}{2}$. Therefore, it exists C, independent of N, such that $\|P_N(u_{0,x})\|_\infty \leq C$ (see analysis of the Gibbs effect in [10]).

We perform the decomposition

$$\begin{aligned}\|(I_N(u_0))_x\|_\infty &\leq \|(I_N(u_0))_x - (P_N(u_0))_x\|_\infty + \|(P_N(u_0))_x\|_\infty \\ &\leq K_1 N^{\frac{3}{2}} \|I_N(u_0) - P_N(u_0)\| + \|P_N(u_{0,x})\|_\infty,\end{aligned}$$

where we have used Bernstein and Nicholsky inequalities and the fact that truncation does permute with differentiation.

Now, since $u_0 \in H_p^1$ it holds that $\|I_N(u_0) - P_N(u_0)\| \leq K_2 \|I_N(u_0) - u_0\|$. Therefore, we can bound

$$\|(I_N(u_0))_x\|_\infty \leq K N^{\frac{3}{2}} \|I_N(u_0) - u_0\| + C.$$

The only thing that remains to check is the behaviour of $\|I_N(u_0) - u_0\|$. We empirically study the L^2 interpolation error. We compute, for $N = \{128, 256, 512, 1024, 2048\}$,

$$\|u_1(T, y_k, x) - I_N(u_1(T, y_k, x))\|, \quad \|u_w(T, y_k, x) - I_N(u_w(T, y_k, x))\|$$

with the Matlab routine *quad* and plot the results in the following Figure.

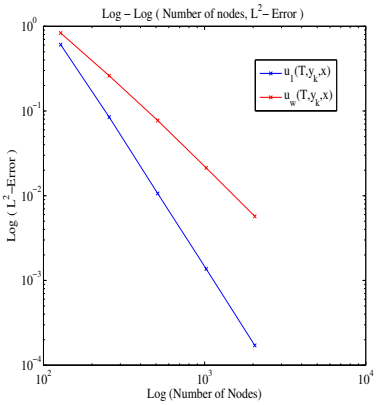

Figure 4.3: Graph (logarithmic scale) of $\|u_1(T, y_k, x) - I_N(u_1(T, y_k, x))\|$ (blue) and $\|u_w(T, y_k, x) - I_N(u_w(T, y_k, x))\|$ (red) for $N = \{128, 256, 512, 1024, 2048\}$ (horizontal axis).

The slopes of the regression lines are -2.95 for u_1 and -1.85 for u_w. The convergence rate seems to be independent of the value of y_k, the Strike or γ. This implies that the regularity condition for u_0 in Proposition 4.3.3 is fulfilled for $j \in \{1, w\}$ and suggest that the expected convergence rate of the numerical solution $H_j^{\mathbf{N}}, j \in \{1, w\}$ of our problem is

$$\|H_w - H_w^N\| \leq CN^{-2}, \quad \|H_1 - H_1^N\| \leq CN^{-s}, \ s \geq 2$$

in the spatial variable.

Localization error

When we extend the function twice and we impose periodic boundary conditions, we are modifying the real terminal conditions of the partial differential equation associated with the No Transaction region and we are inducing a numerical error, called the *localization error*.

If the spatial variable is not bounded, a way of studying the effect of the *localization error* in a fixed domain D (approximation domain) is given in [9]. The procedure would be to check that the difference of the exact solution of the periodic problem and the exact solution of the real problem on D converges to 0 as we increase the limits of the spatial variable before proceeding to the periodic extension.

Remark 4.3.1. Note that the convergence and the localization error analysis are totally independent. In the convergence analysis we have proved that the numerical solution converges to the exact solution of the periodic problem.

In the localization error analysis we will prove that the exact solution of the periodic problem converges to the exact solution of the original problem on the approximation domain for increasing size of the computational domain.

The analysis will be performed over the partial differential equation (4.45):

$$\frac{\partial Q_j}{\partial t} + \left(\alpha - \frac{\sigma^2}{2}\right)\frac{\partial Q_j}{\partial \hat{x}} + \frac{1}{2}\sigma^2\frac{\partial^2 Q_j}{\partial \hat{x}^2} = 0, \quad j \in \{1, w\},$$

where $\hat{x} = \log(S)$.

We recall the bankruptcy function introduced in Subsection 4.2.4. For a fixed $E = E_0$, $X = X_0$, we are going to work with functions $Q_j^{B_{E_0,X_0}}, \quad j \in \{1, w\}$.

We also recall Proposition 4.2.7 which stated that it exists $M = M(X_0, E_0) > 0$ such that

$$0 \leq Q_j^{B_{E_0,X_0}} \leq M, \quad j \in \{1, w\}.$$

Equation (4.45) has to be solved for each value of y, so let $y = y_0$ and $t = t_0 \in [0, T]$. We define $\phi(\hat{x}) = Q_j^{B_{E_0,X_0}}(t_0, y_0, \hat{x})$, where $j = 1$ or $j = w$.

Definition 4.3.4. *For a fixed $L > 0$, we define the approximation domain $[-L, L]$. Let $\hat{x}^* > 0$ be such that $[-L, L] \subset [-\hat{x}^*, \hat{x}^*]$. We define the function*

$$\phi_p^{\hat{x}^*}(\hat{x}) = \begin{cases} \phi(x) & \text{if } \hat{x} \in [-\hat{x}^*, \hat{x}^*], \\ 2\phi_p^{\hat{x}^*}(\hat{x}_0) - \phi_p^{\hat{x}^*}(2\hat{x}^* - \hat{x}) & \text{if } \hat{x} \in [\hat{x}^*, 3\hat{x}^*], \\ \phi_p^{\hat{x}^*}(6\hat{x}^* - \hat{x}) & \text{if } \hat{x} \in [3\hat{x}^*, 7\hat{x}^*], \\ \phi_p^{\hat{x}^*}(\hat{x} \ mod\,([-\hat{x}^*, 7\hat{x}^*])) & \text{if } \hat{x} \notin [3\hat{x}^*, 7\hat{x}^*]. \end{cases}$$

Theorem 4.3.3. *Let $R_p^{\hat{x}^*}(\hat{x}, t)$ and $R(\hat{x}, t)$ be the solutions of*

$$\frac{\partial Q}{\partial t} + \left(\alpha - \frac{\sigma^2}{2}\right)\frac{\partial Q}{\partial x} + \frac{1}{2}\sigma^2\frac{\partial^2 Q}{\partial x^2} = 0,$$

subject to $R_p^{\hat{x}^*}(\hat{x}, t_0) = \phi_p^{\hat{x}^*}(\hat{x})$ and $R(\hat{x}, t_0) = \phi(\hat{x})$.

Let $L > 0$ and $t \leq t_0$. Then, for any $\epsilon > 0$ it exists $\hat{x}_\epsilon > 0$ such that $\forall \hat{x}^* \geq \hat{x}_\epsilon$ it holds that

$$\left|R_p^{\hat{x}^*}(\hat{x}, t) - R(\hat{x}, t)\right| \leq \epsilon, \quad \hat{x} \in [-L, L].$$

Proof. Note that it holds $\forall \hat{x} \in [-L, L]$

$$R_p^{\hat{x}^*}(\hat{x}, t) - R(\hat{x}, t) = \int_{-\infty}^{\infty} \left(\phi_p^{\hat{x}^*}(\hat{x}') - \phi(\hat{x}')\right) \Theta(\hat{x}', \hat{x}, t, t_0) d\hat{x}',$$

where $\Theta(\hat{x}', \hat{x}, t, t_0) = \frac{1}{\sigma\sqrt{2\pi(t_0 - t)}} \exp\left(\frac{-\left[\hat{x}' - (\hat{x} + \left(\alpha - \frac{\sigma^2}{2}\right)(t_0 - t))\right]^2}{2\sigma^2(t_0 - t)}\right)$.

This function can be split in :

$$R_p^{\hat{x}^*}(\hat{x},t) - R(\hat{x},t) = \int_{-\infty}^{-\hat{x}^*} \left(\phi_p^{\hat{x}^*}(\hat{x}') - \phi(\hat{x}')\right) \Theta d\hat{x}' + \int_{\hat{x}^*}^{\infty} \left(\phi_p^{\hat{x}^*}(\hat{x}') - \phi(\hat{x}')\right) \Theta d\hat{x}',$$

because, by construction, $\phi_p^{\hat{x}^*}(\hat{x}') = \phi(\hat{x}'),\ \hat{x}' \in [-\hat{x}^*, \hat{x}^*]$.

By Lemma 4.2.7, $0 \leq \phi(\hat{x}') \leq M$, and this implies, by construction, $0 \leq \phi_p^{\hat{x}^*}(\hat{x}') \leq 2M$. Therefore, we can bound

$$\left|R_p^{\hat{x}^*}(\hat{x},t) - R(\hat{x},t)\right| = 3M \int_{-\infty}^{-\hat{x}^*} \Theta d\hat{x}' + 3M \int_{\hat{x}^*}^{\infty} \Theta d\hat{x}'.$$

The result of the theorem is now straightforward since it is well known (see [9]) that

$$\int_{-\infty}^{-\hat{x}^*} \Theta d\hat{x}' \underset{-\hat{x}^* \to -\infty}{\longrightarrow} 0,$$
$$\int_{\hat{x}^*}^{\infty} \Theta d\hat{x}' \underset{\hat{x}^* \to \infty}{\longrightarrow} 0.$$

□

A numerical example of this result is presented in Subsection 4.4.2.

4.4 Numerical results

4.4.1 Implementation of the method. Remarks

Several temporal implementations for the Fourier method have been tested: explicit Euler, the implicit midpoint rule with Newton method to solve the nonlinear equation and the linearly implicit midpoint rule.

We have chosen the last one because it gave the best results when we compared the error convergence and computational cost. This implementation is given by:

$$\frac{\hat{U}^{n+1} - \hat{U}^n}{\Delta t} = \mathrm{L}\left(\frac{\hat{U}^{n+1} + \hat{U}^n}{2}\right) + \mathrm{NL}\left(\frac{3}{2}\hat{U}^n - \frac{1}{2}\hat{U}^{n-1}\right)$$

Prior to the analysis of the error convergence, we are going to make a remark about several properties of the model that affect the behaviour of the numerical method that has been designed.

The number of shares.

When there are no transaction costs ($\lambda = \mu = 0$), the problem has a solution which is explicitly computable. In this case, we have already mentioned that the optimal trading

strategies of both processes satisfy $y_j^{\mathscr{B}} = y_j^{\mathscr{S}}, \quad j \in \{1, w\}$ and that they were given in the original variables by the formulas:

$$y_1^{\mathscr{B}}(t,S) = y_1^{\mathscr{S}}(t,S) = \frac{\delta(T,t)}{\gamma S}\frac{\alpha - r}{\sigma^2},$$
$$y_w^{\mathscr{B}}(t,S) = y_w^{\mathscr{S}}(t,S) = \frac{\delta(T,t)}{\gamma S}\frac{\alpha - r}{\sigma^2} + \frac{\partial \mathscr{C}(t,T)}{\partial S},$$

where $\frac{\partial \mathscr{C}(t,T)}{\partial S}$ denotes the delta of the European Option price.

For simplicity reasons, we are going to restrict ourselves to the case when $\alpha > r$. Thus, the number of shares in the optimal strategy is always $y \geq 0$ and numerical experiments show that this also holds when transaction costs appear.

It is easy to check that as $S \to 0$ it holds that $y_j^{\mathscr{S}} \to \infty$.

In the numerical method that we have designed, we need to employ quite small values for the logarithmic stock price. Therefore, up to a certain level, the numerical approximation of the Buying/Selling frontiers may reach the limit of the computational domain of the number of shares and we will have to truncate.

On Figure 4.4 we plot the optimal trading strategies which correspond to H_1 (left) and H_w (right). As the logarithmic stock price tends to $-\infty$ (S tends to 0), we can observe that the optimal trading strategy increases. The numerical solution is computed in a finite domain, so up to a certain level we have truncated the solution. In this numerical example, the truncation occurs at $y = 2$.

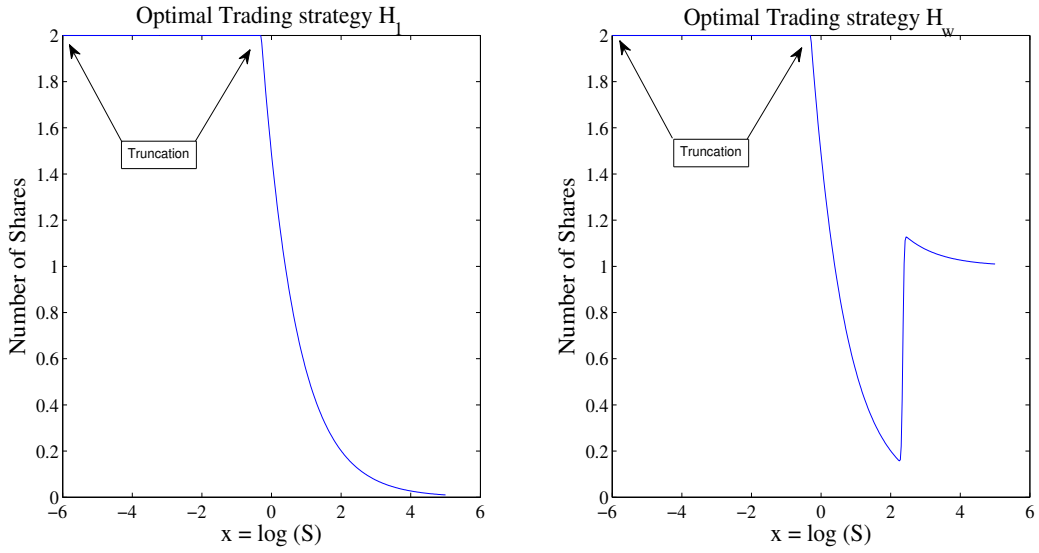

Figure 4.4: Optimal trading strategies, in function of the stock price, when there are no transaction costs.

A numerical error is generated in steps 2-4 of the algorithm of Section 4.3.4, where we have to find the optimal trading strategy and recompute $H_j^{\mathbf{N}},\ j \in \{1, w\}$ in the Buying/Selling regions.

On Figure 4.5 we can observe the effect of this error in the computation of functions $H_1^{\mathbf{N}}$ (left) and $H_w^{\mathbf{N}}$ (right). The blue lines represent the numerical value obtained and the red dashed line the exact value of the function. The zone marked as "share truncation error" is due to the truncation of the number of shares because in that zone we cannot compute a numerical approximation to the frontiers. The regularizing effect is explained below, jointly with the Gibbs effect.

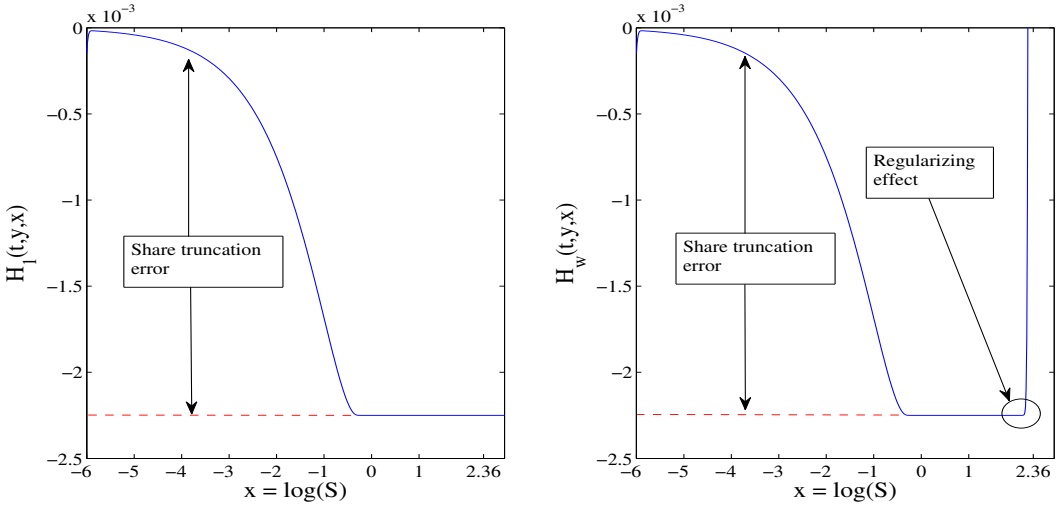

Figure 4.5: Error generated in functions $H_1^{\mathbf{N}}$ and $H_w^{\mathbf{N}}$ due to the finite computational domain of the number of shares.

We note that we can control (or even remove) the truncation error for functions $H_j^{\mathbf{N}},\ j \in \{1, w\}$ just increasing the domain of the number of shares, something that progressively moves this error to the left until it disappears. Besides, since

$$p_w(t_m, \hat{x}) = \frac{\delta(T, t_m)}{\gamma} \left(H_w(t_m, 0, \hat{x}) - H_1(t_m, 0, \hat{x}) \right),$$

some cancellation effect of the error has also been observed. Numerical experiments show that for $y_{\max}$ big enough (covering all the values which correspond to the approximation domain), this error has no perceptible effects in the option price.

The Gibbs effect.

At time $t = T$, function $H_w(T, y, x)$ is continuous but not differentiable. In Figure 4.6 we plot function $H_w(T, 0, x)$ and zoom around $\hat{x}_K$, the point where the function is not differentiable.

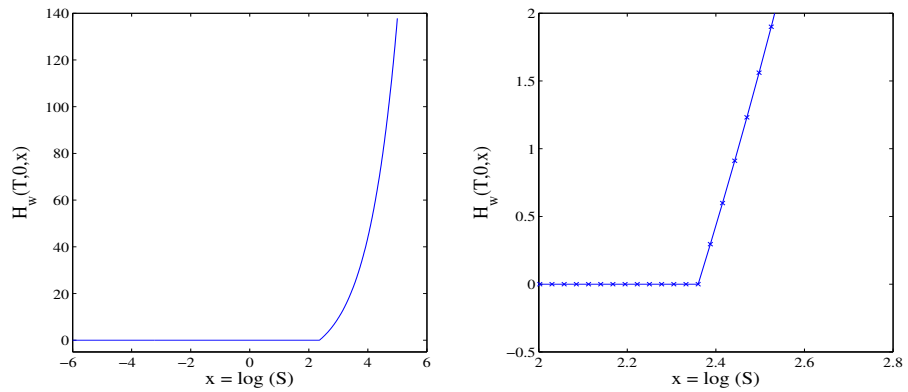

Figure 4.6: Value of $H_w(T, 0, x)$ (left) and zoom around $\hat{x}_K$ (right).

When approximating the function by trigonometric polynomials, this causes some oscillations, known that the Gibbs phenomena. These oscillations will be reflected for a very brief period of time in the computation of the optimal trading strategies.

The regularization effect of the partial differential equation quickly smoothes out the possible singularities, so the true value of function H_w (and therefore the corresponding optimal trading strategies) can be rapidly approximated by its truncated Fourier series. This could be expected from the results of [10]. Numerical experiments suggest that the smoothing velocity depends on Δt and $\Delta \hat{x}$.

The following picture shows a zoom of the encircled zone of Figure 4.5, where the smoothing effect of the partial differential equation around the strike can be observed for $t < T$.

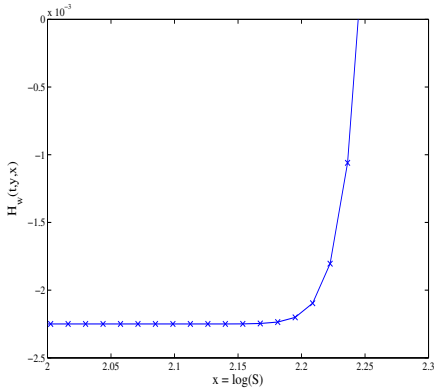

Figure 4.7: Graph of $H_w^{\mathbf{N}}(t, 0, \hat{x})$, t<T (zoom around $\hat{x}_K$)

The computational cost of the method depends on the values of Δt and Δx, but also on the value of the strike $\hat{x}_K = \log(K)$.

The objective of this work was to reduce the impact of the exponential growth of the

objective function. Although we can work now with very big values for the stock or the strike, the exponential growth affects the computational cost.

If we compute options for higher and higher strikes x_K, we can observe that the growth of function H_w becomes more and more steep at $x = x_K$, something that worsens the Gibbs phenomena. This will force us to use smaller values for Δx and Δt in order to reduce the impact of the Gibbs effect and wipe it out soon. A reduction of the computational time cost for long maturity options could be achieved through a variable time-step method.

Discontinuity of the Buying frontier of function H_w

When we have sold an option ($j = w$), the explicit formula of the Buying frontier (when there are no transaction costs), shows that there is a discontinuity at $S = K$ when $t \to T$, so that

$$\lim_{t \to T} \frac{\partial \mathscr{C}(t,T)}{\partial S} = I_{S \geq K}.$$

Numerical experiments show that this behaviour remains when there are transaction costs. Therefore, the regions in which the state space is divided by the frontiers (Selling/Buying/No Transactions Regions) have a jump discontinuity at $t = T$

When we study the convergence of the numerical method for function H_1, where there is not such discontinuity, we obtain a better error convergence in the spatial variable.

As we will see, for function H_w we will not obtain the same rate of error convergence. The reason for this probably lies in the jump discontinuity of the regions or in the fact that function H_w is continuous but not differentiable at $t = T$.

4.4.2 Error convergence, localization error and computational cost

We now proceed to numerically check the rates of convergence of the error, the effect of the localization error and the computational cost of the method. When no transaction costs are present ($\lambda = \mu = 0$), the problem can be explicitly solved. Therefore, we employ the exact function values to check the error behaviour.

For studying the error convergence, we have to choose an approximation domain $[L_{\min}, L_{\max}]$ and a computational domain $[\hat{x}_{\min}, \hat{x}_{\max}]$. We define a set of test points $\{\hat{x}_p\}_{p=0}^{N_p}$ (of the approximation domain):

$$\hat{x}_p = L_{\min} + p\frac{L_{\max} - L_{\min}}{N_p}, \quad p = 0, 1, 2, ..., N_p.$$

It is in this set of points where we will study the time, spatial and number of shares error convergence.

Definition 4.4.1. *Let $f(t, y, \hat{x})$ denote the exact value of a function which can either be H_j, $j \in \{1, w\}$, the option price p_w or the optimal trading strategies $y_j^{\mathscr{B}}, y_j^{\mathscr{S}}$, $j \in \{1, w\}$. We recall that $S = \exp(\hat{x})$.*

Let $f^{\boldsymbol{N}}$ denote the numerical approximation subject to $\boldsymbol{N} = (N_t, N_y, N_{\hat{x}})$, which were given in Definition 4.3.2.

We globally define the mean square error of the numerical approximation of function $f^{\boldsymbol{N}}$ as

$$RMSE\left(f^{\boldsymbol{N}}\right) = \sqrt{\frac{1}{N_p+1}\sum_{p=0}^{N_p}\left(f(\hat{x}_p) - f^{\boldsymbol{N}}(\hat{x}_p)\right)^2}. \tag{4.92}$$

Spatial Error convergence

We fix the parameter values σ=0.1, $\alpha = 0.1$, r=0.085, the strike and maturity ($t = 0$ today)

$$\begin{cases} \hat{x}_K = 2 \ \ (\text{K=7.389}), \\ T = 0.5 \ \ (\text{years}). \end{cases}$$

For this numerical example, we take $[L_{\min}, L_{\max}] = [1, 3]$ and $[\hat{x}_{\min}, \hat{x}_{\max}] = [-5, 5]$. The limits of the computational domain have been taken big enough in order to minimize the effect of the localization error.

For clarifying purposes, we point that this corresponds to an option with strike $K = 7.389$ and that we compute several functions for stock prices $S_p = e^{\hat{x}_p}$ which vary from 2.718 to 20.085 (i.e. for options At and (very) In/Out the money). For the number of shares, we set $y \in [0,\ 2]$. We also set $N_p = 10$ (all the nodes of the approximation domain for $N_{\hat{x}} = 50$).

For the spatial convergence analysis, we take $\Delta y = 2.5 \cdot 10^{-3}$, $\quad \Delta t = 5 \cdot 10^{-5}$ and compute the RMSE for $N_x = \{50, 100, 200, 400, 800, 1600\}$.

The first two functions that we are going to study are $H_j^{\mathbf{N}}$, $j \in \{1, w\}$. We restrict ourselves to $t = y = 0$, i.e., the functions that are employed to compute the option price for a maturity of 0.5 years.

The following picture shows the logarithmic (left) and the semilogarithmic (right) values of RMSE($H_1^{\mathbf{N}}$) (solid-red) and RMSE($H_w^{\mathbf{N}}$) (blue).

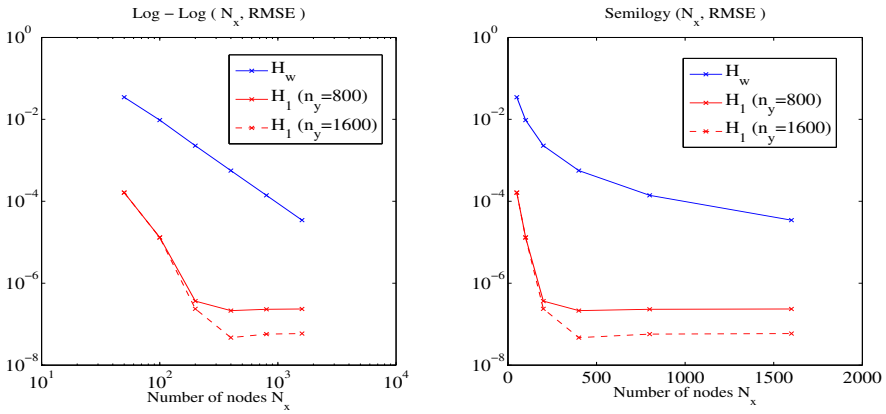

Figure 4.8: Spatial error convergence of functions $H_1^{\mathbf{N}}$ (red) and $H_w^{\mathbf{N}}$ (blue) in both logarithmic (left) and semilogarithmic (right) scales.

The slope of the regression lines are -2.004 for H_w and -4.397 for H_1 (3 first points) in the logarithmic scale (left). In the semilogarithmic scale (right), we see that we might be obtaining the so called "spectral convergence" for function H_1. We realize another experiment with $\Delta y = 1.25 \cdot 10^{-3}$ (dashed-red) to check that the lowest value of the error reached by H_1 (solid-red) was given by the value of Δy.

H_1 and H_w seem to present different error behaviour. Since we are employing the same numerical method for both, the reason of this must lie in the function properties. Function H_1 and its optimal trading strategy are both smooth functions at any time and for any point. On the other hand, H_w is continuous but not differentiable and its optimal trading strategy presents a jump discontinuity, both at maturity and for $x = x_K$.

In order to check numerically that one of this two properties is worsening the error behaviour, we are going to carry out the following experiment with H_w. Time interval is $t \in [0,\ 0.5]$. Since we have the explicit formula when there are no transaction costs, we are going to compute the exact function value at $t = 0.49$ and apply the numerical method in $[0,\ 0.49]$ with the same discretizations for Δt and Δy.

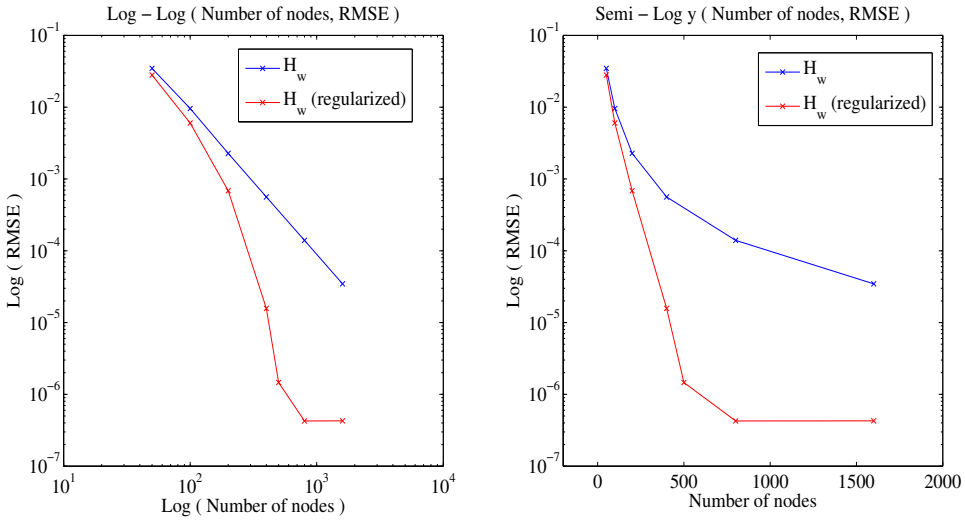

Figure 4.9: Graph of the spatial error convergence of $H_w^{\mathbf{N}}$, for $t \in [0, 0.5]$ (red) and $t \in [0, 0.49]$ (blue).

Function H_w and its optimal trading strategy are smooth functions at any moment/point prior to maturity, so we should obtain a better error convergence for the spatial error. On Figure 4.9 we can observe that the error rate if we include the maturity (blue) is worse that if we do not include it (red). This results are consistent with the upper bounds of the error convergence rate mentioned just after Theorem 4.3.2 (Comments about threshold condition).

Returning to the original experiment, when we have to compute the option price, the function values of H_w are much bigger than those of H_1 so it is the error of H_w the dominant one. The following picture shows the value of $\mathrm{RMSE}(p_w^{\mathbf{N}})$ in logarithmic scale. We recover

the same error convergence of function value H_w, since it is the dominant error in p_w.

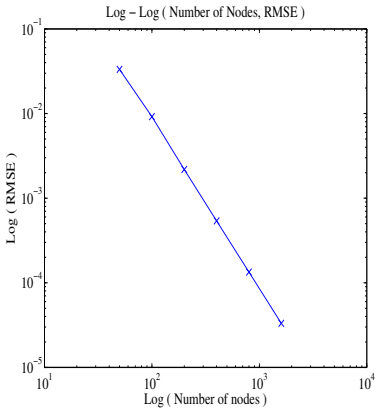

Figure 4.10: Spatial Error convergence of the option price.

We point out that for this numerical method, a relative big number of spatial nodes is needed. We have to remove soon the Gibbs effect for obtaining a good approximation to the optimal trading strategies, specially around the strike ($\hat{x}_K$) zone for function H_w, where the highest errors occur. The number of spatial nodes also depends of the size of the computational domain, which has been taken quite big in this example.

Figure 4.11 shows the absolute value of the difference between the numerical approximation of the option price and the exact option price in the whole computational domain for $N_{\hat{x}} = \{100, 200, 1600\}$. The highest errors occur around the strike zone. The localization error is perceptible, specially at the right limit of the interval.

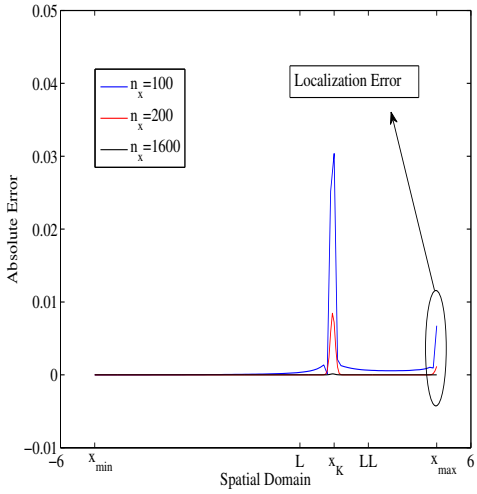

Figure 4.11: Function $H_w^{\mathbf{N}}$ absolute error in the whole computational domain.

As we can check, the size of the error at point $\hat{x}$ depends mostly in the relative position of $\hat{x}$ with respect to $\hat{x}_K$. The localization error is perceptible at the right side of the picture which corresponds to the zone where we extend the functions in the proposed numerical method.

Although the localization error will be studied later on, we mention now that the fact of employing big values for n_x reduces the impact of such error, allowing us to obtain reliable option prices, not only in the approximation domain, but almost in the whole computational domain.

In this model, a priori, there is no linearity in the relation S/K. Although the rate of error convergence is independent of the values of S or K, for clarifying purposes, we are going to study the relative error.

The option prices vary from 0 ($\hat{x}_{\min}$) to 141.36 ($\hat{x}_{\max}$) dollars in the computational domain. Since the error analysis has been done for the specific value of the strike ($K = 7.389$ dollars), we present the following table in order to get an idea of the size of the absolute/relative errors in monetary terms for $N_x = 1600$:

Stock Price (S)	Contract value (dollars)	Absolute Error (dollars)	Relative Error (%)
5.439	10^{-5}	$1.07\cdot 10^{-7}$	1.0679 %
5.974	0.0012	$6.57\cdot 10^{-6}$	0.5235 %
6.520	0.0288	$6.24\cdot 10^{-5}$	0.2167 %
7.028	0.1736	$1.27\cdot 10^{-4}$	0.0733 %
7.389	0.3936	$1.09\cdot 10^{-4}$	0.0278 %
8.014	0.9415	$2.96\cdot 10^{-5}$	0.0031 %
8.584	1.5038	$3.48\cdot 10^{-6}$	0.0002 %
9.025	1.9435	$4.05\cdot 10^{-7}$	$2.08\cdot 10^{-5}$ %
10.037	2.9551	$8.70\cdot 10^{-10}$	$2.94\cdot 10^{-8}$ %

Table 4.1: Absolute and relative errors of the price of the option. For a fixed strike of $K = 7.389$ and different stock prices, we have computed the exact Black-Scholes price of the option. We also compute the absolute and relative errors with respect to the numerical approximation.

The relative errors are quite small. The zone where they are bigger corresponds to option prices which are almost 0. We also mention that for $S \in [0.0067, 4.08]$, the real option prices are $0 \sim 10^{-16}$ (dollars) and the numerical method gives $\sim 10^{-11}$.

Finally, let us study the optimal trading strategies. In Figure 4.12 we can check that numerical approximation of the buying/selling frontiers ($y_j^{\mathscr{B}} = y_j^{\mathscr{S}},\ j \in \{1, w\}$). As it was expected when there are no transaction costs, the buying and selling frontiers collapse and approximate the exact optimal trading strategy, which is explicitly computable.

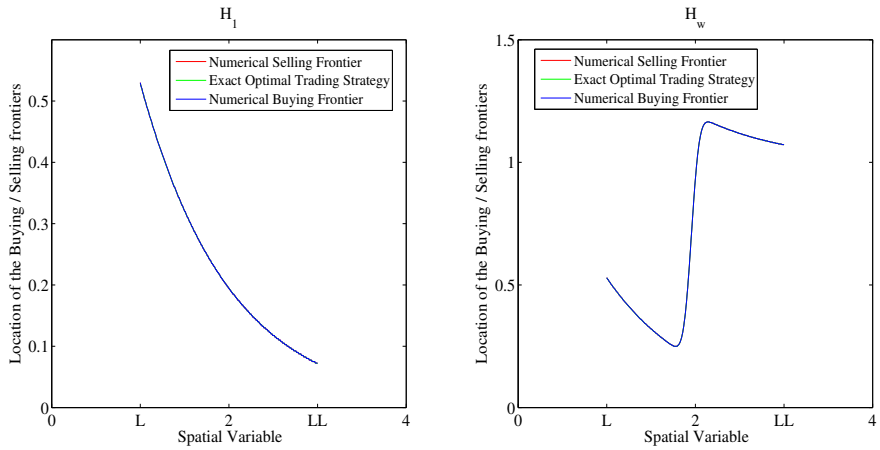

Figure 4.12: Numerical approximation of the Buying / Selling frontiers with no costs.

We compute the RMSE($y_j^{\mathscr{B}}$) for $N_{\hat{x}} = \{50, 100, 200, 400, 800, 1600\}$ and plot the results in logarithmic scale in the following picture.

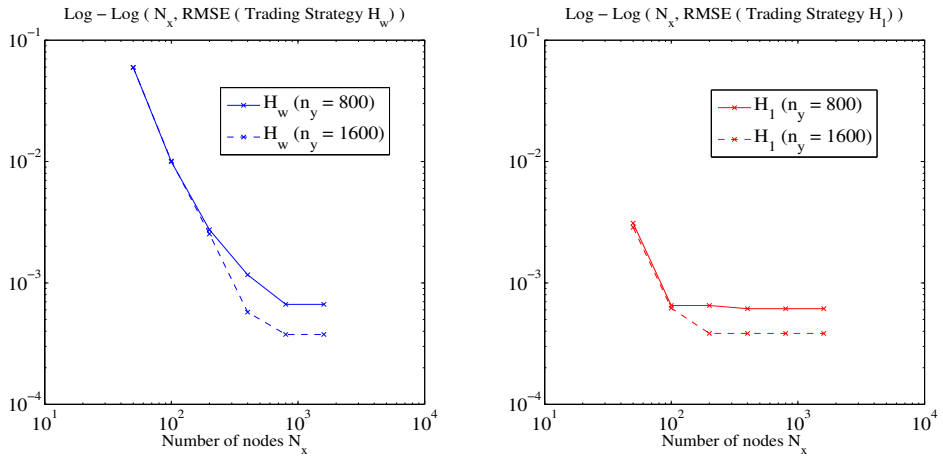

Figure 4.13: Spatial Error convergence of the numerical trading strategies $y_1^{\mathscr{B}}$ (red) and $y_w^{\mathscr{B}}$ (blue) in logarithmic scale.

The slope of the regression line of $y_w^{\mathscr{B}}$ (solid-blue) is -1.87. We recall that for $t = T$, there is a jump discontinuity at $x = x_K$. We carry out a second experiment with $\Delta y = 1.25 \cdot 10^{-3}$ (dashed-blue, dashed-red) to check that the lowest value reached by the error is marked by the size of the mesh of variable y.

Temporal Error convergence

In this experiment, we take the same values as the previous one for the model parameters, the strike and the computational/approximation domains.

We fix $\Delta\hat{x} = 6.25 \cdot 10^{-3}$ ($N_{\hat{x}} = 1600$) and $\Delta y = 2.5 \cdot 10^{-3}$. For the set of test points, we fix $N_p = 320$ (all the nodes of the approximation domain for $N_{\hat{x}} = 1600$)

We take $N_t = \{1, 2, 4, 8, 16, 25, 50, 100, 200, 400, 800, 1600, 3200, 10000\}$ (big values for Δt) because the size of the temporal error in this model is very small compared with other errors.

The following picture shows in logarithmic scale the number of temporal nodes versus the RMSE for functions $H_j^{\mathbf{N}}, j \in 1, w$.

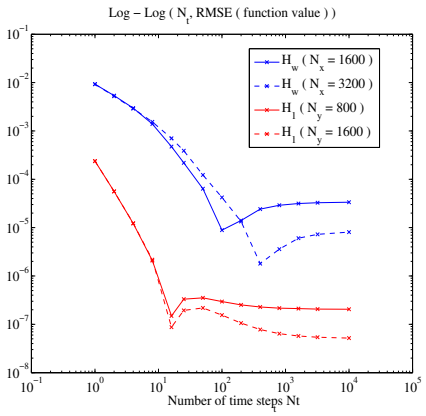

Figure 4.14: Temporal Error convergence of $H_1^{\mathbf{N}}$ (blue) and $H_w^{\mathbf{N}}$ (red) in logarithmic scale.

The slopes of the regression lines are -2.27 for H_1 (4 first points, solid-red) and -1.26 for H_w (7 first points, solid-blue). For function H_w and N_t small, we may not wipe out completely the Gibbs effect and, for bigger values of N_t, we reach very soon the error limit marked by $\Delta\hat{x}$. Perhaps this is the reason why we do not observe an order 2 in time for function H_1.

We carry out a second experiment halving the value of Δy for H_1 (dashed-red) and the value of $\Delta\hat{x}$ for H_w (dashed-blue) to check that the lowest value reached by the errors was respectively given by the size of the meshes of the other two variables.

Concerning the optimal trading strategies, temporal error is also very small.

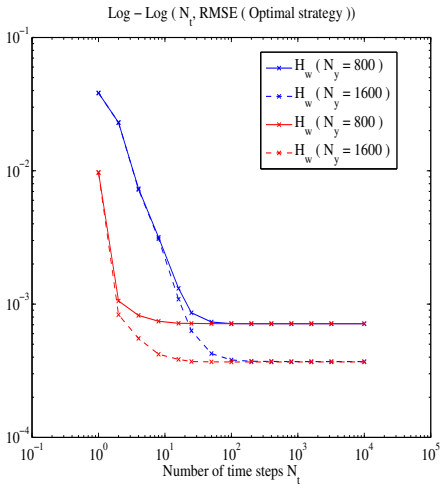

Figure 4.15: Temporal Error convergence of the numerical trading strategies $y_1^{\mathscr{B}}$ (red) and $y_w^{\mathscr{B}}$ (blue) in logarithmic scale.

The slope of the regression line of the optimal trading strategy of H_w is -1.23 (5 first

points, solid-blue). For both functions the lowest value reached by the error is given by the size of Δy in both cases as it can be checked in the experiment where we halve the value of Δy (dashed-blue/red).

Number of shares Error convergence

In this experiment, we take the same values as the previous one for the model parameters and the approximation/computational domains. We fix $\Delta\hat{x} = 6.25 \cdot 10^{-3}$ ($N_{\hat{x}} = 1600$), $\Delta t = 5 \cdot 10^{-5}$ and set $N_p = 320$.

We are going to compute RMSE for $N_y = \{8, 16, 32, 64, 128, 256, 512\}$. The following picture shows the log-log of functions $H_j,\ j \in 1, w$ (left side) and the optimal trading strategies (right side).

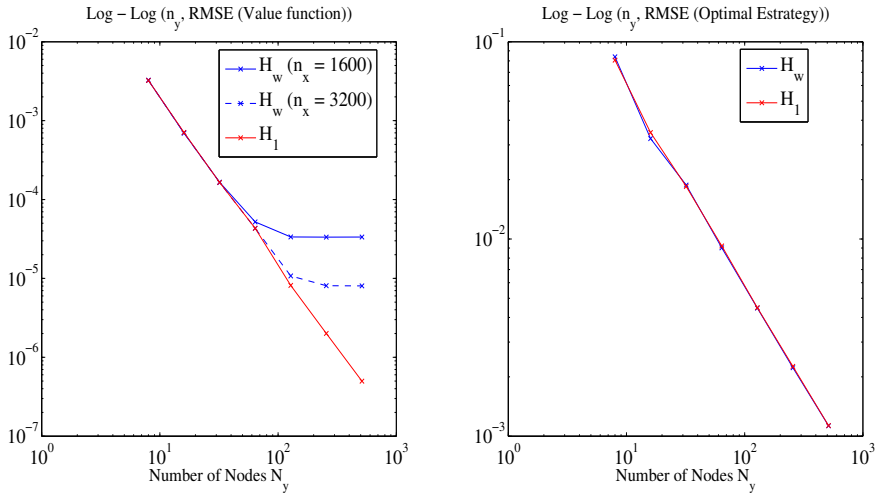

Figure 4.16: Number of shares error convergence of the value functions (left) and the optimal trading strategies (right) with $j = 1$ (red) and $j = w$ (blue) in logarithmic scale.

The slope of the regression lines is -2.11 in the case of functions H_j (red($j = 1$), solid-blue($j = w$)) and -1.01 in the case of the optimal trading strategies. We carry out another experiment (dashed-blue) where $N_{\hat{x}} = 3200$. This experiments shows that the lowest value of the error reached by function H_w (solid-blue) was given by the size of $\Delta\hat{x}$.

Localization Error

We fix the same model parameters of the previous analysis and the same approximation domain $[L_{\min}, L_{\max}] = [1, 3]$. For studying the convergence of the localization error, we propose the following experiment.

The computational domain is defined by $[\hat{x}_{min}, \hat{x}_{\max}] = [L_{\min} - M, L_{\max} + M]$ for $M > 0$ and we define the proportion

$$P(M) = \frac{L_{\max} + M - (L_{\min} - M)}{L_{\max} - L_{\min}}.$$

For the same values of $\Delta\hat{x},\ \Delta y,\ \Delta t$, we compute the RMSE for different values of $P(M)$.

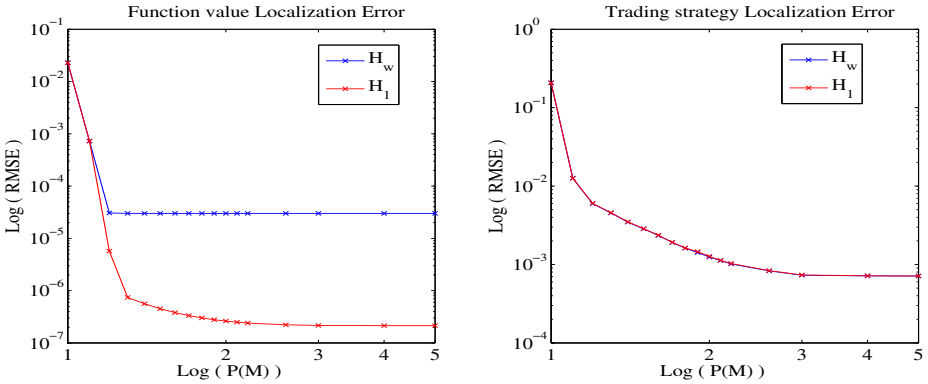

Figure 4.17: Localization Error convergence. Value of RMSE of the function values (left) and optimal trading strategies (right) for $j = 1$ (red) and $j = w$ (blue) for different values of $P(M)$ in logarithmic scale.

The previous picture shows the logarithm of $P(M)$ versus the logarithm of RMSE for the function values and the optimal trading strategies. As it can be checked, as M grows, the size of the localization error decreases as it could be expected from results of Subsection 4.3.5. The limit error is marked by the size of $\Delta\hat{x},\ \Delta y$ and Δt.

Computational cost and scaling problem.

The computational cost of the method will be checked, for example, with the same parameter values for σ, α and r of the previous example and for

$$\begin{cases} \hat{x} = \hat{x}_K = 2 \ \ (\text{S=K=7.389}) \\ T = \dfrac{1}{12} \ \ (\text{years}) \end{cases}$$

The real price of this contract is 0.113409 \$. We set: $\hat{x} \in [-5, 3]$, $y \in [0, 2]$, $\Delta y = 0.02$

Δt \ $\Delta\hat{x}$	$2\cdot 10^{-2}$	10^{-2}	$5\cdot 10^{-3}$
$2.77 \cdot 10^{-3}$	0.11013 (1.86 × 2 sg)	0.11267 (3.5 × 2 sg)	0.11331 (6.86 × 2 sg)
$1.38 \cdot 10^{-3}$	0.11008 (3.40 × 2 sg)	0.11262 (6.62 × 2 sg)	0.11325 (13.38 × 2 sg)
$6.9 \cdot 10^{-4}$	0.11006 (6.60 × 2 sg)	0.11261 (12.82 × 2 sg)	0.11326 (26.32 × 2 sg)

Table 4.2: We represent for different values of Δt (vertical) and different values of $\Delta\hat{x}$ the numerical approximation to the option price and the computational costs (seconds).

For $\Delta\hat{x} = 2\cdot 10^{-3}$, $\Delta t = 6.9 \cdot 10^{-4}$ the price is 0.113401 (68.30×2 sg).

Along the development it was also mentioned that there was a scaling problem if we worked with the original variables. This problem has been greatly reduced with our numerical method.

With the new variables, we can work with very big values for the stock and the strike and also compute options very deep in the money. For example, we can employ the approximated S&P values from year 1992 (examples of Chapter 1) and the same parameter values for σ, α and r. Let

$$\begin{cases} \hat{x}_K = 6.04 \ \ (\text{K}{=}419.89) \\ T = 0.2 \ \ (\text{years}) \end{cases}$$

Retaining the previous discretization for the number of shares and setting the spatial domain $\hat{x} \in [-5, 7]$ and $\Delta\hat{x} = 6 \cdot 10^{-3}$, we obtain

	Real Price	Numerical Solution with $\Delta t = 3.4 \cdot 10^{-5}$
$S = 402.62$	3.28	3.30
$S = 419.89$	11.49	11.52
$S = 473.42$	60.61	60.61

Table 4.3: Example of numerical option prices vs exact option prices with a higher strike ($K = 419.89$) and higher stock prices.

Note that as we increase the value of the strike, we need to reduce the time/spatial partitions in order to obtain the same relative error. This is due to the fact that at $\hat{x} = \hat{x}_K,\ t = T$, the function value H_w is continuous but not differentiable and becomes steeper as we increase the value of x_K, something that worsens the Gibbs effect.

Although we need to refine the partitions it order to wipe it out soon, once done, we do not need to employ such small time partitions. It could be worthy to employ a variable time-step method.

Empirically, the behaviour of the computational cost has been checked to be linear in the number of time steps (N_t) and in the number of shares (N_y) and almost linear in the number of spatial nodes (theoretically $\mathscr{O}(N_{\hat{x}} \log(N_{\hat{x}}))$).

4.4.3 Numerical examples with transaction costs

Now we are going to check the effects of incorporating transaction costs to the pricing model. First, we repeat one of the experiments realized in [22]. The model parameters are:

$$\begin{cases} \lambda = \mu = 0.002, \quad \gamma = 1 \\ S = 19, \quad K = 20 \\ \sigma = 0.05, \quad r = 0.085, \quad \alpha = 0.1. \end{cases}$$

The following figure shows the price difference for all maturities between $T \in [0, 3]$, i.e.

$$\text{Price difference} = p_w - \text{BS},$$

where p_w denotes the option price with transaction costs and BS the Black-Scholes price.

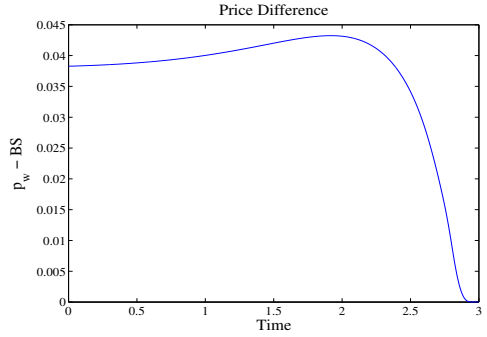

Figure 4.18: Price difference obtained with the Pseudospectral method. The results coincide with the numerical experiment in [22].

We can observe that as $T \to \infty$, the price difference at $t = 0$ approximates to λS, the additional amount of money that is needed to purchase one share. This is empirically justified in [22] with a very natural interpretation: if maturity is big enough, it will be more likely that the option finishes In The money and it is exercised, so the seller will need to have one share.

This behaviour should repeat if we fix a maturity and compute option prices for the same strike but bigger stock prices:

$$S \to \infty \Rightarrow p_w - \text{BS} \to \lambda S,$$

As we can compute now options as In The money as we want, this can be numerically checked. The following example parameters are

$$\begin{cases} \lambda = \mu = 0.002, \quad x_K = 2.8, \quad T = 0.5, \\ \sigma = 0.1, \quad r = 0.085, \quad \alpha = 0.1. \end{cases}$$

and option prices have been computed for several γ and stock prices.

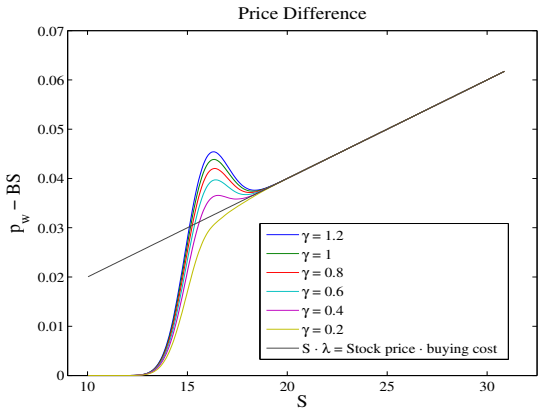

Figure 4.19: Influence of the risk aversion parameter in the price difference vs the stock price.

On the previous Figure we see that $p_w - \text{BS}$ approximates to λS as $S \to \infty$. We can also check the influence of parameter γ, the index of risk aversion. As γ grows, the seller of the option is more and more risk averse which means that he will demand more money to cover him from the possible transaction costs.

Concerning optimal trading strategies, it was conjectured in [22] that there exist two surfaces, which depend on t and S, that lay up and below the optimal trading strategy when there were no transaction costs present. Numerical experiments seem to support this conjecture.

We fix a date t. For H_1 (just optimal investment and no option), we plot in Figure 4.20 for each stock price, the Selling Frontier (red) and the Buying frontier (blue) which lie up and below the optimal trading strategy when there are no transaction costs (green). The left Figure represents the logarithmic scale for the stock price and the right Figure the natural scale.

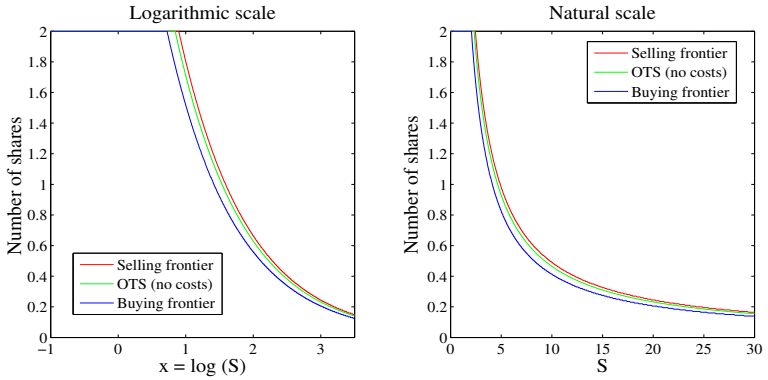

Figure 4.20: Optimal trading strategies of function $H_1^{\mathbf{N}}$ in logarithmic (left) and natural (right) scales with costs (the Selling Frontier (red) and the Buying frontier (blue)) and without costs (green).

For H_w (optimal investment + sold option), we plot in Figure 4.21 the results.

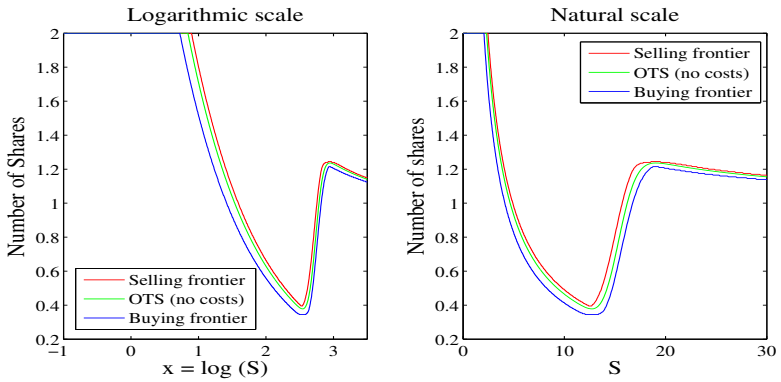

Figure 4.21: Optimal trading strategies of function $H_q^{\mathbf{N}}$ in logarithmic (left) and natural (right) scales with costs (the Selling Frontier (red) and the Buying frontier (blue)) and without costs (green).

On Figure 4.21, for each stock price,we plot the Selling Frontier (red) and the Buying frontier (blue) which lie up and below the optimal trading strategy when there are no transaction costs (green). The left Figure represents the logarithmic scale for the stock price and the right Figure the natural scale.

Other experiments were realized in [22] related with the "overshoot" ratio (OR), which is given by

$$\mathrm{OR} = \frac{(p_w - BS) - \lambda S}{\lambda S}. \tag{4.93}$$

The evolution of OR in function of different parameter values was studied and several statements were made in [22]. The numerical method employed in [22] was the binomial approximation working with variable S. In order to avoid the problems related with the growth of the Exponential Utility, the domain of the stock price was much smaller than the one we employ. Now, we have more information about the OR.

We are going to repeat the experiments, but with different parameter values. Since we can compute prices for many stock prices at once, the Figures will include, when possible, the evolution of the OR with respect to the stock price and to the corresponding parameter.

The common parameters through all the analysis will be:

$$\begin{cases} \lambda = \mu = 0.002, \quad \hat{x}_K = 2.8 \ \ (K = 16.44), \quad T = 0.5, \\ \sigma = 0.1, \quad r = 0.085, \quad \alpha = 0.1, \end{cases}$$

and for each statement just the corresponding parameters will be altered.

The (empirical) properties of the overshoot ratio are:

1. The OR is linear increasing in function of $\log(\gamma)$.
2. $\lim_{S\to 0} = -1$ and $\lim_{S\to\infty} = 0$.

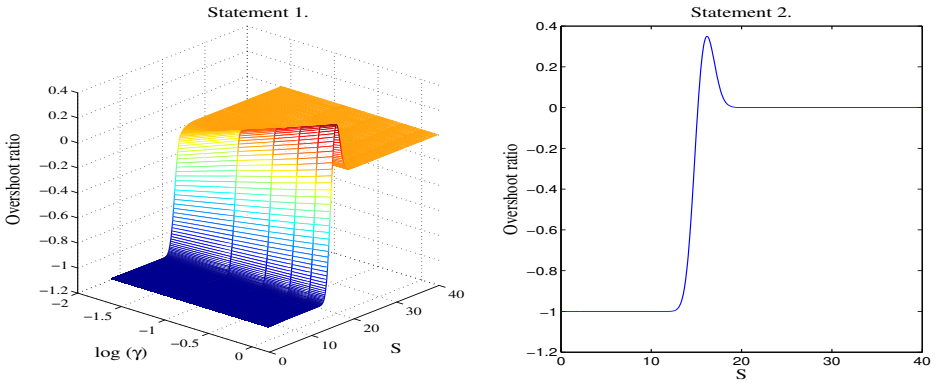

Figure 4.22: Overshoot ratio dependance of $\log(\gamma)$ (left) and S (right).

The first limit comes from (4.93) and the fact that

$$(p_w - BS) << \lambda S \ \text{ if } \ S << K$$

and the second one from $(p_w - BS) \underset{S\to\infty}{\longrightarrow} \lambda S$ (see Figure 4.19).

3. The OR is an increasing function of the volatility σ.
4. The OR is a convex decreasing function of the proportional transaction costs $\lambda = \mu$.

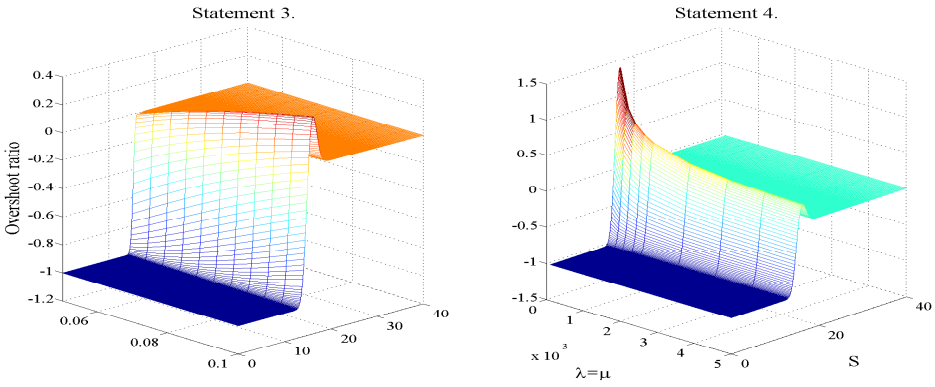

Figure 4.23: Overshoot ratio dependance of σ and $\lambda = \mu$

5. The OR is a convex function of the interest rate r.
6. The OR is a linear decreasing function of the stock's mean growth α.

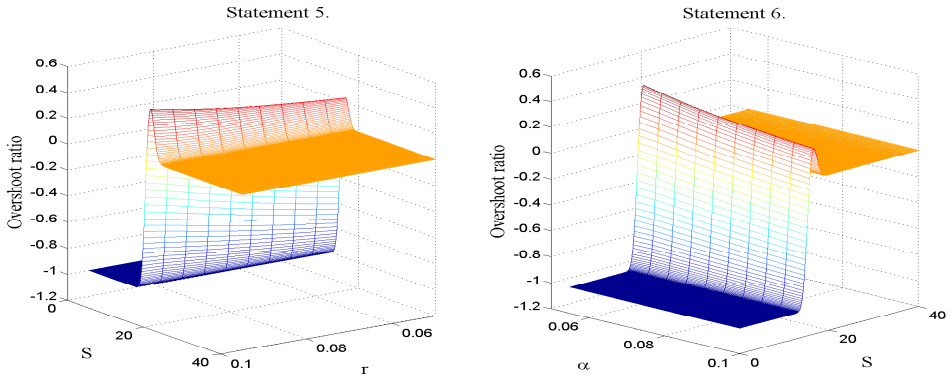

Figure 4.24: Overshoot ratio dependance of r and α.

In Statement 6, the value of interest rate was $r = 0.05$ ($\alpha > r$).

Bibliography

[1] Achdou Y., Pironneau O. (2007): Finite Element Method for Option Pricing. Université Pierre et Marie Curie.

[2] Arregui I., Vázquez C. (2012): Numerical solution of an optimal investment problem with proportional transaction costs. Journal of Computational and Applied Mathematics

[3] Björk T. (2004): Arbitrage Theory in continuous Time. Oxford University Press.

[4] Black F., Scholes (1973): The Pricing of Options and Corporate Liabilities. The Journal of Political Economy, 81, 637-654.

[5] BME Clearing House: Central counterparty entity Regulations.

[6] Bollerslev T. (1986): Generalized Autoregressive Conditional Heteroskedasticity. Journal of Economics, 31, 307-327.

[7] Bollerslev T., Engle R., Daniel (1994): Arch Models. Handbook of Econometrics (IV), Elsevier, 2959-3038.

[8] Breeden, D.T. (1979): An intertemporal Asset Pricing Model with Stochastic Consumption and Investment Opportunities". Journal of financial Economics, 7, 265-296.

[9] Breton M., de Frutos J. (2010): Option Pricing Under Garch Processes Using PDE Methods. Informs, Operations Research, 58, 1148-1157.

[10] Canuto C. et al. (2006): Spectral Methods. Fundamentals in single domains. Springer

[11] Capuzzo-Dolcetta, Lions P.L. (1987): Hamilton-Jacobi equations and state constraints problems, IMA 342, University of Minnesota.

[12] Carmona, R et al. (2009): Indifference Pricing, Princeton University Press.

[13] Christoffersen P., Jacobs K. (2004): Which GARCH Model for Option Valuation?. Management Science, 50, 1204-1221.

[14] Christoffersen P., Heston S., Jacobs K. (2013): Capturing Option Anomalies with a Variance-Dependent Pricing Kernel. Review of Financial Studies, 26, 1963-2006.

[15] Corraldi V. (2000): Reconsidering the continuos time limit of the GARCH(1,1) process. Journal of Econometrics 96 (2000),145-153.

[16] Cox J., Ingersoll J., Ross S. (1985): An Intertemporal General Equilibrium Model of Asset Prices. JSTOR. Econometrica, Volume 53, Issue 2, 363-384.

[17] Cox J., Ingersoll J., Ross S. (1985): A Theory of the Term Structure of Interest rates. Econometrica, Volume 53, 385-408

[18] Crandall M.G. and Lions P.L. (1983): Viscosity solutions of Hamilton-Jacobi equations. Trans. Amer. Math. Soc., 277, 1-42.

[19] Crandall M.G., Ishii H. and Lions P.L. (1990): User's guide to viscosity solutions of second order partial differential equations, Dep. of Mathematics, University of California.

[20] Cvitanić J., Karatzas I. (1996): Hedging and Portfolio Optimization under Transaction Costs: A Martingale Approach, Mathematical Finance, 6(2),133-165.

[21] Davis M.H.A., Norman A.R. (1990): Portfolio selection with transaction costs. Mathematics of Operations Research Vol. 15 N 4.

[22] Davis M.H.A., Panas V.G., Zariphopoulou T (1993): European Option Pricing with transaction costs. Journal of Control and Optimization. Siam. 31, 2, 470-493.

[23] Day M., Yi F. (2009): Finite-Horizon Optimal Investment with Transaction Costs: A Parabolic Double Obstacle Problem.

[24] Duan J.C. (1995): The Garch Option Pricing Model. Mathematical Finance, 5, 13-32.

[25] Duan J.C., Simonato (1998): Empirical Martingale Simulation. Management Science, 44, 1218-1233.

[26] Duan J.C., Hua Zang (2000): Pricing Hang Seng Index options around the Asian financial crisis. A GARCH approach. Elsevier, 1989-2014

[27] Elliot D., Rao K. (1982): Fast Transforms: Algorithms, Analyses, Applications. Academic Press. Inc

[28] Elliot R., Kopp P. (1999): Mathematics of Financial Markets. Springer.

[29] Engle R. (1982): Autoregressive Conditional Heteroscedasticity with Estimates of the Variance of United Kingdom Inflation. Econometrica, 50, 987-1007.

[30] de Frutos J., García-Archilla B., Novo J. (2000): A postprocessed Galerkin method with Chebyshev or Legendre polynomials. Numerische Mathematik, 86, 419-442

[31] Friedman A. (1982): Variational Principles and Free-Boundary problems, Wiley, New York.

[32] García-Archilla B., Novo J., Titi E.S. (1998): Postprocessing the Galerkin method: A novel approach to approximate inertial manifolds. SIAM, 35, 2, 941-972.

[33] Harrel F. (2001): Regression Modeling Strategies. Springer.

[34] Heston S. (1993): A Closed-Form Solution for Options with Stochastic Volatility with Applications to Bond and Currency Options. The Review of Financial Studies, Volume 6, Issue 2, 327-343.

[35] Heston S., Nandi S. (2000): A closed-form GARCH option pricing model. The Review of Financial Studies. Fall, 13, 585-625.

[36] Higgins M.L., Bera A.K. (1992): A Class of Nonlinear ARCH Models. International Economic Review, 33,137-158.

[37] Ishii H., Lions P.L. (1990): Viscosity solutions of fully non-linear second-order elliptic partial differential equations, J. Differential equations, 83, 1, 26-78.

[38] Jarrow R., TurnBull S. (2000): Derivative Securities. South Western.

[39] Johnson N. et al. (2013): The Stock-Bond correlation. PIMCO (Alliance).

[40] Kallsen J., Taqqu M. (1998): Option pricing in ARCH-TYPE models. Mathematical Finance, 8, 13-26.

[41] Karatzas I., Shreve S. (1988): Brownian Motion and Stochastic Calculus. Springer.

[42] Karatzas I. (1989): Optimisation problems in the theory of continuous trading, SIAM J. Control Optim., 27, pp. 1221-1259.

[43] Katsoulakis (1991): State constraint problems for second order fully non-linear degenerate partial differential equations, Ph. D. thesis, Brown University, Providence.

[44] Lions P.L. (1983): Optimal control of diffusion processes and Hamilton-Jacobi-Bellman equations, parts 1 & 2. Comm. Partial Differential Equations, 8, 1101-1174, 1229-1276.

[45] Longstaff F., Schwartz E. (1992): Interest Rate Volatility and the Term Structure: A Two-Factor General Equilibrium Model. JSTOR

[46] Lyuu Y.,Wu C. (2005): On accurate and Provably Efficient GARCH Option Pricing Algorithms. Quantitative Finance, 2, 181-198.

[47] Magill M.J.P., Constatinides G.M. (1976): Portfolio selection with transaction costs. J. Econom. Theory 13, 245-263.

[48] Merton R.C. (1971): Optimal consumption and portfolio rules in a continuous time model, Journal of Economic Theroy 3, 473-413

[49] Merton R.C. (1973): An intertemporal Capital Asset Pricing Model. Econometrica, 42, 867-887.

[50] Multiprod algorithm. www.mathworks.com/matlabcentral/fileexchange/8773-multiple-matrix-multiplications–with-array-expansion-enabled

[51] Nelson D.B. (1990): Arch models as diffusion approximations. Journal of Econometrics 45 (1990), 7-38.

[52] Oksendal B. (1985): Stochastic Differential Equations. Springer

[53] Protter P. (1990): Stochastic Integration and Differential Equations. Springer-Verlag, Berlin

[54] Ritchen P, Trevor R. (1999): Pricing Options under Generalized GARCH and Stochastic Volatility Processes. The Journal of Finance, 54, 377-402.

[55] Rivlin T.J. (1990): Chebyshev Polynomials: From Approximation Theory to Algebra and Number Theory. Wiley, New York, MR1060735(92a:41016)

[56] Shreve S.E., Soner H.M. (1994): Optimal investment and consumption with transaction costs, Annals of Applied Probablity 4, 609,692

[57] Soner H.M. (1986): Optimal control with state-space constraints, SIAM, J. Control Optim., 24, 552-561.

[58] Soner H.M., Shreve S.E., Cvitanić J. (1995): There is no nontrivial hedging portfolio for option pricing with transaction costs. The Annals of Applied Probability 5, 2, 327-355.

[59] Stentof L. (2004): Pricing American Options when the underlying asset follows GARCH processes. Journal of Empiriccal Ginance, 12, 576-611.

[60] Tauchen G. (1985): Diagnostic Testing and Evaluation of Maximum Likelihood Models. Journal of Econometrics, 30, 415-443.

[61] Zhang L., Mykland Per A., Aït-Sahalia Y. (2005): A Tale of Two Time Scales: Determining Integrated Volatility With Noisy High-Frequency Data

[62] Zhu H. (1991): Characacterization of variational inequalities in singular control, Ph.D. thesis, Brown University, Providence, RI.